

Some pages of this thesis may have been removed for copyright restrictions.

If you have discovered material in AURA which is unlawful e.g. breaches copyright, (either yours or that of a third party) or any other law, including but not limited to those relating to patent, trademark, confidentiality, data protection, obscenity, defamation, libel, then please read our [Takedown Policy](#) and [contact the service](#) immediately

THE SYNTHESIS OF BIODEGRADABLE POLYMERS USING
ALUMINIUM ALKOXIDE INITIATORS.

GRAEME KETTLEWELL

Doctor of Philosophy

ASTON UNIVERSITY

March 2001

This copy of the thesis has been supplied on condition that anyone who consults it is understood to recognise that its copyright rests with its author and that no quotation from the thesis and no information derived from it may be published without proper acknowledgement.

Thesis Summary.

Alkyl aluminium alkoxides have been used as initiators for the ring opening polymerisation of ϵ -caprolactone and δ -valerolactone. The effect of the reaction solvent on the kinetics of the polymerisation of ϵ -caprolactone has been studied. The rate of polymerisation was found to be faster in solvents of lower polarity and donor nature such as toluene. In general solvents of higher polarity resulted in a decreased rate of polymerisation. However solvents such as THF or DMF with a lone pair of electrons capable of forming a complex with the aluminium centre slowed the polymerisation further. The size of the monomer also proved to be an important factor in the kinetics of the reaction. The six membered ring, δ -valerolactone has less ring strain than the seven membered ring ϵ -caprolactone and thus the polymerisation of δ -valerolactone is slower than the corresponding polymerisation of ϵ -caprolactone. Both the alkoxide and alkyl group structures have an effect on the polymerisation. In general bulkier alkoxide groups provide greater steric hindrance around the active site at the beginning of the reaction. This causes an induction or a build up period that is related to the both the steric hindrance and also the electronic effects provided by the alkoxide group. The alkyl group structure has an effect throughout the polymerisation because it remains adjacent to the active centre. The number of alkoxide groups on the aluminium centre is also important, using a dialkoxide as an initiator yields polymers with molecular weights approximately half that of the corresponding reactions using a mono alkoxide. Transesterification reactions have also been found to occur after most of the monomer has been consumed. These transesterification reactions are exaggerated as temperature increases. A method of producing tri-block co-polymers has also been developed. A di-hydroxy functional pre-polymer, PHBV, was reacted with an aluminium alkyl to form a di-alkoxide macroinitiator which was subsequently used as an initiator for the polymerisation of ϵ -caprolactone to form an ABA type tri-block co-polymer. The molecular weight and other properties were predictable from the initial monomer/initiator ratios.

KEYWORDS: alkyl aluminium alkoxide, polymer, ϵ -caprolactone, co-polymer, solvent effect.

For Heather

Acknowledgements.

Thanks to Allan and Wendy Amass for advice, assistance and patience.

Also thanks to Colin, Tristan, Hassen and the many others who have worked in 208/209 over the last four years.

Thanks to Mike Perry for NMR analysis and Lynne for stores.

And thanks to my family for their support through the hard bits.

This thesis was kindly funded by the EPSRC.

Contents

| | |
|----------------------------------------------|-----------|
| Summary | 2 |
| Table of contents | 5 |
| List of tables | 14 |
| List of diagrams | 17 |
| List of abbreviations | 18 |
| Aims and objectives | 30 |
| CHAPTER 1 INTRODUCTION | 31 |
| 1.1 Biodegradable polymers | 31 |
| 1.1.1 Applications of biodegradable polymers | 31 |
| 1.1.2.1 Medical applications | 32 |
| 1.1.2.2 Surgical sutures | 32 |
| 1.1.2.3 Tissue adhesion prevention | 32 |
| 1.1.2.4 Bone fixation devices | 32 |
| 1.1.2.5 Drug delivery systems | 33 |
| 1.1.2.6 Agricultural applications | 34 |
| 1.1.2.7 Packaging applications | 34 |
| 1.1.2 Examples of biodegradable polymers | 34 |
| 1.1.3 Natural biodegradable polymers | 35 |
| 1.1.3.1 Poly(peptides) and proteins | 35 |
| 1.1.3.2 Poly(saccharides) | 35 |
| 1.1.3.3 Starch | 36 |

| | | |
|-------------|--------------------------------------------------------------------------------------------------------------------------|-----------|
| 1.1.3.4. | Cellulose | 36 |
| 1.1.4. | Synthetic biodegradable polymers | 37 |
| 1.1.4.1. | Poly(α -hydroxy acids), poly(lactic acid) and poly(glycolic acid) | 37 |
| 1.1.4.2. | Poly(ϵ -caprolactone) | 38 |
| 1.1.4.3. | Poly(hydroxyalkanoates), poly(β -hydroxybutyrate)(PHB), poly(β -hydroxyvalerate)(PHV) and PHBV co-polymers | 40 |
| 1.1.4.4. | Other synthetic polymers | 42 |
| 1.1.5. | Definition of biodegradation | 43 |
| 1.1.6. | Effect of polymer structure on biodegradation | 45 |
| 1.1.6.1. | Morphology | 45 |
| 1.1.6.2. | Glass transition temperature | 46 |
| 1.1.6.3. | Effect of polymer structure and molecular weight | 47 |
| 1.2. | Polymerisation reactions | 48 |
| 1.2.1. | Introduction | 48 |
| 1.2.2. | Ring opening polymerisation | 51 |
| 1.2.2.1. | Ring strain in cyclic molecules | 52 |
| 1.2.2.2. | Ring strain in lactones | 53 |
| 1.2.3. | Ring opening polymerisation of ϵ -caprolactone and other lactones | 56 |
| 1.2.4. | Anionic polymerisation | 58 |
| 1.2.4.1. | Anionic polymerisation of ϵ -caprolactone | 58 |
| 1.2.4.2. | Intra and inter molecular transesterification reactions | 59 |
| 1.2.5. | Free radical polymerisation | 61 |
| 1.2.5.1. | Free radical polymerisation of ϵ -caprolactone | 63 |
| 1.2.6. | Cationic polymerisation | 65 |
| 1.2.6.1. | Cationic ring opening polymerisation of ϵ -caprolactone | 67 |
| 1.2.7. | Co-ordination polymerisation | 69 |
| 1.2.7.1. | Co-ordination or insertion polymerisation of ϵ -caprolactone | 69 |

| | | |
|-------------|------------------------------------------------------------------------------------------------------------|------------|
| 1.2.8. | Enzymatic polymerisation of lactones | 73 |
| 1.2.9. | Living polymerisation | 75 |
| 1.2.9.1. | Kinetics of living polymerisation | 76 |
| 1.2.10. | Effect of solvent on polymerisation | 77 |
| 1.3. | Aluminium alkoxide initiators | 80 |
| 1.3.1. | Introduction | 80 |
| 1.3.2. | Bimetallic μ -oxoalkoxides | 80 |
| 1.3.3. | Aluminium trialkoxides | 82 |
| 1.3.3.1. | Mechanism of polymerisation initiated with aluminium trialkoxides | 82 |
| 1.3.4. | Aggregation alkoxide species | 85 |
| 1.3.4.1. | Aluminium <i>trialkoxides</i> | 86 |
| 1.3.4.2. | Alkyl aluminium alkoxides | 90 |
| 1.3.5. | Transesterification or back biting reactions | 90 |
| 1.3.6. | Effect of the nature of the alkyl group in alkyl aluminium alkoxides on the polymerisation of lactones. | 92 |
| 1.3.7. | Effect of the nature of the alkoxide group in alkyl aluminium alkoxides on the polymerisation of lactones. | 93 |
| 1.3.8. | Effect of the solvent on polymerisation initiated by aluminium alkoxides | 94 |
| 1.3.9. | Telechelic polyesters from aluminium alkoxide initiated polymerisations. | 96 |
| 1.3.10. | Synthesis of block co-polymers using alkoxide macroinitiators | 100 |
| 1.3.11. | 'Immortal' polymerisation of ϵ -caprolactone. | 102 |
| 1.4. | Plan for experimental work | 103 |

| | | |
|------------------|-----------------------------------------------------------------|-----|
| Chapter 2 | Experimental Techniques | 105 |
| 2.1. | Purification of materials | 105 |
| 2.1.1. | Solvents | 105 |
| 2.1.1.1. | THF | 105 |
| 2.1.1.2. | Toluene | 105 |
| 2.1.1.3. | Dichloromethane | 105 |
| 2.1.1.4. | 2,4-Pentanedione | 106 |
| 2.1.1.5. | Methanol | 106 |
| 2.1.1.6. | <i>N,N</i> -Dimethylformamide | 106 |
| 2.1.2. | Drying agents | 106 |
| 2.1.2.1. | Calcium hydride | 106 |
| 2.1.2.2. | Phosphorous pentoxide | 106 |
| 2.1.2.3. | Sodium metal | 106 |
| 2.1.3. | Monomers | 107 |
| 2.1.3.1. | ϵ -caprolactone | 107 |
| 2.1.3.2. | δ -valerolactone | 107 |
| 2.1.3.3. | Poly(hydroxybutyrate-co-valerate) (PHBV) diol. $M_n = 1500$ | 107 |
| 2.1.4. | Others | 107 |
| 2.1.4.1. | <i>N,N</i> -Dimethyl- <i>N</i> -ethylethylenediamine (DMEDA) | 107 |
| 2.1.5. | Initiators | 108 |
| 2.1.5.1. | Triisobutyl aluminium | 108 |
| 2.1.5.2. | Alkyl aluminium alkoxide | 108 |
| 2.1.5.3. | Macro initiators | 108 |
| 2.2. | Polymerisation methods | 109 |
| 2.2.1. | Homo polymerisations | 109 |
| 2.2.2. | Co-polymerisations | 109 |
| 2.2.3. | Sampling reactions | 110 |

| | | |
|-------------------|---------------------------------------------------------------------------------------------------------------------------------------------------------|----------------|
| 2.3. | Techniques for handling air sensitive materials | 111 |
| 2.3.1. | Vacuum line techniques | 112 |
| 2.3.3. | Freeze-thaw degassing Trap to trap distillation | 113 |
| 2.3.4. | Schlenk techniques | 113 |
| 2.3.5. | Argon dry box | 114 |
| 2.4. | Analytical techniques | 114 |
| 2.4.1. | Gel permeation (size exclusion) chromatography | 114 |
| 2.4.1.1. | Molecular weight determination | 116 |
| 2.4.1.2. | Calibration of GPC | 119 |
| 2.4.1.3. | Universal calibration | 120 |
| 2.4.2. | Nuclear magnetic resonance | 120 |
| Chapter 3 | The polymerisation of ϵ-caprolactone using alkyl aluminium alkoxide initiators. | 122 |
| 3.1. | The effect of the reaction medium on the polymerisation of ϵ-caprolactone using diisobutyl aluminium isopropoxide initiator. | 122 |
| 3.1.1. | Introduction | 122 |
| 3.1.2. | The polymerisation of ϵ -caprolactone using toluene as a solvent | 123 |
| 3.1.3. | The polymerisation of ϵ -caprolactone using THF as a solvent | 126 |
| 3.1.4. | The polymerisation of ϵ -caprolactone using DCM as a solvent | 128 |
| 3.1.5. | The polymerisation of ϵ -caprolactone using DMF as a solvent | 130 |
| 3.1.6. | Plots of $\ln([M]_0/[M]_t)$ against time for the polymerisation of ϵ -caprolactone. | 132 |

| | | |
|-------------------|-------------------------------------------------------------------------------------------------------------------------------------------------------|-----|
| 3.1.7. | Plots of $\ln(DP_{n_{\infty}}-DP_{n_t})$ vs time for the polymerisation of ϵ -caprolactone using diisobutyl aluminium isopropoxide initiator | 139 |
| 3.1.8. | Overall comparison of apparent rate constants in toluene, DCM and THF. | 142 |
| 3.1.9. | The dependence of M_n on conversion | 147 |
| 3.1.10. | Initiator efficiency and initiator concentration | 150 |
| 3.2. | Mono alkoxide and dialkoxide aluminium initiators | 151 |
| 3.2.1. | Results of the polymerisation of ϵ -caprolactone Using alkyl aluminium mono and di alkoxides | 151 |
| 3.3. | Aggregation of initiator molecules | 153 |
| 3.3.1. | Effect of solvent on the aggregation of initiator molecules. | 153 |
| 3.4. | Effect of temperature on the rate of polymerisation | 156 |
| 3.5. | Transesterification reactions in the polymerisation of ϵ-caprolactone using alkyl aluminium alkoxide initiators | 163 |
| 3.5.1. | Effect of solvent on transesterification | 163 |
| 3.5.2. | Effect of temperature on transesterification reactions | 166 |
| Chapter 4. | The polymerisation of ϵ-caprolactone using functional aluminium alkoxides. | 170 |
| 4.1. | Introduction | 170 |
| 4.1.1. | Synthesis of functional aluminium alkoxides | 170 |
| 4.1.2. | Functional aluminium alkoxides synthesised | 171 |

| | | |
|-------------|----------------------------------------------------------------------------------------------------------------------------------------------------------------------------------|-----|
| 4.1.3. | Unsuccessful dialkyl aluminium alkoxide synthesis | 172 |
| 4.2. | The polymerisation of ϵ-caprolactone using functional aluminium alkoxide initiators | 172 |
| 4.2.1. | The polymerisation of ϵ -caprolactone using aromatic alkoxide initiators | 173 |
| 4.2.2. | The polymerisation of ϵ -caprolactone using <i>diisobutyl</i> aluminium phenoxide initiator | 173 |
| 4.2.3. | <i>Diisobutyl</i> aluminium <i>p</i> -methoxyphenoxide as an initiator for the polymerisation of ϵ -caprolactone | 176 |
| 4.2.4. | <i>Diisobutyl</i> aluminium 2,6-di <i>tert</i> -butyl phenoxide as an initiator for the polymerisation of ϵ -caprolactone | 180 |
| 4.2.5. | <i>Diisobutyl</i> aluminium cyclohexanoxide as an initiator for the polymerisation of ϵ -caprolactone | 184 |
| 4.2.6. | The polymerisation of ϵ -caprolactone using <i>diisobutyl</i> aluminium cyclopentoxide as an initiator | 187 |
| 4.2.7. | <i>Diisobutyl</i> aluminium <i>n</i> -butoxide as an initiator for the polymerisation of ϵ -caprolactone | 191 |
| 4.2.8. | <i>Diisobutyl</i> aluminium <i>tert</i> -butoxide as an initiator for the polymerisation of ϵ -caprolactone | 196 |
| 4.2.9. | <i>Diisobutyl</i> aluminium <i>iso</i> -propoxide as an initiator for the polymerisation of ϵ -caprolactone | 198 |
| 4.3. | The effect of alkyl group structure on the kinetics of the polymerisation of ϵ-caprolactone using dialkyl aluminium alkoxide initiators. | 201 |
| 4.3.1. | Introduction | 201 |
| 4.3.2. | The effects of alkyl group structure on the dependence of $\ln(DP_{n_{\infty}}-DP_{n_t})$ versus time | 202 |
| 4.4. | Summary of the effect of alkoxide group structure on the kinetics of the polymerisation of ϵ-caprolactone using dialkyl aluminium alkoxide initiators | 214 |
| 4.5. | NMR analysis of functional terminated poly(ϵ-caprolactone) | 226 |

| | | |
|---------------------------------------------------------------------------------|----------------------------------------------------------------------------------------------------------------------------------------------------------------------------------------|-----|
| 4.5.1. | ¹³ C NMR analysis of poly(ϵ -caprolactone) | 226 |
| 4.5.2. | ¹ H NMR analysis of poly(ϵ -caprolactone). | 227 |
| 4.5.3. | NMR analysis of <i>diisobutyl</i> aluminium 2,6-di- <i>tert</i> butyl phenoxide initiated poly(ϵ -caprolactone) | 229 |
| 4.5.4. | NMR analysis of <i>diisobutyl</i> aluminium <i>p</i> -methoxy phenoxide initiated poly(ϵ -caprolactone) | 231 |
| 4.5.5. | NMR analysis <i>diisobutyl</i> aluminium <i>n</i> -butoxide initiated poly(ϵ -caprolactone) | 233 |
| Chapter 5. Homo-polymerisations of δ-valerolactone | | 235 |
| 5.1 | Polymerisation of valerolactone | 235 |
| 5.1.1. | The polymerisation of δ -valerolactone in THF using <i>diisobutyl</i> aluminium <i>isopropoxide</i> initiator. | 237 |
| 5.1.1.1. | NMR analysis of poly(δ -valerolactone) | 239 |
| 5.1.2. | The polymerisation of δ -valerolactone in toluene. | 244 |
| 5.1.3. | The polymerisation of δ -valerolactone in dichloromethane | 247 |
| 5.1.4. | The dependence of M_n on conversion | 249 |
| 5.1.5. | First order plots of $\ln([M]_0/[M]_t)$ versus time | 251 |
| 5.1.6. | The effect of reaction solvent on plots of $\ln(DP_{n_{\infty}} - DP_n)$ versus time | 257 |
| 5.1.7. | The effect of initiator concentration on k_p | 260 |
| 5.1.8. | Comparison of rate of polymerisation of ϵ -caprolactone and δ -valerolactone using <i>diisobutyl</i> aluminium <i>isopropoxide</i> in solvents of different polarities | 266 |

| | | |
|-------------------|------------------------------------------------------------------------------------|-----|
| Chapter 6 | The synthesis of block co-polymers using aluminium alkoxide macroinitiators | 269 |
| 6.1. | Synthesis of triblock co-polymers | 269 |
| 6.2. | NMR analysis of co-polymers. | 272 |
| 6.2.1. | ^1H NMR of co-polymers | 273 |
| 6.2.2. | Calculation of molecular weights using ^1H NMR. | 277 |
| 6.2.3. | ^{13}C NMR spectra | 279 |
| 6.3. | Effect on molecular weight of aluminium alkyl added | 281 |
| Chapter 7. | Further Work | 283 |
| Chapter 8. | Conclusions | 286 |
| References | | 289 |

List of Tables

Chapter 1

| | | |
|------------|-----------------------------------------------------------------------------|----|
| Table 1.1. | Common biodegradable polymers | 35 |
| Table 1.2. | Comparison of bond angles of lactones. | 54 |
| Table 1.3. | Values of free energy of ring opening for lactones of increasing ring size. | 55 |
| Table 1.4 | Polymerisability of lactones | 55 |
| Table 1.5. | Number of active sites per initiator molecule. | 87 |
| Table 1.6. | Rate constants of propagation | 93 |
| Table 1.7. | Functional polymers synthesised using aluminium alkoxides | 97 |

Chapter 3

| | | |
|------------|------------------------------------------------------------------------------------------------------------------------------------|-----|
| Table 3.1. | Molecular weight and conversion data for the polymerisation of ϵ -caprolactone using toluene as a solvent. | 123 |
| Table 3.2. | Molecular weight and conversion data for the polymerisation of ϵ -caprolactone using THF as a solvent. | 126 |
| Table 3.3. | Molecular weight and conversion data for the polymerisation of ϵ -caprolactone using DCM as a solvent. | 128 |
| Table 3.4 | Molecular weight and conversion data for the polymerisation of ϵ -caprolactone using DMF as a solvent. | 130 |
| Table 3.5. | Dielectric constants of solvents used in polymerisations. | 143 |
| Table 3.6. | Apparent rate constant of polymerisation of ϵ -caprolactone in solvents of differing polarity. | 144 |
| Table 3.7. | Molecular weight data from the polymerisation of ϵ -caprolactone in using <i>isobutyl</i> aluminium <i>diisopropoxide</i> | 151 |
| Table 3.8. | Degree of initiator association in three solvents. | 155 |

| | | |
|----------------------|-------------------------------------------------------------------------------------------------------------------------------------------------------------------------------------------------------------------------------------------------------|-----|
| Table 3.9. | Molecular weights and molecular weight distributions obtained from samples taken from the polymerisation of ϵ -caprolactone using <i>diisobutyl</i> aluminium <i>isopropoxide</i> in toluene at a range of temperatures from -31°C to +40°C. | 156 |
| Table 3.10. | Molecular weight and conversion data from polymerisation of ϵ -caprolactone over 9 days at 25°C | 162 |
| Table 3.11 | Molecular weights obtained from the polymerisation of ϵ -caprolactone at a range of temperatures from 40°C to 100°C using <i>diisobutyl</i> aluminium <i>isopropoxide</i> initiator in toluene. | 133 |
| Chapter 4 | | |
| Table 4.1. | Alcohols used in synthesis of aluminium alkoxides | 171 |
| Table 4.2. | Aluminium alkoxides attempted | 172 |
| Table 4.3. | Molecular weight and conversion data from the polymerisation of ϵ -caprolactone using <i>diisobutyl</i> aluminium phenoxide as an initiator | 174 |
| Table 4.4 | Molecular weight and conversion data obtained from the polymerisation of ϵ -caprolactone using <i>diisobutyl</i> aluminium <i>p</i> -methoxyphenoxide | 177 |
| Table 4.5. | Molecular weight and conversion data obtained from the polymerisation of ϵ -caprolactone using <i>diisobutyl</i> aluminium 2,6- <i>di-tert</i> -butyl phenoxide in toluene at 25°C | 181 |
| Table 4.6. | Molecular weight and conversion data obtained from the polymerisation of ϵ -caprolactone using <i>diisobutyl</i> aluminium cyclo-hexanoxide in toluene at 25°C | 185 |
| Table 4.7. | Molecular weight and conversion data obtained from the polymerisation of ϵ -caprolactone using <i>diisobutyl</i> aluminium cyclopentoxide in toluene at 25°C. | 188 |
| Table 4.8. | Molecular weight and conversion data from the polymerisation of ϵ -caprolactone using <i>diisobutyl</i> aluminium <i>n</i> -butoxide in toluene at 25°C | 192 |
| Table 4.9. | Molecular weight data from the polymerisations of ϵ -caprolactone using <i>diisobutyl</i> aluminium <i>tert</i> -butoxide in toluene at 25°C | 196 |

| | | |
|----------------------|-----------------------------------------------------------------------------------------------------------------------------------------------------------------------------------------------------------------------------------------------------------------------------|-----|
| Table 4.10. | Molecular weight and conyversion data from the polymerisation of ϵ -caprolactone using <i>diisobutyl</i> aluminium <i>iso</i> -propoxide in toluene at 25°C | 198 |
| Table 4.11 | Molecular weight and conversion data obtained from the polymerisation of ϵ -caprolactone using diethyl aluminium <i>n</i> -butoxide in toluene at 25°C | 202 |
| Table 4.12. | Apparent rate constant $L \text{ mol}^{-1} \text{ sec}^{-1}$ for the polymerisation of polymerisation of ϵ -caprolactone using <i>diisobutyl</i> aluminium <i>n</i> -butoxide and diethyl aluminium <i>n</i> -butoxide initiator and toluene as a solvent at 25°C. | 204 |
| Table 4.13. | Apparent rate constants of polymerisation for the polymerisation of ϵ -caprolactone using <i>diisobutyl</i> aluminium alkoxide initiators in toluene at 25°C. | 214 |
| Table 4.14. | Slope of linear section of $\{1/[I]_0\} \ln([M]_0/[M]_t)$ against time plot | 216 |
| Table 4.15 | Build up period, t_i for the polymerisation of ϵ -caprolactone using <i>diisobutyl</i> aluminium alkoxide initiators in toluene at 25°C | 219 |
| Chapter 5 | | |
| Table 5.1. | Molecular weight and conversion data obtained from polymerisations of δ -valerolactone using <i>diisobutyl</i> aluminium <i>isopropoxide</i> initiator in THF | 237 |
| Table 5.2. | Molecular weight and conversion data obtained from polymerisations of δ -valerolactone using <i>diisobutyl</i> aluminium <i>isopropoxide</i> initiator in toluene | 244 |
| Table 5.3. | Molecular weight and conversion data obtained from polymerisations of δ -valerolactone using <i>diisobutyl</i> aluminium <i>isopropoxide</i> initiator in DCM | 246 |
| Table 5.4 | Apparent rate constant of polymerisation of δ -valerolactone in solvents of differing polarity | 260 |
| Table 5.5. | Mean degree of association in THF and DCM | 265 |
| Table 5.6. | Values of free energy of ring opening for lactones of increasing ring size | 267 |
| Table 5.7. | Comparison of bond angles of lactones | 268 |

Chapter 6

| | | |
|------------|---------------------------------------------------------------------------------------------------------------|-----|
| Table 6.1. | Results of the formation of PCL-PHBV-PCL block co-polymers using alkyl aluminium PHBV-alkoxide macroinitiator | 271 |
| Table 6.2. | Resonances in ^1H NMR spectrum of PCL-PHBV-PCL co-polymer | 274 |
| Table 6.3. | Molecular weights by GPC and NMR of PHBV-PCL co-polymers. | 278 |
| Table 6.4 | Ratio of reactants in co-polymerisation. | 281 |
| Table 6.5. | Molecular weight with varying aluminium alkyl concentration. | 281 |

List of Figures

Chapter 1

| | | |
|--------------|----------------------------------------------------------------------------------------------------------------------|----|
| Figure 1.1. | Monomeric structure of starch and cellulose | 35 |
| Figure 1.2. | Structures of poly(lactic acid) and poly(glycolic acid) | 37 |
| Figure 1.3. | Structure of poly(ϵ -caprolactone) | 38 |
| Figure 1.4 | Structure of polyhydroxyalkanoates | 40 |
| Figure 1.5. | Structure of poly(β -hydroxybutyrate) and poly(β -hydroxyvalerate). | 40 |
| Figure 1.6. | Poly(urethane), poly(amide), poly(anhydride). Synthetic biodegradable polymers. | 42 |
| Figure 1.7. | Poly condensation of diacid and diol | 48 |
| Figure 1.8. | General equation for ring opening polymerisation | 51 |
| Figure 1.9. | Cycloalkane strain versus ring size | 53 |
| Figure 1.10. | Ring strain in cyclo alkanes and lactones | 54 |
| Figure 1.11. | Mechanism of anionic polymerisation of lactones. | 58 |
| Figure 1.12. | Transesterification reactions in the polymerisation of (ϵ -capro)lactone with anionic initiator species | 60 |
| Figure 1.13. | Decomposition of benzoyl peroxide to form radical Species | 62 |
| Figure 1.14. | Termination via combination | 63 |
| Figure 1.15. | Termination via disproportionation | 63 |
| Figure 1.16. | Reaction between MDO and AIBN | 64 |
| Figure 1.17. | Initiation, propagation and termination of cationic polymerisation using protonic/ Brønsted acid initiators. | 65 |
| Figure 1.18. | Reaction of catalyst complex with isobutylene | 66 |
| Figure 1.19. | Termination via unimolecular rearrangement of the ion Pair | 67 |
| Figure 1.20. | Termination via bimolecular transfer reaction with Monomer | 67 |
| Figure 1.21. | Mechanism of cationic polymerisation of ϵ - ϵ -caprolactone | 68 |
| Figure 1.22. | Tin octoate polymerisation mechanism | 71 |

| | | |
|----------------------|-------------------------------------------------------------------------------------------------------------------------------------------------------------------------------------------------------------------------|-----|
| Figure 1.23. | Active-dormant species in tin octoate polymerisation of ϵ - ϵ -caprolactone | 71 |
| Figure 1.24. | Side reactions in tin alkoxide initiated polymerisation of ϵ - ϵ -caprolactone | 72 |
| Figure 1.25. | Structure of aluminium alkoxides | 80 |
| Figure 1.26. | Structure of bimetallic μ -oxoalkoxide and aluminium Alkoxides | 81 |
| Figure 1.27. | Co-ordination-insertion mechanism of polymerisation of a lactone | 83 |
| Figure 1.28. | π -complexation of the monomer with the aluminium centres | 84 |
| Figure 1.29. | Propagation and reformation of oxonium ion. | 84 |
| Figure 1.30. | Trisolvated six co-ordinate $\text{Al}(\text{iPrO})_3(\text{monomer})_3$ complexes | 87 |
| Figure 1.31. | Initiator in presence and absence of monomer. | 89 |
| Figure 1.32. | Solvation of alkyl aluminium alkoxide by ϵ -caprolactone in toluene. | 95 |
| Figure 1.33. | Solvation of alkyl aluminium alkoxide by THF and lactone. | 95 |
| Figure 1.34. | Formation of PS-PCL diblock co-polymers using aluminium alkoxides and 'living' radical polymerisation | 99 |
| Figure 1.35. | Scheme for the preparation of PHB- <i>b</i> -poly(esters) by the formation of PHB-O-AlEt ₂ macroinitiator species and subsequent ring opening polymerisation of ϵ -caprolactone or lactide monomers | 101 |
| Figure 1.36. | (5, 10, 15, 20 tetraphenylporhinato) aluminium alkoxide. | 102 |
| Chapter 2 | | |
| Figure 2.1. | Removal of organo aluminium compounds using acetylacetone to form aluminium acetylacetonate. | 110 |
| Figure 2.2. | Sampling reaction equipment including Omnifit valve. | 111 |
| Figure 2.3. | Vacuum Line | 112 |
| Figure 2.4 | Schematic diagram of GPC apparatus | 116 |

| | | |
|-------------|--------------------------------------------------------|-----|
| Figure 2.5. | Calibration Curve for GPC using polystyrene standards. | 119 |
|-------------|--------------------------------------------------------|-----|

Chapter 3

| | | |
|--------------|---------------------------------------------------------------------------------------------------------------------------------------------------------------------------------|-----|
| Figure 3.1. | Effect of solvent on plot of M_w/M_n versus time for the polymerisation of ϵ -caprolactone in solvents of varying polarity | 125 |
| Figure 3.2. | First order plot for the polymerisation of ϵ -caprolactone in toluene at 25°C using <i>diisobutyl</i> aluminium <i>isopropoxide</i> initiator. | 132 |
| Figure 3.3. | First order plot for the polymerisation of ϵ -caprolactone in THF at 25°C using <i>diisobutyl</i> aluminium <i>isopropoxide</i> initiator. | 132 |
| Figure 3.4 | First order plot for the polymerisation of ϵ -caprolactone in DCM at 25°C using <i>diisobutyl</i> aluminium <i>isopropoxide</i> initiator. | 133 |
| Figure 3.5. | Dependence of build up period on initiator concentration for the polymerisation of ϵ -caprolactone in various solvents. | 134 |
| Figure 3.6. | Plot of $1/[I]_0 \ln[M]_0/[M]_t$ against time for the polymerisation of ϵ -caprolactone using toluene as a solvent. | 136 |
| Figure 3.7. | Plot of $1/[I]_0 \ln[M]_0/[M]_t$ against time for the polymerisation of ϵ -caprolactone using THF as a solvent. | 137 |
| Figure 3.8. | Plot of $1/[I]_0 \ln[M]_0/[M]_t$ against time for the polymerisation of ϵ -caprolactone using DCM as a solvent. | 138 |
| Figure 3.9. | Plot of $\ln(DP_{n_0}-DP_{n_t})$ vs time for the polymerisation of ϵ -caprolactone in toluene at 25°C using <i>diisobutyl</i> aluminium <i>isopropoxide</i> initiator. | 141 |
| Figure 3.10. | Plot of $\ln(DP_{n_0}-DP_{n_t})$ vs time for the polymerisation of ϵ -caprolactone in THF at 25°C using <i>diisobutyl</i> aluminium <i>isopropoxide</i> initiator. | 141 |

| | | |
|--------------|------------------------------------------------------------------------------------------------------------------------------------------------------------------------------------------------------------------|-----|
| Figure 3.11. | Plot of $\ln(DP_{n_0}-DP_{n_t})$ vs time for the polymerisation of ϵ -caprolactone in DCM at 25°C using <i>diisobutyl</i> aluminium <i>isopropoxide</i> initiator | 142 |
| Figure 3.12. | Comparison of apparent rate constants versus initiator concentration in solvents of varying polarity. | 144 |
| Figure 3.13. | Possible association of aluminium alkoxide and THF molecules | 146 |
| Figure 3.14. | Co-ordination of DMF with aluminium alkoxide. | 147 |
| Figure 3.15. | The dependence of molecular weight on conversion for the polymerisation of ϵ -caprolactone in toluene. | 148 |
| Figure 3.16. | The dependence of molecular weight on conversion for the polymerisation of ϵ -caprolactone in THF. | 148 |
| Figure 3.17. | The dependence of molecular weight on conversion for the polymerisation of ϵ -caprolactone in DCM. | 149 |
| Figure 3.18. | Plot of initiator efficiency versus initiator concentration for the polymerisation of ϵ -caprolactone. | 150 |
| Figure 3.19. | Plot of M_n against $1/[I]_0$ for the polymerisation of ϵ -caprolactone using <i>diisobutyl</i> aluminium <i>isopropoxide</i> and <i>isobutyl</i> aluminium <i>diisopropoxide</i> in toluene at 25°C. | 152 |
| Figure 3.20. | Plot of $-\ln(k_p)$ versus $-\ln[I]_0$ for the polymerisation of ϵ -caprolactone using <i>diisobutyl</i> aluminium <i>isopropoxide</i> in toluene, THF, and DCM at 25°C | 154 |
| Figure 3.21. | The effect of temperature on the first order plot for the polymerisation of ϵ -caprolactone using <i>diisobutyl</i> aluminium <i>isopropoxide</i> in toluene. | 158 |
| Figure 3.22. | Dependence of M_n versus conversion for the polymerisation of ϵ -caprolactone using <i>diisobutyl</i> aluminium <i>isopropoxide</i> at various temperatures. | 159 |
| Figure 3.23. | Plot of $\ln(DP_{n_0}-DP_{n_t})$ versus temperature for the polymerisation of ϵ -caprolactone using <i>diisobutyl</i> aluminium <i>isopropoxide</i> at various temperatures. | 160 |
| Figure 3.24. | Arrhenius plot of $\ln k_p$ against $1/T$ for the polymerisation of ϵ -caprolactone in toluene using <i>diisobutyl</i> aluminium <i>isopropoxide</i> . | 160 |
| Figure 3.25. | Decrease in molecular weight with time of poly(ϵ -caprolactone) in toluene and THF | 163 |

| | | |
|----------------------|-------------------------------------------------------------------------------------------------------------------------------------------------------------------------------|-----|
| Figure 3.26. | Plot of M_w/M_n versus time for the polymerisation of ϵ -caprolactone. | 164 |
| Figure 3.27. | Effect of reaction temperature on a plot of polydispersity against time for the polymerisation of ϵ -caprolactone at various temperatures. | 167 |
| Figure 3.28. | Plot of molecular weight against time the polymerisation of caprolactone at various temperatures. | 168 |
| Figure 3.29. | Intramolecular transesterification reaction. | 169 |
| Chapter 4 | | |
| Figure 4.1. | Dialkyl aluminium phenoxide | 173 |
| Figure 4.2. | Dependence of M_n on conversion for the polymerisation of ϵ -caprolactone using diisobutyl aluminium phenoxide as an initiator | 175 |
| Figure 4.3. | First order for the polymerisation of ϵ -caprolactone using diisobutyl aluminium phenoxide as an initiator | 175 |
| Figure 4.4 | Diisobutyl aluminium <i>p</i> -methoxyphenoxide | 176 |
| Figure 4.5. | Dependence of M_n on conversion for the polymerisation of ϵ -caprolactone using diisobutyl aluminium <i>p</i> -methoxy phenoxide in toluene at 25°C | 178 |
| Figure 4.6. | Interactions between aluminium centre and <i>p</i> -methoxy group | 178 |
| Figure 4.7. | First order plot for the polymerisation of ϵ -caprolactone using diisobutyl aluminium <i>p</i> -methoxy phenoxide initiator | 179 |
| Figure 4.8. | Plot of $\ln(DP_{n_o}-DP_{n_i})$ against time for the polymerisation of ϵ -caprolactone | 179 |
| Figure 4.9. | Diisobutyl aluminium di- <i>tert</i> -butyl phenoxide | 181 |
| Figure 4.10. | Dependence of M_n on conversion for the polymerisation of ϵ -caprolactone using diisobutyl aluminium di- <i>tert</i> -butyl phenoxide initiator in toluene at 25°C | 182 |
| Figure 4.11. | Diisobutyl aluminium di- <i>tert</i> -butyl phenoxide | 182 |

| | | |
|--------------|------------------------------------------------------------------------------------------------------------------------------------------------------------------------------|-----|
| Figure 4.12. | Plot of $\ln(DP_{n_0}-DP_{n_t})$ against time for the polymerisation of ϵ -caprolactone using diisobutyl aluminium di <i>tert</i> -butyl phenoxide | 183 |
| Figure 4.13. | First order plot for the polymerisation of ϵ -caprolactone using diisobutyl aluminium 2,6-di- <i>tert</i> -butyl phenoxide initiator | 184 |
| Figure 4.14. | Dialkyl aluminium cyclohexanoxide. | 185 |
| Figure 4.15. | Dependence of M_n on conversion for the polymerisation of ϵ -caprolactone in toluene using diisobutyl aluminium cyclohexanoxide at 25°C | 185 |
| Figure 4.16. | First order plot for the polymerisation of ϵ -caprolactone using diisobutyl aluminium cyclohexanoxide initiator in toluene at 25°C. | 187 |
| Figure 4.17. | Dialkyl aluminium cyclopentanoxide | 187 |
| Figure 4.18. | Dependence of M_n on conversion for the polymerisation of ϵ -caprolactone using diisobutyl aluminium cyclopentoxide in toluene at 25°C | 189 |
| Figure 4.19. | First order plot for the polymerisation of ϵ -caprolactone using diisobutyl aluminium cyclopentoxide in toluene at 25°C | 190 |
| Figure 4.20. | Plot of $\ln(DP_{n_0}-DP_{n_t})$ against time for the polymerisation of ϵ -caprolactone using diisobutyl aluminium cyclopentoxide initiator in toluene at 25°C | 190 |
| Figure 4.21. | Dialkyl aluminium <i>n</i> -butoxide | 193 |
| Figure 4.22. | Dependence of M_n on conversion for the polymerisation of ϵ -caprolactone using diisobutyl aluminium <i>n</i> -butoxide in toluene at 25°C | 193 |
| Figure 4.23. | First order plot for the polymerisation of ϵ -caprolactone in toluene using diisobutyl aluminium <i>n</i> -butoxide in toluene at 25°C | 194 |
| Figure 4.24. | Plot of $\ln(DP_{n_0}-DP_{n_t})$ against time for the polymerisation of ϵ -caprolactone in toluene using diisobutyl aluminium <i>n</i> -butoxide in toluene at 25°C | 195 |
| Figure 4.25. | Dialkyl aluminium <i>tert</i> -butoxide | 197 |
| Figure 4.26. | First order plot for the polymerisation of ϵ -caprolactone in toluene | 197 |
| Figure 4.27. | Dialkyl aluminium isopropoxide | 198 |

| | | |
|--------------|---------------------------------------------------------------------------------------------------------------------------------------------------------------------------------------------------------------------|-----|
| Figure 4.28. | First order plot for the polymerisation of ϵ -caprolactone using <i>diisobutyl</i> aluminium <i>iso</i> -propoxide initiator | 200 |
| Figure 4.29. | Plot of $\ln(\text{DP}_{n_{\infty}} - \text{DP}_n)$ against time for the polymerisation of ϵ -caprolactone using diethyl aluminium <i>n</i> -butoxide initiator and toluene as a solvent at 25°C | 203 |
| Figure 4.30. | Plot of $\ln(\text{DP}_{n_{\infty}} - \text{DP}_n)$ against time for the polymerisation of ϵ -caprolactone using <i>diisobutyl</i> aluminium <i>n</i> -butoxide initiator and toluene as a solvent at 25°C | 203 |
| Figure 4.31. | Plot of apparent rate constant against initial initiator concentration to show the effect of alkyl group structure | 204 |
| Figure 4.32. | Plot of $\ln([M]_0/[M]_t)$ against time for the polymerisation of ϵ -caprolactone using diethyl aluminium <i>n</i> -butoxide initiator in toluene at 25°C | 205 |
| Figure 4.33. | Plot of $\ln([M]_0/[M]_t)$ against time for the polymerisation of ϵ -caprolactone using <i>diisobutyl</i> aluminium <i>n</i> -butoxide initiator in toluene at 25°C | 206 |
| Figure 4.34. | Build up period against initial initiator concentration for the polymerisation of ϵ -caprolactone using dialkyl aluminium <i>n</i> -butoxide in toluene at 25°C | 207 |
| Figure 4.35. | Plot of M_n against conversion for the polymerisation of ϵ -caprolactone using diethyl aluminium <i>n</i> -butoxide initiator in toluene at 25°C | 208 |
| Figure 4.36. | Plot of M_n against conversion for the polymerisation of ϵ -caprolactone using <i>diisobutyl</i> aluminium <i>n</i> -butoxide in toluene at 25°C | 209 |
| Figure 4.37. | Plot of M_w/M_n against time for the polymerisation of caprolactone using diethyl aluminium <i>n</i> -butoxide as an initiator | 209 |
| Figure 4.38. | Plot of M_n against time for the polymerisation of caprolactone using <i>diisobutyl</i> aluminium <i>n</i> -butoxide as an initiator | 211 |
| Figure 4.39. | The effect of the alkoxide group structure on the apparent rate constant k_{app} . | 215 |
| Figure 4.40. | The effect of the alkoxide group structure on the length of the build up period | 230 |

| | | |
|------------------|----------------------------------------------------------------------------------------------------------------------------------------------------------------|-----|
| Figure 4.41. | The structures of <i>diisobutyl</i> aluminium cyclohexanoxide and <i>diisobutyl</i> aluminium <i>iso</i> -propoxide | 222 |
| Figure 4.42. | Rotation about C-O bond. | 223 |
| Figure 4.43. | <i>Diisobutyl</i> aluminium 2,6- <i>di-tert</i> butylphenoxide | 225 |
| Figure 4.44. | Poly(ϵ -caprolactone). | 226 |
| Figure 4.45. | ^{13}C NMR of poly(ϵ -caprolactone) | 226 |
| Figure 4.46. | Poly(ϵ -caprolactone). | 227 |
| Figure 4.47. | ^1H NMR of poly(ϵ -caprolactone) | 228 |
| Figure 4.48. | ^{13}C NMR of <i>diisobutyl</i> aluminium <i>di-tert</i> -butyl phenoxide initiated poly(ϵ -caprolactone) | 229 |
| Figure 4.49. | ^1H NMR spectrum of <i>di-tert</i> -butyl phenoxide initiated poly(ϵ -caprolactone) | 230 |
| Figure 4.50. | ^{13}C NMR of <i>diisobutyl</i> aluminium <i>para</i> -methoxy phenoxide initiated poly(ϵ -caprolactone) | 231 |
| Figure 4.51. | ^1H NMR of <i>diisobutyl</i> aluminium <i>p</i> -methoxy phenoxide initiated poly(ϵ -caprolactone) | 232 |
| Chapter 5 | | |
| Figure 5.1. | Structure of poly(δ -valerolactone) | 239 |
| Figure 5.2. | ^1H NMR spectra of poly(δ -valerolactone) | 239 |
| Figure 5.3. | Structure of poly(δ -valerolactone)-poly(THF) copolymer | 240 |
| Figure 5.4 | Ratio of intensities of protons adjacent to carbonyl carbon and acyl oxygen as reaction proceeds | 241 |
| Figure 5.5. | Mechanisms of the polymerisation of δ -valerolactone using alkyl aluminium alkoxide initiator and THF as a solvent. | 243 |
| Figure 5.6. | Dependence of initiator efficiency on initiator concentration in all solvent used for the polymerisation of δ -valerolactone | 247 |
| Figure 5.7. | Dependence of polydispersity on time for the polymerisation of δ -valerolactone | 248 |
| Figure 5.8. | Dependence of M_n on conversion for the polymerisation of δ -valerolactone using <i>diisobutyl</i> aluminium <i>isopropoxide</i> and THF as a solvent | 249 |

| | | |
|--------------|-------------------------------------------------------------------------------------------------------------------------------------------------------|-----|
| Figure 5.9. | Dependence of M_n on conversion for the polymerisation of δ -valerolactone using diisobutyl aluminium isopropoxide and DCM as a solvent | 250 |
| Figure 5.10. | Dependence of M_n on conversion for the polymerisation of δ -valerolactone using diisobutyl aluminium isopropoxide and toluene as a solvent | 250 |
| Figure 5.11. | Effect initiator concentration on first order plot for the polymerisation of δ -valerolactone in THF | 251 |
| Figure 5.12. | Effect of initiator concentration on first plot of $\ln([M]_0/[M]_t)$ versus time for the polymerisation of δ -valerolactone in toluene | 252 |
| Figure 5.13. | First order plot for the polymerisation of δ -valerolactone in DCM | 252 |
| Figure 5.14. | Plot of induction period against initiator concentration for the polymerisation of δ -valerolactone in THF, toluene and DCM | 253 |
| Figure 5.15. | Effect of initiator concentration on plot of $1/[I]_0 \ln([M]_0/[M]_t)$ against time using toluene as a solvent | 254 |
| Figure 5.16. | Effect of initiator concentration on plot of $1/[I]_0 \ln([M]_0/[M]_t)$ against time using DCM as a solvent | 255 |
| Figure 5.17. | Effect of initiator concentration on plot of $1/[I]_0 \ln([M]_0/[M]_t)$ against time using THF as a solvent | 255 |
| Figure 5.18. | The effect of initiator concentration on plot of $\ln(DPn_{\infty} - DPn_t)$ vs time for the polymerisation of δ -valerolactone in THF at 25°C | 257 |
| Figure 5.19. | Plot of $\ln(DPn_{\infty} - DPn_t)$ against time for the polymerisation of δ -valerolactone in DCM at 25°C | 258 |
| Figure 5.20. | Plot of $\ln(DPn_{\infty} - DPn_t)$ against time for the polymerisation of δ -valerolactone in toluene at 25°C | 259 |
| Figure 5.21. | Graph of apparent rate of propagation versus initiator concentration for the polymerisation of δ -valerolactone in DCM, THF and toluene | 261 |
| Figure 5.22. | Dependence of structure of propagating species on solvent polarity | 261 |
| Figure 5.23. | Structure of THF and δ -valerolactone | 263 |

| | | |
|------------------|--------------------------------------------------------------------------------------------------------------------------------------------------------------------------------------|-----|
| Figure 5.24. | Solvation of alkyl aluminium alkoxide by THF and lactone | 264 |
| Figure 5.25. | Effect of solvent on plot of $-\ln k_p$ versus $-\ln[I]_0$ for the polymerisation of δ -valerolactone using diisobutyl aluminium isopropoxide in toluene, THF and DCM at 25°C | 265 |
| Figure 5.26. | Graph of apparent rate constant of propagation for the polymerisation of ϵ -caprolactone and δ -valerolactone in toluene, DCM and THF | 266 |
| | | |
| Chapter 6 | | |
| Figure 6.1. | Formation of macroinitiator | 269 |
| Figure 6.2. | Formation of triblock co-polymers using aluminium alkoxide macroinitiator | 270 |
| Figure 6.3. | Effect of volume of ϵ -caprolactone added on molecular weight of co-polymers | 272 |
| Figure 6.4. | Structure of PHBV-PCL co-polymer and numbers used in NMR labels | 273 |
| Figure 6.5. | ^1H NMR spectrum of PCL-PHBV-PCL co-polymer | 273 |
| Figure 6.6. | Expansion of methylene protons adjacent to acyl oxygen in poly(ϵ -caprolactone) segment | 274 |
| Figure 6.7. | Expansion of 0.9 ppm - 1.70 ppm area of ^1H NMR of PCL-PHBV-PCL co-polymer | 275 |
| Figure 6.8. | ^1H NMR of PHBV-PCL co-polymer, proton on tertiary carbon resonance | 276 |
| Figure 6.9. | ^1H NMR spectrum of PCL-PHBV-PCL co-polymer. | 277 |
| Figure 6.10. | Plot of molecular weight of co-polymer against ϵ -caprolactone added. | 278 |
| Figure 6.11. | PHBV-PCL co-polymer structure | 279 |
| Figure 6.12. | ^{13}C NMR spectra of PCL-PHBV-PCL co-polymer | 279 |
| Figure 6.13. | Close up of carbonyl peaks in ^{13}C NMR spectra of PHBV-PCL block co-polymers. | 280 |
| Figure 6.14. | Plot of molecular weight of PHBV-PCL co-polymer against volume of aluminium alkyl. | 282 |

List of abbreviations.

| Abbreviation | Full name |
|-------------------|----------------------------------------------------------------------|
| [A*] | concentration of active species |
| AcAc | acetyl acetone |
| AIBN | azobisisobutyronitrile |
| ATRP | atom transfer radical polymerisation |
| BIOPOL | trade name for PHBV |
| [CL] ₀ | initial monomer concentration |
| DCM | dichloromethane |
| ΔG_p | Gibbs free energy of polymerisation |
| ΔH_p | Enthalpy of polymerisation |
| ΔS_p | Entropy of polymerisation |
| DMEDA | Dimethylethylethylenediamine |
| DMF | N,N'-dimethylformamide |
| DP _n | degree of polymerisation |
| DTBP | di- <i>tert</i> -butyl peroxide |
| GPC | gel permeation chromatography |
| HPLC | high performance liquid chromatography |
| K | Mark-Houwink parameter |
| η | intrinsic viscosity of a polymer in a solvent at a given temperature |
| k_b | rate constant of back biting |
| k_p | rate constant of propagation |
| MDO | 2-methylene-1,3-dioxepane |
| [M] ₀ | monomer concentration at time = 0 |
| [M] _t | monomer concentration at time = t |
| M_n | number average molecular weight |
| M_w | weight average molecular weight |
| M_w/M_n | molecular weight distribution, polydispersity |

| | |
|-------------|----------------------------------------------------|
| N_i | weight of molecules with molecular weight N_i |
| NMR | nuclear magnetic resonance |
| n_{OR}/Al | number of active alkoxide sites per aluminium atom |
| PCL | poly(ϵ - ϵ -caprolactone) |
| PHB | poly(hydroxybutyrate) |
| PHBV | poly(hydroxybutyrate-co-hydroxyvalerate) |
| PHV | poly(hydroxyvalerate) |
| ROP | ring opening polymerisation |
| T | temperature |
| T_g | glass transition temperature |
| THF | tetrahydrofuran |
| V_r | retention volume |
| W_i | weight of molecules with molecular weight M_i |
| v | Mark-Houwink parameter |

Aims and objectives.

The aim of the project is to synthesise biodegradable co-polymers of poly(hydroxybutyrate-co-valerate) and poly(ϵ -caprolactone). Poly(hydroxybutyrate-co-valerate) and poly(ϵ -caprolactone) are in general immiscible in blends with greater than 10-15% poly(ϵ -caprolactone). Therefore a compatibiliser is needed to prevent phase separation. A co-polymer of poly(hydroxybutyrate-co-valerate) and poly(ϵ -caprolactone) would be suitable for this task. The molecular weight of the co-polymer needs to be controlled and predictable for the compatibiliser to be effective. In order to achieve this aim the mechanism of the polymerisation needs to be fully understood. It is proposed that a series of polymerisations of homo-polymerisations of ϵ -caprolactone should elucidate the mechanism of the polymerisation and any factors which effect the properties of the polymers produced. Reaction temperature, medium, monomer and initiator type and structure will all be varied in an attempt to gain an understanding of the reaction mechanism. Once the mechanism and any influencing factors have been identified then a method of producing controlled co-polymers should be clear.

Chapter 1.

Introduction.

1.1 Biodegradable polymers.

In recent years considerable interest has been shown towards the use and development of biodegradable plastics for a variety of applications. As the use of polymers in packaging and other commodities has increased, so attempts to solve the problems associated with their disposal has increased the demand for biodegradable plastics.⁽¹⁻⁵⁾ Indeed, plastic waste totals around 6% by weight of Western European municipal waste but around 20-25% of waste by volume.⁽⁶⁾ The largest component by far of municipal waste is paper, but because plastic materials have lower densities than paper they therefore they occupy a greater volume and have a far higher impact on the environment. If this large volume of waste could be lowered by the use of biodegradable plastics, then harm to the environment could be minimised. The current interest in biodegradable polymers has also been initiated by constantly changing legislation and through an increasing environmental consciousness on the part of the public.

1.1.1. Applications of biodegradable polymers⁽⁷⁾

1.1.1.1. Medical applications.

A great deal of attention has also been paid towards developing degradable polymers for use in medical applications. Polymers which are to be used in a biomedical context must be tailored to meet a number of specific and important requirements. If tissue irritation is to be minimised then the polymer should be soft and pliable. This means that the polymer must have little or no crystallinity and a glass transition temperature below body temperature. The material used must be totally compatible with the body, including of course the degradation products which must also be non toxic.⁽⁸⁾

The main applications for such polymers include:

1.1.1.2. Surgical sutures⁽⁹⁾

Severe tissue damage such as a deep laceration or a bone fracture may be incapable of unassisted healing. Sutures may hold the tissue together until the healing is completed naturally. Degradable sutures are designed to degrade once healing is complete, eliminating the need for surgical removal at a later date.

1.1.1.3. Tissue adhesion prevention

Temporary barriers can be used to prevent tissue adhesion after surgery.

1.1.1.4. Bone fixation devices⁽¹⁰⁾

Since bone is much weaker than the metal devices which are commonly used to hold fractured bones in place, the premature removal of such implants can considerably weaken the bone resulting in a re-fracture. Thus biodegradable implants

can meet the requirements of a support during the process of bone healing and will disappear completely after a few months when the injury has healed. This eliminates the need for further surgery to remove a metal implant possibly causing further tissue damage and trauma.

1.1.1.5. Drug delivery systems⁽¹¹⁾

Controlled release drug delivery devices are designed to limit or slow the rate of drug release relative to the rate offered by fast release systems such as tablets or capsules containing the same drug. Originally, some studies into the sustained release of drugs from implanted devices centred on the use of materials based on silicone rubber. However because of the lack of degradability of these polymers, they have to be surgically removed if potential future health problems are to be eliminated.⁽¹²⁾ The use of biodegradable implants ensures that the concentration of the drug remains constant in the body, and thus remaining above therapeutic levels

Synthetic polymers have been studied for use as biodegradable, controlled drug release devices. With only a few exceptions, the most suitable method for achieving this delayed drug release is via the use of biodegradable polymers that slowly degrade, erode, or dissolve.⁽¹³⁾ Aliphatic poly(esters) are widely used as synthetic polymeric biomaterials in the medical field with poly(hydroxyacids) in particular having many important applications as biodegradable polymers. Their primary function in the biomedical context is controlling the release of the drug in a predictable manner by the progressive erosion of the polymer backbone. The chemical and physical properties of these polymers can be carefully altered by selecting the repeat units.⁽¹²⁾ Therefore the rate of degradation and other properties of the polymer may be suited to purpose by the use of co-polymers as these may often offer properties intermediate to those of the corresponding homo-polymers.

1.1.1.6. Agricultural applications

Degradable materials are also of interest in agriculture as mulches and plant containers. Mulches allow growers to use synthetic films in order to aid plant growth. The mulches then degrade, avoiding the cost of removing the protective layer. The aim of these is often to conserve moisture and control the temperature, helping to reduce weed and insect infestation and thus increasing the rate of growth. Common polymers used in such applications include poly(vinyl alcohol) and poly(vinyl chloride) blended with starch.⁽⁷⁾

1.1.1.7. Packaging applications.

The properties required of a material for use in food packaging depend upon the environment in which the product will be used. Food which is to be kept frozen requires different materials from those which need to be placed in the oven. Materials based on poly(hydroxybutyrate) (PHB) for example are susceptible to bacteriological attack and may be unsuitable for some food packaging applications.

1.1.2. Examples of biodegradable polymers.

There are a number of broad classes available for summarising the types of polymers which may be described as biodegradable. Degradable polymers may be produced by either synthetic or natural methods. Natural biodegradable polymers are commonly synthesised by enzyme catalysed chain growth polymerisations within plant cells. A few examples of both natural and biodegradable polymers are shown in the table below:

| Type | Comments | Example |
|-----------------|------------------------------------------------------------|----------------------------------------------------|
| Polyester | Most widely used, formed by a number of different methods. | Polyester Polylactones Polyhydroxyalkanoates |
| Polyamides | Structurally modified only | Hydroxylated nylon |
| Polyurethanes | Structurally modified only | Hydrophilic ether urethanes |
| Polypeptides | Natural | Polyaminoacids |
| Polysaccharides | Natural origin | Dextran |
| Proteins | Natural origin | Collagen, gelatin |

Table 1.1. Common biodegradable polymers.⁽¹⁴⁾

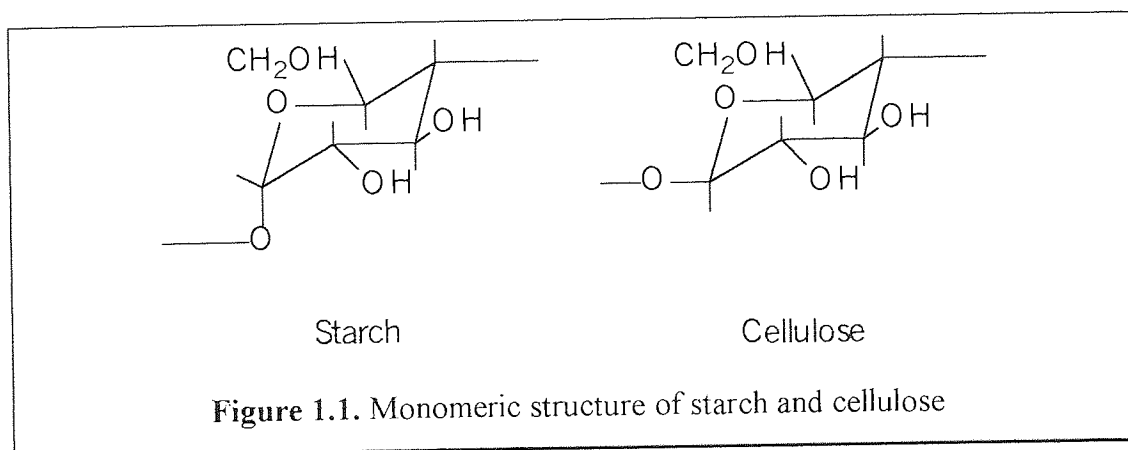
1.1.3. Natural biodegradable polymers.⁽⁷⁾

1.1.3.1. Poly(peptides) and proteins.

Such materials are commonly used in the form in which they are found in nature. Gelatin an animal protein is a water soluble, biodegradable polymer which is extensively used in pharmaceutical and biomedical applications.⁽¹⁵⁾

1.1.3.2. Poly(saccharides).

The most common of these materials are cellulose and starch. Both are composed of D-glucopyranoside units linked together by acetal bonds. (see below)



1.1.3.3. Starch

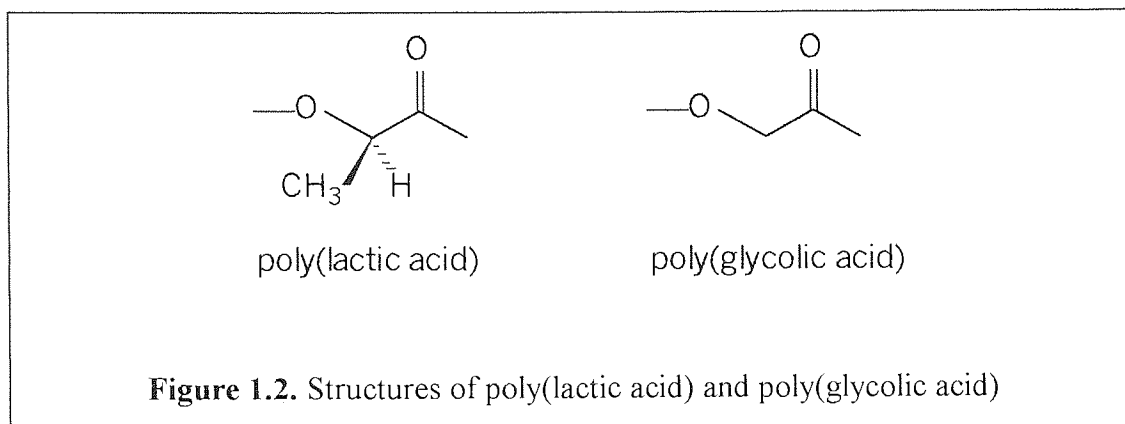
Starch is a polymer which occurs widely in plants such as potatoes, rice and corn. It is a polymer of glucose in which the monosaccharide units are linked via the 1,4'- α -glycoside bonds. Starch can be separated into two fractions, amylose (20%) and amylopectin (80%).⁽¹⁶⁾ Amylopectin has a more complex structure involving via 1,6'- α -glycoside branches, it has a cross linked structure which is attacked by glucosidases.

1.1.3.4. Cellulose

Cellulose consists of one repeat unit, namely D-glucose linked via 1,4'- β -glycoside bonds in a very large polymer chain (see figure 1.1) as in the disaccharide compound, cellobiose. It is highly crystalline and is used in nature as a structural material to impart rigidity to plants. Cellulose is also insoluble in all common solvents. Cellulose is often processed and used as a derivative such as cellulose acetate, which is commercially known as acetate rayon.⁽¹⁶⁾

1.1.4. Synthetic biodegradable polymers

1.1.4.1. Poly(α -hydroxy acids), poly(lactic acid) and poly(glycolic acid).

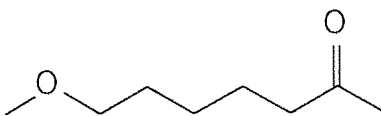


The most commonly used synthetic, biodegradable polymers are poly(lactic acid) and poly(glycolic acid).⁽¹⁷⁾ These two polymers and their co-polymers are used in a variety of medical applications. PLA and PGA degrade slowly by hydrolysis and the degradation products are non toxic, *l*-lactic acid and glycolic acid are found endogenously and *d*-lactic acid is eliminated from the body. PGA for example, is completely absorbed within two to three months of implantation. The lactic acid generated by the hydrolysis of poly(lactic acid) is incorporated into the tricarboxylic acid cycle and is then excreted as carbon dioxide and water.⁽¹⁸⁾ These properties make poly(lactic acid) and poly(glycolic acid) biocompatible and hence they exhibit little or no local toxicity on administration into the body. For use in pharmaceutical applications however, poly(lactic acid) is often unsuitable because the rate of degradation is too slow. Co-polyesters of poly(lactic acid) and poly(glycolic acid) are therefore the most widely used resorbable materials for drug delivery systems.⁽¹⁹⁾ The degradation rate of poly(glycolic acid) is faster because the ester groups of the glycolic acid units are more sensitive to hydrolysis and the degradation of PGA is therefore faster than the degradation of PLA. This results in a polymer which has properties that are more useful for controlled drug release devices. However if too much glycolic acid, i.e. more than 50%, is added, then the resulting co-polymer has

blocks of glycolic acid which render the co-polyester insoluble in common solvents.⁽²⁰⁾

The mechanical characteristics and the degradation rate of PLA depend on the configuration of the lactic acid used. Since lactic acid has a chiral carbon atom, (L), (D) and (DL) configurations are available. The polymeric (L) and (D) stereoisomers are crystalline whilst the racemic form is largely amorphous.

1.1.4.2. Poly(ϵ -caprolactone).



poly(ϵ -caprolactone)

Figure 1.3. Structure of poly(ϵ -caprolactone).

As an alternative to PLA and PGA homo and co-polymers, poly(ϵ -caprolactone) (PCL) degrades slower and is more useful for devices with a desired life time of one to two years.⁽¹¹⁾ Poly(ϵ -caprolactone) is useful for applications such as the controlled release of contraceptive drugs where a minimum useable life of between six and twelve months is desirable although uses of over twelve months are more common. Copolymers of PCL with PLA reduce the useable life of a poly(ϵ -caprolactone) controlled release device, making it more suitable when a lifespan of less than one year is desirable⁽²¹⁾

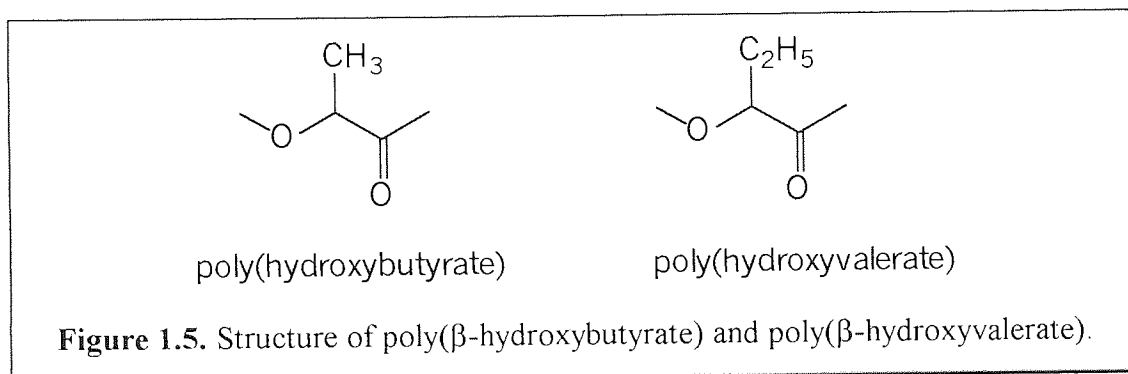
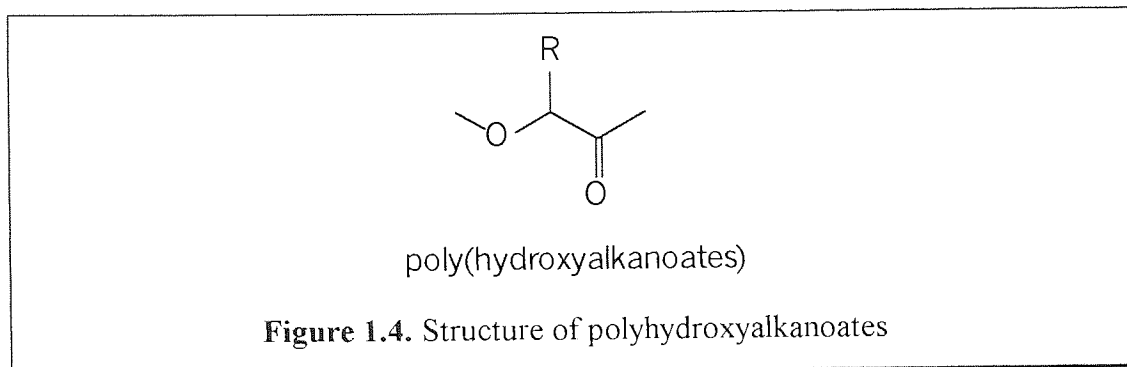
Poly(ϵ -caprolactone) can be produced with varying molecular weights by a range of catalysts. It can also be co-polymerised with a vast range of other monomers such as lactide and glycolide to produce biodegradable polymers with the desired degradation time and properties.

Amongst poly(esters), which are the most common family of biodegradable polymers, poly(ϵ -caprolactone) occupies a unique position since it is at the same time biodegradable and miscible with a large variety of polymers.⁽²²⁾ Synthetic polymers such as poly(ϵ -caprolactone) can be immiscible in a blend with naturally occurring polymers such as poly(β -hydroxybutyrate). The poor interfacial adhesion in the blends of such polymers results in inferior mechanical properties. Block co-polymers are often used in non-reactive blending, the constituents are blended in the presence of preformed block or graft co-polymers which act as compatibilisers.⁽²³⁾

Poly(ϵ -caprolactone) itself is a semi crystalline polymer with a melting point of approximately 60°C and it has a glass transition temperature of -60°C. High molecular weight poly(ϵ -caprolactone) may be classed as a tough, crystalline polymer with a moderate melting point. The crystallinity of poly(ϵ -caprolactone) varies with its molecular weight and for molecular weights of 100000 and greater the crystallinity is around 40%. When the molecular weight is lowered to 5000, the percentage of crystallinity increases to around 80%. Since the degree of crystallinity is vital in considering the rate of degradation, it can be seen that the molecular weight of a polymer will affect degradation.

Poly(ϵ -caprolactone) is soluble in a wide range of solvents at room temperature. Amongst others it is soluble in THF, chloroform, DCM, benzene, toluene and carbon tetrachloride

1.1.4.3. Poly(hydroxyalkanoates)-poly(β -hydroxybutyrate) (PHB), poly(β -hydroxyvalerate) (PHV) and PHBV co-polymers.



Poly(β -hydroxyalkanoates) are another widely used types of biodegradable polymer and this group of materials includes poly(β -hydroxybutyrate) and its co-polymers with β -hydroxyvalerate. The alkyl side groups are methyl for β -hydroxybutyrate units and ethyl for β -hydroxyvalerate units. Poly(esters) with longer alkyl substituents, up to heptyl and above, can be produced using a range of bacteria.⁽⁷⁾ PHBV co-polymers, produced commercially by Monsanto as BIOPOL, are especially useful in packaging applications. PHB is a crystalline thermoplastic with a melting point in the range 160-180°C depending on the molecular weight of the sample.⁽²⁴⁾ The glass transition temperature of PHB and PHBV co-polymers have been reported to be in the range -5 to +20°C, appearing to be independent of copolymer composition but more dependent on the thermal history of the sample.⁽²⁵⁾ PHB has a Tg in the region of +5°C and a melting point of 180°C. These properties

combine with a high degree of crystallinity to make PHB very brittle. In order to overcome this co-polymers are formed, commonly with PHV which can produce more useable materials.

Poly(β -hydroxybutyrate) a naturally occurring polyester produced by bacteria, is known to be a biodegradable polymer. The homopolymer PHB is produced in nature by a wide range of microorganisms to store carbon and energy. Bacterially produced PHB and PHBV are considered to be genuinely biodegradable materials because their corresponding rates of chemical hydrolysis are very slow.⁽²⁶⁾ Indeed the rate is so slow that it was previously thought that they were inert to chemical hydrolysis.⁽²⁷⁾ However, adding microorganisms to such polymers leads to their rapid degradation into water and carbon dioxide.⁽²⁸⁾ Microbially produced polymers have an advantage over synthetic polymers in that if the extraction from the organism is efficient, then there are none of the potentially toxic catalyst residues remaining that may be present if synthetic polymers are used. However such polymers and especially PHB homopolymer tend to exhibit a brittleness that develops during storage at room temperature and thus limits the range of possible uses.⁽²⁹⁾ This phenomenon is probably due to morphological changes. It has been reported that PHB, which has been stored at room temperature for a few weeks, is less soluble in chloroform than its freshly synthesised counterpart. It would seem therefore that the crystallinity of PHB increases in order to enhance its stability. The polymer can be returned to its amorphous state by heating in boiling chloroform. Reported uses of PHB in pharmaceutical applications are apparently limited but that is not to say that PHB or its copolymers are not useful in the preparation of sustained release devices.

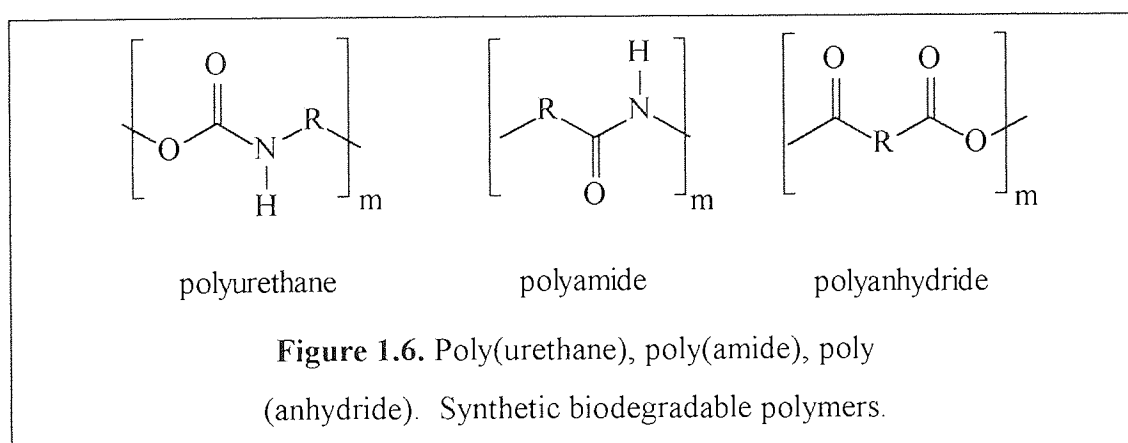
'BIOPOL' copolyesters are produced by a two stage fermentation process. 'BIOPOL is compostable, renewable and recyclable and therefore offers additional options alongside established techniques for waste management. In order to overcome some of the problems associated with bacterial PHB, e.g. high melting point, both PHB and PHBV can be synthesised synthetically.⁽³⁰⁾ The physical

properties and biodegradation rate of 'BIOPOL' depend upon factors including the amount of hydroxy valerate in the polymer, molecular weight, degree of crystallinity, surface area and the environment in which it is placed.⁽³¹⁾ Applications for PHB and PHBV for packaging have been limited however because of their high cost relative to commodity plastics such as poly(ethylene). A viable option to overcome such high costs is to produce blends of PHBV with other polymers such as cellulose acetate butyrate (CAB) which can lower the price significantly.⁽³²⁾

Although the properties of PHB can be varied by the inclusion of hydroxy valerate, the extent to which the properties may be modified is limited and the use of blending techniques is valuable. Polymer blends, such as PHB and PCL are commonly incompatible. Useful physical properties such as modulus, tensile strength, impact strength and permeability may be adversely affected by incompatibility in a polymer blend. A common method of altering the physical properties of a polymer blend is to use a plasticiser such as dialkyl phthalates or aliphatic esters, although these materials may present toxicity problems in a biomedical context.⁽³³⁾ Poly(ϵ -caprolactone) has been used as a polymeric plasticiser to alter the physical properties of polymers.

1.1.4.4. Other synthetic biodegradable polyesters.

Modified polyurethanes, polyamides and polyanhydrides may be used as biodegradable polymers.



Poly(amides) contain the same amide linkage as proteins yet their rates of degradation are so slow that they are often reported to be non-degradable.⁽⁷⁾ The introduction of pendant substituents decreases crystallinity and improves the rate of degradation.

Polyanhydrides have two sites available to degradation via hydrolysis.

1.1.5. Definition of biodegradation.

There is a lack of a common consensus on a definition of biodegradation. Many have attempted to define it and a summary of what biodegradation is may be as follows. *Biodegradation is the natural process by which organic chemicals such as polymers are converted to smaller, simpler compounds by the action of enzymes and/or chemical decomposition. The process can be chemical in nature, by oxidation or hydrolysis, or a biological degradation catalysed by enzymes. The chemical process is homogeneous in nature, taking place throughout the amorphous regions of the structure. The attack by enzymes takes place initially on the polymer surface only.*

However, the true biodegradability of many of these polymers can be brought into question. Poly(lactic acid) and poly(glycolic) acid are known to degrade into their respective acids, which, if used in implantable devices are excreted from the body via the Krebs's cycle as water and carbon dioxide. It can be said that a truly biodegradable plastic will undergo disassembly to CO₂ and biomass in a composting infrastructure leaving no persistent or toxic residue.

Other terms such as 'bioerosion' can confuse the issue over what biodegradation actually is. Bioerosion requires an actual loss from the polymer which can be affected by a range of properties that cannot always be specified due to their complex nature. Phrases such as bioadsorbable and bioresorbable refer to the material and its degradation within the body.⁽³⁴⁾

A number of standards authorities have attempted to produce definitions for biodegradable plastics, which are listed below.⁽⁷⁾

ISO 472: 1998. A plastic designed to undergo a significant change in its chemical structure under specific environmental conditions resulting in a loss of some properties that may vary as measured by standard test methods appropriate to the plastics and application in a period of time that determines its classification. The change in chemical structure results from the action of naturally occurring micro-organisms.

ASTM sub committee D20.96 proposal. Degradable plastics are plastic materials that undergo bond scission in the backbone of a polymer through chemical, biological and/or physical forces in the environment at a rate which leads to fragmentation or disintegration of the plastics.

Japanese Biodegradable Plastic Society.⁽³⁵⁾ Biodegradable plastics are polymeric materials which are changed into lower molecular weight compounds where at least one step in the degradation process is through metabolism in the presence of naturally occurring organisms.

DIN 103.2 working group on biodegradable polymers. Biodegradation of a plastic material is a process leading to naturally occurring end products.

1.1.6. Effect of polymer structure on biodegradation.

The structure of a polymer affects its biodegradability and not all polymers therefore are biodegradable. Since natural macromolecules such as starch, cellulose and proteins are generally degraded in biological systems by hydrolysis followed by oxidation, it is not surprising that most of the reported synthetic biodegradable polymers also have a hydrolysable link. One of the most striking features of a comprehensive list of biodegradable polymers is the over-whelming number of esters and ester derivatives that have been exploited as biodegradable materials because of the presence of a hydrolytically labile ester bond. Heterochain polymers, and in particular those containing oxygen and/or nitrogen atoms in the main chain such as amide, enamine, ester, urea, and urethane are all susceptible to hydrolysis.⁽³⁶⁾ However, since most of these polymers are hydrophobic, hydrolysis, even where it is possible, proceeds slowly.⁽³⁷⁾ Factors which affect the degradation rate, include hydrolysable links along the polymer backbone, electronic and steric effects, morphology, molecular weight and physical properties such as Tg.

Since most of the enzyme catalysed reactions occur in an aqueous media, the balance between the hydrophobic and hydrophilic nature of the polymer affects its biodegradability. A polymer that contains both hydrophobic and hydrophilic segments appears to biodegrade faster than polymers that contain hydrophobic segments only.

In order for a synthetic polymer to be susceptible to enzymatic degradation, the polymer chain must be flexible enough to fit into the active site of the enzyme. Thus more rigid polymers are often considered to be inert to biodegradation.

1.1.6.1. Morphology.

Polyesters in particular have two distinct biodegradation phases. The first is diffusion of water into the amorphous regions of the polymer matrix and then this is

followed by random hydrolytic chain scission. The second stage begins when the majority of the amorphous regions have been eroded and hydrolysis is then associated with the crystalline regions of the polymer. The degree of crystallinity of the polymer therefore increases as degradation proceeds. It would appear that amorphous polymers are therefore more suited to applications as biodegradable polymers than those which have a higher degree of crystallinity. Indeed the rate of biodegradation of 'BIOPOL' has been found to increase with decreasing degree of crystallinity and this effect has also been observed in other polyesters.⁽³⁸⁾

Proteins, unlike synthetic polymers do not have regular repeating units along the polymer backbone and this irregularity leads to a decreased tendency to crystallise. This fact assists biodegradation by making the hydrolysable sites accessible to enzymes, a property which many synthetic polymers do not possess. It also may be reasonable to say therefore that polymers with long and irregular repeat units are less likely to crystallise and hence may be biodegradable.

1.1.6.2. Glass transition temperature.

Since biodegradation depends largely upon diffusion of water into the polymer matrix, the glass transition temperature (T_g) of the polymer is important. A polymer above its T_g is likely to be flexible and hence water will be able to diffuse into the polymer easier. Hydrolysis of the labile bonds will therefore take place more quickly than in a polymer below its T_g .

The T_g of poly(ϵ -caprolactone) samples can be altered by co-polymerisation. The T_g of co-polymers can be estimated using the Fox equation:

$$(1/T_g)_{12} = (W_1/T_{g1})_1 + (W_2/T_{g2})_2 \quad 1.1.$$

Where W_1 and W_2 refer to the mass fractions of monomers 1 and 2.

Only those polymers with a T_g below body temperature are in a rubbery state and exhibit a high permeability. This becomes evident as a comparison of the permeability of PLA with co-polymers of increasing poly(ϵ -caprolactone) content.

1.1.6.3. Effect of polymer structure and molecular weight.

It is apparent that synthetic polymers are generally biodegradable to different extents depending on chain coupling (ester > ether > amide > urethane) and molecular weight (lower > higher).

There have been many studies on the effect of molecular weight on the biodegradation of plastic materials.⁽⁷⁾ Many of the differences observed are so small as to be negligible. Plastics however do remain relatively immune to microbial attack as long as the molecular weight remains high. Despite this it has been found that the crystallinity of poly(ϵ -caprolactone) varies with its molecular weight and for molecular weights of 100000 and greater the crystallinity is around 40%. When the molecular weight is lowered to 5000, the percentage of crystallinity increases to around 80%. Since the degree of crystallinity is vital in considering the rate of degradation, it can be seen that the molecular weight of a polymer will affect its degradation.

The hydrophobic/hydrophilic nature of the polymer will also affect the rate of degradation of a polymer sample. It has been stated that the degradation of hydrophilic polymers is faster than that of hydrophobic ones. However as a rider it is important to note that if a polymer is water soluble, then that should not be taken to mean that it is biodegradable.⁽³⁹⁾ Considering the case of PLA and PGA, the ester groups of PGA are more sensitive to degradation than those of PLA. The rate of hydrolysis of PGA is faster than that for PLA therefore. The same can be said when comparing poly(α -hydroxy acids) and poly(ϵ -caprolactone). Poly(ϵ -caprolactone) with its longer alkyl chain is more hydrophobic than PLA and PGA and the rate of degradation is known to be much slower.

1.2. Polymerisation reactions.

1.2.1. Introduction.

The formation of polymers can be classified into two different mechanisms, condensation (step growth) and chain growth (addition) reactions, a distinction depending both upon the mechanism of the reaction, and the polymerisation product. This distinction was first made by Carothers and co-workers in the late 1920's.⁽⁴⁰⁾

Step growth polymers, which include poly(esters) and poly(amides) are formed from polyfunctional molecules which have been reacted together with the elimination of a small molecule such as water but which can also be ammonia, hydrogen chloride or carbon dioxide. Step growth polymerisation however does not necessarily always involve the loss of a small molecule. Poly(urethanes) for example may be formed by the reaction of a diisocyanate with a diol, a reaction which does not involve the elimination of any molecule. This reaction is made possible because of the highly electrophilic nature of the carbon atom in the isocyanate.⁽⁴¹⁾ A typical example of a step growth reaction would be the polyesterification reaction involving a diol and a diacid.

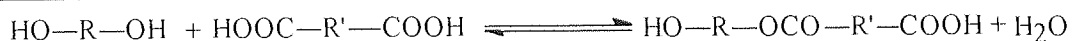


Figure 1.7. Poly condensation of diacid and diol

Should the water be removed as it is produced, then no equilibrium is established and the reaction proceeds until long polymer chains are formed. The formation of polymers of high molecular weight is therefore difficult using step growth reactions. Such reactions are often carried out at high temperatures in order to facilitate both fast reaction times and to aid the removal of the small molecule produced (H₂O in this example). To achieve the high molecular weights which are synonymous with high conversions then the equilibrium in fig 1.7. must be displaced

towards the right (the polymer). This is commonly achieved by a decrease in the pressure of the reaction system which may however result in the loss of a small amount of reactants.

When Flory analysed the kinetics of step growth reactions, he assumed that the functional groups present in the monomeric and polymeric species are both equally reactive. Thus monomer is equally likely to react with both monomer and polymer. Carothers set forth a relationship between the degree of polymerisation and the extent of the reaction which is known as the *Carothers equation*. The number of repeat units of the polymer is equal to the number of bifunctional monomers present at the start of the reaction. The number average degree of polymerisation (DP_n) is defined therefore as the average number of repeat units per polymer chain and is given as total number of monomer molecules present divided by the number present at time t ;

$$DP_n = [M]_t/[M]_0 = N_t/N_0 \quad 1.2.$$

where N_t = Number molecules at time, t .

If we combine this with an equation for the extent of the reaction p ,

$$[M]_t = [M]_0 - [M]_0 p = [M]_0(1-p) \quad 1.3.$$

or

$$N_t = N_0(1-p)$$

then we can see that

$$\begin{aligned} DP_n &= N_0/N_0(1-p) & 1.4. \\ &= 1/(1-p) \end{aligned}$$

Equation 1.4. $1/(1-p)$ is the *Carothers equation* and is valid for the step growth reaction of two difunctional molecules. Using this equation it can be seen that the degree of polymerisation is dependent on the extent of the reaction. If $p = 0.9$, (i.e. 90% conversion), then $DP_n = 10$ and when $p = 0.99$, (i.e. 99% conversion), then $DP_n = 100$. Thus as the reaction proceeds, the rate of increase of DP_n with time decreases. From this it can be deduced that for high molecular weights to be formed then unpractically long reaction times are required. In order to produce a polymer of a desired molecular weight, the reaction must be stopped at a certain time and hence a certain value of p . In order to do this accurately, the amounts of each reactant in the mixture must be carefully controlled. An accurately controlled stoichiometric imbalance of reactants can also be used in order to produce a polymer of the desired molecular weight.

Chain growth polymerisations proceed via the successive addition of a monomer to a growing polymer chain end. The growth at this active centre leads to the formation of a macromolecule in which propagation continues until termination, which may be either via transfer reaction or a terminating agent. Chain growth polymerisation proceeds with at least three distinct reactions, initiation where the active centre is formed, propagation, which is a series of identical events, namely the repeated addition of a monomer unit to the active centre, and termination or transfer where the growing chain is destroyed. Unlike in the case of condensation polymerisation where the polymer is a residue of the monomer, a polymer formed by step growth polymerisation has the same composition as the monomer used.

Chain growth polymerisation itself can be divided into different classes according to the nature of the growing end. It may be an ionic species, either anionic or cationic, a free radical, or a co-ordination system such as Ziegler-Natta or metathesis systems where the monomer is bonded to the initiator or catalyst species.

1.2.2. Ring opening polymerisation.

Ring opening polymerisation can be said to bridge the gap between step growth and chain growth polymerisation mechanisms. Poly(esters), poly(ethers) and poly(carbonates) may be synthesised by both polymerisation techniques, e.g. poly condensation reactions of alcohols and acids, and by chain growth reactions such as the ring opening polymerisation of lactones, cyclic ethers and cyclic carbonates respectively. A general expression for the ring opening polymerisation is shown as the following general equation in which a cyclic molecule is opened to produce a linear polymer:

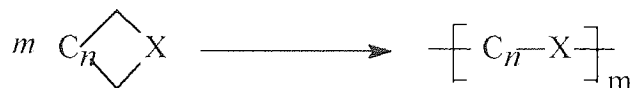


Figure 1.8. General equation for ring opening polymerisation

The functional group, X, may be one of a number of hetero atoms, such as oxygen, nitrogen, sulfur, phosphorous, silicon, a combination of two or more hetero atoms, or a functional group e.g. a vinylic bond, an ester or amide group etc. The polymers which result from the ring opening of these monomers, with the exception of cycloalkenes, possess the respective functional groups along the polymer backbone.

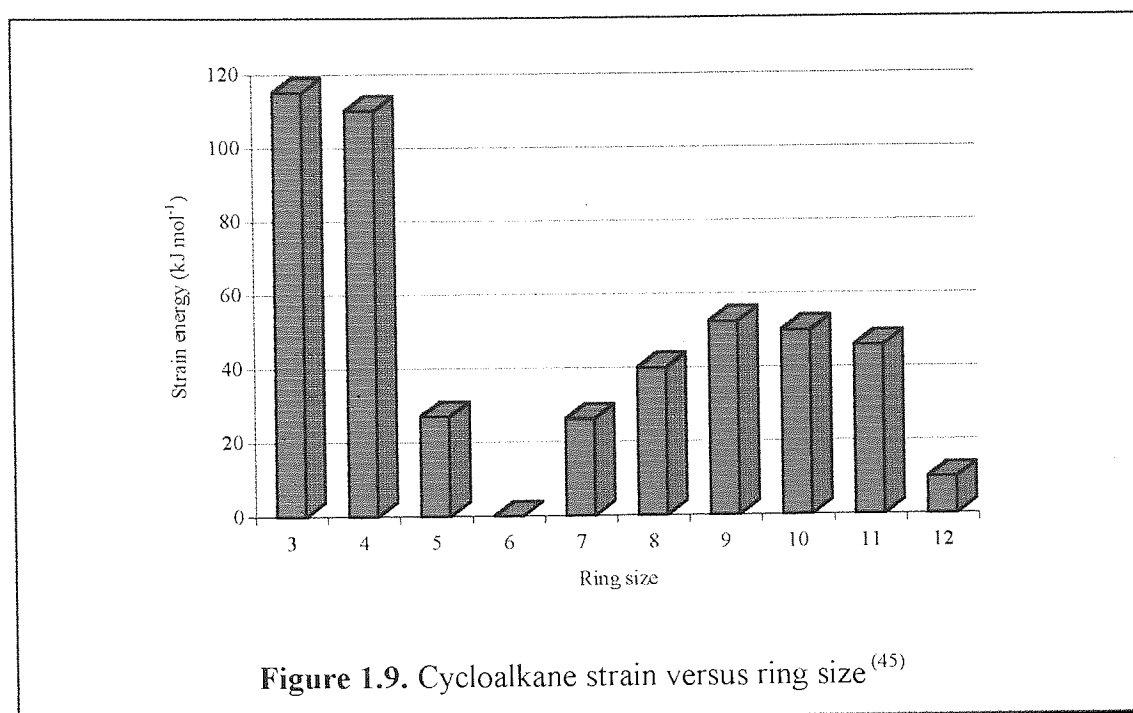
In order for the ring opening to proceed, the thermodynamics of the ring opening must be favourable⁽⁴²⁾ and therefore not all cyclic molecules are suitable for ring opening reactions. The tendency towards polymerisation of a cyclic monomer depends partly upon the existence of, and the extent of any ring strain, the reactivity of any functional groups within the ring, the polymerisation conditions and the initiator used. The primary driving force for the ring opening of small rings however, is the relief of the ring strain present. The nature of any substituents which may be present on the ring can also affect the polymerisation of cyclic monomers.

1.2.2.1 Ring strain in cyclic molecules.

It is well known that sp^3 hybridised carbon has a tetrahedral structure and that it possesses an angle between unstrained bonds of 109.5° . The concept of angle strain comes from the compression or expansion of a bond from the ideal tetrahedral angle. In cycloalkanes, the ring can pucker in order to adopt a more stable form which allows the bond angles to be as close to tetrahedral or 109.5° as possible. A greater degree of stability is attained therefore when ring strain is lower. Considering specific cycloalkanes, the three and four membered rings of cyclopropane and cyclobutane are highly strained whereas the six membered ring of cyclohexane, in its chair as opposed to boat form, is totally unstrained.

The main constituents of ring strain are bond angle strain, bond stretching or compression, repulsion between eclipsed hydrogen atoms (conformational strain, bond torsion), and non bonding interactions between substituents attached to different parts of the ring.⁽⁴³⁾ Substituents on cyclic monomers in general have a detrimental effect on the ring opening polymerisation. The polymerisation of unsubstituted caprolactam has been widely reported, whereas the substituted lactams, 3-methylcaprolactam and *N*-methylcaprolactam cannot be polymerised.⁽⁴⁴⁾ The reduced reactivity of *N*-substituted lactams is presumably due to steric hindrance at the reaction site.

A plot of ring size versus ring strain in cycloalkanes is shown below in figure 1.9. This shows the decrease in ring strain as we move from the quite highly strained three and four membered rings of cyclopropane and butane to the totally unstrained ring of cyclohexane. Larger rings are still strained although when compared to cyclopropane and butane, deviations from the normal tetrahedral bond angle of 109.5° are less and therefore ring strain is lower.



For cyclic molecules of ring size five to seven, the thermodynamic parameters upon which ring opening polymerisation depends are determined by the chemical structure of monomer.

1.2.2.2. Ring strain in lactones.

The thermodynamic polymerisability of cyclic monomers can be estimated by the change in free energy of polymerisation during ring opening. The size and nature of the ring are important factors in determining the free energy of ring opening. As was discussed in the previous section, cyclic molecules possess bond angles which differ from those in a linear molecule. The extent of the deviation from this angle is an indication of the ring strain present in the monomer. Table 1.2. shows the deviation from the *n*-ester bond angle values which are found in common lactones.

| | Ring Size | Bond angle (°) | | |
|--------------------------|-----------|----------------|--------------|--------------|
| | | C-O-(C=O) | O-(C=)-C | C-C-C |
| γ -butyrolactone | 5 | 109.0 | 110.3 | 102.1 |
| γ -valerolactone | 5 | 109.0 | 110.4 | 102.1 |
| δ -valerolactone | 6 | 121.0 | 114.9 | 113.9 |
| ϵ -caprolactone | 7 | 125.5 | 117.6 | 114.4 |
| Equilibrium value | | 109.5 | 110.0 | 110.5 |

Table 1.2. Comparison of bond angles of lactones.⁽⁴⁶⁾

It can be seen that as the size of the lactone ring increases from five to seven, that the deviation of the bond angle from the equilibrium value, i.e. that of a linear ester also increases. Comparison of this data with the values shown in the graph below, fig 1.10., show that ring strain correlates with bond angle distortion. We therefore say that the ring strain in lactones increases as ring size increase from 5 to 7.

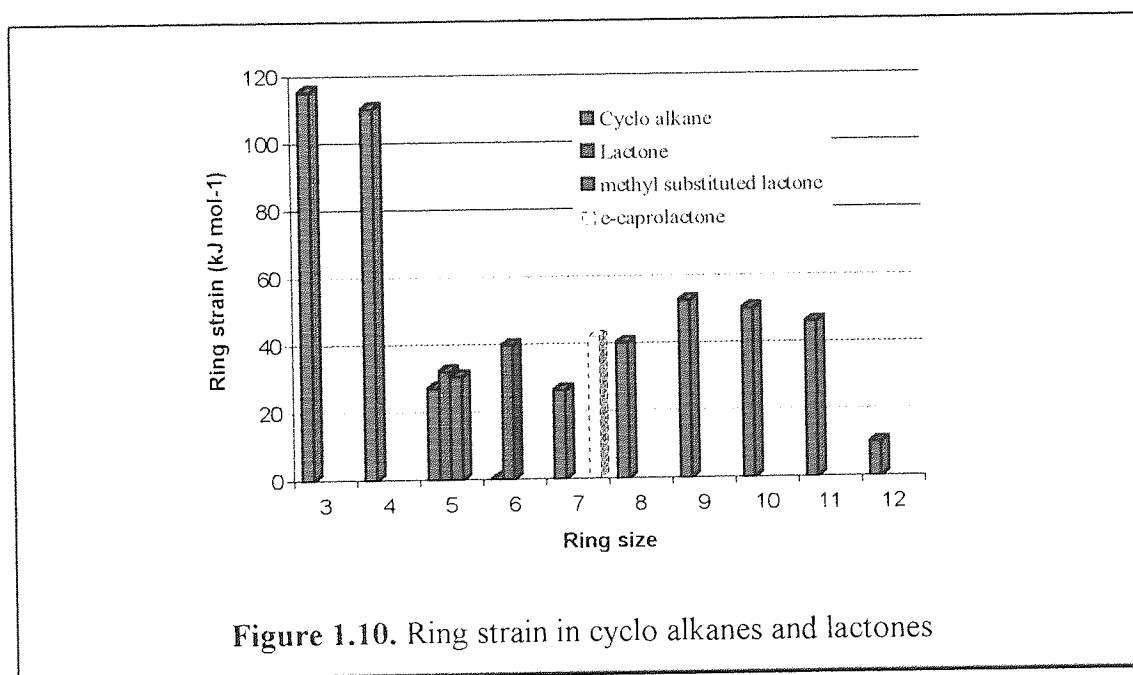


Figure 1.10. Ring strain in cyclo alkanes and lactones

The polymerisability of cyclic monomers can also be estimated by the change of free energy of polymerisation during ring opening.⁽⁴³⁾ A prerequisite for a ring opening reaction to proceed is that it has to be a thermodynamically favourable reaction. The free energy of the polymerisation is given by equation 1.5

$$\Delta G_p < 0 \text{ and } \Delta G_p = \Delta H_p - T\Delta S_p.$$

1.5.

Providing that the polymer has the same repeat unit as the monomer, then the free energy of polymerisation is independent of the polymerisation mechanism. The free energy of ring opening is however affected by the size, nature, and substituents on the ring. Values for the free energy of ring opening of lactone monomers, (ΔG_p) are shown in the table below for lactones of ring size 5, 6, and 7.

| | Ring Size | ΔG_p (kJ mol ⁻¹) |
|--------------------------|-----------|--------------------------------------|
| γ -butyrolactone | 5 | + 12.6 |
| δ -valerolactone | 6 | - 8.0 |
| ϵ -caprolactone | 7 | - 12.8 |

Table 1.3. Values of free energy of ring opening for lactones of increasing ring size.

(46)

It can be seen from this data that the ring opening polymerisation of the five membered ring γ -butyrolactone can be considered to be thermodynamically unfavourable whilst the ring opening polymerisation of δ -valerolactone and ϵ -caprolactone would appear to be favourable, a statement supported by the published literature.

In order to summarise this data on ring opening of different sized lactones, table 1.4. shows the polymerisability of lactones from β -propiolactone upwards

| Ring size | | | | | |
|-----------|---|---|---|---|----|
| 4 | 5 | 6 | 7 | 8 | 9+ |
| + | - | + | + | + | + |

Table 1.4. Polymerisability of lactones
(+ polymerises, - does not polymerise)

Thus only the five membered rings of γ -butyrolactone and γ -valerolactone are unpolymerisable.

A negative value of ΔG_p however is not necessarily an indication that a cyclic molecule will partake in ring opening polymerisation. Indeed the ΔG_p value for all cycloalkanes with the exception of cyclohexane is negative,⁽⁴³⁾ yet there is no ring opening polymerisation of any of these molecules. This is due however to a lack of any catalysts which are suitable for the ring opening of such molecules rather than an actual thermodynamic reason.

1.2.3. Ring opening polymerisation of ϵ -caprolactone and other lactones.

The polymerisation of a lactone was first reported in 1903 when Beisswenger and Fichter reported that δ -valerolactone polymerised after a short length of time.⁽⁴⁷⁾ The formation of poly(ϵ -caprolactone) via the ring opening polymerisation of a lactone was first reported by Carothers in the 1930's.⁽⁴⁸⁾ Carothers was also the first to notice that the five membered rings of γ -butyrolactone and γ -valerolactone would not polymerise.

The ring opening polymerisation of lactones does provide a convenient route to poly(esters) which is unimpeded by the long reaction times and high temperatures which are characteristic of condensation polymerisations. The polymerisation of ϵ -

caprolactone can be effected by five different mechanisms and these can be roughly divided into the following classes, anionic, cationic, co-ordination, free radical and enzymatic, which will be discussed within the next few pages. Each of these methods affords different degrees of control of polymer characteristics, namely molecular weight, molecular weight distribution, and end groups nature.

1.2.4. Anionic polymerisation

A variety of basic initiators have been used to initiate anionic polymerisation including covalent or ionic metal amides such as NaNH_2 , $\text{LiN}(\text{C}_2\text{H}_5)_2$, hydroxides, cyanides, phosphines, amines or organometallic compounds such as alkyl lithium compounds. Szwarc and co-workers⁽⁴⁹⁾ have also investigated the polymerisation of styrene using sodium naphthalenide, a radical anion. The reaction involves the transfer of an electron from the sodium to naphthalene. This radical anion then transfers an electron to a vinylic monomer such as styrene to form a styryl radical anion.

1.2.4.1. Anionic polymerisation of ϵ -caprolactone

The anionic polymerisation of ϵ -caprolactone has been widely reported. A vast number of initiator systems, over 50 in fact, have been reported to be suitable for the ring opening polymerisation of lactones. Initiation is most common with alkali metal alkyls and alcoholates such as *n*-, *s*-, *t*-butyl lithium, lithium or potassium *tert*-butoxide or lithium diisopropylamide.

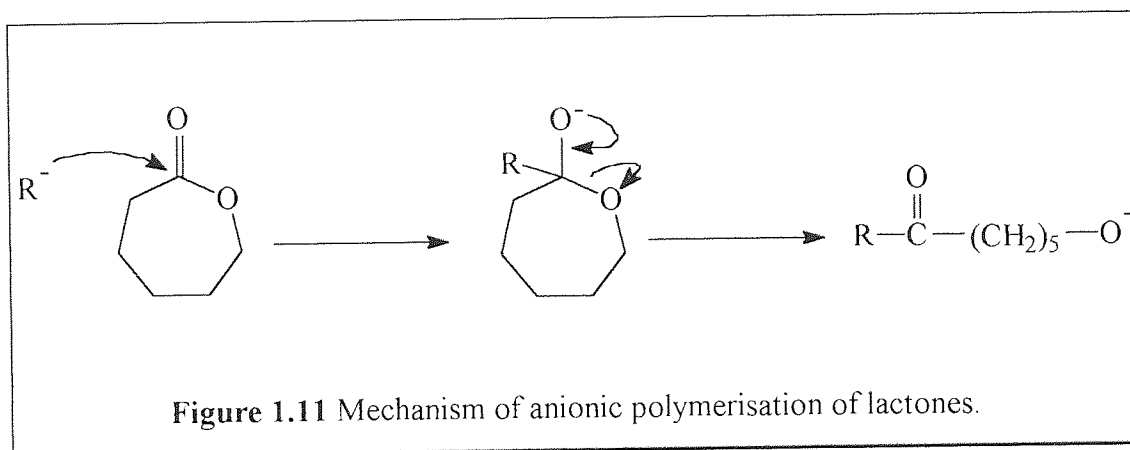


Figure 1.11 Mechanism of anionic polymerisation of lactones.

Organolithium compounds are a common method of initiating the polymerisation of ϵ -caprolactone.⁽⁵⁰⁾ Lithium *t*-butoxide⁽⁵⁰⁾, and *n*-, *s*-⁽⁵⁰⁾ and *t*-butyl lithium along with lithium diisopropylamine are all known to be suitable for the ring opening polymerisation of ϵ -caprolactone. The rate of reaction using lithium alkyl

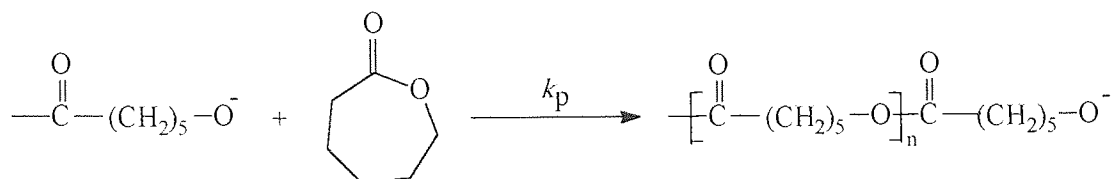
initiators is fast with quantitative conversion being achieved in less than 6 minutes. It was found by Morton and Wu⁽⁵⁰⁾ that the molecular weight distribution broadens as the reaction proceeds, indicating the presence of the transesterification reactions discussed in section 1.2.4.2. When transesterification does occur often the polymerisation proceeds with the formation of a linear polymer which is then followed by back biting reactions which break down the polymer into cyclic oligomers.⁽⁵¹⁻⁵²⁾

1.2.4.2. Inter and intra molecular transesterification reactions.

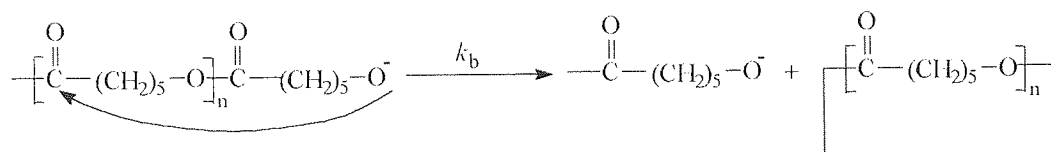
In the anionic ring opening polymerisation of lactones, chain transfer to the ester linkages on the polymer chain may take place and this is known as a 'back biting' reaction. This phenomenon was first reported by Yamashita and co-workers⁽⁵¹⁻⁵²⁾ and results in the formation of cyclic oligomers and an accompanying broadening of the molecular weight distribution of the polymer.

A mechanism for these intra and inter molecular transesterification reactions is as follows:

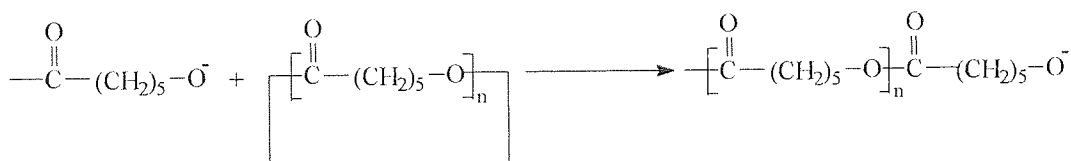
Propagation:



Intra molecular transesterification (back biting) formation of macrocycles:



This can be reversed by the reaction of a growing species and a macrocyclic polymer:



Inter molecular transesterification takes place according to the following mechanism

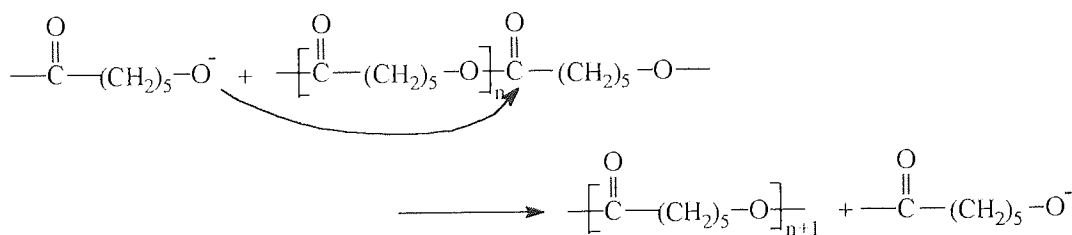


Figure 1.12. Transesterification reactions in the polymerisation of (ϵ -capro)lactone with anionic initiator species. ⁽⁵³⁾

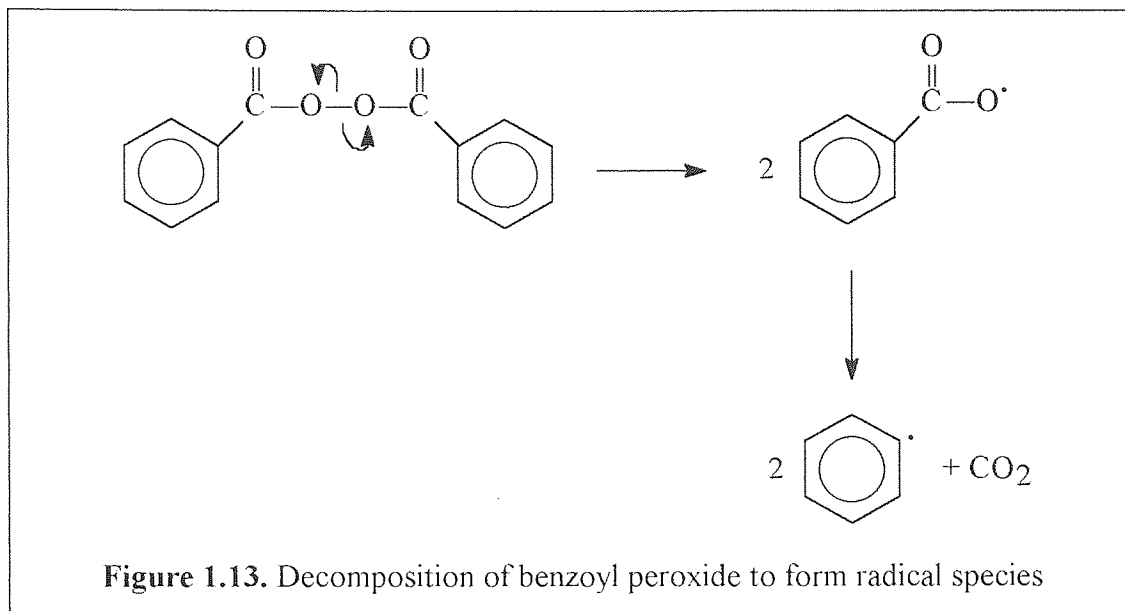
The use of pseudoanionic co-ordination systems such as aluminium alkoxides allows the polymerisation to proceed without significant formation of macrocycles. The back biting reaction and propagation are essentially two different reactions, having rate constants k_b and k_p respectively. It can be expected therefore that the formation of macrocyclic molecules should be dependent in some way on the ratio of

k_p/k_b . It can be assumed therefore that if k_p is much greater than k_b , then propagation will predominate over back biting and a linear polymer will result. Slomkowski and co-workers found that the formation of macrocycles can be kinetically suppressed by the use of initiators which produce active species with a reduced reactivity.⁽⁵⁴⁻⁵⁵⁾ Indeed the polymerisation of ϵ -caprolactone using aluminium alkoxide initiators is known to be slower than the polymerisation initiated with other anionic initiators. With an increase in the use of biodegradable poly(esters) derived from lactones in biomedical applications, the requirement for well defined linear polymers is becoming ever more important.

1.2.5. Free radical polymerisation

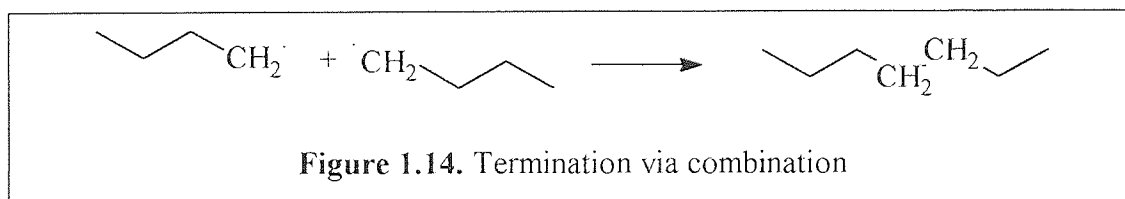
Polymerisation of unsaturated monomers may be brought about by the use of anionic, cationic or radical species. A free radical is an atomic or molecular species whose normal bonding has been modified so that an unpaired electron remains associated with the new structure.

Radical polymerisation consists of three steps, initiation, propagation and termination. Initiation comprises the formation of the radical, often by the homolytic dissociation of a species such as the thermal decomposition of benzoyl peroxide, or the photolytic degradation of AIBN (azobisisobutyronitrile). Whilst decomposition of the initiator species may be quantitative, it may be so that not all radicals will initiate chain propagation. Primary recombination may occur when two radicals combine to form an inactive species.

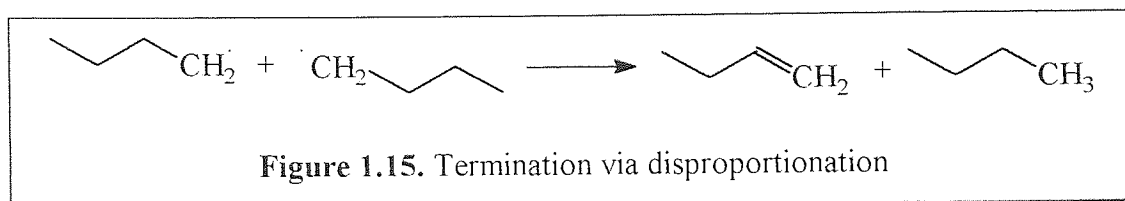


The second stage of initiation is the addition of this radical to the first monomer molecule in order to produce the chain initiating species M^{\cdot} . Propagation then proceeds via the successive addition of monomer M^{\cdot} until termination.

Propagation could continue until all monomer has been consumed but free radicals are particularly reactive species and this is likely to lead to termination. Two radicals may react with each other via combination, leading to the formation of a polymer of increased molecular weight.



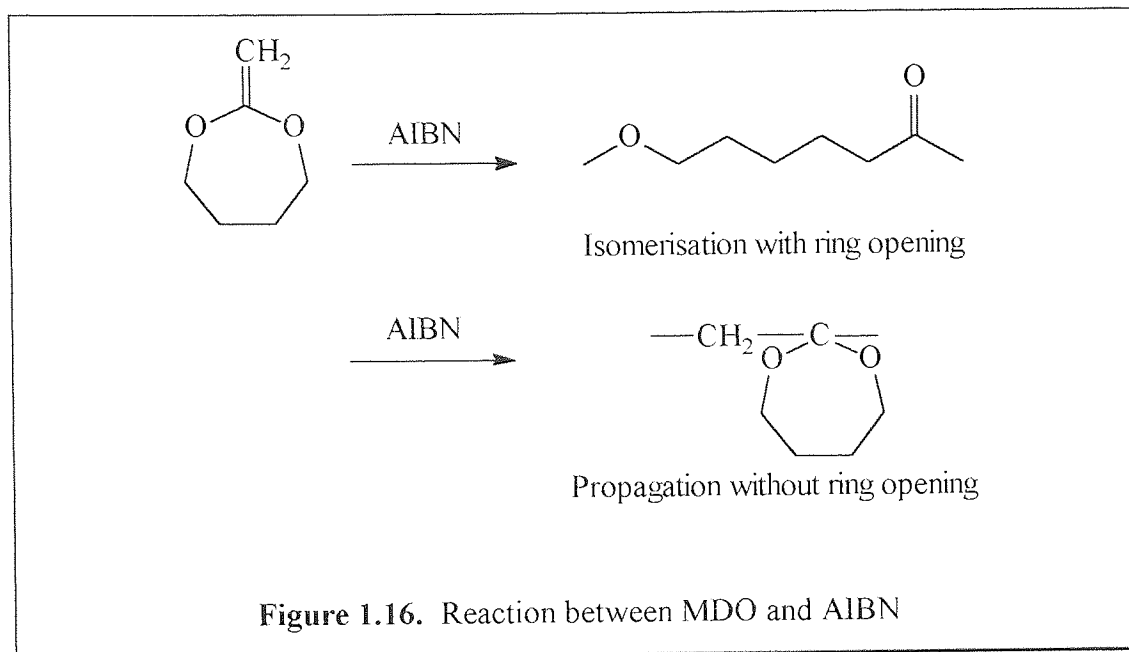
Disproportionation which involves the abstraction of a hydrogen from one end to give two dead polymers can also occur.



Termination may occur via either or both mechanisms, depending on the reaction conditions. The readiness at which these termination reactions can take place means that polymers produced via a free radical mechanism often have a broad molecular weight distribution. Controlled radical polymerisation methods can be used to limit termination and transfer reactions although they are outside the limits of this study.

1.2.5.1. Free radical polymerisation to form poly(ϵ -caprolactone).

Whilst the use of anionic, cationic, co-ordination, and enzymatic methods of initiating the ring opening polymerisation of ϵ -caprolactone are commonly reported, investigations into free radical techniques are rare. Indeed the actual polymerisation of ϵ -caprolactone using free radical techniques appears to be unreported. More commonly, the free radical polymerisation of an isomer of ϵ -caprolactone, 2-methylene-1,3-dioxepane (MDO) (figure 1.16.) is utilised in order to produce poly(ϵ -caprolactone). MDO in the presence of radical initiators such as AIBN or DTBP, can undergo ring opening polymerisation to form poly(ϵ -caprolactone) via a free radical mechanism. This method can also be used to form co-polymers with other vinylic monomers such as styrene, ethylene or methacrylates.⁽⁵⁶⁾ However because of the exocyclic vinyl bond present in MDO, this method of polymerisation does not necessarily produce a polymer which is 100% poly(ϵ -caprolactone). Cyclic ketene acetals such as MDO can also polymerise without ring opening to form a substituted polymer with pendant acetal groups.

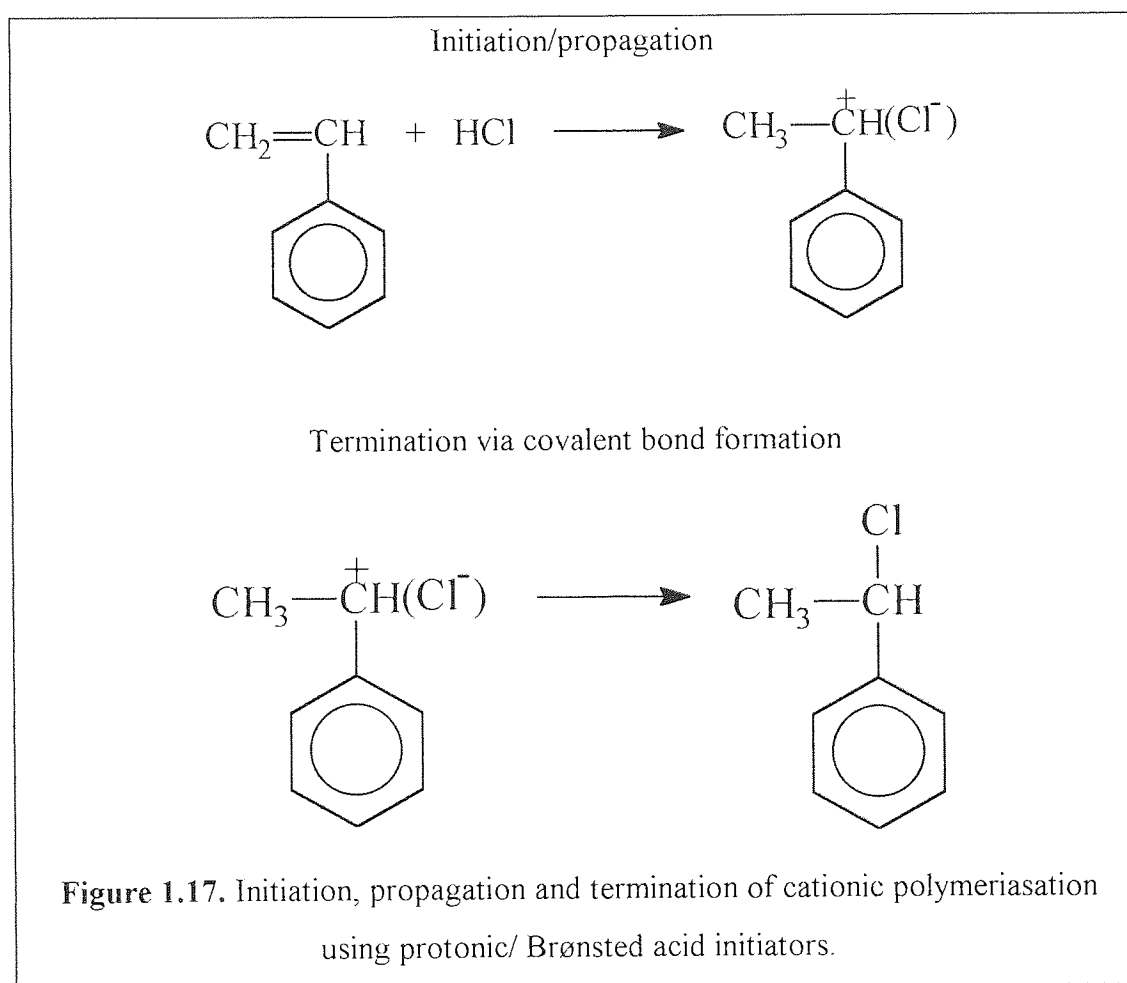


Bailey et al⁽⁵⁶⁾ reported the polymerisation of cyclic ketene acetals at 125°C in *t*-BuOH using AIBN (azobisisobutyronitrile) or DTBP (di-*tert*-butyl peroxide) initiator. It was found by the use of ¹H and ¹³C NMR analysis that in the formation of poly(ϵ -caprolactone) the ring opening of MDO was quantitative using this technique. MDO was also copolymerised with various vinylic monomers and again propagation proceeded entirely via ring opening and only poly(ϵ -caprolactone)-copoly(vinyl monomer) was formed, there was no propagation of MDO without ring opening. Jin and Gonsalves⁽⁵⁷⁾ co-polymerised MDO with various vinyl phosphorous compounds to introduce phosphonic acid and dimethylphosphonate groups into a polymeric-inorganic hybrid material.

Whilst MDO appears to be a commercially unavailable product, presumably because of high cost, the use of this technique would afford an economical route to otherwise inaccessible co-polymers with such as styrene, methyl methacrylate and vinyl acetate. Other methods of producing these co-polymers such as the use of bromo terminated poly(ϵ -caprolactone) and ATRP techniques may be more suitable for producing the well defined polymers which conventional radical mechanisms would appear to be unable to do.

1.2.6. Cationic polymerisation.

Various initiators can be used to bring about the polymerisation of monomers with electron releasing substituents. These may include protonic or Brønsted acids such as HCl, H₂SO₄, HClO₄. The initiation of olefins is brought about by the protonation of the double bond. Care must be taken in selecting an initiator where the anion is not highly electrophilic as this can terminate the protonated bond by the formation of a covalent bond.



This method of drawing the anion close to the cationic propagating species shows that the ionic species do not exist as free ions but as ion pairs. The nature of

the ion pair is dependent upon the polarity of the solvent used in the polymerisation, a phenomenon discussed fully in section 1.2.10.

A much more important method of initiating the cationic polymerisation of vinylic monomers is the use of Lewis acids. These include metal halides such as, BF_3 , AlCl_3 , TiCl_4 , SnCl_4 , organometallic derivatives including RAlCl_2 , R_2AlCl or R_3Al and oxy halides, POCl_3 , CrO_2Cl , or VOCl_3 . On their own however, Lewis acids are not particularly active and they require the use of a co-catalyst to act as a proton donor. Common co-catalysts can be divided into two sub classes, proton donors e.g. water or alcohols, and cation donors such as *t*-butyl chloride or triphenylmethyl fluoride. An example would be the polymerisation of *isobutylene* by dry boron fluoride which is dormant under anhydrous conditions. When trace amounts of water are added however the reaction is rapid.

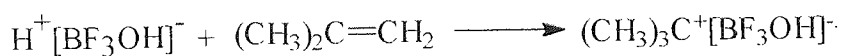
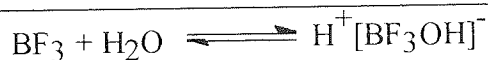


Figure 1.18. Reaction of catalyst complex with isobutylene

The nature of the co-catalyst complex can dramatically affect the rate of the polymerisation reaction. The activity of the initiator-co-catalyst complex is dependent on its ability to donate a proton or cation to the monomer, which in turn depends upon the initiator, co-catalyst and monomer.

Termination reactions in cationic polymerisations are thought to take place by a unimolecular rearrangement of the ion pair;

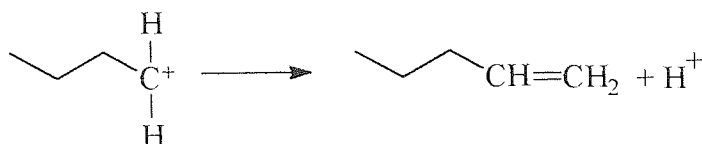


Figure 1.19. Termination via unimolecular rearrangement of the ion pair

or alternatively via bimolecular transfer reaction with a monomer;

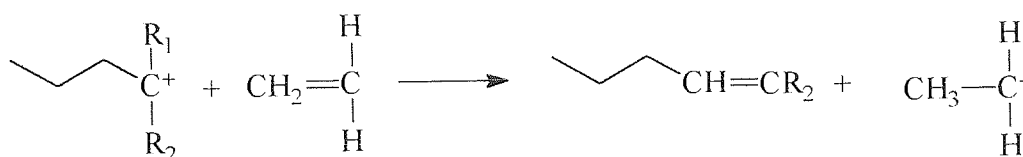
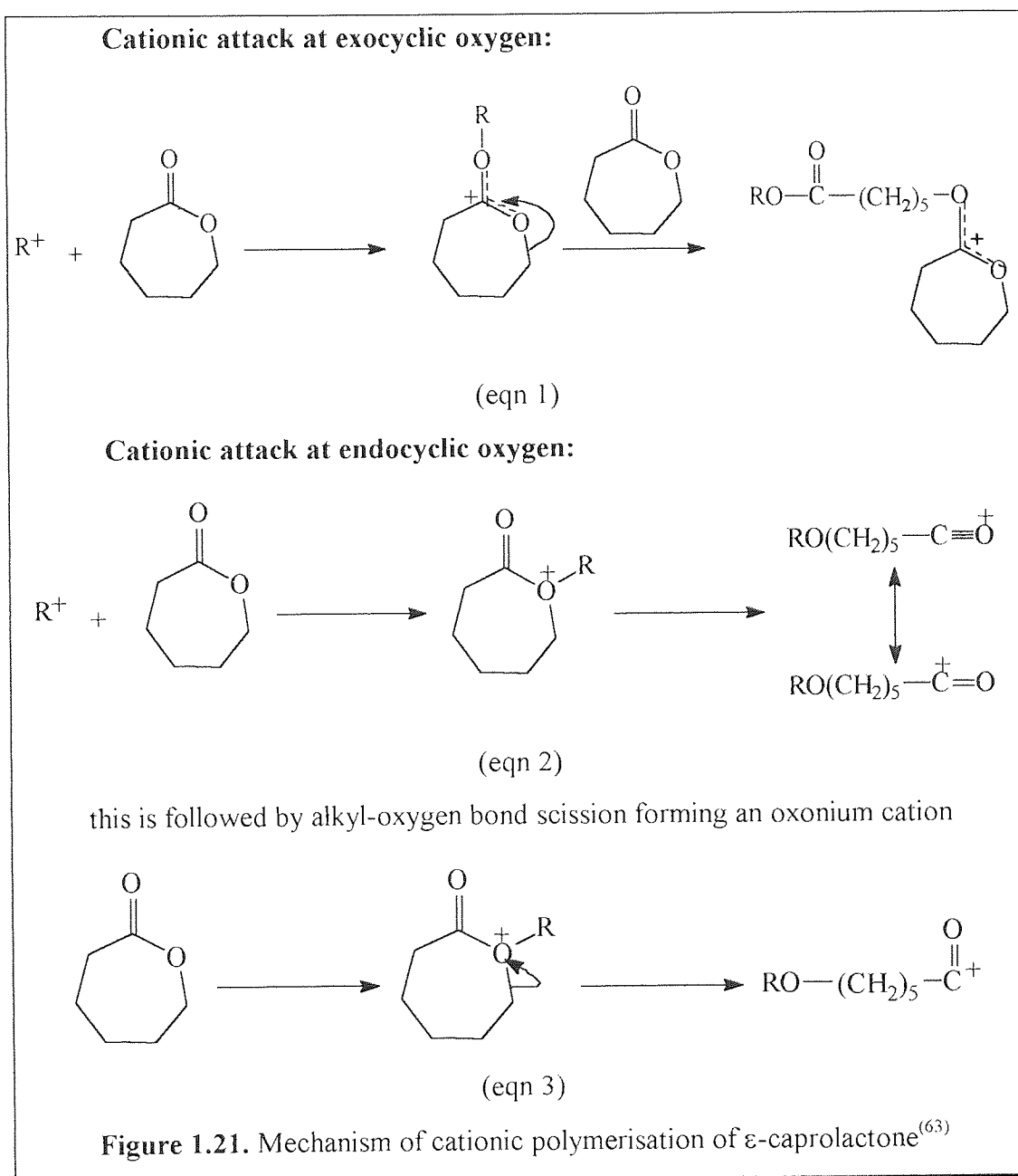


Figure 1.20. Termination via bimolecular transfer reaction with a monomer

1.2.6.1. Cationic ring opening polymerisation of ϵ -caprolactone.

The cationic ring opening polymerisation of ϵ -caprolactone, and other lactones, has been studied comparatively little, especially when compared to anionic and co-ordination systems. The first reported cationic polymerisation of ϵ -caprolactone was with the allyl carbocation derived from AgPF_6 and allyl chloride.⁽⁵⁸⁾ The reaction however was very slow with only 75% conversion being achieved in 3 days. A number of broad types of cationic initiators have been used to polymerise ϵ -caprolactone including, acylium perchlorate⁽⁵⁹⁻⁶⁰⁾ methyl trifluoromethanesulfonate⁽⁶¹⁾, metal halides⁽⁶²⁾, halonium salts.⁽⁶³⁾ A novel approach to the cationic polymerisation of ϵ -caprolactone was reported in 1991 by Djelali and co-workers.⁽⁶⁴⁾ ϵ -Caprolactone was polymerised to a high molecular weight using metallic (V, Ti, Cr, Al, Hg) cations which had been generated electrochemically in situ using sacrificial anodes. Tsubokawa et al⁽⁶⁵⁾ also polymerised various lactones using acylium perchlorate which had been grafted onto carbon fibre particles.

Two different mechanisms for the polymerisation of ϵ -caprolactone using cationic species have been formulated. Since a lactone molecule has two nucleophilic centres, which are the endo and exocyclic oxygen atoms then the exact mechanism of cationic polymerisation depends upon which of these centres is attacked. Attack at the exocyclic (carbonyl) oxygen leads to the formation of an oxonium ion active species. eqn 1 in figure 1.21. and alkyl oxygen bond scission. An attack at the lactone's endocyclic oxygen atom produces an acylium cation from the scission of the acyl oxygen bond (eqn 2. below).



During the polymerisation reaction, when initiated using cationic species, lactones undergo transesterification reactions including the back biting reactions that also occur during anionic polymerisations

1.2.7. Co-ordination polymerisation.

1.2.7.1. Co-ordination or insertion polymerisation of lactones.

Co-ordination polymerisation is one of the most versatile methods of preparing poly(lactones) and co-polymers of lactones and lactides. This technique affords control of molecular weights, high conversions and control of the nature of the polymer end groups. As discussed in section 1.2.4.1., lactones, when polymerised by ionic mechanisms, have a tendency to undergo side reactions which lead to the formation of macrocycles. The use of pseudoanionic co-ordination systems such as aluminium alkoxides allows polymerisation to proceed without the formation of macrocycles. In such systems the rate of transesterification when compared to the rate of propagation is slow, leading to linear polyesters with a narrow molecular weight distribution. Hence the kinetics of the reaction may be used to control the extent of the side reactions which lead to the formation of macrocycles.

Another extremely useful facet of a polymerisation reaction involving the insertion of the monomer unit into an active initiator bond is the incorporation of catalyst residue into the polymer to form a functionally terminated polymer. Further to this, the co-ordination-insertion mechanism allows the polymerisation of substituted lactones without racemisation of the polymer.⁽⁶⁶⁾

In general all covalent metal alkoxides with free *p* or *d* orbitals react as co-ordination or complexation initiators and not as ionic initiators. Many different transition metal compounds have been used in the co-ordination polymerisation of ϵ -

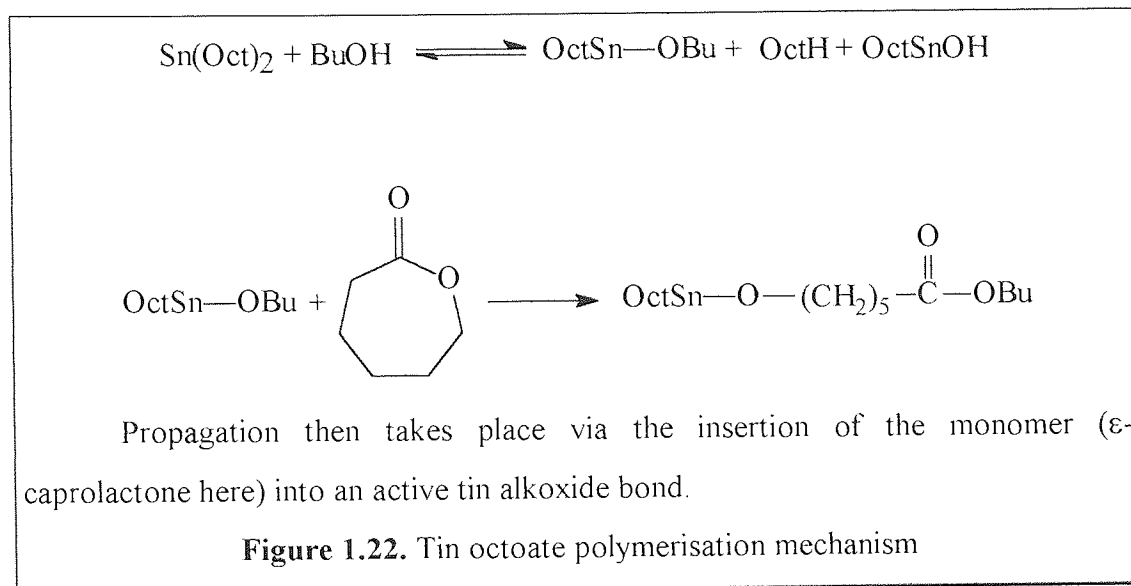
caprolactone and indeed other lactones. These include aluminium alkoxides (see section 1.3), tin alkoxides,⁽⁶⁶⁻⁶⁸⁾ tin octoate,⁽⁶⁹⁻⁷¹⁾ tin halides⁽⁶⁶⁾ titanium alkoxides,⁽⁶⁷⁾ zirconium alkoxides,⁽⁶⁷⁾ alkyl aluminium compounds,⁽⁷²⁾ zinc alkoxides,^(68, 73) alkyl zinc compounds,⁽⁷⁴⁻⁷⁹⁾ samarium complexes,⁽⁸⁰⁻⁸¹⁾ yttrium alkoxides.⁽⁸²⁻⁸⁴⁾

Zinc metal has also been used by Vert and co-workers⁽⁸⁵⁾ in the co-polymerisation of L-lactide and ϵ -caprolactone although they do report little to elucidate the actual mechanism of the polymerisation. Other papers report the polymerisation of lactones with zinc compounds. Both Doi and Tanahashi⁽⁸⁶⁾ and Lenz and co-workers⁽⁸⁷⁾ have reported the polymerisation of β -butyrolactone with a $\text{ZnEt}_2/\text{H}_2\text{O}$ and $\text{AlEt}_3/\text{H}_2\text{O}$ systems respectively.⁽⁸⁸⁻⁹¹⁾ Zinc compounds are particularly useful as initiators for the polymerisation of ϵ -caprolactone for biomedical uses. Zinc is a trace metal found in the body and hence catalyst residues may cause less toxicity problems than other metal species such as tin or aluminium.

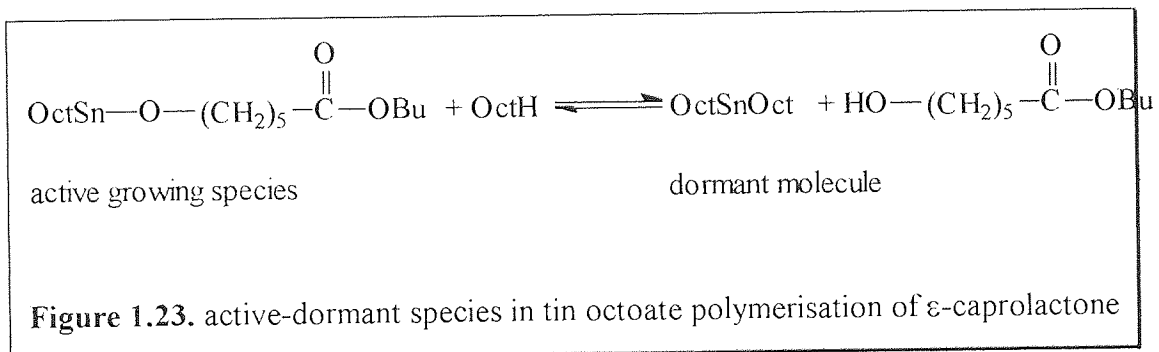
Trialkyl aluminium compounds and primary amines have been used in conjunction to initiate the polymerisation of ϵ -caprolactone⁽⁹²⁾ The mechanism of this polymerisation, involving the co-ordination of an alkyl aluminium/amine complex with the lactone results in the formation of an amine terminated poly(ϵ -caprolactone) chain. It has been proved that the amine has merely co-ordinated with and not reacted with the alkyl aluminium to form an aluminium amine initiator. Teysie and his co-workers concluded that this system did in fact display living characteristics rather like the similar aluminium alkoxide initiated reactions.

Tin compounds are widely used as initiators for the ring opening polymerisation of lactones. Whilst tin octoate ($\text{Sn}(\text{OOct})_2$) in particular is widely used for the polymerisation of ϵ -caprolactone, the mechanism of the polymerisation is under some debate. According to Penczek and co-workers⁽⁹³⁾ in THF, the polymerisation proceeds via an active tin(II) alkoxide bond formed from $\text{Sn}(\text{Oct})_2$. When *n*-butanol and $\text{Sn}(\text{Oct})_2$ are reacted at 80°C in THF as a solvent, 2-ethylhexanoic acid and/or butyl 2-ethylhexanoate are formed. This led to the

conclusion that an exchange product, (Octan-O-Sn-OBu) is formed which acts as an initiator, e.g.:



However, results from the same group also suggest that intentionally introducing octanoic acid into the reaction shows that a reversible activation-deactivation step takes place during the polymerisation:



Penczek et al reported that for the polymerisation of ϵ -caprolactone using tin octoate, that no transfer reactions are present, except transesterification reactions, which broadens the molecular weight distribution by increasing the weight average molecular weight M_w rather than decreasing M_n . This is probably due to the existence of bimolecular transesterification. They do however report that this method of polymerising ϵ -caprolactone is a living system, indicated by a linear

dependence of $-\ln\{1-M_n[P_n]/((114.14)[CL]_0)\}$ with time, where $[P_n]$ is the concentration of growing species and $[CL]_0$ is the initial monomer concentration.

Other studies into the polymerisation of lactones using tin alkoxides have found that the most likely mechanism for the polymerisation is also of a co-ordination insertion type. In their studies into the polymerisation of β -D,L-butyrolactone with butyl tin methoxides, Kricheldorf and co-workers⁽⁶⁸⁾ have found that side reactions may take place other than the formation of cyclic oligomers due to back biting transesterification reactions. They propose that an elimination process such as the one displayed in figure 1.24. may be present in reactions which proceed via an insertion mechanism.

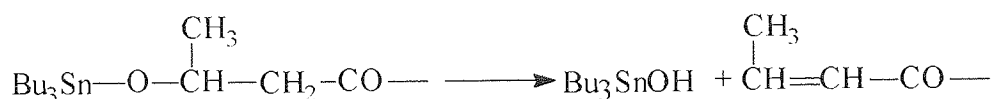


Figure 1.24. Side reactions in tin alkoxide initiated polymerisation of ϵ -caprolactone

They proved that the polymerisation proceeds via cleavage of the acyl oxygen bond of the lactone as opposed to the alkyl oxygen bond.

More exotic systems involving the use of rare earth metal complexes have also been reported. Evans and Katsumata⁽⁸¹⁾ used divalent samarium compounds as initiators for the polymerisation of ϵ -caprolactone. Samarium iodide, alkyls, metallocene, and amides, all complexed with THF have been used as initiators. All the systems produced polymers in quantitative conversion although the molecular weight distributions (polydispersity) were broad and in the region of 1.3 - 3.2. The authors report that the species retain their ability for further propagation once all the monomer has been consumed, an indication that the system may be living. They do not however offer any kinetic details in support of this.

Yttrium alkoxides have also been used for the polymerisation of ϵ -caprolactone alkoxides. The yttrium alkoxide, tris(2,6-di-*tert*-butylphenoxy)yttrium is reported as being inactive as an initiator for the polymerisation of ϵ -caprolactone due to its sterically hindered nature.⁽⁸³⁾ The less sterically hindered yttrium triisopropoxide⁽⁸²⁾ is a more suitable initiator formed by the reaction of tris(2,6-di-*tert*-butylphenoxy)yttrium and *isopropyl* alcohol.

Strongly basic lanthanide compounds have to be avoided however because side reactions are encountered identical to those using purely anionic initiators.⁽⁸⁴⁾

1.2.8. Enzymatic polymerisation of lactones.

The utilisation of enzymatic methods of initiating the ring opening polymerisation of lactones is a recently reported phenomenon. Kohn and co-workers⁽⁹⁵⁾ reported the synthesis of poly(ϵ -caprolactone) using the enzyme *porcine pancreatic lipase* (PPL). The reaction was very slow however with conversions approaching 100% only after around 26 days. The molecular weight distribution of the polymer produced in this reaction is unreported however. Uyama and Kobayashi⁽⁹⁶⁾ polymerised ϵ -caprolactone using lipase enzymes *P.flourescens*, *Candida cylindracea* and PPL. They reported that *P.flourescens* gave a polymer of molecular weight $M_n = 7700$ with a conversion of 92% after 10 days. MacDonald and his co-workers⁽⁹⁷⁾ also polymerised ϵ -caprolactone using PPL catalyst and butanol initiator. They achieved 100% conversion after 4 days at 65°C with a polydispersity of between 1.4 and 1.9 in heptane. Nobes et al⁽⁹⁷⁾ reported the polymerisation of lactones other than ϵ -caprolactone (β -propiolactone, β -butyrolactone and γ -butyrolactone) to form poly(hydroxyalkanoates) of varying molecular weights. Their work however yielded little more than oligomers of molecular weights of no more than 1000 for all reactions except ϵ - ϵ -caprolactone, and one with β -propiolactone, which was subsequently repeated and yielded a low molecular weight polymer. Other papers have reported the ring opening polymerisation of lactones catalysed by enzymes.⁽⁹⁹⁻¹⁰²⁾ All except Bisht⁽¹⁰¹⁾ and

Henderson⁽¹⁰²⁾ however have failed to produce anything that could be considered more than an oligomer, although Bisht's work on the polymerisation of ω -pentadecalactone did produce high molecular weight polymers with a molecular weight of around 35000, albeit with a polydispersity of 2.4. One major drawback of these reactions is the very long length of time they require. A reaction time of nearly 60 days has been reported in some cases before quantitative conversion is achieved.⁽⁹⁴⁾

Henderson and co-workers⁽¹⁰²⁾ have reported that the polymerisation of ϵ -caprolactone using PPL as the catalyst and *n*-butylamine initiator can be considered to be a living system. Plotting M_n against conversion and a derivation of $\log([M]_0/[M]_t)$ against time, they obtained linear plots indicating a lack of transfer reactions and proving that monomer consumption follows first order kinetics. However, it can also be said that for low values of M_n , the presence or lack of chain transfer cannot be observed from M_n versus conversion plots.

1.2.9. Living polymerisation.

A living system can be described as a polymerisation in which propagation proceeds in the absence of termination or transfer reactions until all monomer has been consumed. It has also been proposed that the growing chains remain active indefinitely once all monomer has been consumed. This hypothesis has been reviewed slightly in recent years to be defined as that the chains remain active for a period sufficiently long enough for further monomer addition or reaction to be completed. However, whatever the definition used, in a polymerisation which is considered to be living, the rate constant of termination and transfer are equal to zero.

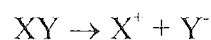
Living polymerisation was first described by Szwarc.⁽¹⁰³⁾ He reported the reaction of styrene with sodium naphthalenide and the accompanying colour change from green to red. On the subsequent addition of more styrene, the red colour remained and the solvent boiled. It was concluded therefore that the red solution was active and that the styrene was polymerising exothermically. After destroying the active species with the addition of methanol, it was found that all of the styrene had been converted into poly(styrene). The reaction was discovered to have been free of any termination or chain transfer reactions and the resulting polymer chains had retained capacity for growth.⁽¹⁰⁴⁾ Thus the term *living polymers* became applied to those polymers which retained their ability to grow whenever monomer is supplied. This lack of a formal termination step is a very useful tool in the preparation of block copolymers when sequential addition of monomer can be made to a reaction once the initial polymerisation has been concluded.

A living system will only remain so if the reaction is not terminated, either deliberately or accidentally, by the inclusion of trace impurities in the reaction medium. Moisture on or in the reaction vessel leads to the termination of living anionic polymerisation reaction by forming a hydroxy anion which is insufficiently nucleophilic to reinitiate polymerisation. Oxygen and carbon dioxide from the

atmosphere are also capable of terminating anionic polymerisation reactions by adding to the propagating species and forming peroxy and carboxyl anions. Strictly controlled reaction conditions in which all traces of these terminating agents are excluded are necessary.

1.2.9.1. Kinetics of living polymerisations.⁽⁴¹⁾

A living polymerisation involves no formal termination step, and so the reaction scheme shown below will hold true,



Scheme 1.1. Reaction scheme of living polymerisation

It can be assumed that the initiator is completely dissociated in the solvent before the monomer is added. Under these conditions when monomer is brought into contact with the initiator, all the chains will be initiated at the same time, leading to a polymer with a narrow molecular weight distribution.

If the initial initiator concentration is $[I]$, $[YM_1^-] = [I]$ if all the initiator is converted to propagating centres and then the rate of propagation is,

$$\frac{-d[M]}{dt} = k_p[YM^-][M] \quad 1.6.$$

since the monomer concentration is expected to decay in a first order manner

$$\ln \frac{[M]_0}{[M]} = k_p [I] t$$

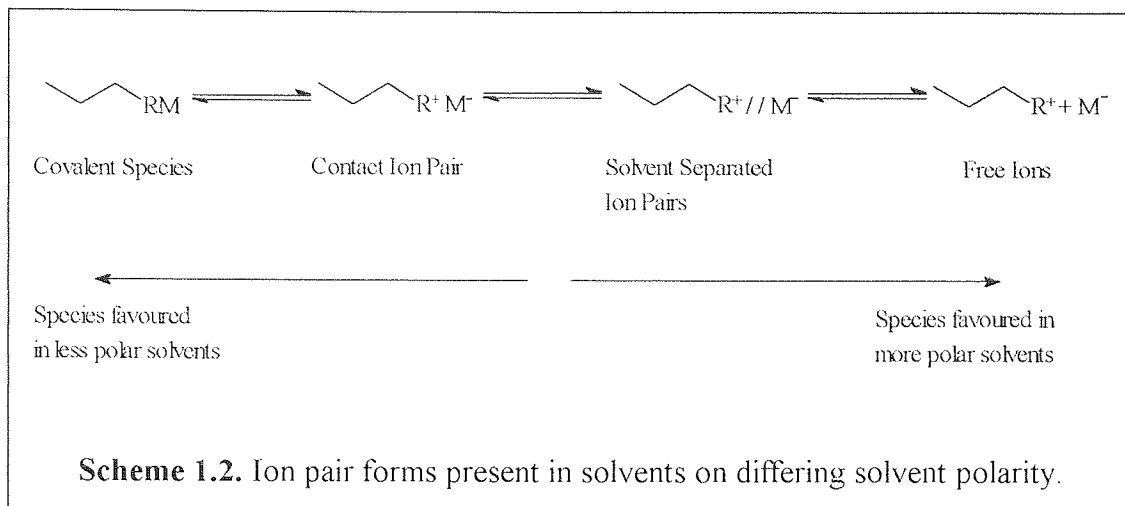
1.7.

Thus a linear graph of $\ln\{[M]_0/[M]\}$ vs time which indicates the concentration of propagating centres is constant if the reaction is living and the reaction is first order in monomer.

1.2.10. Effect of solvent on polymerisation.

The nature of the solvent can have a profound effect on the polymerisation. A solvent must be able to dissolve the monomer, initiator and the polymer being formed and not react with any of these species or the propagating centre. Using alkali metal alkyl initiators in the solvents of low dielectric constant (ϵ) which are commonly used in polymerisations, such as toluene, the alkali metal cation is associated with the anion. Carbanion pairs form a significant proportion of active centres in polar solvents such as dioxane, although dissociation into free ions does occur. Whilst the extent of this dissociation is limited in THF, it cannot be ignored because the reactivity of free anions is much greater than that of the corresponding ion pairs. Ion pairs can exist in solution in different forms, from the covalent species through separated ion pairs to free ions.

So depending on solvent, temperature and gegen ion, the active species can be present in several forms as summarised in the scheme below.



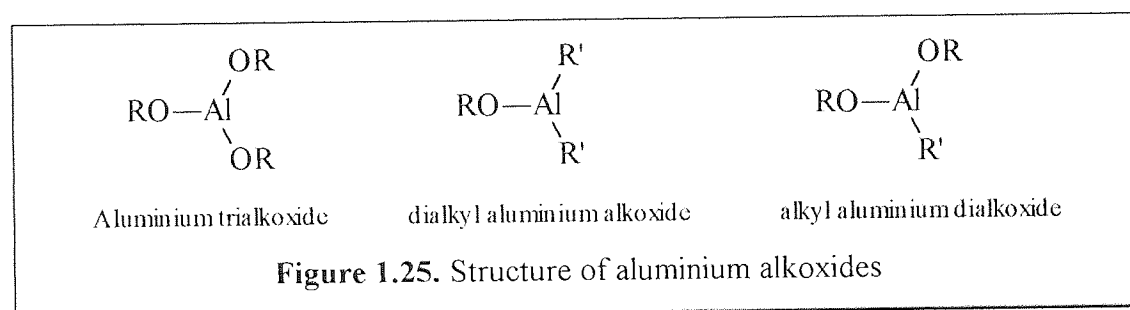
Any of these species may be active in the polymerisation of monomers but it is unlikely that all will be present in a given solvent. In low polarity solvents the species on the left of the scheme above are favoured, whilst those on the right are the species that are present in solvents of higher polarity. Such highly polar solvents are desirable for ionic polymerisations but are often not used because they either destroy the initiator, (e.g. water, alcohol) or form stable complexes with it (e.g. ketones).⁽¹⁰⁵⁾ The covalent species found in solvents of lower polarity are often unreactive and can usually be ignored. In solvents that have an electron donating group, such as dioxane ($\epsilon = 7.3$), the solvent is able to complex with the cation, especially in cationic polymerisations and in co-ordination systems with aluminium metal centres. If more than one propagating species is present in the reaction, and if conversion between ion pairs, solvent separated and free ions is rapid, then the propagating species will exist in each of the forms at different times in the reaction. The rate of propagation is therefore an average of the rate for each active species. However, should one form be much more reactive than the rest, and assuming rapid exchange between each, then the molecular weight and distribution will be associated with the faster propagating species. If the propagating species do not interconvert, i.e. there are two or more distinct propagating centres, then the molecular weight distribution will be bi or even multi modal, with each peak representing a separate growing species.

In general, the rate constant of propagation will be higher for free ions than that of the same reaction involving an ion pair. Thus for purely ionic reactions, the rate of propagation is faster in solvents of a higher polarity than in less polar media. However for systems involving the polymerisation of lactones with alkyl aluminium alkoxides the opposite is true. It has been found that for polymerisations in toluene, THF and acetonitrile (respective dielectric constants = 2.4, 7.6, and 37.5) that the rate of polymerisation decreased as the dielectric constant of the solvent increased.⁽¹⁰⁶⁾ This observation is indicative of a co-ordination system such as this. If the polymerisation involved ionic species, then the propagation rate would decrease as the dielectric constant of the reaction media increased. However, the rate of polymerisation in THF using this system is effected by the co-ordination of the solvent molecules with the catalyst.

1.3. Aluminium alkoxide initiators.

1.3.1. Introduction.

It was reported by Teyssie and co-workers over twenty years ago that the living polymerisation of ϵ -caprolactone and other lactones could be promoted by bimetallic (Al,Co) or (Zn,Al) μ -oxo alkoxides.⁽¹⁰⁷⁻¹⁰⁹⁾ Since then aluminium trialkoxides and alkyl aluminium alkoxides (figure 1.25) have been used for the ring opening polymerisation of lactones lactides and cyclic anhydrides.^(68, 92, 106, 110-124, 135-137) The use of such initiators, and the living mechanism associated with them allows the avoidance of formation of cyclic oligomers and leads to linear chains of a predictable molecular weight and a narrow molecular weight distribution. The use of other metal alkoxide initiators has been reported in the literature, including lithium,⁽¹²⁵⁾ yttrium,⁽⁸²⁾ tin,^(66, 68) titanium,⁽⁶⁸⁾ zinc,⁽⁶⁸⁾ and zirconium.⁽⁶⁸⁾



1.3.2. Bimetallic μ -oxoalkoxides.

A reproducible preparation of well defined compounds containing several metal atoms linked together by μ -oxo bridges was first reported by Osgan and Teyssie in 1967.⁽¹²⁶⁾ The nature of the catalyst, having the formula depicted in figure 1.26. below, can be altered by changing the nature of the metals M_2^p (Al^{III} , Ti^{IV} ...) and M_1^{II} (Zn, Co, Fe, Mo,...) and of the alkoxide groups, (*isopropoxy*, *n*- or *sec*-butoxy,...). These initiators have been synthesised by the thermal condensation between aluminium *isopropoxide* and (Zn) acetate in a 2:1 molar ratio at around 200°C in decalin for 8 hours.⁽¹⁰⁷⁾

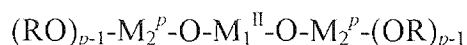


Figure 1.26 Structure of bimetallic μ -oxoalkoxide.

The polymerisation of lactones promoted by such initiators is unimpeded by transfer or termination under aprotic conditions and the concentration of propagating species remains constant throughout. These observations, characteristic of living polymerisations, have been observed for all polymerisable lactones in the presence of both *n*-butoxy and *iso*-propoxy Zn,Al μ -oxoalkoxides. The mechanism of chain propagation has also been determined. The lactone molecule is found to insert into the Al-OR bond of the catalyst, this involves an acyl oxygen cleavage of the lactone ring. The insertion occurs in a manner which maintains the binding of the chain to the catalyst through an alkoxide rather than carboxylate link. This corresponds to a co-ordinated anionic insertion mechanism. It appears that the number of growing chains per catalyst molecule varies with the catalyst composition and the mean degree of association. The polymer resulting from this polymerisation possesses a terminal hydroxyl group from the hydrolysis of the catalyst and the other end group is fixed by the nature of the initial alkoxide initiator. Hence a method for the production of telechelic polyesters is available using bimetallic μ -oxoalkoxides.

The high solubility of bimetallic μ -oxoalkoxides in organic solvents can be attributed to a co-ordinative association in solution, resulting in an aggregated structure. This phenomenon is due to the presence of a lone pair of electrons on the alkoxide oxygen which will occupy the vacant co-ordination position on the metal atoms. The mean degree of aggregation is lower in more polar solvents such as dichloromethane when compared to *n*-heptane and lower when linear (*n*-butoxy) alkoxide groups are replaced by bulkier (*iso*-propoxy) groups.

It has been reported⁽¹⁰⁹⁾ that the co-ordinative association of the bimetallic μ -oxoalkoxides in solution effects the kinetics of the polymerisation. The ϵ -polymerisation of caprolactone is first order in monomer using toluene as a solvent. However as the concentration of monomer is increased, the rate constant appears to decrease. This can be attributed to an increase in the dielectric constant (ϵ) increasing with the monomer concentration. Changing the nature of the metals, alkoxide groups, solvent and temperature does not alter the order in monomer. The order in catalyst does however depend upon the structure of the alkoxide used and thus the degree of association.

1.3.3. Aluminium Trialkoxides.

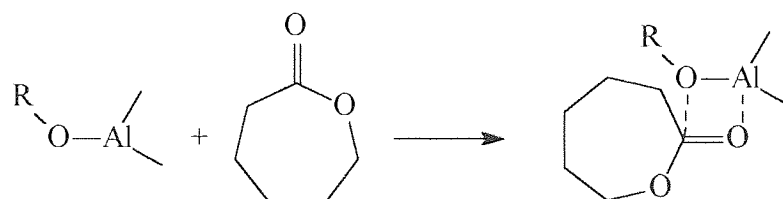
Aluminium alkoxides such as aluminium triisopropoxide have been used for around 40 years as initiators for ring opening polymerisation.⁽¹²⁷⁾ Aluminium triisopropoxide, in particular, is well known as an effective initiator for the living ring opening polymerisation (ROP) of ϵ -caprolactone,⁽⁷²⁾ lactides.^(122,123) and cyclic anhydrides.⁽¹²⁸⁾

1.3.3.1. Mechanism of polymerisation initiated with aluminium trialkoxides.

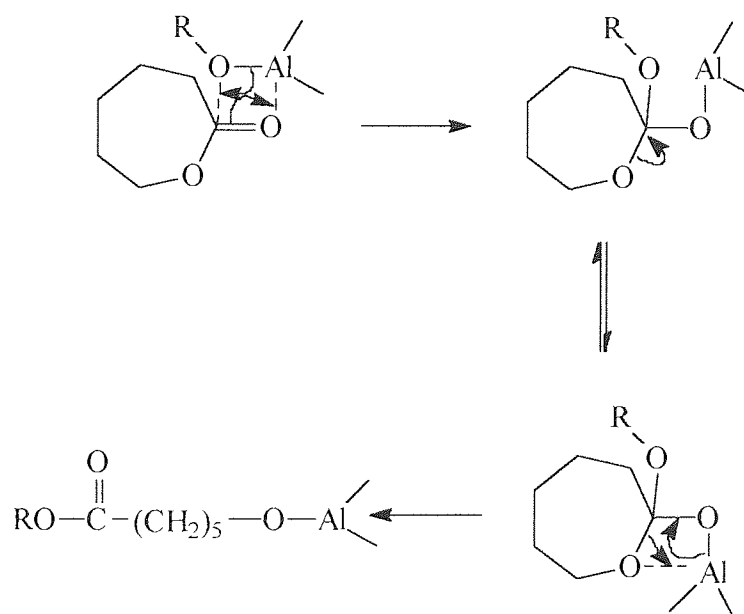
Earlier it was mentioned that bimetallic μ -oxoalkoxides initiate the polymerisation of lactones via the scission of the acyl oxygen bond of the lactone. Kinetic and structural data support the notion that the polymerisation proceeds via the same 'co-ordination-insertion' type mechanism with monomer insertion into the active Al-O bond.

The first step of the reaction with lactones is the complexation or co-ordination of monomers at the most nucleophilic site of the lactone, the carbonyl oxygen. The next step is the insertion of the lactone into the metal alkoxide bond via a cleavage of the acyl oxygen bond of the lactone. The name 'co-ordination-

insertion' mechanism affords a clear distinction between such a reaction and one involving free ions or ion pairs. Reaction begins with co-ordination of monomer and initiator,



Which is followed by insertion of the lactone into the active Al-O bond via the acyl oxygen cleavage in the monomer

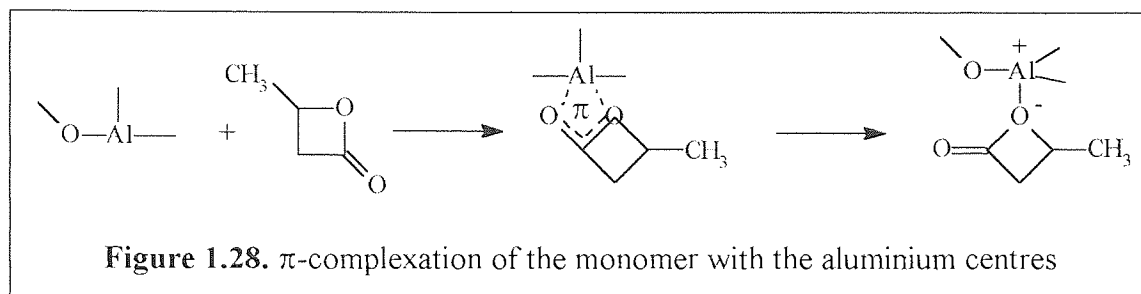


Propagation then continues by the same mechanism

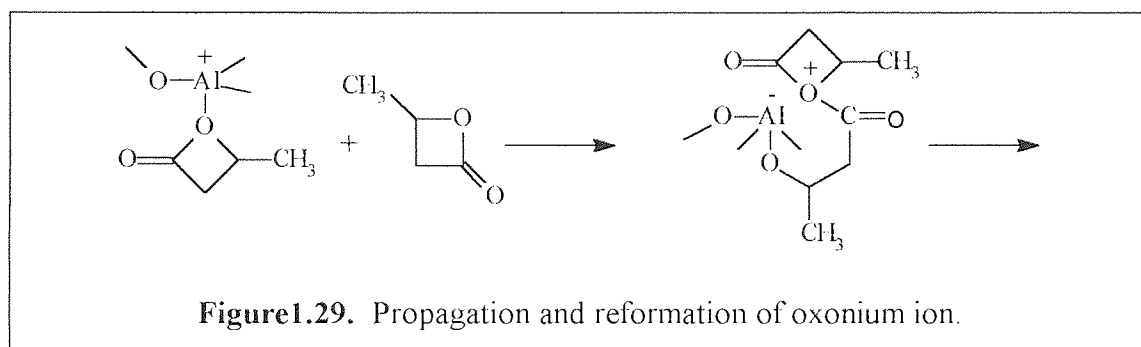
Figure 1.27. Co-ordination-insertion mechanism of polymerisation of a lactone

Shelton et al⁽⁷⁴⁾ proposed a different mechanism for the polymerisation of lactones using aluminum alkoxides. They assumed π -complexation of the monomer with the

aluminium centres as shown in figure 1.28 followed by localization and formation of a sigma bond between aluminium and oxygen.



Propagation then occurs by attack of the oxonium ion by the acyl oxygen of the lactone and reformation of the oxonium ion.

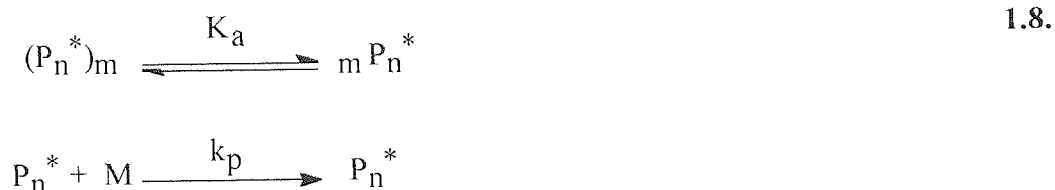


A cyclic intermediate is formed and this retained throughout the reaction as the polymer chain grows.

1.3.4. Aggregation of alkoxide species.

Aluminium based initiators are known to have a high tendency to aggregate. The growing species are also known to aggregate in the same manner despite the size of the alkoxy moiety (the growing polymer) increasing. Penzcek⁽¹³⁷⁾ calculated the degree of aggregation m and used this to determine the corresponding equilibrium constants K_a and rate constant k_p .

Assuming that only the non aggregated species (P_n^*) partake in propagation and that the aggregated species ($(P_n^*)_m$) are inactive then,



reversibility of the propagation step is ignored because $[I]_c < 10^{-2}$ mol/l

and then assuming

$$[I]_0 = [P_n^*] + m[(P_n^*)_m] \quad \mathbf{1.9.}$$

but if $[I]_0$ is high then $[(P_n^*)_m] \gg [P_n^*]$ and thus,

$$[(P_n^*)_m] = [I]_0/m \quad \mathbf{1.10.}$$

then using equation 1.8.

$$[P_n^*] = K_a^{-1/m} [(P_n^*)_m]^{1/m} \quad \mathbf{1.11.}$$

and combining equations 1.10 and 1.11

$$Pn^* = (1/m)^{1/m} K_a^{1/m} [I]_0^{1/m} \quad 1.12.$$

and then the kinetic solution to scheme 1.8. is

$$-d[M]/dt = k_p[M](1/m)^{1/m} K_a^{1/m} [I]_0^{1/m} \quad 1.13.$$

where $[M]$ is the instantaneous monomer concentration,

then,

$$\ln([M]_0/[M]) = (1/m)^{1/m} k_p K_a^{1/m} [I]_0^{1/m} t \quad 1.14.$$

and thus

$$\ln\{(1/t) \ln([M]_0/[M])\} = \ln[(1/m) k_p K_a^{1/m}] + (1/m) \ln[I]_0 \quad 1.15.$$

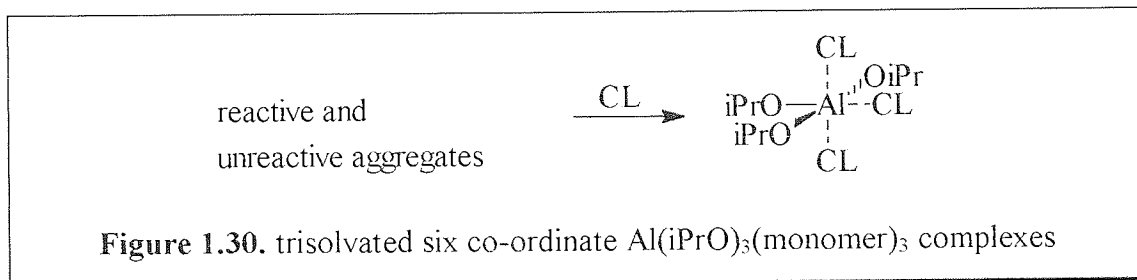
and so a plot of $-\ln\{(1/t) \ln([M]_0/[M])\}$ against $-\ln[I]_0$ will have a gradient of $1/m$, the reciprocal of the mean degree of association. Since $\{(1/t) \ln([M]_0/[M])\}$ is equal to the gradient of a first order plot of $\ln([M]_0/[M]_t)$ against time, which is equal to k_p , then a plot of $-\ln(k_p)$ against $-\ln[I]_0$ will have a slope equal to m , the mean degree of association/

1.3.4.1. Aluminium trialkoxides

Alkyl aluminium alkoxides and aluminium alkoxides are known to co-ordinate or aggregate in solution^(106, 113, 118)

A study by Teyssie and co-workers focused upon the co-ordinative structure of aluminium triisopropoxide in toluene both before and after the addition of a co-ordinating monomer.⁽¹²⁹⁾ They found that according to ^{27}Al NMR, an equilibrium exists between the trimer and tetramer species of $\text{Al}(\text{iPrO})_3$ in toluene. Addition of

the non polymerisable lactone γ -butyrolactone resulted in this equilibrium being altered leading to a monomeric alkoxide species. It was postulated that these 'monomeric' species are in fact trisolvated six co-ordinate $\text{Al}(\text{iPrO})_3(\text{monomer})_3$ complexes.



In a further paper concerning the kinetics of lactone polymerisation using aluminium trisopropoxide, Teyssie⁽¹¹³⁾ studied the structure and co-ordinative association of the propagating species. They found that the number of active sites on the catalyst is dependent upon the monomer used (table 1.5).

| Initiator | Monomer | Solvent | n_{OR}/Al |
|----------------------------------------|--------------------------|---------|---------------------------|
| $\text{Al}(\text{iPrO})_3$ | lactide | toluene | 3.0 |
| $\text{Al}(\text{iPrO})_3$ | ϵ -caprolactone | toluene | 1.0 |
| $\text{Al}(\text{iPrO})_3$ | ϵ -caprolactone | THF | 1.0 |
| $\text{Et}_2\text{AlOCH}_2\text{CH}_3$ | ϵ -caprolactone | toluene | 1.0 |

Table 1.5. Number of active sites per initiator molecule.

The polymerisations of both lactide and ϵ -caprolactone were found to be living in toluene at 0°C and 70°C. From a plot of D_{pn} against monomer/initiator ratio it appeared that each alkoxide group participated in the polymerisation of lactide, $n_{\text{OR}}/\text{Al} = 3.0$. In contrast $n_{\text{OR}}/\text{Al} = 1.0$ when ϵ -caprolactone was being polymerised. Thus one and three chains are respectively being grown per aluminium atom. In the case of ϵ -caprolactone, it may be that there is one poly(ϵ -caprolactone) chain per aluminium atom or that only a fraction of the $\text{Al}(\text{iPrO})_3$ initiates but then each molecule propagates three poly(ϵ -caprolactone) chains per aluminium atom. Teyssie differentiated between these proposals using viscosity measurements on the chains before and after deactivation.

They found that when lactide is polymerised by $\text{Al}(\text{iPrO})_3$, the degree of association of the living chains ($\text{DA} = 3$) agreed with the mean number of active alkoxide groups per chain ($n_{\text{OR}}/\text{Al} = 3$). However in the case of the polymerisation of ϵ -caprolactone, the degree of association was higher with an aged $\text{Al}(\text{iPrO})_3$ solution ($\text{DA} = 11.3$) than n_{OR}/Al which is equal to 1.0. The aged solution contained a 45/55 ratio of three and four aggregated species, A_3/A_4 . The degree of association when freshly prepared $\text{Al}(\text{iPrO})_3$ was used decreased to 2.75, where the $\text{Al}(\text{iPrO})_3$ solution comprised 90% of the A_3 species. The authors concluded that there was an equilibrium between A_3 and A_4 species and that it is an important equilibrium. Penzcek also concluded that there may be inter molecular co-coordinative interactions taking place.⁽¹³⁸⁾

The average degree of association m was calculated to be the same ($m=1$) for both lactide and ϵ -caprolactone in toluene indicating that the living aluminium *trialkoxide* centres do not associate in toluene. The value of $\text{DA} = 3$ obtained for lactide polymerisation is obtained because of the three armed shaped growing chains. Provided that the unreactive A_4 aggregates are taken into account, then the same conclusion holds for ϵ -caprolactone polymerisation. $\text{Al}(\text{iPrO})_3$ tetramer is much more stable than the trimer, hence the assumption that the active species in the polymerisation of ϵ -caprolactone is a trimer.

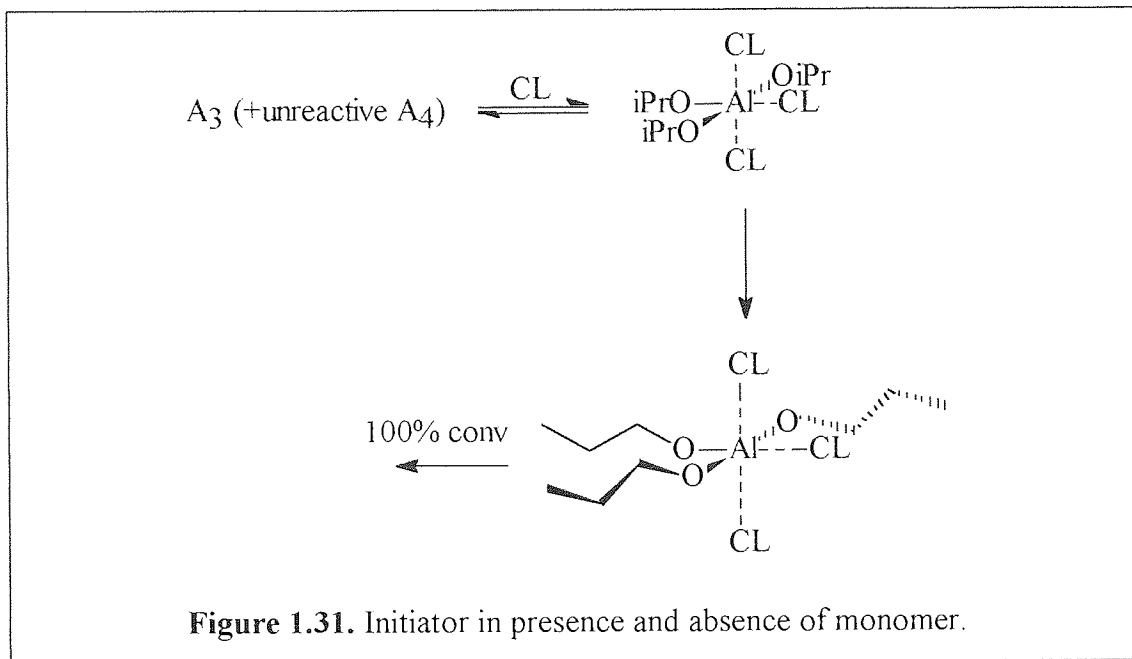


Figure 1.31. Initiator in presence and absence of monomer.

The nature of the solvent does not appear to have an effect on the average number of active alkoxide groups per aluminium; it was found that the number of active alkoxide sites per aluminium was, $n_{OR}/Al = 1$ in both THF and toluene.⁽¹³⁹⁾ Teyssie et al⁽¹¹³⁾ observed that the rate of polymerisation of ϵ -caprolactone was slower in THF than in toluene. Since THF is a well known solvating agent, the ether oxygen is able to compete with the carbonyl groups of lactones and lactides for coordination on the aluminium.

Penzcek⁽¹⁴⁰⁾ found that both the molecular weights and molecular weight distribution of poly(L,L-lactide) were affected by the aggregation form of the aluminium triisopropoxide. Experimentally determined M_n values were found to be close to calculated values when aluminium triisopropoxide trimer A_3 was used as an initiator. This indicates an absence of side reactions, quantitative initiation, and since M_n increased linearly with time, that the polymerisation was living. However when polymerisation was brought about with the tetramer A_4 M_n values exceeded theoretical values, presumably because of slow initiation. Molecular weight distribution was found to be slightly higher for polymer prepared with the aluminium triisopropoxide tetramer A_4 . The MWD was found to increase with conversion, supposedly because of side reactions such as inter molecular transesterification.

1.3.4.2 Alkyl aluminium alkoxides.

Dialkyl aluminium alkoxides are also known to be associated as dimers or trimers in the solid state or in solution. The alkyl substituent does have an effect on the mean degree of association. When the alkyl group is small such as ethyl, then trimers are formed. Dimers are formed when the alkyl group is bulkier such as *isobutyl*.

Each alkoxide group is known to participate in the polymerisation of ϵ -caprolactone and lactide. In contrast to this the alkyl groups are considered to be inactive under normally anhydrous conditions.⁽¹⁴¹⁻¹⁴²⁾

1.3.5. Transesterification or 'back biting' reactions.

Studies of anionic and cationic polymerisations of ϵ -caprolactone and δ -valerolactone indicate that ionic chain ends promote transesterification reactions. *Intramolecular* transesterifications cause degradation and formation of cyclic oligomers whilst *intermolecular* transesterification modifies the sequence of copolymers which prevents the formation of block copolymers. Both of these mechanisms can cause a broadening of the molecular weight distribution of the polymer sample.

Kricheldorf and co-workers⁽⁶⁸⁾ compared the effect different metal alkoxides had on the extent of transesterification. Commercially available poly(ϵ -caprolactone) was dissolved in an inert solvent and combined with, aluminium, zinc, titanium, zirconium and tin alkoxides at 100°C and 150°C. The extent of degradation was measured and the results summarised. It was found that aluminium triisopropoxide did not induce back biting reactions even after 4 days at 150°C. The order of reactivity of the alkoxides towards back biting was $\text{Al}(\text{O}-i\text{-Pr})_3 < \text{Zn}(\text{O}-n\text{-Pr}) < \text{Ti}(\text{O}-n\text{-Bu})_4 < \text{Bu}_3\text{SnOMe} < \text{Bu}_2\text{Sn}(\text{OMe})_2$.

Modification of the active centre of initiators leads to a change in the mechanism of propagation and they decrease the reactivity of the formation of macrocycles.⁽¹³⁰⁾ This can be summarised by the ratio k_p/k_b where k_p and k_b represent the rates of propagation with monomer and back biting leading to formation of macrocycles respectively. It was found that the use of diethyl aluminium methoxide in the polymerisation of ϵ -caprolactone led to the formation of linear molecules by kinetic enhancement of the linear polymer.⁽⁵³⁾ An initiator where $k_p \gg k_b$ would lead to the formation of linear molecules over cyclics.

Penzcek⁽¹¹⁶⁾ did however state that side reactions leading to the formation of macrocycles and intermolecular transesterification are unimportant until the reaction has reached greater than 99% conversion. This is presumably because the monomer is a much more reactive species than the polymer. Once the reaction has approached quantitative conversion, then reaction with the polymer becomes more likely than with the remaining monomer.

Teyssie⁽¹²²⁾ in his paper on the polymerisation of lactides, noted that above molecular weights of 90,000, the molecular weight distribution of the polymers broadened with time and that percentage conversion also decreased as molecular weight increased. This was claimed as an indication of the presence of side reactions which were more important than at low conversions. Furthermore they reported that intramolecular transesterification reactions can cause a decrease in the weight average molecular weight, thus broadening the molecular weight distribution. *Intermolecular* transesterification would also increase the polydispersity. Interestingly they also reported that the production of high molecular weight polymers, through low initiator concentrations was much more sensitive to impurities in the reaction.

Little would appear to have been reported as regards the effect of temperature on the transesterification reactions present in the polymerisation of ϵ -caprolactone. However Teyssie et al⁽¹²²⁾ reported the effect of temperature on the

transesterification reactions in lactide polymerisations. They found that the overall rate of polymerisation increases and that the polydispersity broadens with temperature. For a polymerisation carried out at 75°C, the molecular weight remained constant at long reaction times and close to the theoretical maximum value, M_n . The polydispersity and weight average molecular weight of the polymer however broadened, which was attributed to the presence of intermolecular transesterification.

The apparent absence of side reactions at conversions less than 99% does suggest that propagation does not involve ionic structures. This leads further to the suggestion that the propagation proceeds via a pseudo anionic co-ordination insertion type mechanism. Teyssie et al^(72, 123, 131) found that using alkyl aluminium alkoxide and aluminium alkoxide initiators that the polymerisation of ϵ -caprolactone was under kinetic control.

1.3.6 Effect of the nature of the alkyl group in alkyl aluminium alkoxides on the polymerisation of lactones.

The nature of the alkyl group in alkyl aluminium alkoxides was found by Penczek and co-workers⁽¹¹⁶⁾ to have an effect on the formation of macrocycles after complete (99.9%) conversion. They reported that when comparing *isobutyl* and ethyl alkyl groups, that formation of linear polymers is more enhanced with bulkier alkyl substituents.

The structure of the alkyl group can affect the mean degree of association of the initiator species in solution. Teyssie et al⁽¹¹³⁾ found that the partial order in initiator concentration depends on the alkyl substituent. When the alkyl group was ethyl, the partial order in initiator was 1/3, whilst the partial order in initiator was 1/2 when the alkyl group was the bulkier *isobutyl* group. These correspond to the formation of trimers and dimers respectively.

1.3.7. Effect of the structure of the alkoxide group in alkyl aluminium alkoxides on the polymerisation of lactones.

The structure of the alkoxide group is believed to have no significant effect on the polymerisation of lactones using alkyl aluminium alkoxides. Penzcek and Duda⁽¹⁴³⁾ reported that the rate constant of propagation (k_p) for ϵ -caprolactone in THF was independent of the initiator within experimental error as shown in table 1.6.

| Initiator | $k_p/L \text{ mol}^{-1} \text{ s}^{-1}$ |
|-------------------------------------------------------------------|-----------------------------------------|
| $(\text{C}_2\text{H}_5)_2\text{AlOCH}_2\text{CHCH}_2$ | 3.9×10^{-2} |
| $(\text{C}_2\text{H}_5)_2\text{AlOC}_2\text{H}_5$ | 3.9×10^{-2} |
| $(i\text{-C}_4\text{H}_9)_2\text{AlOCH}_3$ | 3.9×10^{-2} |
| $(\text{C}_2\text{H}_5)_2\text{AlOCH}_2\text{CHCH}_2\text{.NN}^*$ | 4.5×10^{-2} |

Table 1.6. Rate constants of propagation

* alkoxide complexed with DMEDA

It would seem therefore that the nature of the alkoxide group in fact has no effect on the observed rate constant of polymerisation. The addition of an amine, *N,N*-dimethyl-*N'*-ethylethylene diamine(DMEDA) presumably prevents the alkoxides aggregating thus increasing slightly the rate of propagation.

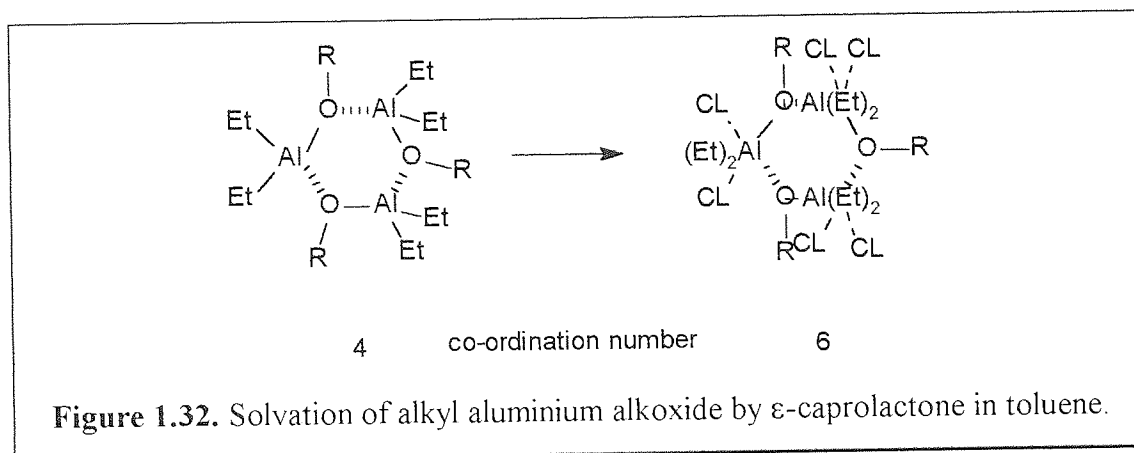
Teyssie and co-workers^(111, 124) also investigated the effect of the alkoxide group on the rate of polymerisation. The polymerisation of ϵ -caprolactone using various aluminium alkoxides showed little or no variation in the polymerisation rate.

1.3.8. Effect of the solvent on polymerisations initiated by aluminium alkoxides.

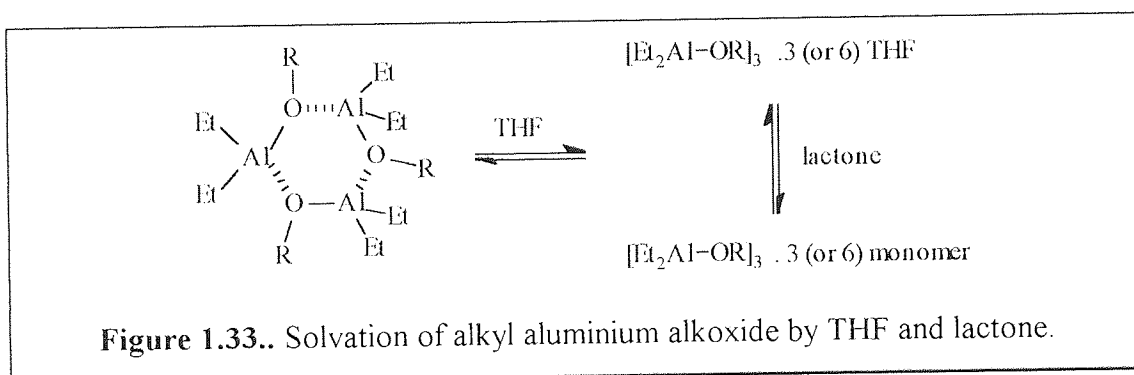
Biela and Duda ⁽¹⁰⁶⁾ studied the effect of the solvent on the polymerisation of ϵ -caprolactone using dialkyl aluminium alkoxides. Using solvents of different dielectric constants and solvating power, benzene, THF and acetonitrile, it was found that the most polar solvent, acetonitrile breaks down the aggregates into not aggregated, i.e. reactive species. In both THF and benzene the equilibrium between aggregated (not reactive/dormant) and unaggregated species still persists but at low concentrations the amount of aggregated species may be negligibly small.

Since both lactones and the active alkoxide centre are polar, an increase in the solvent dielectric constant (ϵ) should lead to an increase in the apparent rate of propagation. However Duda, ⁽¹⁰⁶⁾ noted the opposite to be true for alkyl aluminium alkoxides, that is the rate constant of propagation is lower in acetonitrile than in THF and benzene. This was attributed to the specific solvation of the growing alkoxide by the dipolar solvents. Consistent with the 'co-ordination-insertion' mechanism postulated for the polymerisation of lactones using alkyl aluminium alkoxides, substitution of toluene for more polar solvents such as THF, results in a reduction in the observed rate of polymerisation.⁽¹⁴⁴⁾

In pure toluene the ²⁷Al NMR of diethyl aluminium bromoethoxide shows only one absorption corresponding to a tetrahedrally co-ordinated aluminium atom.⁽⁷⁾ This is consistent with the trimer reported for ethyl substituents on aluminium alkoxides. Dimers may also be present but ²⁷Al NMR cannot differentiate between the two species. When a lactone is added, a new peak is observed corresponding to an octahedral aluminium which is attributed to the solvation of the aluminium by two lactone molecules or the dissociation of the trimer into single alkoxide species. Since the alkoxide is known to remain in the aggregated state during the polymerisation the former hypothesis is likely to be true.



A similar experiment carried out in THF indicates two new additional ^{27}Al NMR peaks which can be attributed to alkyl aluminium alkoxide trimers solvated by one THF per aluminium, or two THF molecules per alkyl aluminium alkoxide trimer. Again when a lactone is added, another peak is observed attributable to solvation of the initiator by the lactone. These peaks indicate competition between the solvent and monomer for the solvation of the aluminium atoms.



Intermacromolecular aggregation interactions are apparently not disturbed by the presence of a lactone or other monomer. The active alkyl aluminium monoalkoxide species in THF in the presence or absence of monomers participate in a dynamic aggregation equilibrium. When a lactone is added to the alkyl aluminium monoalkoxide solution in THF, a cyclic trimer solvated by the monomer is formed. The lactone insertion does need a fast reversible dissociation of the monomer solvated aggregates in order to insert into the active alkoxide bond since the aggregates are an inactive species. Propagating alkoxide sites are stabilised by

intermolecular co-ordinative associations, the cyclic trimers illustrated in figure 1.31 above and by association with THF.

1.3.9. Telechelic polyesters from aluminium alkoxide initiated polymerisations.

In section 1.3.2. it was mentioned that bimetallic μ -oxoalkoxides and aluminium isopropoxide initiate the polymerisation of lactones in such a way that the acyl oxygen bond of the lactone is cleaved. It is characteristic of this mechanism that the alkoxide group of the initiator forms the 'dead' end of the polymer. Thus using carefully selected alkoxide groups for the initiator, it is possible to form a wide range of telechelic polyesters.

Teyssie⁽¹⁴⁵⁾ reported that the end functionalisation of poly(ϵ -caprolactone) using alkoxide initiators could be extended to other polymerisable lactones such as δ -valerolactone and β -propiolactone, and lactides. They also reported that α -hydroxy, ω -X functional poly(ϵ -caprolactone) can be coupled in quantitative conversions with an aromatic diisocyanate or an aromatic diacid chloride. An α,ω -X-functional poly(ϵ -caprolactone) of double the previous molecular weight was thus obtained.

One of the most widely formed telechelic poly(lactones) synthesised using aluminium alkoxides is the vinylic terminated polymer.^(116, 120) A wide variety of functional aluminium alkoxides have been used for the synthesis of telechelic polymers and some of these have been summarised in table 1.7.

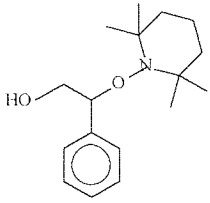
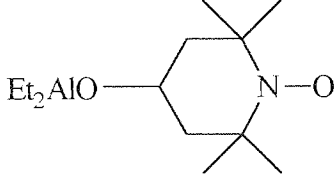
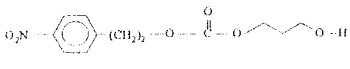
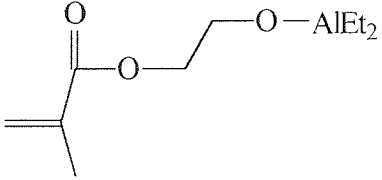
| Alkoxide group | Functional Polymer | Reference |
|----------------------------------------------------------------------------------------|--------------------------------------------------------------------------------------|-----------|
| $(\text{CH}_3\text{CH}_2)_2\text{AlOCH}_3$ | PCL-OMe | 113, 116 |
| $(\text{CH}_3\text{CH}_2)_2\text{AlOCH}_2\text{CH}=\text{CH}_2$ | PCL-O- $\text{CH}_2\text{CH}=\text{CH}_2$ | 113, 116 |
| $(\text{CH}_3\text{CH}_2)_2\text{AlO}(\text{CH}_2)_2\text{Br}$ | PCL-O- $(\text{CH}_2)_2\text{Br}$ | 113 |
| $(\text{CH}_2)_{10}\text{Br}$ | PCL-O- $(\text{CH}_2)_{10}\text{Br}$ | 111 |
| $\text{CH}_3\text{CH}_2\text{AlOCH}_2\text{CH}_2\text{CH}=\text{CH}_2$ | PCL-O- $\text{CH}_2\text{CH}_2\text{CH}=\text{CH}_2$ | 114 |
|  | TEMPO terminated PCL suitable for ATRP with styrene and other vinylic monomers | 132 |
|  | TEMPO terminated PCL suitable for ATRP with styrene and other vinylic monomers | 115 |
| $\text{O}_2\text{N}-\text{C}_6\text{H}_4-(\text{CH}_2)_2-\text{AlEt}_2$ |  | 133 |
| $\text{Si}-\text{O}-\text{AlEt}_2$ | | 114 |
| $\text{PHB}-\text{O}-\text{AlEt}_2$ | PHB- <i>b</i> -PCL | 134 |
| $\text{H}_2\text{C}=\text{CH}-\text{C}_6\text{H}_4-\text{CH}_2-\text{O}-\text{AlEt}_2$ | | 114 |
|  | Methacryloyl terminated poly(ϵ -caprolactone) | 114, 120 |

Table 1.7. Functional polymers synthesised using aluminium alkoxides

The synthesis of functional polymers using aluminium alkoxides follows the same mechanism as that of normal polymers.

Jerome⁽¹³²⁾ and Osagawa⁽¹¹⁵⁾ have both synthesised by different routes poly(ϵ -caprolactone) with a 2,2,6,6-tetramethylpiperidine-1-oxyl (TEMPO) end group. This allows the formation of poly(ϵ -caprolactone) co-polymers with vinylic monomers such as styrene. In both cases this TEMPO supported PCL was used as a polymeric counter radical for the radical polymerisation of styrene with quantitative efficiency.

Jerome and co-workers used two different approaches to the synthesis, both resulting in the same product, a poly(styrene)-*b*-poly(ϵ -caprolactone) co-polymer. In the first method, 4-hydroxy-TEMPO was reacted with aluminium triisopropoxide to form an aluminium alkoxide initiator (figure 1.37). This was subsequently reacted with ϵ -caprolactone resulting in a TEMPO terminated poly(ϵ -caprolactone) polymer. Subsequently, 'living' free radical polymerisation atom transfer radical polymerisation (ATRP) was utilised in order to polymerise styrene to form the co-polymer. The reverse route was also used, with styrene being polymerised first prior to the aluminium alkoxide polymerisation of ϵ -caprolactone.

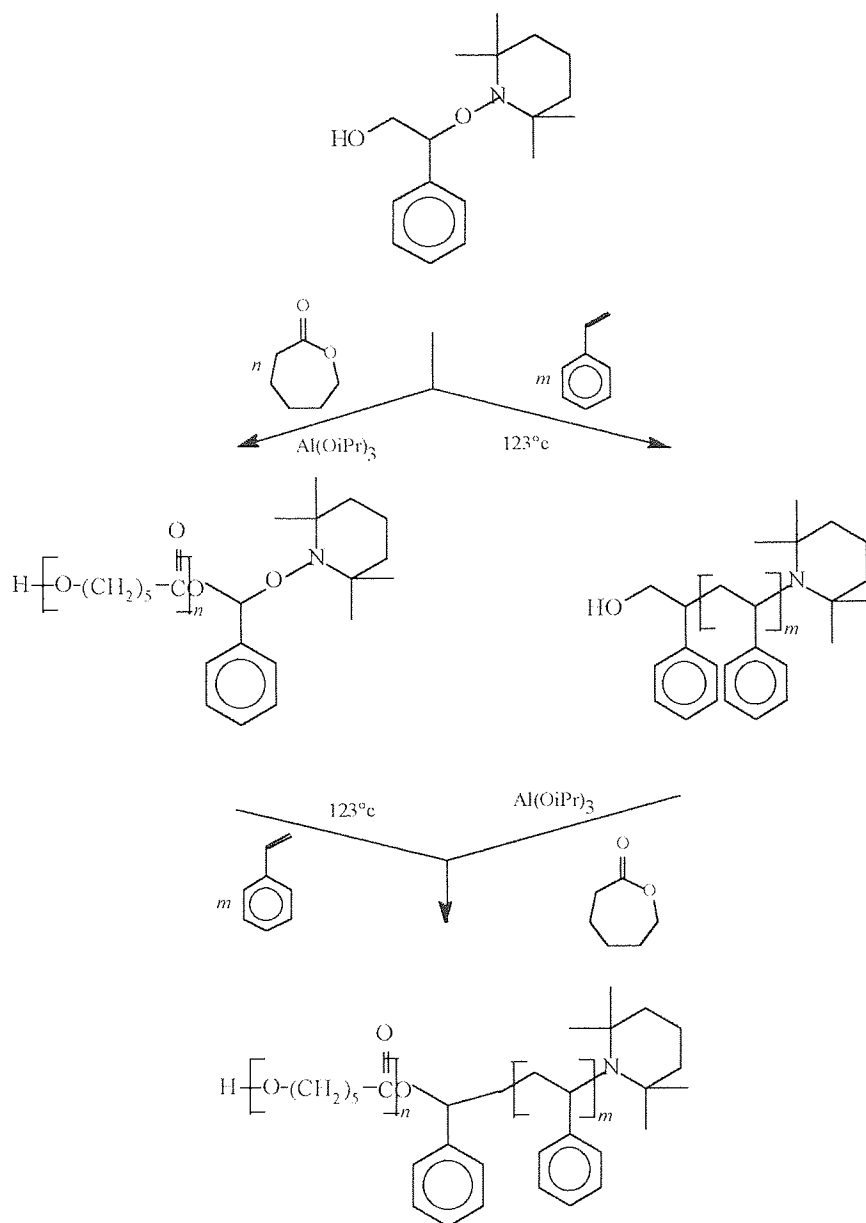


Figure 1.34. Formation of PS-PCL diblock co-polymers using aluminium alkoxides and ‘living’ radical polymerisation.

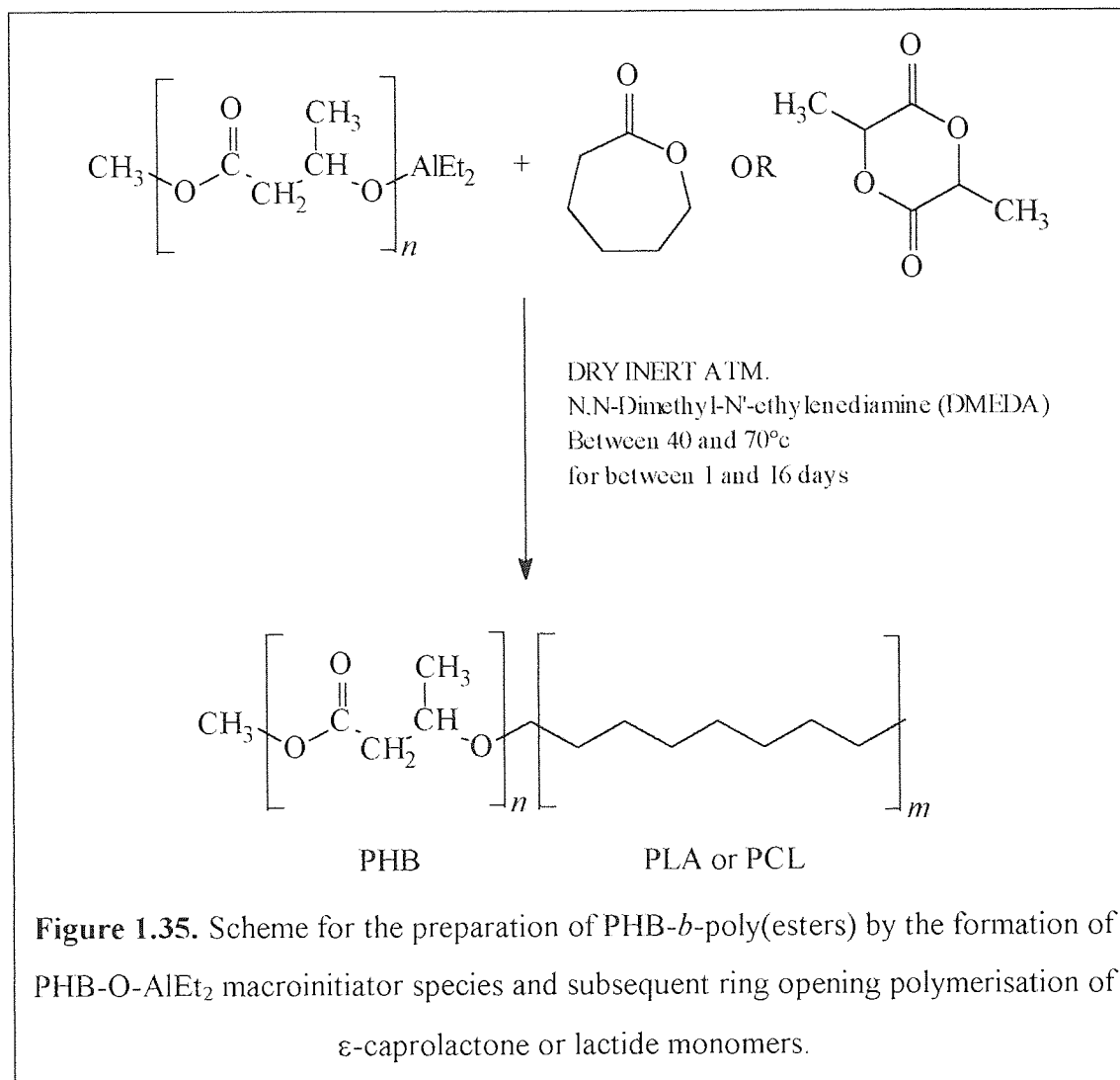
In a second method, tribromoethanol, was reacted with triethyl aluminium to form an alkoxide initiator which was used to form tribromo substituted poly(ϵ -caprolactone). This bromo functionality was subsequently utilised in the ATRP of methylmethacrylate using a nickel catalyst, resulting in a PMMA-*b*-PCL co-polymer.

In a similar method, Yoshida and Osagawa⁽¹¹⁵⁾ used 4-hydroxy TEMPO and reacted this with triethyl aluminium. They found that reacting 4-hydroxy TEMPO

with triethyl aluminium in a 1:1 ratio produced an inactive initiator. This was due to TEMPO being unable to exist with the strong basicity of the alkyl aluminium, probably producing an inactive amine compound. Secondly they reacted triethyl aluminium with a three molar equivalent of 4-hydroxy-TEMPO. This did result in an initiator which was suitable for the ring opening polymerisation of ϵ -caprolactone. This resulted in a TEMPO terminated polymer which was reacted with styrene using benzoyl peroxide to form a diblock co-polymer.

1.3.10. Synthesis of block co-polymers using alkoxide macroinitiators.

A natural extension to the use of functional alkoxides to produce telechelic polymers is to use a macroinitiator in order to form a block co-polymer, in effect a poly(lactone) with another polymer as end group. Gross and co-workers⁽¹³⁴⁾ reacted low molecular weight ($M_n = 2200$) PHB which had been degraded from a molecular weight of 121000 by acid catalysed methanolysis. The PHB-O-AlEt₂ macroinitiator was subsequently reacted with either ϵ -caprolactone or lactide to yield a diblock co-polymer of predictable molecular weights (figure 1.35).



In his paper concerning the formation of hydroxy terminated polymers, Teyssie⁽⁹²⁾ reported the use of short dialcohol units and alkyl aluminium to form a difunctional initiator. This was then reported to have been used as initiator for the ring opening polymerisation of ε-caprolactone forming a triblock copolymer with a central alkyl block. As a final paragraph to this paper, the possibility of using α,ω-dihydroxy prepolymers as the diol was briefly mentioned. This would lead to the possibility of the formation of a triblock copolymer consisting of lateral biodegradable PCL chains.

1.3.11. 'Immortal' Polymerisation of ϵ -caprolactone.

A rather interesting paper was published by Inoue and co-workers.⁽¹¹⁷⁾ They reported the polymerisation of ϵ -caprolactone using (5, 10, 15, 20 tetraphenylporhinato) aluminium alkoxide $\{(TPP)AlOR\}$ (figure 1.36). The polymerisation of ϵ -caprolactone proceeded even in the presence of protic species such as alcohols which would be expected to terminate a polymerisation initiated with a more conventional aluminium alkoxide.

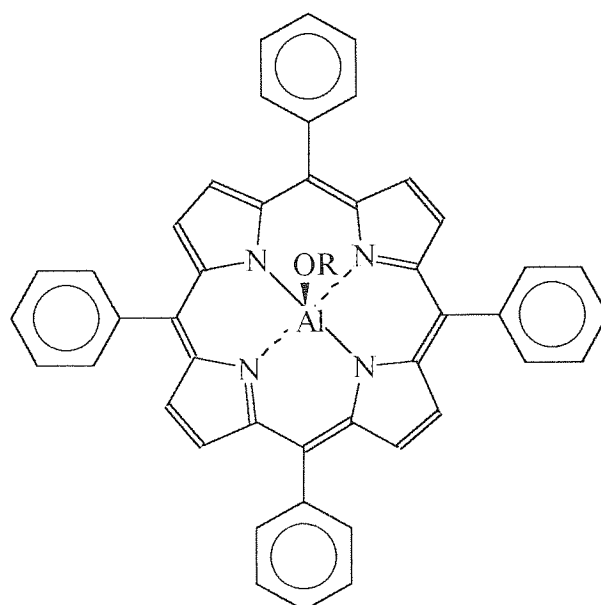


Figure 1.36. (5, 10, 15, 20 tetraphenylporhinato) aluminium alkoxide.

ϵ -Caprolactone was polymerised using $\{(TPP)AlOMe\}$ and quantitative conversion was obtained in around 13 days at 50°C without using solvent. Methanol was present in the system in a ratio of $\{(TPP)AlOMe\}/MeOH = 1/9$ and $\{(TPP)AlOMe\}/\epsilon\text{-CL} = 200$. A value of M_n of 2100 and M_w/M_n of 1.12 was achieved. It is reported that the number of polymer molecules was equal to the sum of the number of aluminium and methanol molecules. Thus the 'immortal' polymerisation of ϵ -caprolactone in the presence of methanol is apparent.

1.4. Plan for experimental work.

The use of alkyl aluminium alkoxides as initiators for the polymerisation of lactones and lactides gives a route to polyesters that is largely free of side reactions such as transesterification ^(68, 92, 106, 110-124, 135-137). Penzcek⁽¹¹⁶⁾ found that bulkier alkoxide groups such as isobutyl help promote the growth of linear polymers compared to less bulky alternatives such as ethyl. The effect of altering the structure of the alkoxide group has also been investigated and is reported to have no effect on the polymerisation ^(111, 124, 143). Most of the alkoxides investigated in this context however have been small, linear alkoxides such as methoxy, ethoxy and *n*-propoxy. A greater variety of alkoxide groups have been used to synthesise functional terminated poly(ϵ -caprolactone) although little appears to have been reported as to the effect of these groups on the kinetics of the polymerisation. Benzene appears to have been a successful solvent for the polymerisation of ϵ -caprolactone using alkyl aluminium alkoxide initiators although THF and acetonitrile have also been used ^(106, 144).

In order to help elucidate the mechanism of the polymerisation of ϵ -caprolactone, a series of homo-polymerisations using an alkyl aluminium alkoxide initiator will be carried out. It is proposed that by varying the alkoxide group structure, using linear, branched and cyclic aliphatic alkoxides, in addition to aromatic alkoxides will help achieve this. The reaction solvent will be varied using polar and non-polar solvents, and solvents capable and incapable of co-ordinating with the initiator. The structure of the alkyl group will also be varied.

Gross (134) used hydroxy terminated PHB to form an alkyl aluminium alkoxide initiator that was used to initiate the polymerisation of lactide or ϵ -caprolactone. A dihydroxy terminated PHBV should therefore be able to be used to form an aluminium alkoxide initiator that can be reacted with ϵ -caprolactone to form an ABA type triblock co-polymer. The best reaction conditions for this reaction should have

been identified by the preceding work involving the homo-polymerisation of ϵ -caprolactone.

Chapter 2.

Experimental Techniques.

2.1. Purification of materials.

2.1.1. Solvents.

2.1.1.1 THF

Tetrahydrofuran was purchased from Fisher Chemical Co. as HPLC grade. For use as a solvent in polymerisations it was dried over calcium hydride and distilled under vacuum at room temperature.

2.1.1.2. Toluene

Toluene was obtained from Fisher Chemical Co. as standard lab. grade. For use as a solvent in polymerisations it was dried over calcium hydride and distilled under vacuum at room temperature.

2.1.1.3. Dichloromethane

Dichloromethane was bought from Romil Chemicals Company, unstabilised 99.9% purity. It was dried over calcium hydride and distilled under argon into a dried flask immediately before use.

2.1.1.4 2,4-Pentandione

2,4-Pentandione was obtained from Aldrich Chemical Co, stored in a refrigerator and used as supplied.

2.1.1.5. Methanol.

Methanol was supplied by Fisher Chemical Co, and used as supplied for the precipitation of polymers.

2.1.1.6. *N,N*-Dimethylformamide.

Supplied as HPLC grade by Fisher Chemical Company. The solvent was dried over calcium hydride and then distilled under vacuum at room temperature using a vacuum line.

2.1.2. Drying agents

2.1.2.1 Calcium Hydride

Purchased from Avacado Research Chemicals and used as supplied.

2.1.2.2. Phosphorus pentoxide

From Aldrich Chemical Co. Used as supplied.

2.1.2.3 Sodium metal

Washed with *n*-hexane to remove oil. Tarnished surfaces were removed and the metal was pressed into wire.

2.1.3. Monomers

2.1.3.1 ϵ -caprolactone

Supplied by Lancaster Synthesis Ltd. as 99+%. Dried overnight over calcium hydride and distilled under reduced pressure, (0.05-0.2mm Hg, approx. 60°C). Stored in a desiccator under argon.

2.1.3.2 δ -valerolactone

Supplied by Lancaster Synthesis Ltd. as 99% purity. Dried overnight over calcium hydride and distilled under reduced pressure, (0.05-0.2mm Hg, approx. 45°C). Stored in a desiccator under argon.

2.1.3.3. Poly(hydroxybutyrate-co-valerate) (PHBV) diol. $M_n=1500$

Supplied by Monsanto. Dried under vacuum at 40°C for 48 hours prior to use.

2.1.4. Others

2.1.4.1 *N,N*-Dimethyl-*N*-ethylethylenediamine (DMEDA).

Supplied by Aldrich Chemical Co. Dried over calcium hydride and distilled under vacuum.

2.1.5. Initiators

2.1.5.1 *Triisobutyl aluminium.*

Supplied by Aldrich Chemical Co. as 99+% purity in a 'sure-pac' metal cylinder and used as supplied. Transferred to the required vessel using Schlenk techniques.

2.1.5.2 *Alkyl aluminium alkoxide*

Synthesised by the following method.

Alkyl aluminium alkoxides were prepared by reaction of an alcohol and trialkylaluminium⁽¹²⁴⁾. The selected alcohol was slowly injected through a rubber septum into a flask containing a 0.31M solution of *triisobutylaluminium* in toluene. The flask had been previously dried at 240°C, flamed and purged with argon. The solution was stirred at room temperature for 3 hours. The reaction vessel was maintained at atmospheric pressure throughout.

Synthesis of aluminium monoalkoxides relied upon the stoichiometric reaction of *triisobutyl aluminium* with a molar equivalent of the appropriate alcohol. Similarly, the preparation of aluminium dialkoxides required the reaction of a 2 molar equivalent of alcohol with $\text{Al}(\text{iBu})_3$. Once formed, alkyl aluminium alkoxide initiators were used immediately.

2.1.3.3. *Macro initiators*

Synthesised by the following method.

Poly(hydroxybutyrate-co-valerate) (PHBV) diol macroinitiators were prepared by addition of *triisobutylaluminium* to the previously dried PHBV diol⁽¹³⁴⁾

Triisobutylaluminium was added to excess of *N,N*-Dimethyl-*N*-ethylethylenediamine (DMEDA) in a 1:2 ratio (1.3×10^{-3} : 2.6×10^{-3} mol) in 2 cm^3 of dichloromethane. In a separate ampoule 1.0 g (6×10^{-4} mol) of dried PHBV diol was dissolved in 15 cm^3 of dichloromethane. The PHBV solution was then transferred to the ampoule containing the alkyl aluminium/DMEDA/dichloromethane solution using a dried syringe and the mixture stirred for 3 hours at room temperature.

2.2. Polymerisation Methods

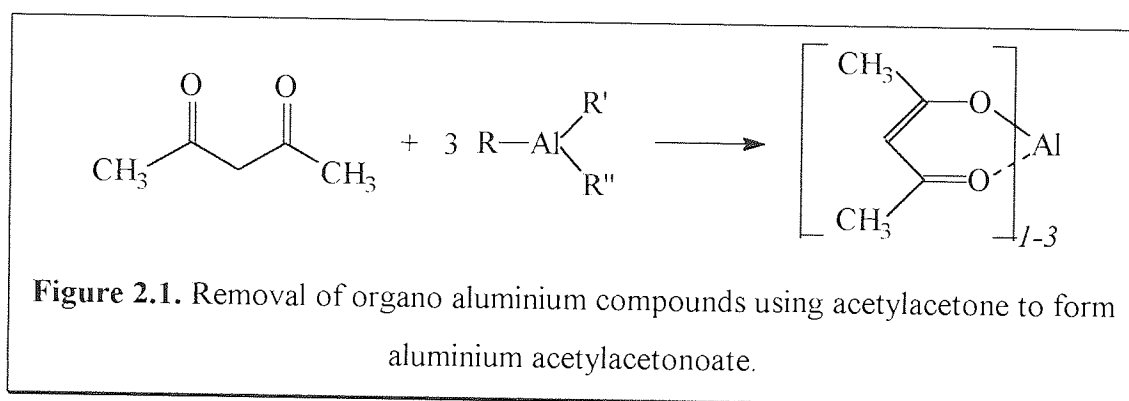
2.2.1 Homo-polymerisations.

A previously dried reaction vessel equipped with a greaseless PTFE tap was used for polymerisations. The required solvent was distilled directly into the reaction flask either from the dichloromethane still or from a vacuum line for all other solvents. The monomer and then the initiator were subsequently transferred into the reaction vessel using a dried glass syringe under an argon blanket. The polymers synthesised were isolated by precipitation in an approximately a 10 fold excess of cold methanol. The solid polymer was removed by filtration and then dried under vacuum at 50°C for 24 hours.

2.2.2. Co-polymerisations

Block co-polymers were formed by using a macroinitiator. The macroinitiator was first formed by the method described in section 2.1.3.3. After the macroinitiator had been formed by stirring triisobutyl aluminium, PHBV diol and DMEDA together in DCM for 3 hours at room temperature, the required amount of monomer was added by a dry glass syringe using the Schlenck technique. Co-polymerisation took place and co-polymers were isolated by precipitation in cold methanol and then removed via vacuum filtration with a cold sintered glass funnel. This technique did not necessarily destroy the Al-O bonds in the initiator. In order to

remove any remaining organo aluminium compounds the product was redissolved in approximately 75cm³ of 2,4-pentanedione (AcAc). The carbonyl groups of the AcAc co-ordinated with the aluminium atoms which were then removed. The AcAc/PHBV-*b*-PCL slurry was dissolved in chloroform and then reprecipitated in the normal way. The solid polymer was then removed by filtration before being dried under vacuum at 50°C for 24 hours.



2.2.3. Sampling reactions.

Polymerisations of this type are extremely sensitive to traces of moisture and it is very difficult to extract samples of the polymerising system by syringe without destroying some of the catalyst sites in the remaining liquid. To overcome this problem an apparatus was developed to enable sample extraction without contaminating the remaining liquid. The apparatus used for this procedure is shown in figure 2.2. it differed from normal systems by containing a side arm constructed from a glass HPLC column. Samples could then be removed from the reaction without introducing impurities through the Omnifit using a syringe. The vessel was kept at atmospheric pressure throughout using an argon bubbler.

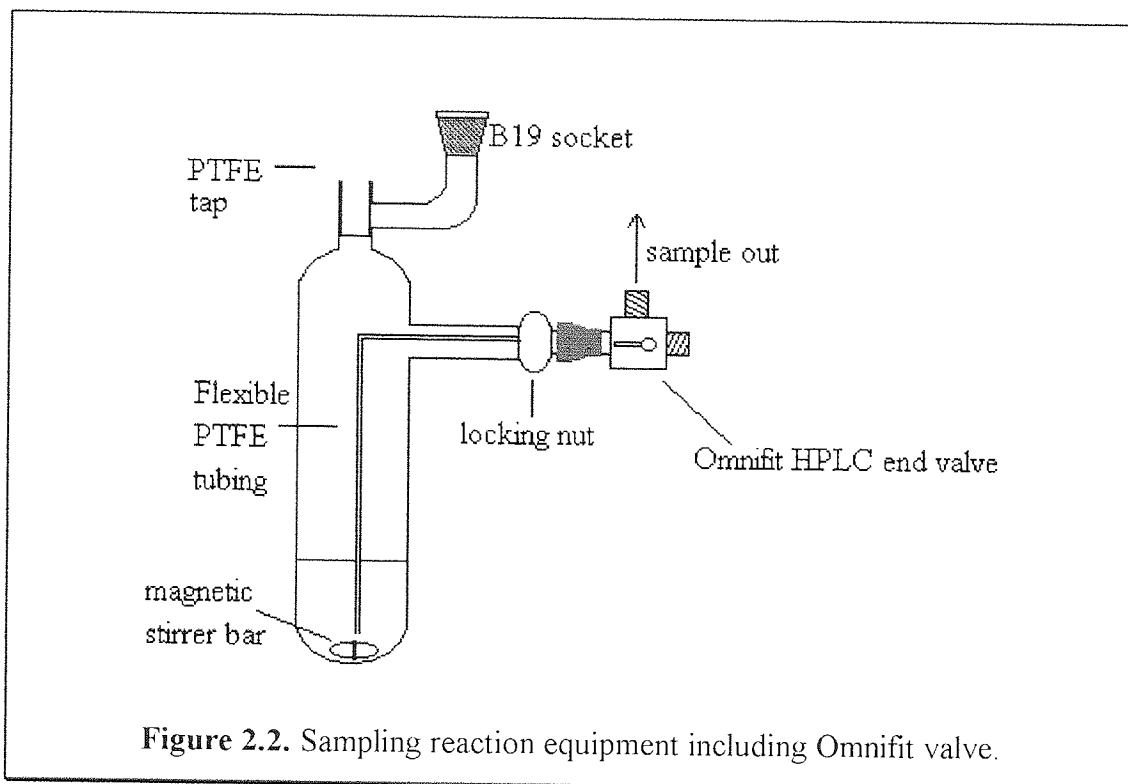


Figure 2.2. Sampling reaction equipment including Omnifit valve.

The preparation of the polymer solution was identical to that described previously.

2.3. Techniques for handling air sensitive materials.

Living polymerisations are by nature, extremely sensitive to impurities including oxygen and moisture. Solvents and reactants, where necessary, should be handled in air free conditions. These can be achieved by using high vacuum techniques or alternatively under an inert atmosphere using Schlenk techniques.

All glassware used for polymerisations, solvents, monomers and initiators was cleaned thoroughly with toluene and acetone to remove any organic or polymer residues. It was then soaked in Decon 90 to and then rinsed with acetone and dried at 240°C in an oven for at least 24 hours. It was then flamed under vacuum and flushed with argon before use.

2.3.1. Vacuum Line techniques.

A larger vacuum line was used for trap to trap distillation of solvents than for small amounts of reactants in order to save time. The main body of the vac line (see fig 2.3.) consisted of a glass manifold connected to taps and joints to which flasks could be attached. The manifold was connected to a Leybold rotary pump via a large PTFE tap and a mercury diffusion pump connected in series. When these were used in combination pressures as low as 10^{-5} mmHg could be achieved, as measured using a Vacustat[®].

Liquid nitrogen traps were used either side of the mercury diffusion pump, which served to prevent contamination of the atmosphere and to condense vapour coming from the manifold during evacuation of the manifold.

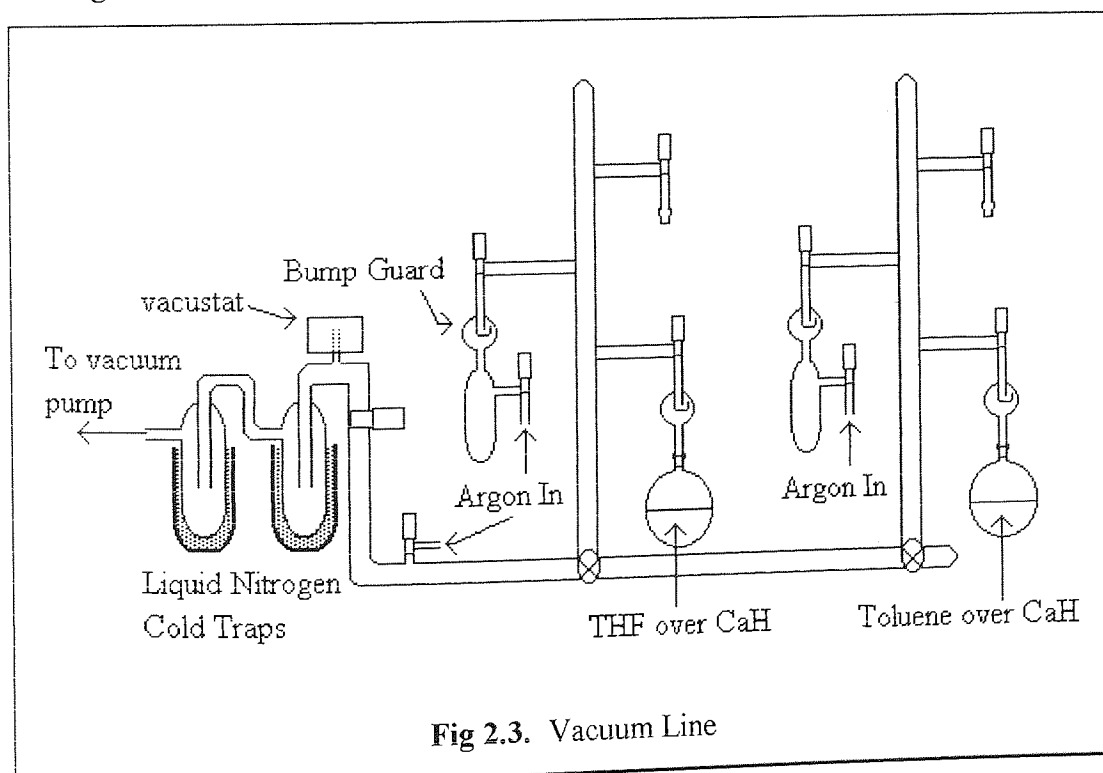


Fig 2.3. Vacuum Line

2.3.2. Freeze-thaw degassing

In order to distil liquids efficiently under high vacuum they first need to be thoroughly degassed. The freeze thaw technique of degassing was carried out by

immersing the vessel containing the solvent in liquid nitrogen, therefore freezing the liquid. Once frozen, the vessel was then opened to the vacuum line and evacuated completely. The vessel was then sealed and the contents allowed to thaw, thus releasing any dissolved gasses. This procedure was then repeated several times until the pressure in the manifold showed no increase when the flask containing the frozen liquid was opened to it.

In some cases, this technique may be unsuitable. Such would include when the flask containing the liquid is too large to fit into a Dewar, as when using the solvent line, or when toluene is being distilled. Toluene has a tendency to form a glass when frozen, which may lead to the vessel cracking whilst the toluene thawed. In these cases the vessel is opened directly to the pump resulting in the liquid bubbling as dissolved gases are evolved. The tap was closed when the bubbling subsides into a slow distillation into the traps. Whilst this technique is not ideal in some cases it is the only option available.

2.3.3. Trap to trap distillation

Degassed liquids can be distilled from vessel to vessel using a technique known as trap to trap distillation. A flask containing degassed solvent was attached under vacuum to the manifold and a reaction vessel was attached to the vacuum line and evacuated before emersion in liquid nitrogen contained in a Dewar. The main tap on the manifold is closed, the tap of the liquid containing vessel is opened and the required volume of solvent is allowed to distil into the receiver flask.

2.3.4. Schlenk techniques

In order to handle sensitive materials under an inert atmosphere, vessels which required addition of further reagents were connected to an argon line. A slight positive pressure of argon was maintained whilst the vessel was opened, usually by the removal of a greaseless tap. Argon was then allowed to flow through the body

of the tap such that the flow prevented contamination by back diffusion of moisture and oxygen. The tap to the apparatus was removed and the materials could be added or removed using a dry syringe with an argon stream flowing.

2.3.5 Argon dry box

A dry box was supplied by Halco Engineering Ltd. to enable materials to be stored and handled under a dry, inert atmosphere. The dry box maintained an argon atmosphere which was continuously recycled through absorbent columns to remove oxygen and moisture. A BASF R311 catalyst was used to remove oxygen and a 3 Å molecular sieve to absorb water. A double door port was used to place and remove vessels from the dry box without contaminating the main atmosphere. The inner door was sealed, the outer door opened and the apparatus placed in the port. The port was evacuated and filled with argon three times before the inner door was opened.

2.4. Analytical Techniques.

2.4.1 Gel Permeation (Size exclusion) Chromatography.^(41, 135)

Gel Permeation Chromatography (GPC) is normally used as an analytical procedure for separating molecules according to their size and to obtain molecular weight averages (M_n , M_w) or information on the molecular weight distribution of polymers. The method depends on the use of mechanically stable, highly cross-linked gels, which have a distribution of different pore sizes and can, by means of a sieving action, effect separation dictated by molecular volume of a polymer sample.

The non-ionic gel stationary phase is comprised of cross-linked polystyrene particles which do not significantly swell in the carrier solvent. A range of pore sizes is fundamental to the success of the size fractionation, which depends on two

processes. These processes are, separation by size exclusion, which is the most important and a dispersion process, controlled by molecular diffusion which may lead to artificial broadening of the molecular weight distribution.

The separation process can be explained as a solute band being moved along the column by the solvent. The solute molecules repeatedly diffuse in and out of the pores of the packing during this passage. Larger solute molecules, which have the largest effective volume in solution, elute faster than smaller molecules because they are less able to penetrate the pores of the column packing. Solutes of two quite distinct sizes can be resolved into two peaks shown on the resulting chromatogram. All peaks detected are of a finite width. Even for solutes of the same size, the elution peak will be broader than expected because of the mixing effects in the injector, column, detector and connecting tubing.

The system used consists of a Knauer HPLC 64 pump and a filter before a Polymer Laboratories 5 μ m pre column in order to remove any suspended particles. Two Polymer Laboratories columns, one mixed bed and one with an exclusion limit of 10⁴Å were connected in series. This was later changed when the uniform pore size column was replaced by another mixed bed column in order to improve resolution. Unstabilised HPLC grade THF was pumped through the system at 1 cm³ min⁻¹. An Alltech recycler was fitted to prevent wastage of solvent. The eluent was monitored by a Knauer differential refractometer and a Perkin-Elmer LC 85B variable wavelength spectrometer which were connected in series. The refractometer and UV detector were connected to a Polymer Laboratories DCU and a PC running PL Caliber version 7.1 software to analyse the data. Only the differential refractometer was used because the polymers synthesised showed no suitable λ_{\max} .

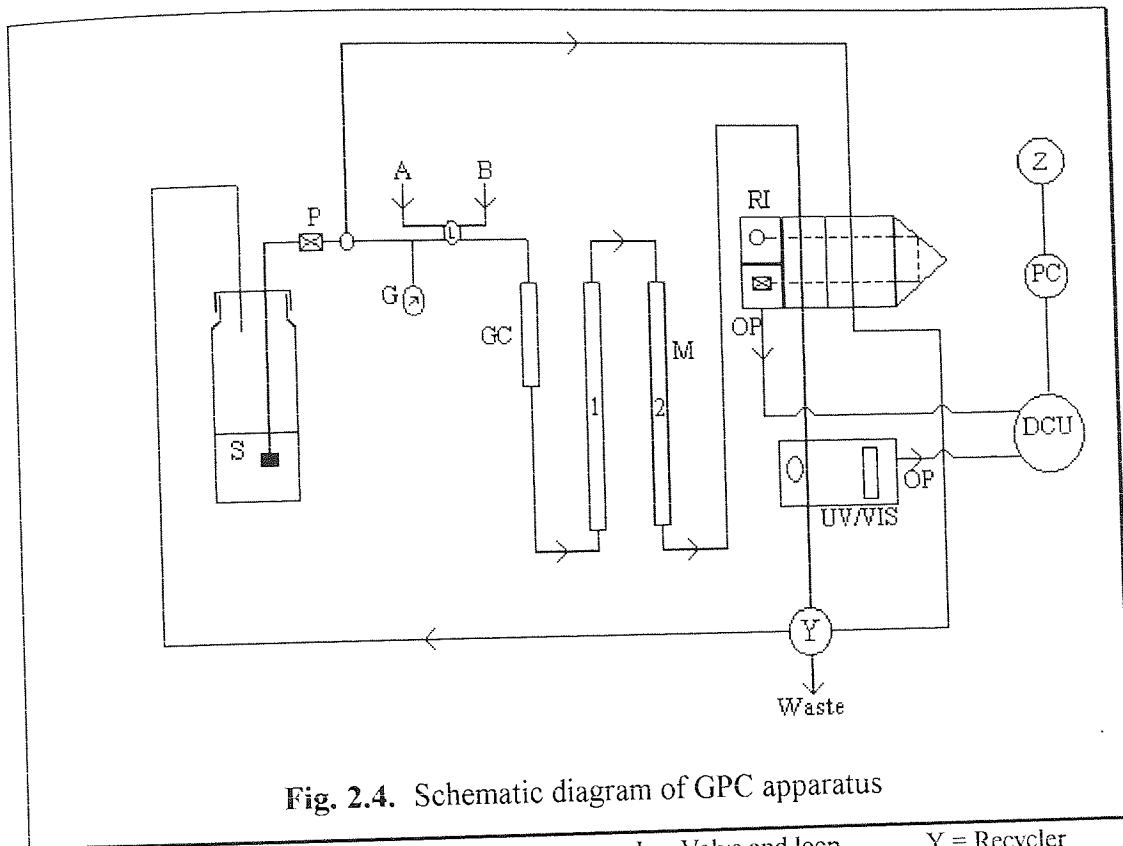


Fig. 2.4. Schematic diagram of GPC apparatus

| | | | |
|-----------------------|----------------------|--------------------------|-----------------------------|
| S = Solvent reservoir | A = Injection port | L = Valve and loop | Y = Recycler |
| | | Injector | |
| P = Pump | B = Waste | GC = Guard or pre column | DCU = Detector control unit |
| G = Pressure gauge | OP = Output | RI = Refractometer | PC = Computer |
| X = Valve | M = Mixed bed column | UV/VIS = Spectrometer | Z = Printer |

Further to this, samples of copolymers were sent for analysis by GPC using chloroform as a solvent at RAPRA Technology Ltd. The system used there was the same as the system used at Aston.

2.4.1.1. Molecular weight determination.

The raw data GPC curve is actually a molecular size distribution curve, unless a concentration sensitive detector is used and then the GPC curve is a distribution curve in weight concentration. With calibration data, the raw data is converted into a

molecular weight distribution curve and the respective molecular weight can be calculated.

A convenient method of measuring the 'average' chain length in a polymer sample gives a value known as M_n , the number average molecular weight. M_n has historically been measured by methods such as vapour phase osmometry, membrane osmometry, boiling point elevation or by end group determination from titration. One of the advantages of methods such as these lies in the fact that they are absolute. That is they give actual molecular weights without calibration. Molecular weights determined by GPC are only absolute if the necessary calibration was carried out with standards of the same molecular type. If not, the molecular weights are often given as relative to a poly(styrene) standard.

M_n has been defined as the mass of the sample in grams, $\sum W_i$ or $\sum N_i M_i$ divided by the total number of chains present N , which is $\sum N_i$. Where W_i and N_i are the weight and number of molecules of molecular weight M_i , respectively, and i is an incrementing index over all molecular weights present.

Therefore

$$M_n = \frac{\sum N_i M_i}{\sum N_i} = \frac{\sum W_i}{\sum (W_i / M_i)} \quad 2.1.$$

and from GPC

$$M_n = \frac{\sum_{i=1}^N h_i}{\sum_{i=1}^N (h_i / M_i)} \quad 2.2.$$

where h_i is the GPC curve height at the i th volume increment and M_i the molecular weight of the species eluted at the i th retention volume. This is assuming

that h_i is proportional to solute concentration and M_i is sampled in equal volume increments.

M_w , the weight average molecular weight is defined as follows,

$$M_w = \frac{\sum NiM_i^2}{\sum NiMi} = \frac{\sum WiMi}{\sum Wi} \quad 2.3.$$

and from GPC,

$$M_w = \frac{\sum_{i=1}^N (hiMi)}{\sum_{i=1}^N hi} \quad 2.4.$$

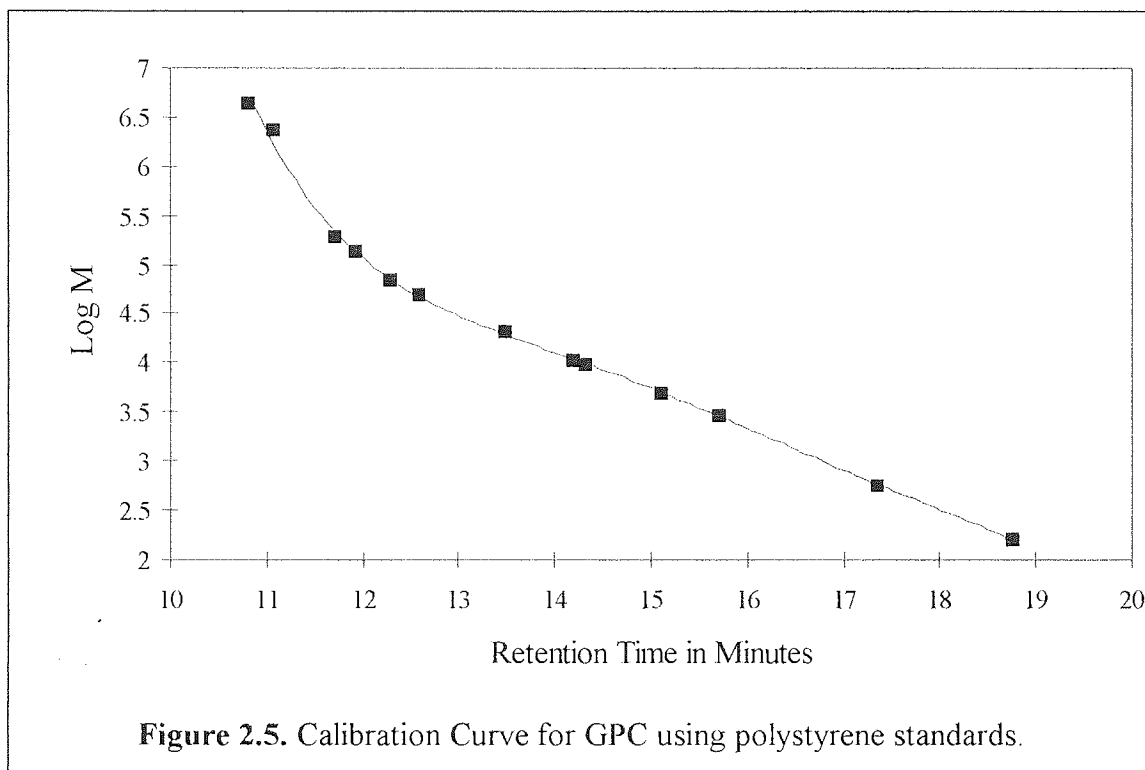
The value of M_w is always bigger than M_n , except for samples which are monodisperse, when they are identical.

The ratio M_w/M_n is a measure of the width of the polymer molecular weight distribution, being equal to 1 for a monodisperse system and very large for a cross linked polymer.

A more general and meaningless value M is often used. This is often used to denote the general term molecular weight rather than the more specific weight or number average molecular weight.

2.4.1.2. Calibration of GPC

In order for the elution volume to be correlated to the molecular weight of the polymer sample



In order to obtain values for M_i in equations 2.1 to 2.4 it was necessary to determine how the molecular weight of eluted polymer varied with elution volume. This was achieved by calibrating the columns using polystyrene standards of known molecular weight and molecular weight distribution ($\overline{M}_w/\overline{M}_n$) less than 1.1. The logarithm of the molecular weight was plotted against elution volume and a 5th order polynomial equation obtained. Figure 2.5. shows the calibration curve obtained.

Since the hydrodynamic volume of a given molecular weight varies with polymer type, this calibration only provides absolute molecular weights for samples of polystyrene. However it is possible to obtain molecular weights for polymers other than the calibrant by using the universal calibration method.

2.4.1.3. Universal Calibration.

A universal calibration curve is obtained by plotting $\log[\eta].M$ against the retention volume V_r , for a given carrier solvent and temperature. A universal calibration curve can be constructed to relate V_r , which depends on the interstitial void volume and M , assuming that the hydrodynamic volume of a macromolecule is related to the product $[\eta].M$, where $[\eta]$ is the intrinsic viscosity for the polymer in the solvent used at a given temperature. The absolute molecular weight may then be calculated using the following method. If the universal calibration curve is valid then,

$$\log [\eta]_s M_s = \log [\eta]_u M_u \quad 2.5.$$

where u and s denote the unknown and standard respectively. Since chains of equal molar mass will swell differently in the same solvent to the standard, then the hydrodynamic volumes will not always be the same. A correction is therefore applied based on knowledge of the Mark-Houwink relations, $[\eta]_s = K_s M_s^{v_s}$. The molar mass is then

$$\log M_u = \frac{1}{1+v_u} \cdot \log \left[\frac{K_s}{K_u} \right] + \frac{1+v_s}{1+v_u} \cdot \log M_s \quad 2.6.$$

Therefore a calibration curve constructed for polystyrene standards can be used to determine M for other polymers if the Mark-Houwink Parameters are known.

2.4.2. Nuclear magnetic resonance spectroscopy.

Fourier transform high resolution ^1H and ^{13}C N.M.R. were carried out using a Bruker AC 300 spectrometer. Solutions of the samples were prepared in deuterated chloroform with a small quantity of tetramethyl silane as reference. For ^{13}C analysis

the P.E.N.D.A.N.T pulse technique was used, with methyl and methine carbons appearing as positive peaks and methylene and quaternary carbons as negative peaks. The spectra were analysed using WinNMR software supplied by Bruker.

Chapter 3.

The polymerisation of ϵ -caprolactone using alkyl aluminium alkoxide initiators.

In order to gain an understanding of the polymerisation of ϵ -caprolactone using dialkyl aluminium alkoxide initiators, it was necessary to establish the magnitude of effects that the following variables have on the polymerisation and its kinetics. Reaction medium, temperature, monomer and initiator structure have all been varied in an attempt to gain an understanding of the reaction mechanism. These variables have been dealt with in turn in the following three chapters.

3.1. The effect of the reaction medium on the polymerisation of ϵ -caprolactone using *diisobutyl aluminium isopropoxide* initiator.

3.1.1. Introduction.

Polymerisations of ϵ -caprolactone have been carried out using a toluene solution of *diisobutyl aluminium isopropoxide* as an initiator and solvents of different polarity and donating power. The reaction conditions were,

- Temperature 25°C
- $[\epsilon\text{-CL}] = 2.1 \text{ ml}^{-1}$
- $[I] = \text{varied}$
- Inert atmosphere
- Toluene solvent

Aliquots of a recorded volume were withdrawn from the reaction at timed intervals using the Omnifit apparatus described in chapter 2, section 2.2.3. The samples were removed and placed into a weighed beaker containing approximately 10ml of THF. Methanol was added to the THF/polymer solution in order to terminate the growing chains. The solvent was evaporated off in a fume cabinet and then the polymer was dried to a constant weight under vacuum at 50°C.

3.1.2. The polymerisation of caprolactone using toluene as a solvent.

| $[I]_0 \text{ ml}^{-1}$ | Time (mins) | % Conv | M_n | M_w | M_w/M_n |
|---------------------------------|-------------|--------|-------|-------|-----------|
| 3.6×10^{-2} (GKS06) | 4 | 4 | 5000 | 10400 | 2.1 |
| | 8 | 6 | 6500 | 10200 | 1.6 |
| | 15 | 17 | 11000 | 16000 | 1.4 |
| | 21 | 42 | 16800 | 21900 | 1.3 |
| | 42 | 62 | 18700 | 24900 | 1.3 |
| | 60 | 98 | 17400 | 26400 | 1.5 |
| 1.8×10^{-2} (GKS05) | 8 | 4.0 | 1900 | 3300 | 1.7 |
| | 18 | 16.3 | 4700 | 7500 | 1.6 |
| | 28 | 48.8 | 8400 | 11500 | 1.3 |
| | 34 | 87.6 | 15200 | 18900 | 1.3 |
| 1.0×10^{-2} (GKS27) | 20 | 1 | - | - | - |
| | 35 | 2 | - | - | - |
| | 60 | 3.6 | 2400 | 12700 | 2.4 |
| | 105 | 14.4 | 11900 | 18700 | 1.6 |
| | 125 | 69.4 | 14800 | 24100 | 1.6 |
| | 185 | 94.6 | 17500 | 25700 | 1.5 |
| 6.7×10^{-3} (GKS28) | 45 | 2.4 | - | - | - |
| | 65 | 2.0 | - | - | - |
| | 100 | 11.6 | 10000 | 13500 | 1.30 |
| | 150 | - | 14300 | 14300 | 2.0 |
| | 275 | 74.0 | - | - | - |

Table 3.1. Molecular weight and conversion data for the polymerisation of ϵ -caprolactone using toluene as a solvent.

The expected value for the molecular weight using the first initiator concentration ($[I]_0 = 3.6 \times 10^{-2} \text{ ml}^{-1}$) would be 6730 at 100% conversion. Since $M_n = 17400$ was obtained at 98% conversion it is likely that less than one chain is being initiated per alkoxide moiety, the actual $[I]$ is less than $[I]_0$. The polydispersity of

the sample narrows to 1.3 at the peak molecular weight at 42 minutes and then increases to 1.50 as molecular weight decreases. It is likely that some form of degradation of the polymer chain is taking place once maximum conversion has been achieved. Indeed the presence of transesterification reactions of lactides has been reported after quantitative conversion has been reached. ⁽¹²²⁾

At $[I]_0 = 1.8 \times 10^{-2} \text{ ml}^{-1}$ the molecular weight expected for this reaction would be 13300 at 100% conversion, but at 88% conversion the actual molecular weight is 15200. Again less than one chain is being initiated per alkoxide moiety, alternatively the molecular weights are relative to a poly(styrene) standard and it may be that these molecular weights are not actual. The polydispersity of these samples does narrow appreciably as the reaction proceeds from 1.7 to a narrower value of 1.3 as the reaction ends.

In the reaction carried out at $[I]_0 = 1.0 \times 10^{-2} \text{ ml}^{-1}$, the very small amount of polymer produced at the start of the reaction in the first two samples prevented any analysis by GPC being carried out. It is unlikely that such a low conversion is entirely due to the presence of initiator residue because polymer has certainly been produced. In this reaction, the initiator concentration was $[I] = 1.0 \times 10^{-2} \text{ ml}^{-1}$, so there would approximately 0.002 grams of initiator per 2ml aliquot removed from the reaction. This equates to 0.4% so any value for the percentage conversion over 0.4% undoubtedly contains polymer. The theoretical molecular weight would be around 26100 for this reaction, so it would appear that the molecular weight of the samples produced is too low, possibly because of more than one alkoxide moiety per aluminium centre being active. It is more likely that experimental error such as the addition of an excess of initiator is the cause however.

The molecular weights of polymers produced using toluene as a solvent do not appear to be the same as the values predicted from values of $[M]_0/[I]_0$. The initiator efficiency is less than 100%, there is less than one chain being initiated per alkoxide moiety. Any initiator aggregates may not be forming correctly, which may

lead to a quantity of inactive initiator being formed and inter initiator interactions may be the reason for this.

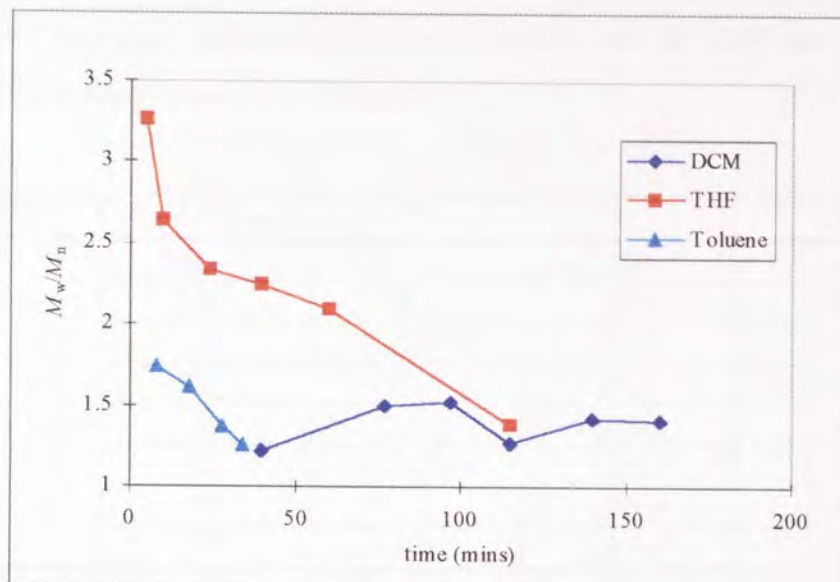


Figure 3.1. Effect of solvent on plot of M_w/M_n versus time for the polymerisation of ϵ -caprolactone in solvents of varying polarity

It is noticeable that the polydispersity of the samples decreases as the reaction proceeds. This is partly indicative of a living polymerisation system where the majority of polymer chains are formed very early in the reaction. Differences in chain length are greatest at the onset but narrow as polymerisation proceeds.

The theoretical molecular weight distribution M_w/M_n is given by equation 3.1.

(41)

$$M_w/M_n = 1 + v/(v+1)^2 \quad 3.1.$$

where v is the kinetic chain length.

Therefore as the chain lengthens, the theoretical molecular weight distribution narrows.

3.1.3. The polymerisation of ϵ -caprolactone using THF as a solvent.

In order to ascertain the effect of polarity and donor nature of the solvent on the propagation reactions, polymerisations were carried out in THF and the results compared with those obtained in toluene.

| $[I]_0$ ml ⁻¹ | Time (mins) | % Conv | M_n | M_w | M_w/M_n |
|---------------------------------|-------------|--------|-------|-------|-----------|
| 3.6×10^{-2} (GKS11) | 5 | 1.7 | 500 | - | - |
| | 9 | 8.3 | 1000 | 6000 | 5.9 |
| | 14 | 22.9 | 2100 | 8100 | 3.8 |
| | 22 | 29.2 | 5100 | 12500 | 2.5 |
| | 28 | 33.3 | 6800 | 14300 | 2.1 |
| | 37 | 54.2 | 11100 | 17900 | 1.6 |
| | 50 | - | 12200 | 20100 | 1.7 |
| | 60 | - | 13900 | 23000 | 1.7 |
| 1.8×10^{-2} (GKS02) | 15 | - | 4900 | 7900 | 1.6 |
| | 35 | 16.6 | 9220 | 13800 | 1.5 |
| | 50 | 48.9 | 10900 | 15500 | 1.4 |
| | 65 | 64.6 | 14800 | 18400 | 1.3 |
| | 80 | 70.8 | 15700 | 20800 | 1.3 |
| | 95 | 87.4 | 15800 | 21200 | 1.3 |
| 1.0×10^{-2} (GKS12) | 5 | 8.3 | 900 | 2900 | 3.3 |
| | 10 | 16.7 | 930 | 2500 | 2.6 |
| | 24 | 27.1 | 4300 | 10100 | 2.3 |
| | 40 | 37.5 | 6820 | 15300 | 2.2 |
| | 60 | 56.3 | 11300 | 23600 | 2.1 |
| | 115 | 98.2 | 27400 | 37700 | 1.4 |
| 6.7×10^{-3} (GKS26) | 35 | 2.1 | 900 | - | - |
| | 55 | 9.8 | 6500 | 7600 | 1.2 |
| | 85 | 37.5 | 8400 | 13100 | 1.6 |
| | 135 | 86.7 | 12800 | 20200 | 1.6 |
| | 165 | 61.4 | 15000 | 24500 | 1.6 |
| | 215 | 77.3 | 16200 | 26900 | 1.6 |
| | 275 | 99.9 | 11600 | 20200 | 1.8 |

Table 3.2. Molecular weight and conversion data for polymerisation of ϵ -caprolactone using THF as a solvent.

Considering the reaction carried out at $[I]_0 = 3.6 \times 10^{-2}$ ml⁻¹ there seems to be a similar degree of control over the polymerisations carried out in THF to that was

using toluene as a solvent. At the same initiator concentration used in toluene, the initiator efficiency was around 37% and in THF it is about 32%. The polydispersities are a little broader in THF compared to those obtained using toluene. A minimum value for M_w/M_n of 1.6 is reached in THF compared to 1.3 in toluene. It may be that the co-ordination between the solvent and the aluminium centres discussed in section 3.1.8. is the reason for such a broadening. If the aluminium centre is complexed with the solvent and an equilibrium between this and the monomer complex exists, then this equilibrium will have an effect on the concentration of growing chain. Assuming the solvent co-ordinated species cannot propagate then other centres, which are co-ordinated with the monomer, will propagate and the molecular weight distribution will broaden.

The same pattern is observed when a lower concentration of initiator is used, $[I]_0 = 1.8 \times 10^{-2} \text{ ml}^{-1}$. The polydispersities of the polymers produced in THF (1.3) are broader than those polymers synthesised in toluene (1.3). The initiator efficiency is also similar to the corresponding reaction in toluene, about 73% compared to 77% in toluene. In the polymerisation of ϵ -caprolactone using THF as a solvent at $[I]_0 = 1.0 \times 10^{-2} \text{ ml}^{-1}$, the theoretical molecular weight would be 26200 at 100% conversion. Initiator efficiency is about 94% in this case, more than the corresponding reaction in toluene or DCM.

In the reaction at $[I]_0 = 6.7 \times 10^{-3} \text{ ml}^{-1}$ the number average molecular weight was 16200, which was approximately 55% of the expected molecular weight at 77% conversion and the polydispersity increased as the reaction proceeded. It is likely therefore that impurities entered this reaction and possibly caused the destruction of initiating moieties and then subsequently leading to the termination of the growing chains.

3.1.4. The polymerisation of ϵ -caprolactone using DCM as a solvent.

To gain and understanding of the effect which solvent polarity and donor nature have on the propagation mechanism, polymerisations were carried out using DCM as a solvent and the results compared with those obtained on toluene.

| $[I] \times 10^2 \text{ ml}^{-1}$ | Time (mins) | % Conv | M_n | M_w | M_w/M_n |
|-----------------------------------|-------------|--------|-------|-------|-----------|
| 1.8×10^{-2} (GKS22) | 25 | 29.6 | 10300 | 15900 | 1.6 |
| | 55 | 45.8 | 14300 | 22000 | 1.6 |
| | 90 | 80.0 | 15900 | 25400 | 1.7 |
| | 120 | 95.0 | 16700 | 27500 | 1.6 |
| 1.0×10^{-2} (GKS25) | 15 | 0.8 | - | - | - |
| | 30 | 1.7 | - | - | - |
| | 40 | 1.7 | 1400 | 1700 | 1.2 |
| | 77 | 8.1 | 6500 | 9700 | 1.5 |
| | 97 | 15.2 | 7300 | 11200 | 1.5 |
| | 115 | 28.1 | 16400 | 20900 | 1.3 |
| | 140 | 31.0 | 15500 | 22000 | 1.4 |
| | 160 | 38.0 | 18200 | 25700 | 1.4 |
| 6.7×10^{-3} (GKS21) | 25 | 1.7 | 1800 | 2300 | 1.3 |
| | 110 | 25.2 | 12900 | 19000 | 1.5 |
| | 140 | 56.0 | 18300 | 29400 | 1.6 |
| | 160 | 28.7 | 16600 | 28700 | 1.7 |
| | 200 | 74.2 | 17200 | 32900 | 1.9 |
| | 240 | 91.7 | 25700 | 48600 | 1.9 |

Table 3.3. Results of the polymerisation of ϵ -caprolactone using DCM as a solvent.

The polymerisations carried out using DCM as a solvent also appear to have incomplete initiation. The molecular weight in the reaction at $[I]_0 = 1.8 \times 10^{-2} \text{ ml}^{-1}$ should be around 13000 after all the monomer has been consumed. In this case it is actually 16720 at 95% conversion and the molecular weight distribution is also broader in DCM than in THF.

At a lower concentration of initiator, $[I]_0 = 1.0 \times 10^{-2} \text{ ml}^{-1}$, the initiator efficiency of this reaction is still not 100%. At 100% conversion, a theoretical molecular weight of 26200 would be expected, but at 38% conversion the molecular

weight was 18180 which corresponds to an initiator efficiency of 55%. The molecular weight distribution is slightly narrower than the corresponding reaction in toluene and similar to the corresponding reaction using THF as a solvent. In the reaction with $[I]_0 = 6.7 \times 10^{-3} \text{ ml}^{-1}$ a maximum theoretical value for M_n is 39400. At 91.7% conversion the actual molecular weight is 25730. The initiator efficiency is 71%, about the same as the corresponding reactions carried out in THF and toluene. The molecular weight distribution is probably broad because of some termination by impurities accidentally leaking into the reaction.

3.1.5. The polymerisation of ϵ -caprolactone using DMF as a solvent.

DMF was chosen as an initiator because it is polar and its donor nature is similar to that of ϵ -caprolactam, which is known to be polymerised using aluminium alkoxide initiators. It should therefore help to ascertain the effect of the solvent on the propagation reactions.

| $[I] \times 10^2 \text{ ml}^{-1}$ | Time (mins) | % Conv | M_n | M_w | M_w/M_n |
|-----------------------------------|-------------|--------|-------|-------|-----------|
| 3.6×10^{-2} (GKS30) | 45 | 4.3 | - | - | - |
| | 115 | 9.4 | - | - | - |
| | 1425 | 53.6 | - | - | - |
| 1.8×10^{-2} (GKS10) | 30 | - | 200 | 190 | - |
| | 60 | 14.6 | 380 | 600 | 1.57 |
| | 105 | 22.9 | 1910 | 2830 | 1.48 |
| | 155 | 33.3 | 2940 | 4030 | 1.37 |
| | 300 | 27.6 | 4170 | 6120 | 1.47 |
| | 4300 | 64.7 | - | - | - |
| 1.0×10^{-2} (GKS31) | 65 | 1.2 | - | - | - |
| | 125 | 2.6 | - | - | - |
| | 210 | 1.4 | - | - | - |
| | 290 | 2.9 | - | - | - |
| | 390 | 3.1 | - | - | - |
| | 525 | 31.8 | - | - | - |
| 6.7×10^{-3} (GKS29) | 130 | 1.2 | - | - | - |
| | 180 | 0.8 | - | - | - |
| | 250 | 1.6 | - | - | - |
| | 310 | 1.2 | - | - | - |
| | 410 | 2.0 | - | - | - |
| | 1320 | 3.1 | - | - | - |

Table 3.4. Molecular weight and conversion data from the polymerisation of ϵ -caprolactone using DMF as a solvent.

It is apparent from table 3.4. that the rate of polymerisation of ϵ -caprolactone using *diisobutyl aluminium isopropoxide* as an initiator and DMF as a solvent is very slow. Indeed, in the slowest reaction, $[I]_0 = 6.7 \times 10^{-3} \text{ ml}^{-1}$, only 3 percent conversion was achieved after 22 hours. Such low conversions effectively prevent the use of GPC in order to analyse the polymer samples obtained. One other

problem observed when using DMF as a solvent is that it is insufficiently volatile for distillation to be carried out. If a large volume is to be distilled in order to allow aliquots to be withdrawn, then 5 to 6 hours were required for the distillation.

A further problem associated with using DMF is that the solvent is not easily removed from the polymer sample after it has been removed from the reaction medium. Periods of up to 7 days under vacuum have been required in order to obtain a polymer which has been dried to a constant weight.

3.1.6. Plots of $\ln([M]_0/[M]_t)$ vs time for the polymerisation of ϵ -caprolactone.

First order plots have been constructed for the polymerisation of ϵ -caprolactone using *diisobutyl* aluminium *isopropoxide* as the initiator in solvents of different polarity.

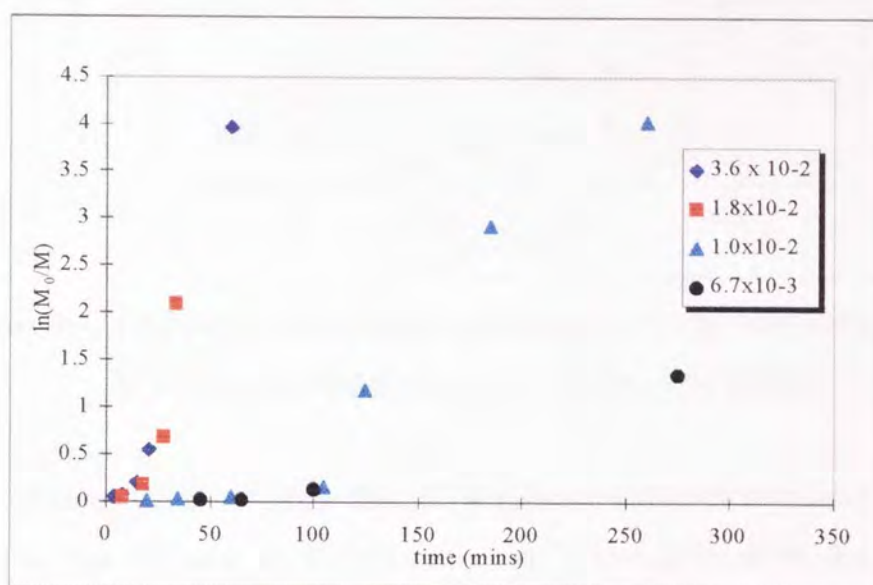


Figure 3.2. First order plot for the polymerisation of ϵ -caprolactone in toluene at 25°C using *diisobutyl* aluminium *isopropoxide* initiator.

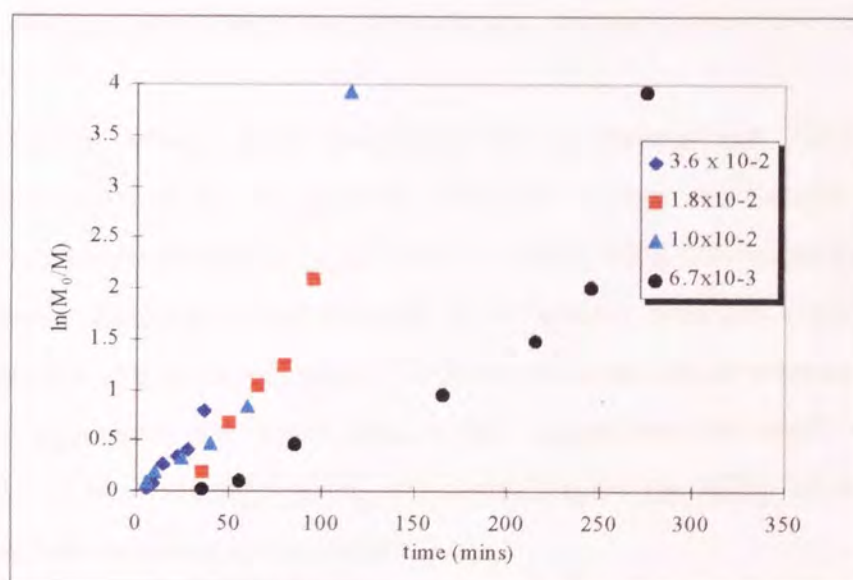


Figure 3.3. First order plot for the polymerisation of ϵ -caprolactone in THF at 25°C using *diisobutyl* aluminium *isopropoxide* initiator.

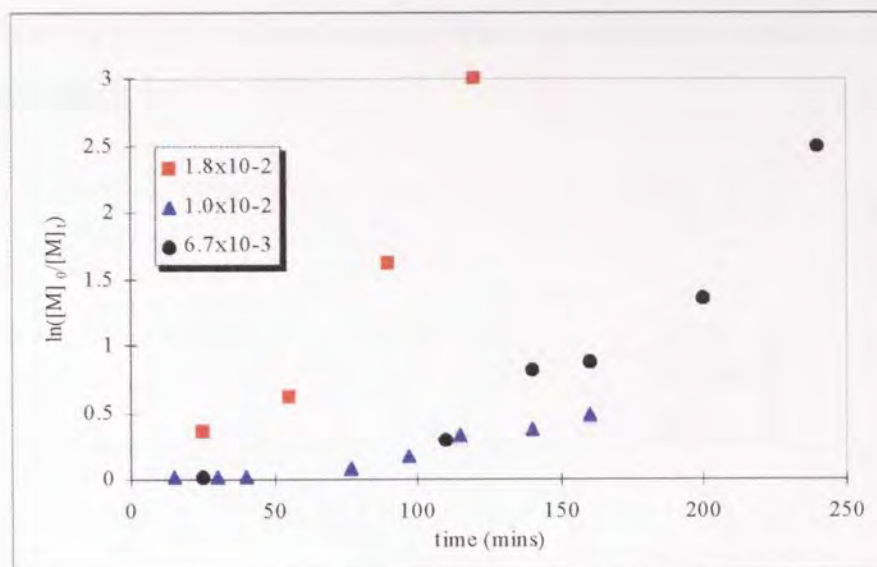


Figure 3.4. First order plot for the polymerisation of ϵ -caprolactone in DCM at 25°C using diisobutyl aluminium isopropoxide initiator.

Figures 3.2 to 3.4 show that the dependence of initiator concentration on a first order plot for each of the solvents used. These plots show that the rate of polymerisation builds up; brought about by an increase in the concentration of active species. The rate of polymerisation then enters a steady growth period, indicated by a linear plot. The build up period present in each reaction appears to be related to the concentration of initiator used, increasing as initiator concentration decreases.

Similar effects have been observed by Jerome and Teyssie⁽¹¹³⁾, when $\text{Al}(\text{iPrO})_3$ was used for the polymerisation of lactones and lactides. They used cryometric measurements to prove that the ring opening polymerisation of lactones when using aluminium triisopropoxide as an initiator does not begin immediately. The addition of a polar monomer is believed to cause a slow rearrangement of the initiator aggregates that are present in the toluene solution used. They further suggest that the induction period, (t_i) depends upon the ability of the initiator to complex with the monomer molecules.

A decrease in the concentration of initiator diisobutyl aluminium isopropoxide used has produced an increase in the build up period, t_i . This is most

likely to be due to the increased reaction time expected when a lower concentration of initiator is used.

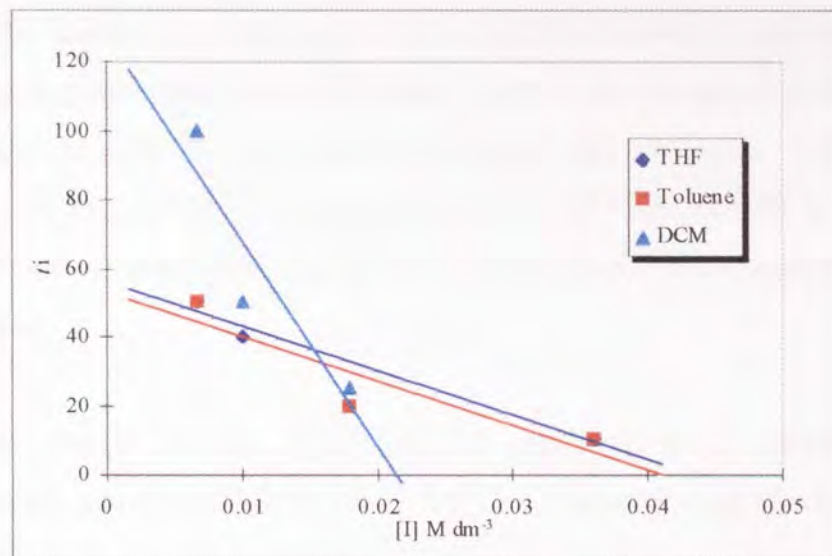


Figure 3.5. Dependence of build up period on initiator concentration for the polymerisation of ϵ -caprolactone in various solvents.

The build up period appears to be longer when more polar solvents are used, figure 3.5. The slower rate of polymerisation observed in polar solvents can be attributed to a lower effective concentration of active centres in such solvents. This could be because the monomer has to displace a solvent molecule from the co-ordination sphere of the complex. Since the rate of propagation would be expected to be slower for co-ordination reactions such as these in more polar solvents, then an increased t_i would be expected. If the polymerisation of ϵ -caprolactone using *diisobutyl* aluminium *isopropoxide* were in fact an ionic reaction, as opposed to a co-ordination-insertion type mechanism, then it would be expected that the opposite would be true, that t_i would decrease as solvent polarity increased and the rate of polymerisation would increase in polar solvents.

An increase in the polarity of a solvent used is known to cause ionic species to separate from contact ion pairs through solvent separated ion pairs to free ions.

Assuming that the alkyl aluminium alkoxide, the monomer (ϵ -caprolactone) or the growing species are not ionic but still polar, then the principle of ionic nature and solvent polarity may be extended to encompass a co-ordination reaction such as this. The negative lactone monomer may be separated from the positive aluminium centre in the same way two ionic species would be. Thus as solvent polarity increases, then the distance between the monomer and initiator also increases. Teyssie's⁽¹¹³⁾ insistence that the time (t_i) is dependent upon the ability of the initiator to co-ordinate with the monomer is supported by the increase in t_i with increasing solvent polarity reported here.

The linearity of the plots after the build up period shows that the polymerisation of ϵ -caprolactone using diisobutyl aluminium isopropoxide is free of termination reactions. The concentration of growing species present in the reaction is shown to remain constant as propagation proceeds. A change in the number of growing species present, i.e. termination reactions would show in the first order plot as a decrease in the gradient. Such decreases in slope occur towards the end of a reaction once the monomer concentration has decreased significantly and hence the rate of propagation has decreased.

A linear plot should be obtained if $1/[I]_0 \cdot \ln[M]_0/[M]_t$ is plotted against t . This plot is obtained from the following derivation,

If

$$-d[M]/dt = k_p [M][A^*] \quad 3.2.$$

Then

$$\ln[M]_0/[M]_t = k_p [A^*]t \quad 3.3$$

So

$$1/[A^*]\ln[M]_0/[M]_t = k_p t$$

3.4.

and assuming that the concentration of active species is equal to the initial initiator concentration then if $1/[I]_0 \cdot \ln[M]_0/[M]_t$ is plotted against time all points should then lie on a straight line for a living polymerisation. These values have been plotted for each of the solvents used (figures 3.6. - 3.8.)

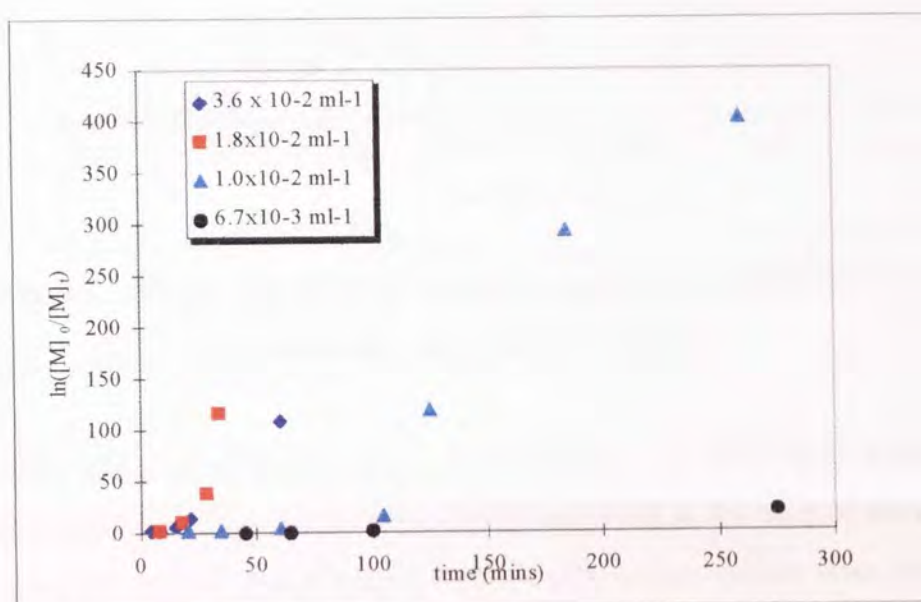


Figure 3.6. Plot of $1/[I]_0 \cdot \ln[M]_0/[M]_t$ against time for the polymerisation of ϵ -caprolactone using toluene as a solvent.

A plot of $1/[I]_0 \cdot \ln[M]_0/[M]_t$ against time for the polymerisation of ϵ -caprolactone using toluene as a solvent (figure 3.6.) shows that the plot is not linear. The gradient of this plot is k_p , the rate of polymerisation. The plot is like the first order plot, that is linear after an initial build up period. This build up period presumably occurs because of a gradual increase in the concentration of growing centres.

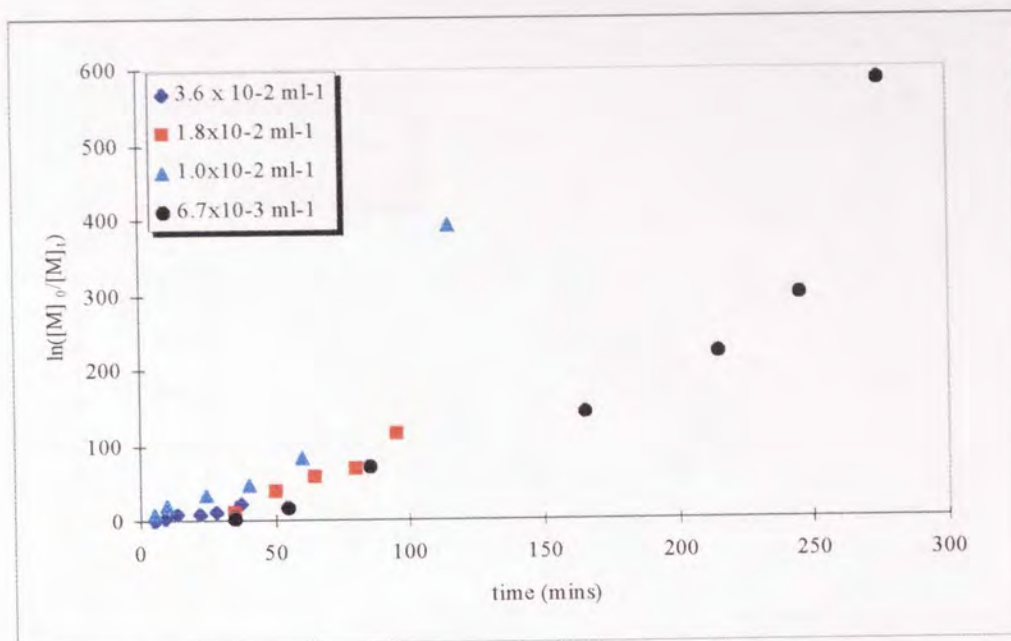


Figure 3.7. Plot of $1/[I]_0 \cdot \ln([M]_0/[M]_t)$ against time for the polymerisation of ϵ -caprolactone using THF as a solvent.

When THF was used as the reaction solvent, the plot of $1/[I]_0 \cdot \ln([M]_0/[M]_t)$ against time (figure 3.7.) also appears to have a build up period at the start of the reaction. It can probably be said that the concentration of growing species does not remain constant throughout the reaction but in fact increases until after the build up period. After this build up period the concentration of growing species appears to remain constant.

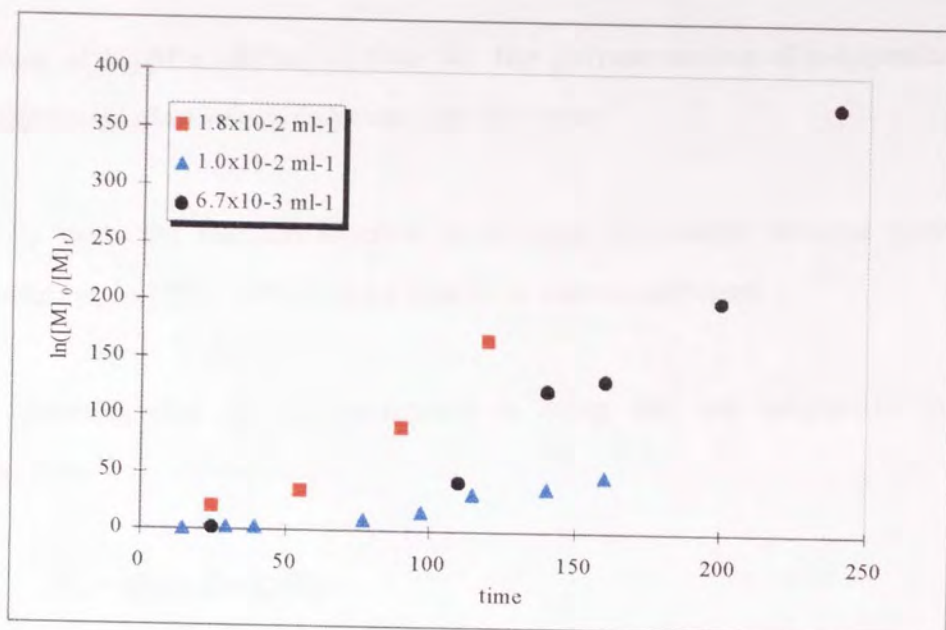


Figure 3.8. Plot of $1/[I]_0 \cdot \ln[M]_0/[M]_t$ against time for the polymerisation of ϵ -caprolactone using DCM as a solvent.

The same build up period and subsequent period of growth that were observed when THF and toluene were used as a solvent were also seen when DCM was used as a solvent (figure 3.8.)

3.1.7 Plots of $\ln(DP_{n_0}-DP_{n_t})$ vs time for the polymerisation of ϵ -caprolactone using diisobutyl aluminium isopropoxide initiator.

To study the reaction kinetics, plots using the number average degree of polymerisation, $\ln(DP_{n_0}-DP_{n_t})$ versus time have been constructed.

Assuming that the polymerisation is living and not subject to transfer reactions then,

$$DP_n = ([M]_0 - [M]_t) / [I]_0 \quad 3.5.$$

where

DP_n = number average degree of polymerisation

$[M]_0$ = initial monomer concentration

$[M]_t$ = monomer concentration at time t

$[I]_0$ = initial initiator concentration, equivalent to the concentration of growing species

the monomer concentration at time t is,

$$[M]_t = [M]_0 e^{-kt} \quad 3.6.$$

where k is the apparent rate constant and incorporates the concentration of growing centres

Substituting 3.6 into 3.5 gives the number average degree of polymerisation as

$$DP_n = ([M]_0 - [M]_0 e^{-kt}) / [I]_0 \quad 3.7.$$

which simplifies to

$$DP_n = \{[M]_0 - (1 - e^{-kt})\} / [I]_0 \quad 3.8.$$

At time $t = \infty$ when all the monomer has been consumed, then

$$DP_{n\infty} = [M]_0 / [I]_0 \quad 3.9.$$

inserting equation 3.9. into 3.8. gives

$$DP_n = DP_{n\infty} (1 - e^{-kt}) \quad 3.10.$$

rearranging and taking natural logarithms gives

$$\ln\{1 - (DP_n / DP_{n\infty})\} = -kt \quad 3.11.$$

which is the same as

$$\ln(DP_{n\infty} - DP_n) = \ln(DP_{n\infty}) - kt \quad 3.12.$$

Thus for a living polymerisation with fast initiation, a linear plot with a negative gradient equal to the apparent rate constant of propagation and a y intercept equal to $\ln(DP_{n\infty})$ is obtained when $\ln(DP_{n\infty} - DP_n)$ is plotted against time

When a plot of $\ln(DP_{n\infty} - DP_n)$ versus time is plotted then the value of $DP_{n\infty}$ calculated from the y intercept should be equal to that calculated from the ratio $[M]_0 / [I]_0$. On occasions the actual value of $DP_{n\infty}$ has been different from the theoretical value and in these cases the value of $DP_{n\infty}$ used has been the closest match between the actual and theoretical values as calculated from the y -axis intercept.

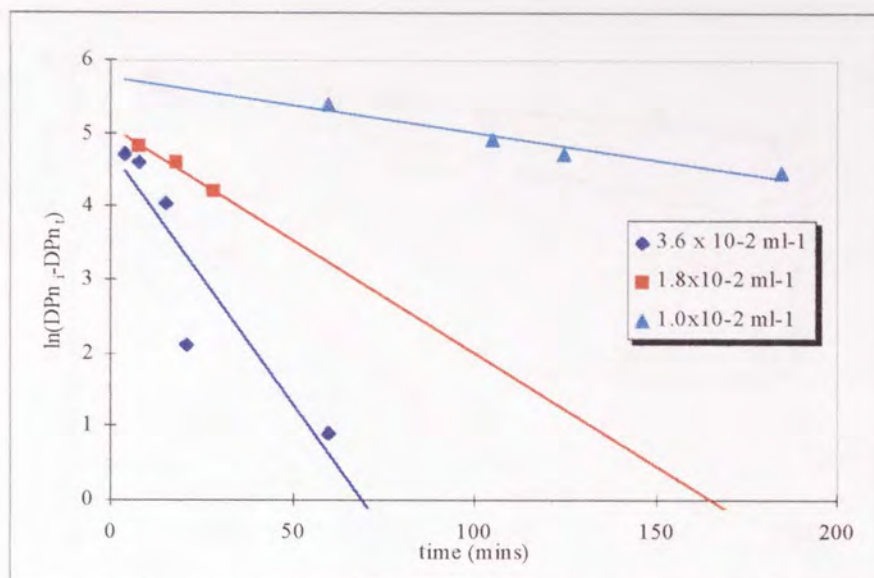


Figure 3.9. Plot of $\ln(DP_{n_{\infty}}-DP_{n_t})$ vs time for the polymerisation of ϵ -caprolactone in toluene at 25°C using *diisobutyl* aluminium *isopropoxide* initiator.

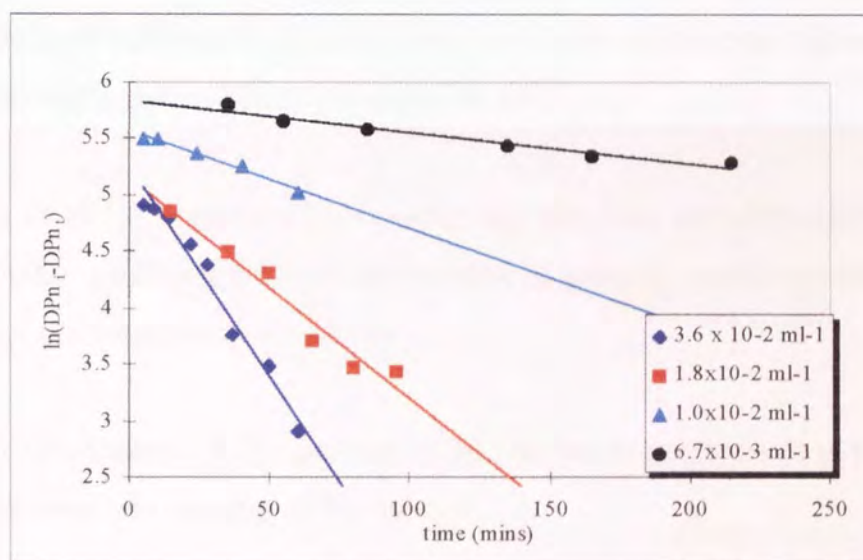


Figure 3.10. Plot of $\ln(DP_{n_{\infty}}-DP_{n_t})$ vs time for the polymerisation of ϵ -caprolactone in THF at 25°C using *diisobutyl* aluminium *isopropoxide* initiator.

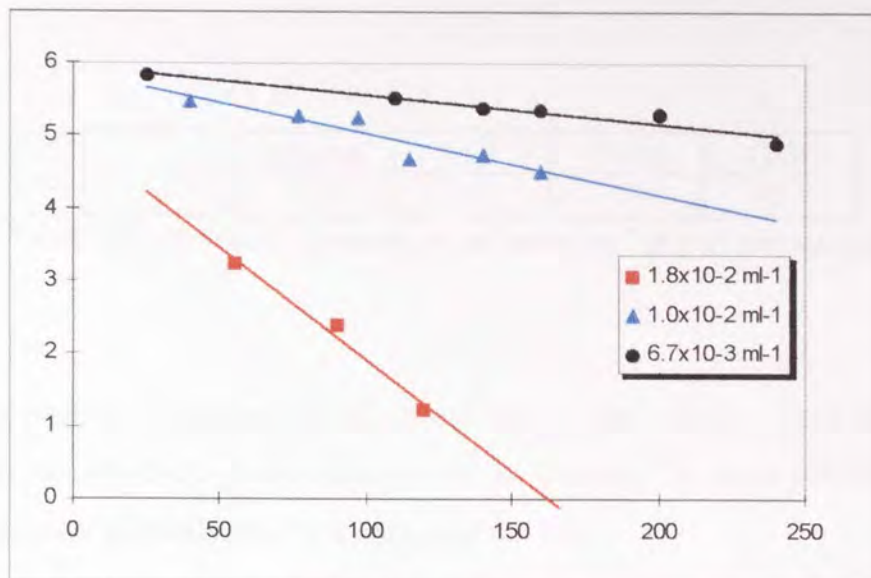


Figure 3.11. Plot of $\ln(DP_{n_x} - DP_{n_1})$ vs time for the polymerisation of ϵ -caprolactone in DCM at 25°C using diisobutyl aluminium isopropoxide initiator

Plots of $\ln(DP_{n_x} - DP_{n_1})$ versus time have been constructed (figures 3.9. to 3.11.) from molecular weight data obtained by GPC

In all of the polymerisations carried out, the plots of $\ln(DP_{n_x} - DP_{n_1})$ versus time are linear, indicating that the concentration of growing species remains constant throughout the polymerisation reaction.

From equation 3.9. the gradient of the plot has been calculated to be equal to $-k_p$, the apparent rate constant of the reaction.

3.1.8. Overall comparison of apparent rate constants in toluene, DCM and THF.

The apparent rate constant of polymerisation of ϵ -caprolactone using diisobutyl aluminium isopropoxide has been calculated in each of the solvents used as summarised in table 3.5 below. Toluene, THF, DCM and DMF have the dielectric constants which are displayed in table 3.5.

| | | | | |
|------------|---------|-----|-----|------|
| | toluene | THF | DCM | DMF |
| ϵ | 2.4 | 7.6 | 8.9 | 36.7 |

Table 3.5. Dielectric constants of solvents used in polymerisations.

In chapter 1, section 1.2.10., it was shown that polarity of the solvent can have a profound effect on the reaction and its kinetics. In ionic polymerisations, aprotic solvents generally lead to solvation of the ions.

Scheme 1.2 (page 48) describes the effect of the polarity on the structure of the propagating species. In general low polarity solvents favour the presence of structures on the left hand side of the equilibrium.

The covalent species on the left of the diagram is usually found to be much less reactive than the free ions on the right. More polar solvents such as acetonitrile or nitrobenzene are therefore expected to result in a faster rate of polymerisation than those of a less polar nature e.g. *n*-alkanes and toluene. This is certainly the case in systems such as butadiene or styrene polymerised anionically.

The apparent rate constant for the polymerisation of ϵ -caprolactone using *diisobutyl* aluminium *isopropoxide* was calculated from the gradient of the $\ln(DP_{n_0} - DP_{n_t})$ versus time plot. The dependence of the apparent rate constant for the solvents used is displayed in table 3.6. The results obtained for the polymerisations carried out in DMF are not displayed here because conversions were so low that GPC analysis was impossible. The dielectric constants of the solvents are included in the table.

| [I] ₀ ml ⁻¹ | Apparent rate constant x 10 ² | | |
|-----------------------------------|------------------------------------------|------------------|------------------|
| | Toluene (ε = 2.4) | THF (ε = 7.6) | DCM (ε = 8.9) |
| 3.6 x 10 ⁻² | 6.89 | | |
| 1.8 x 10 ⁻² | 3.09 | | |
| 1.0 x 10 ⁻² | 0.74 | | |
| 3.6 x 10 ⁻² | | 3.73 | |
| 1.8 x 10 ⁻² | | 1.95 | |
| 1.0 x 10 ⁻² | | 0.87 | |
| 6.7 x 10 ⁻³ | | 0.28 | |
| 3.6 x 10 ⁻² | | | 5.26 |
| 1.8 x 10 ⁻² | | | 2.97 |
| 1.0 x 10 ⁻² | | | 0.85 |
| 6.7 x 10 ⁻³ | | | 0.4 |

Table 3.6. Apparent rate constant of polymerisation of ε-caprolactone in solvents of differing polarity.

The recorded apparent rate constants have then been plotted against initiator concentration in the figure below, figure 3.12.

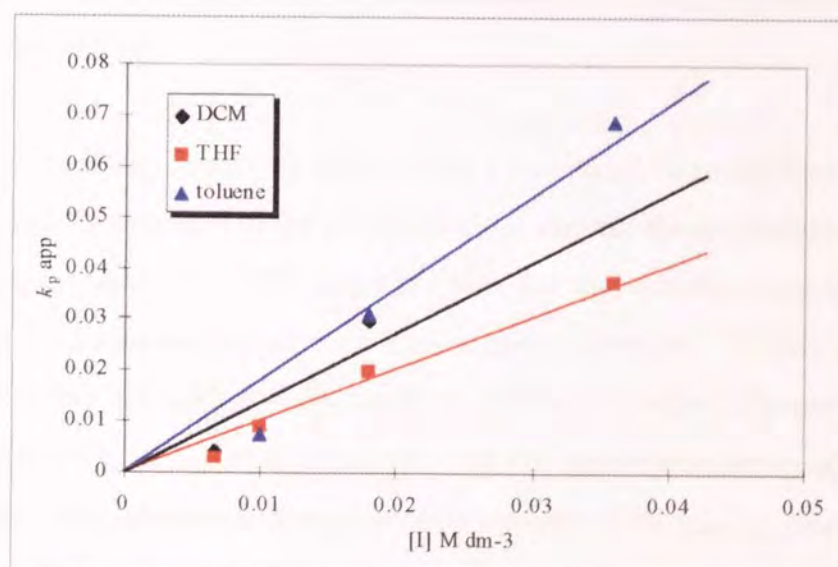


Figure 3.12. Comparison of apparent rate constants versus initiator concentration in solvents of varying polarity.

The rate of polymerisation of ε-caprolactone in toluene, which is the least

polar solvent used ($\epsilon = 2.4$) appears to be the fastest when compared to THF, DCM and DMF. This is the opposite of what would be expected if the mechanism of the polymerisation were a purely ionic one. This may indicate, although not confirm, that the mechanism of the polymerisation of lactones using alkyl aluminium alkoxide initiators is not an ionic one but a co-ordination type system.

However the dependence of rate constant on polarity of the solvent is not a simple relationship since inspection of the data shows that contrary to expectations that the rate of polymerisation in the next most polar solvent, THF, does not have the next slowest rate. The rate of polymerisation in DCM ($\epsilon = 8.9$) appears to be faster than that in THF ($\epsilon = 7.4$), a result which would not necessarily be expected. One of two explanations may be possible. It may be that in these solvents, the reaction may be taking place via an ionic mechanism as opposed to the co-ordination type mechanism proposed by Jerome and Penzcek. This explanation would be feasible because in the more polar solvent ion separation would be greater, increasing the rate of reaction. This however would be an unlikely explanation, aluminium-oxygen bonds are strong and dissociation of the aluminium-alkyl bond to form a carbonium ion would be unlikely.

A more likely scenario is one in which a co-ordination mechanism occurs and THF participates somehow in the polymerisation, slowing the propagation rate. The oxygen atom present in the THF ring has a lone pair and this may occupy the vacant sp^3 -orbital on the aluminium atoms. Jerome and co-workers⁽¹¹³⁾ have shown that THF does in fact co-ordinate with diethyl aluminium ethoxide in the polymerisation of δ -butyrolactone. It is probable therefore that this type of interaction takes place in the reaction using *disobutyl* aluminium *isopropoxide*. This may be summarised by the diagram below (figure 3.13.)

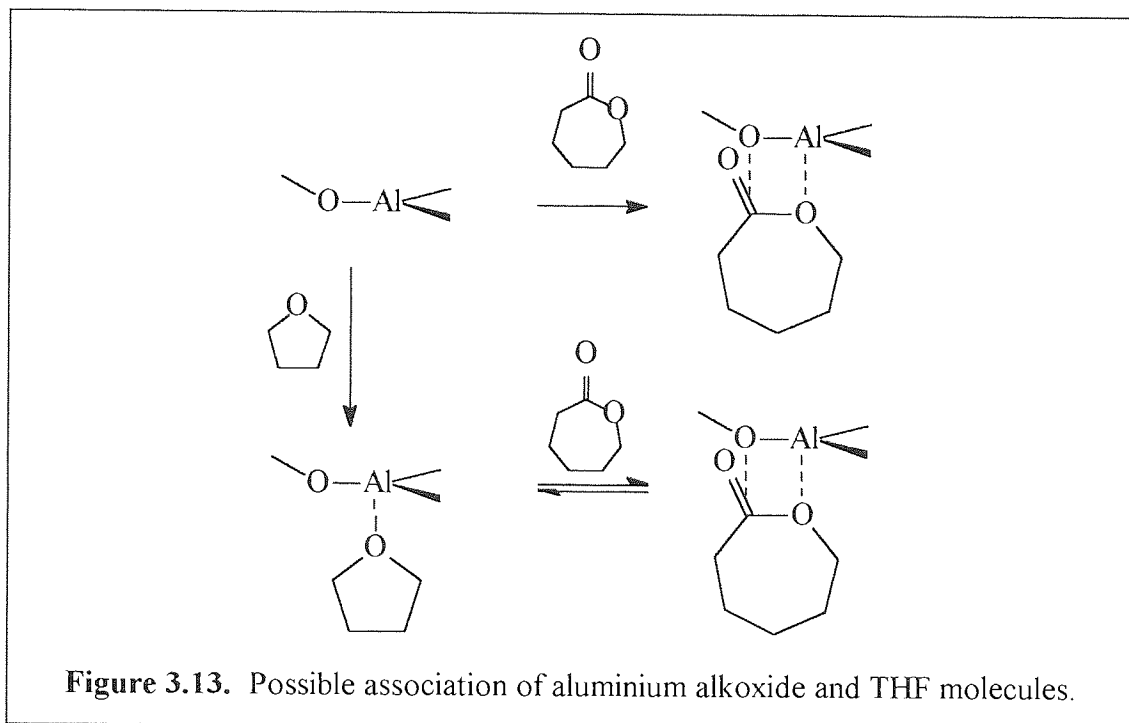
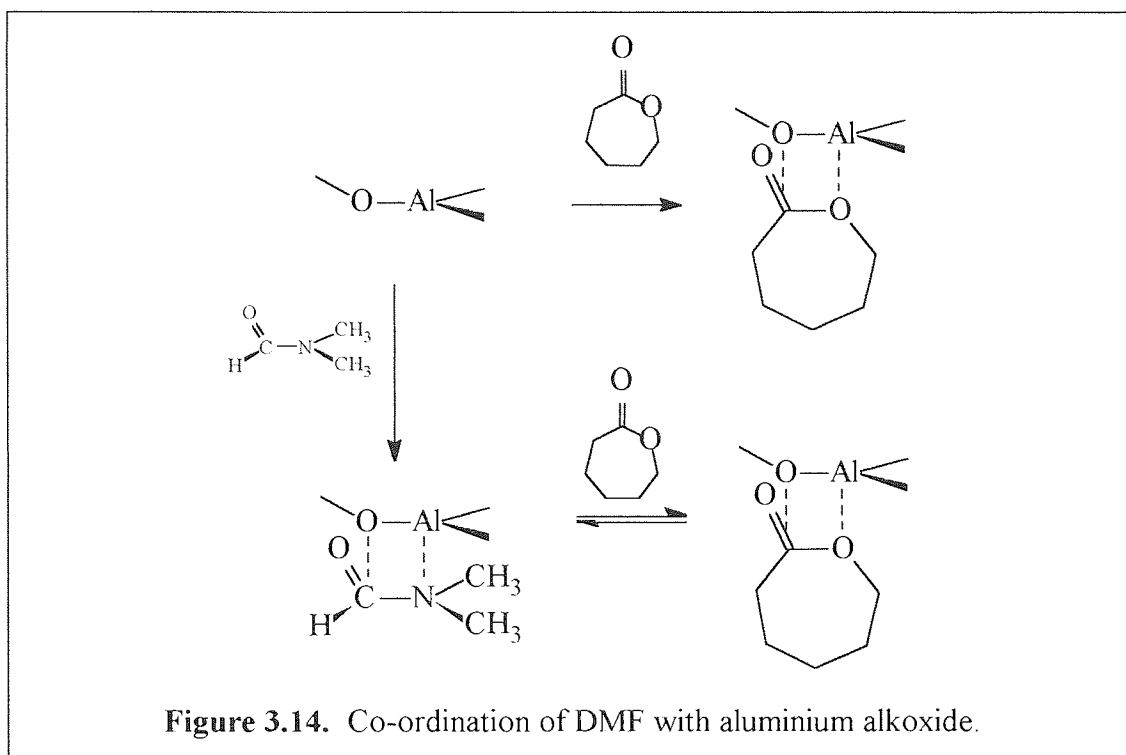


Figure 3.13. Possible association of aluminium alkoxide and THF molecules.

If solvent participates in the polymerisation mechanism by co-ordinating with the aluminium centres, then there could be a slower rate of propagation in THF than may be expected. Propagation can only take place when a monomer molecule first displaces the solvent molecule from the co-ordination sphere of the propagating centre and then any initiator aggregate dissociates to allow propagation by complexation of the monomer. Since an associated ϵ -caprolactone molecule must be displaced by the solvent before it propagates, it is unsurprising that propagation is slower in co-ordinating solvents.

The rate of polymerisation in DMF has not been calculated because yields have been insufficient for GPC analysis, it is clear however that the polymerisation in this solvent is considerably slower than the other three solvents used. Percentage conversions achieved are still low, less than 20 percent, after 24 or more hours. An explanation for this would be similar to that for the rate of polymerisation being slower than expected in THF. Amines are known to co-ordinate with aluminium alkyls via the nitrogen atom in the amine⁽⁹²⁾. It is entirely possible therefore that DMF is also co-ordinating with the aluminium atoms (figure 3.14.).



Proof that using the highly polar solvent DMF results in a slowed rate of reaction further confirms that a co-ordination mechanism rather than a purely ionic mechanism occurs in the polymerisation of ϵ -caprolactone using diisobutyl aluminium isopropoxide.

In summary, whilst the dielectric constant of the solvent increases in the order toluene, THF, DCM, DMF, the apparent rate of polymerisation appears to follow the order toluene>DCM>THF>DMF. Therefore the donor nature of the solvent, as well as the dielectric constant of the solvent must also be taken into account when considering the effect of the solvent on the polymerisation kinetics.

3.1.9. The dependence of M_n on conversion

Plots of M_n against percentage conversion have been constructed from the tables of results obtained from the polymerisation of ϵ -caprolactone using diisobutyl aluminium isopropoxide.

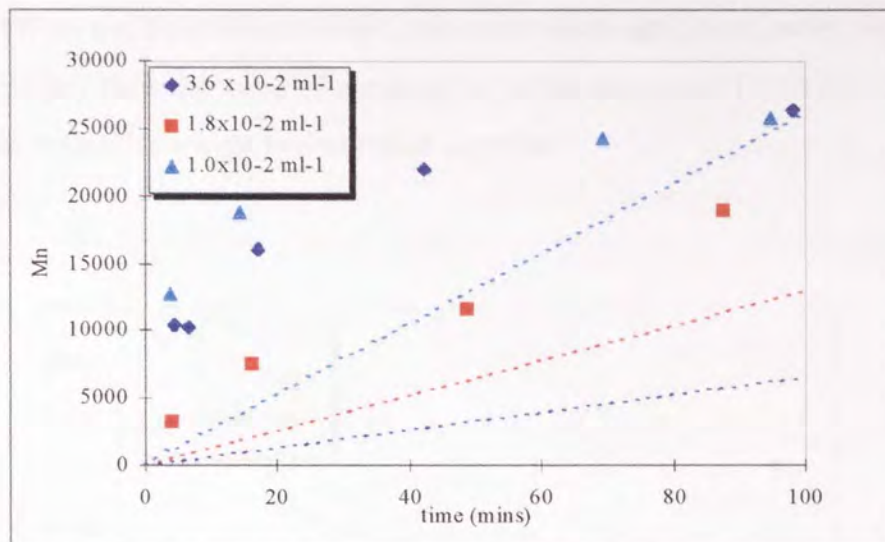


Figure 3.15. The dependence of molecular weight on conversion for the polymerisation of ϵ -caprolactone in toluene.

The plots from the polymerisations carried out in toluene all show the number average molecular weight is higher than the theoretical value (dotted lines) for all concentrations of initiator.

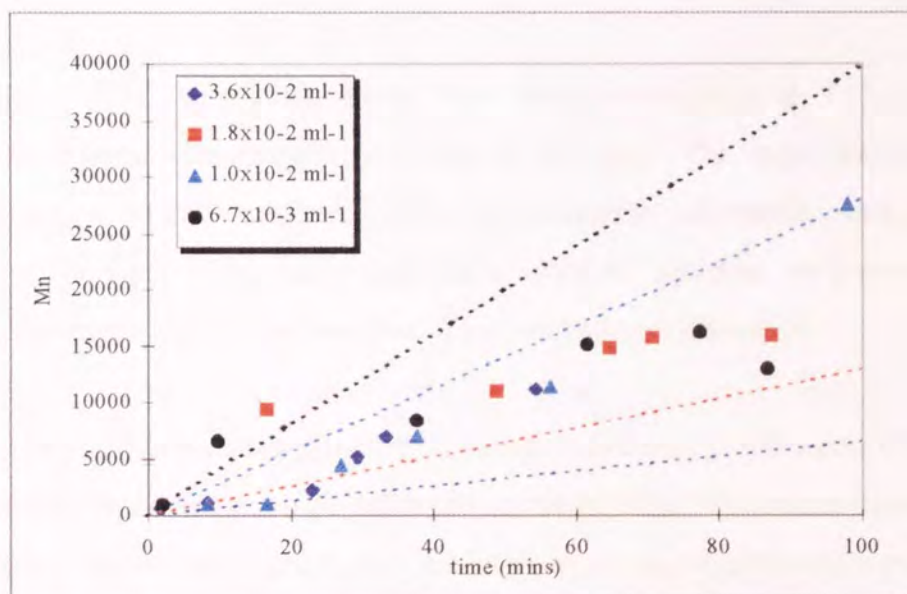


Figure 3.16. The dependence of molecular weight on conversion for the polymerisation of ϵ -caprolactone in THF.

Using THF as a solvent has produced polymers which again have molecular weights that are higher than expected. An exception is the reaction at $[I]_0 = 6.7 \times 10^{-3} \text{ ml}^{-1}$ where the molecular weight is lower than expected.

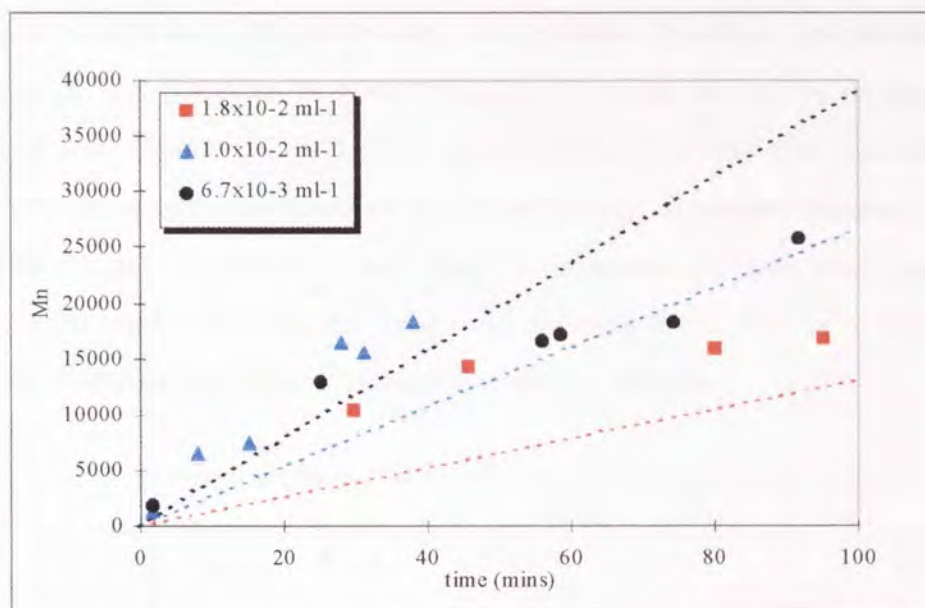


Figure 3.17. The dependence of molecular weight on conversion for the polymerisation of ϵ -caprolactone in DCM.

Plot of M_n versus conversion have been plotted (figures 3.15-3.17) and appear to be linear with a positive intercept on the y-axis. The linear plots indicate a lack of termination and transfer reactions. If termination and transfer reactions were occurring then a plot of M_n versus conversion would not be linear, the gradient of the plot would change as the concentration of growing species decreased.

The positive y-intercept on the M_n versus conversion plot is a confirmation of the existence of the induction period noted on the $\ln([M]_0/[M]_t)$ versus time plot. If no induction period was present, then an intercept at the origin would occur. The positive intercept shows that polymer growth is occurring with a limited conversion.

It can be said quite clearly that the polymerisation of ϵ -caprolactone using *diisobutyl aluminium isopropoxide* is a living system. Plots of $\ln([M]_0/[M]_t)$ and $\ln(DP_{n_x}-DP_{n_t})$ versus time and of M_n versus conversion are linear.

3.1.10. Initiator efficiency and initiator concentration.

The results from the polymerisations shown in tables 3.1-3.4 indicate that the molecular weights of the polymers produced are not the same as the theoretical molecular weights at 100% conversion. It is probable therefore that the initiator is inefficient or that there are termination reactions present during the reaction. The first order plots (figures 3.2-3.4) show a linear period of growth after the initial build up proves that termination reactions are not occurring. A general broadening of the molecular weight distribution would also be expected and this does not occur. Therefore the explanation that the initiator is less than 100% efficient is more likely. It is likely therefore that some of the initiator may be inactive.

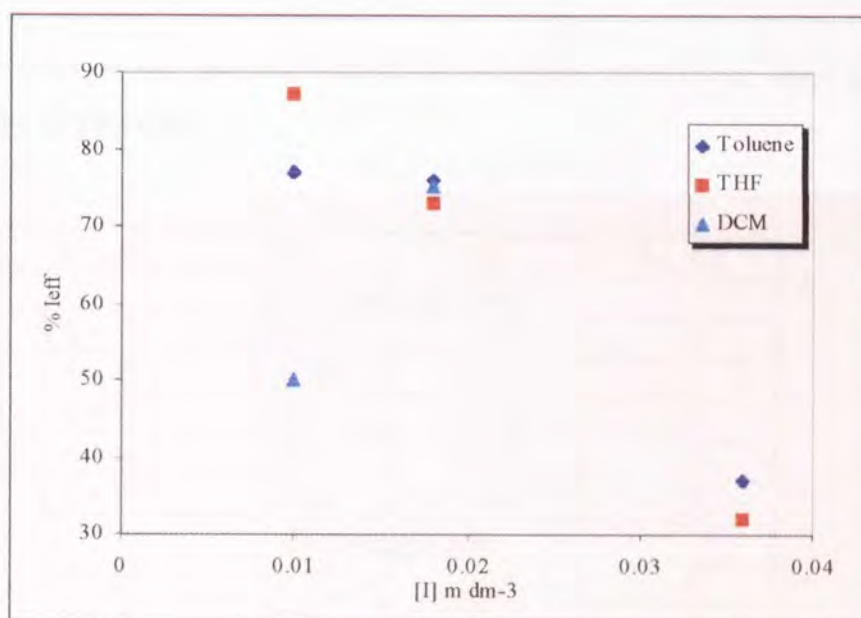


Figure 3.18. Plot of initiator efficiency versus initiator concentration for the polymerisation of ϵ -caprolactone.

It is obvious from previous data presented in this thesis that the efficiency of the initiator is not 100% for the system under study. When plotted against initiator concentration in each solvent, it is apparent that initiator efficiency is a function of initiator concentration. It is possible that at higher initiator concentrations, the rearrangement of the initiator to allow propagation is impeded by inter initiator

interactions.

3.2. Mono alkoxide and dialkoxide aluminium initiators.

In order to understand the mechanism of propagation it was necessary to determine the effect of the number of alkoxide substituents on the aluminium centre. Mono and diisopropoxide aluminium *isobutyls* were synthesised by the stoichiometric reaction of dried and distilled *iso*-propyl alcohol and triisobutyl aluminium in toluene according to the procedure described in section 2.1.5.2. ϵ -Caprolactone was polymerised using each alkoxide initiator and using THF as a solvent.

3.2.1. Results of the polymerisation of ϵ -caprolactone using alkyl aluminium mono and di alkoxides.

| $[I]_0 \text{ ml}^{-1}$ | M_n | M_w | M_w/M_n |
|-------------------------|-------|-------|-----------|
| monoisopropoxide | | | |
| 6.6×10^{-2} | 11000 | 14500 | 1.2 |
| 3.6×10^{-2} | 12200 | 12800 | 1.2 |
| 1.8×10^{-2} | 15200 | 19100 | 1.3 |
| 1.4×10^{-2} | 17800 | 21600 | 1.2 |
| 1.0×10^{-2} | 13000 | 15900 | 1.2 |
| diisopropoxide | | | |
| 6.6×10^{-2} | 6800 | 10400 | 1.5 |
| 3.6×10^{-2} | 8800 | 11200 | 1.3 |
| 1.8×10^{-2} | 8100 | 10200 | 1.3 |
| 1.4×10^{-2} | 7000 | 9200 | 1.3 |
| 1.0×10^{-2} | 13000 | 15600 | 1.2 |

Table 3.7. Molecular weight data from the polymerisation of ϵ -caprolactone in using *isobutyl* aluminium diisopropoxide

A plot of M_n against $1/[I]_0$ has been constructed for each of the sets of results obtained using each alkoxide initiator (figure 3.19).

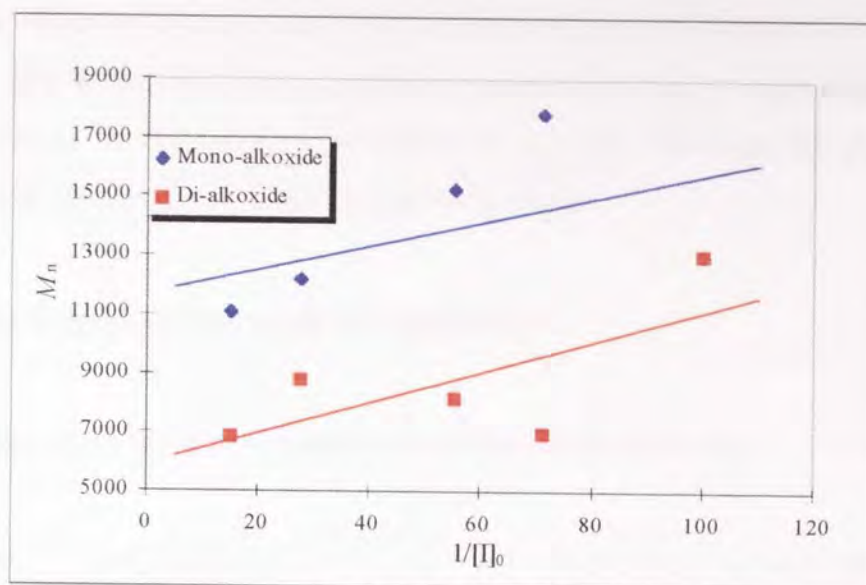


Figure 3.19. Plot of M_n against $1/[I]_0$ for the polymerisation of ϵ -caprolactone using *diisobutyl* aluminium *isopropoxide* and *isobutyl* aluminium *diisopropoxide* in toluene at 25°C.

The plot of M_n against $1/[I]_0$ (figure 3.19) shows that molecular weight of polymers produced using the di-alkoxide is approximately twice that of the polymers produced using the corresponding mono-alkoxide. Clearly each alkoxy moiety is active in the polymerisation of ϵ -caprolactone.

Jerome ⁽¹¹³⁾ found that when lactide was polymerised in toluene using aluminium *triisopropoxide* initiator, that each alkoxide moiety was active in the polymerisation. However when the monomer was ϵ -caprolactone there was only one active site per aluminium centre. It was also reported that there was also only one active site per aluminium centre when the initiator was diethyl aluminium ethoxide and the monomer was ϵ -caprolactone.

Here a di-alkoxide initiator has produced polymers with molecular weights approximately half those of the corresponding reactions using a mono-alkoxide and therefore there are two active sites per aluminium centre. Jerome ⁽¹¹³⁾ stated that there is only one active site per aluminium centre when ϵ -caprolactone was polymerised using either a mono or a tri alkoxide. It is probable that the tri-alkoxide

initiator is solvated in such a way that prevents initiation by each of the alkoxide moieties. The di-alkoxide initiator, perhaps because of the bulkier alkyl and alkoxide groups, may be forming different structures in solution. Therefore this may allow each alkoxide group to initiate separate growing chains.

3.3. Aggregation of the initiator molecules.

3.3.1. Effect of solvent on the aggregation of initiator molecules.

It is known⁽¹³⁷⁾ that aluminium alkoxides associate in solution and this is believed to be a feature that is transferred to the growing species, despite the increase in size of the alkoxy moiety. Using equation 1.15 from section 1.3.4, values of $\ln(k_p)$ versus $\ln[I]_0$ were plotted for the polymerisation of ϵ -caprolactone using diisobutyl aluminium isopropoxide in various solvents at 25°C (figure 3.21).

It is shown (equations 3.13 to 3.17.) that the reciprocal of the gradient of the plot in figure 3.16 is equal to the average degree of association of the initiator aggregates. Thus the average degrees of association of diisobutyl aluminium isopropoxide in solvents of differing polarity have been calculated and are displayed in table 3.8.

Penzcek and Duda assumed that in the reversible aggregation of the growing species, that only the non-aggregated species (P_n^*) are active in propagation whereas the aggregated species ($(P_n^*)_m$) are not.



and assuming a living system, i.e. no termination reactions occur, then the total initiator concentration $[I]_0$ is,

$$[I]_0 = [P_n^*] + [(P_n^*)_m] \quad 3.15.$$

if

$$[(P_n^*)_m] \gg [P_n^*] \quad 3.16.$$

then

$$[(P_n^*)_m] = [I]_0/m \quad 3.17.$$

Therefore the concentration of aggregated species is equal to the initiator concentration at time $t = 0$, divided by the degree of aggregation, m .

As can be seen from equation 3.13 one initiator aggregate or m -mer reversibly dissociates into m monomeric initiator molecules. This would be true assuming that the initiator aggregate was say a dimer or a trimer, that m was in fact an integer. It may be the case when $m < 1$ that one initiator aggregate does not dissociate into individual molecules before propagation occurs, but that one or more initiator aggregates or aluminium centres associate into a larger aggregate in order to propagate.

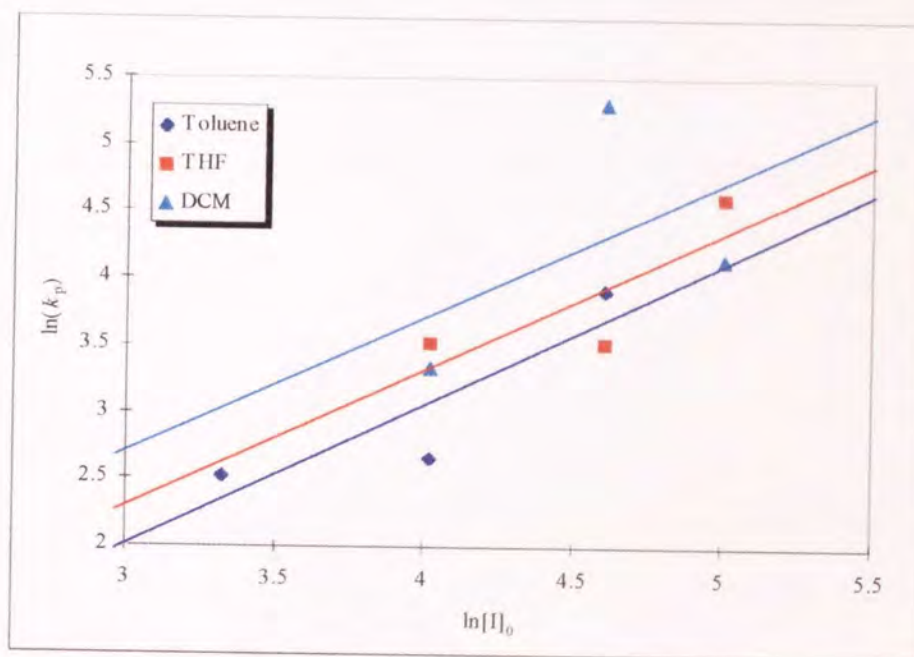


Figure 3.20. Plot of $\ln(k_p)$ versus $\ln[I]_0$ for the polymerisation of ϵ -caprolactone using diisobutyl aluminium isopropoxide in toluene, THF, and DCM at 25°C

The results from figure 3.21 are shown in table 3.8.

| Solvent | Gradient | Degree of association m |
|---------|----------|---------------------------|
| Toluene | 1.03 | 0.94 |
| THF | 1.03 | 0.97 |
| DCM | 1.01 | 0.99 |

Table 3.8. Degree of initiator association in three solvents.

A value for m , the average degree of association in excess of 1 would be expected. According to Jerome ⁽¹¹³⁾, aluminium alkoxide initiator molecules are believed to aggregate in solution. The degree of association, m , calculated from the gradient of the plots in figure 3.20 is equal to 1. It appears that no aggregated initiator molecules are being formed using diisobutyl aluminium *isopropoxide* initiator in THF, toluene or DCM.

3.4. Effect of temperature on the rate of polymerisation.

ϵ -Caprolactone has been polymerised using diisobutyl aluminium isopropoxide in toluene over a range of temperatures from -31°C to $+40^{\circ}\text{C}$. Samples were removed at recorded intervals, precipitated in methanol and dried to a constant weight under vacuum.

| Temperature | Time (mins) | % Conv | M_n | M_w | M_w/M_n |
|----------------------------------|-------------|--------|-------|-------|-----------|
| -31°C (GKS97) | 30 | 18.9 | 7610 | 9760 | 1.28 |
| | 50 | 15.8 | 10660 | 14160 | 1.33 |
| | 60 | 18.3 | 11760 | 15560 | 1.32 |
| | 70 | 22.9 | 14190 | 17960 | 1.27 |
| | 85 | 29.6 | 15260 | 20140 | 1.32 |
| | 95 | 33.5 | 16240 | 21640 | 1.33 |
| | 110 | 43.0 | 16620 | 23120 | 1.39 |
| -3°C (GKS98) | 10 | 6.6 | 4710 | 6080 | 1.29 |
| | 25 | 19.8 | 7560 | 11390 | 1.51 |
| | 35 | 27.7 | 12070 | 15200 | 1.26 |
| | 45 | 37.4 | 13740 | 17760 | 1.29 |
| | 55 | 44.9 | 15060 | 19740 | 1.31 |
| | 65 | 58.8 | 16420 | 21780 | 1.33 |
| 25°C (GKS05) | 8 | 4.0 | 1890 | 3270 | 1.73 |
| | 18 | 16.3 | 4650 | 7500 | 1.61 |
| | 28 | 48.8 | 8370 | 11500 | 1.37 |
| | 34 | 87.6 | 15160 | 18910 | 1.25 |
| 40°C (GKS99) | 5 | 1.4 | 960 | 1370 | 1.43 |
| | 15 | 19.1 | 7880 | 10040 | 1.27 |
| | 20 | 50.9 | 12160 | 15930 | 1.31 |
| | 25 | 92.6 | 20650 | 26110 | 1.26 |
| | 30 | 94.8 | 23650 | 32650 | 1.38 |

Table 3.9. Molecular weights and molecular weight distributions obtained from samples taken from the polymerisation of ϵ -caprolactone using diisobutyl aluminium isopropoxide in toluene at a range of temperatures from -31°C to $+40^{\circ}\text{C}$.

Poly(ϵ -caprolactone) appears to be soluble in toluene above 25°C at all concentrations. At lower temperatures such as -31°C , the growing polymer chains

appear to be less soluble in toluene. At -31°C , after 95 minutes, or approximately 34% conversion, the solution became heterogeneous, there were small amounts of solid forming on the inside of the reaction flask. After a further 15 minutes, at 43% conversion, the polymer became totally solid and the reaction was removed from the freezer. After being heated gently with a hair dryer, the solution became totally homogeneous again. At -3°C the homogeneity of the reaction was also not retained to the end of the reaction. At a higher conversion, about 45%, the reaction started to become slightly solid and at 65 minutes or 60% conversion, it had become totally solid. Like the solution at -31°C it also became homogeneous after warming to room temperature. The melting point of toluene is -95°C , lower than any temperature achieved during the reaction. Therefore the changes observed in the reaction solution are more likely to be as a result of a change in the solubility of the polymer, rather than the mixture freezing.

At 40°C the reaction is much faster than at lower temperatures. The molecular weight distribution is quite narrow, decreasing from 1.43 to 1.26 at the end of the polymerisation before broadening slightly on prolongation of the reaction. It is likely that a transesterification reaction begins to occur as monomer concentration decreases.

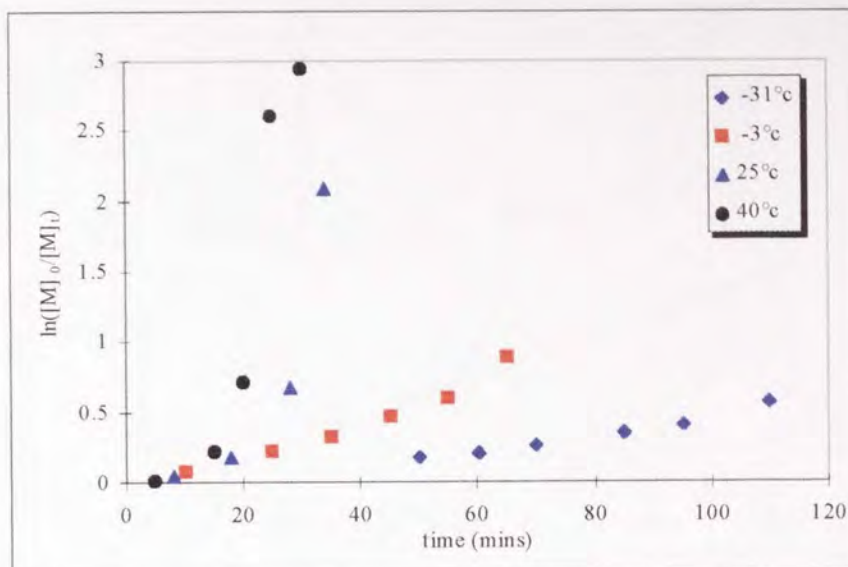


Figure 3.21. The effect of temperature on the first order plot for the polymerisation of ϵ -caprolactone using diisobutyl aluminium isopropoxide in toluene.

The plots of $\ln([M]_0/[M]_t)$ against time (figure 3.21.) are all curved. An induction period appears to be present at each of the temperatures used. The curvature of the plots is more gradual in the case of the reaction carried out at -3°C and -31°C which are almost linear. After the inflexion point which is clearly defined in the plots taken from the reactions at 25° and 40°C the plots do appear to be linear. At lower temperatures, -3°C and -31°C , the induction period does not initially appear to be present but a straight line plot shows that there is an intercept on the x-axis and hence an induction period at around 10 minutes and 27 minutes respectively.

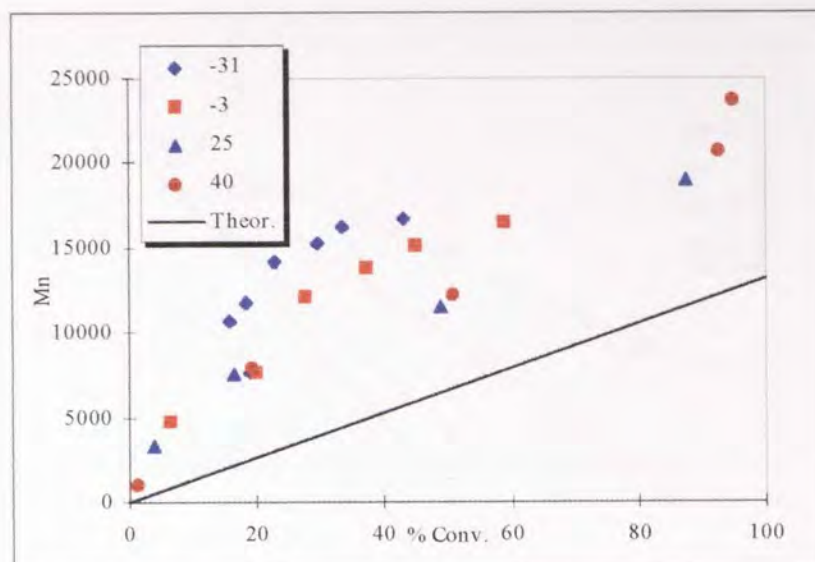


Figure 3.22. Dependence of M_n versus conversion for the polymerisation of ϵ -caprolactone using diisobutyl aluminium isopropoxide at various temperatures.

The plots of M_n against conversion all show molecular weights above the theoretical molecular weight at all conversions (figure 3.22.). Control over the molecular weight seems to be greatest at 25°C. Below this temperature, the polymerisation proceeds until the limit of solubility is reached and the solution becomes solid as the polymer is no longer soluble. The rate of initiation is slower at lower temperatures and this leads to higher molecular weight polymers being formed. At 40°C the molecular weight distribution is as broad (1.3-1.4) as the reactions at lower temperatures. The molecular weight is closer to the theoretical values than those reactions carried out at lower temperatures but except the reaction at 25°C. It may be therefore that at lower temperatures, initiation using diisobutyl aluminium isopropoxide is slower, and that at higher temperatures transesterification reactions occur, both of which lead to a broader molecular weight distribution.

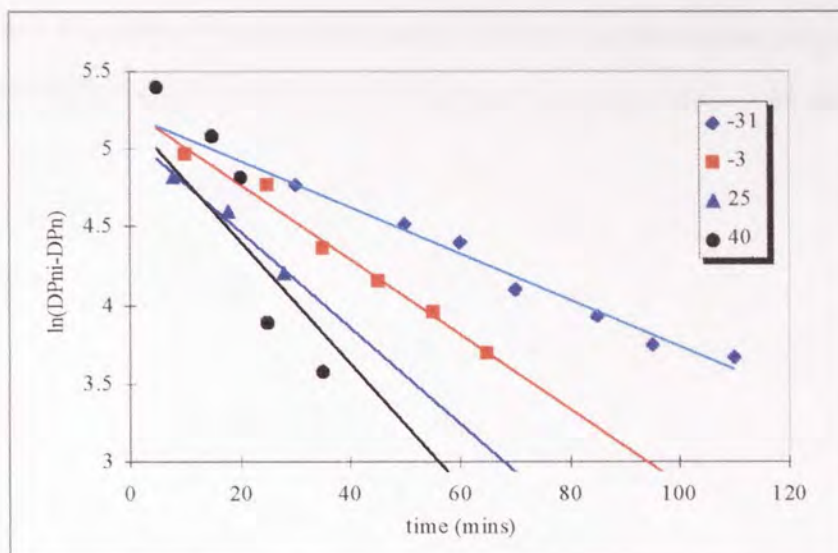


Figure 3.23. Plot of $\ln(DP_{n_x} - DP_{n_t})$ versus temperature for the polymerisation of ϵ -caprolactone using *diisobutyl aluminium isopropoxide* at various temperatures.

A plot of $\ln(DP_{n_x} - DP_{n_t})$ versus time (figure 3.23.) shows that the rate of polymerisation increases with increasing temperature as expected.

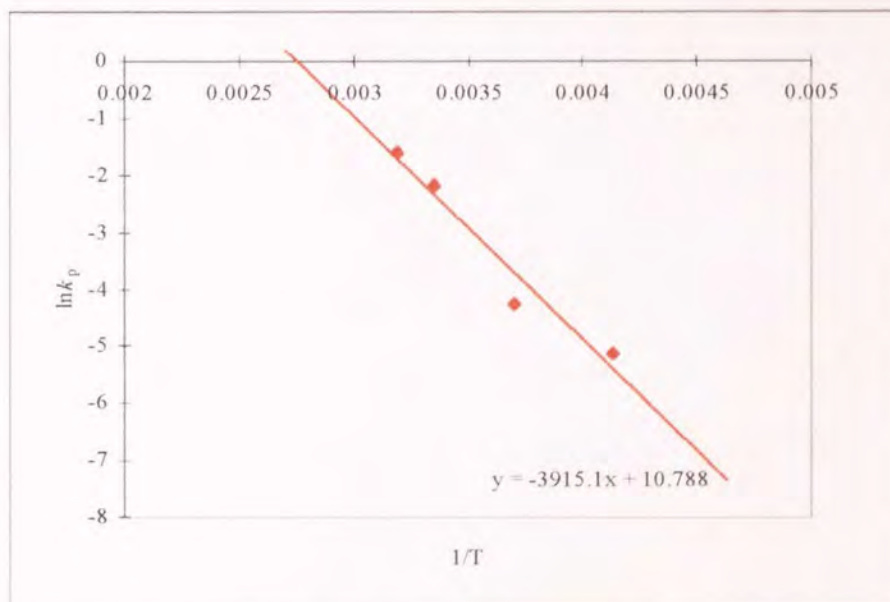


Figure 3.24. Arrhenius plot of $\ln k_p$ against $1/T$ for the polymerisation of ϵ -caprolactone in toluene using *diisobutyl aluminium isopropoxide*.

The activation energy can be calculated from the gradient of a plot of the $\ln k_p$ against $1/T$ multiplied by R , the Gas Constant. The gradient of the plot in figure 3.24

is 3915 and therefore the activation energy for the polymerisation of ϵ -caprolactone using *diisobutyl* aluminium *isopropoxide* initiator in toluene is 32.5 kJ mol⁻¹.

3.5. Transesterification reactions in the polymerisation of ϵ -caprolactone using alkyl aluminium alkoxide initiators.

The presence of back biting or transesterification when anionic initiators are used for the polymerisation of caprolactone is well documented ⁽⁵¹⁻⁵²⁾ (section 1.2.4.2.) The polymerisation of lactones and lactides using aluminium alkoxide initiators is known to be largely free of back-biting side reactions. An investigation into the effect of time and temperature on the molecular weight and polydispersity of the samples has been undertaken.

3.5.1. Effect of solvent on transesterification.

Two sealed vessels were used for the polymerisation of ϵ -caprolactone with *diisobutyl* aluminium *isopropoxide* as an initiator using toluene and THF as solvents. The vessels were kept at 25°C and a sampled daily, carefully removing a sample using a dry syringe under an argon blanket to ensure that there was no contamination of the reaction by impurities. Samples were obtained by precipitation in methanol and dried to a constant weight under vacuum at 40°C. Molecular weight was analysed by GPC.

| Days | Toluene | | | THF | | |
|------|---------|-----------|---------------|-------|-----------|---------------|
| | M_p | M_w/M_n | % of M_{n0} | M_p | M_w/M_n | % of M_{n0} |
| 0 | 34700 | - | 100 | 7200 | 1.6 | 100 |
| 1 | 32700 | 2.0 | 94 | 5700 | 2.4 | 79 |
| 2 | 27800 | 2.2 | 80 | 7700 | - | - |
| 5 | 21000 | 2.4 | 60 | - | - | - |
| 6 | 20200 | 2.4 | 58 | 5900 | 1.9 | 81 |
| 7 | 18200 | 3.1 | 52 | 2200 | 4.5 | 31 |
| 9 | 17000 | 2.7 | 48 | 1800 | 5.7 | 25 |

Table 3.10. Molecular weight and conversion data from polymerisation of ϵ -caprolactone over 9 days at 25°C

(M_p values used due to appearance of bimodal peaks with time)

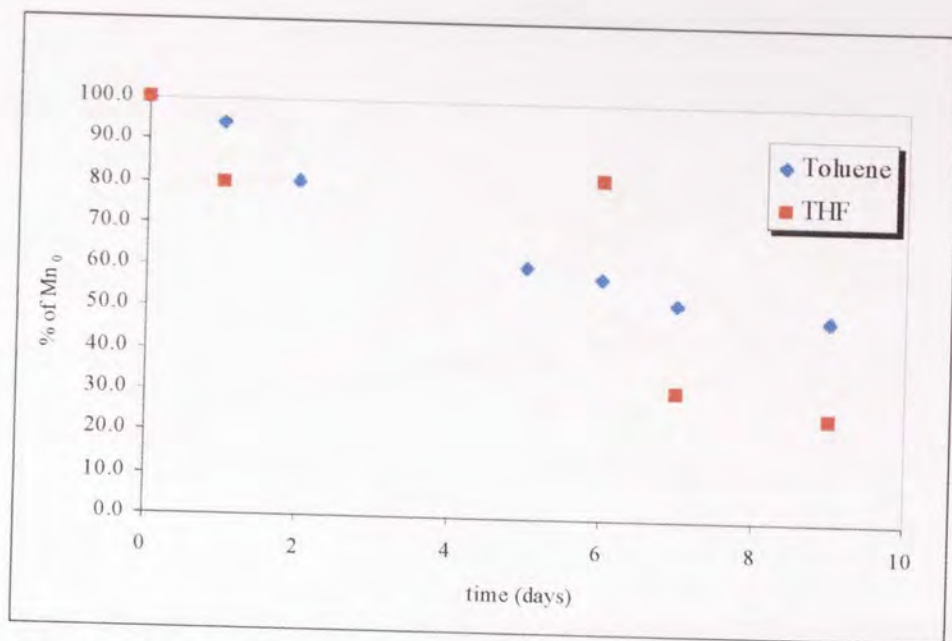


Figure 3.25. Decrease in molecular weight with time of poly(ϵ -caprolactone) in toluene and THF.

The initial molecular weights of the polymers produced in each solvent were not the same, but the percentage of the peak molecular weight by which they decreased on continued exposure to the catalyst are similar (fig 3.25). In THF the molecular weight fell from around 7200 to 1900, a 75% decrease in molecular weight and the polydispersity increased to 5.7, forming a bimodal distribution. Whilst the actual decrease in molecular weight in toluene was greater, the percentage decrease was smaller, only 48%. When the two are compared on a graph, there appears to be little difference in the decrease in molecular weight (figure 3.25.).

The molecular weight distribution of the polymers increase with time, indicating further the presence of transesterification reactions (figure 3.26).

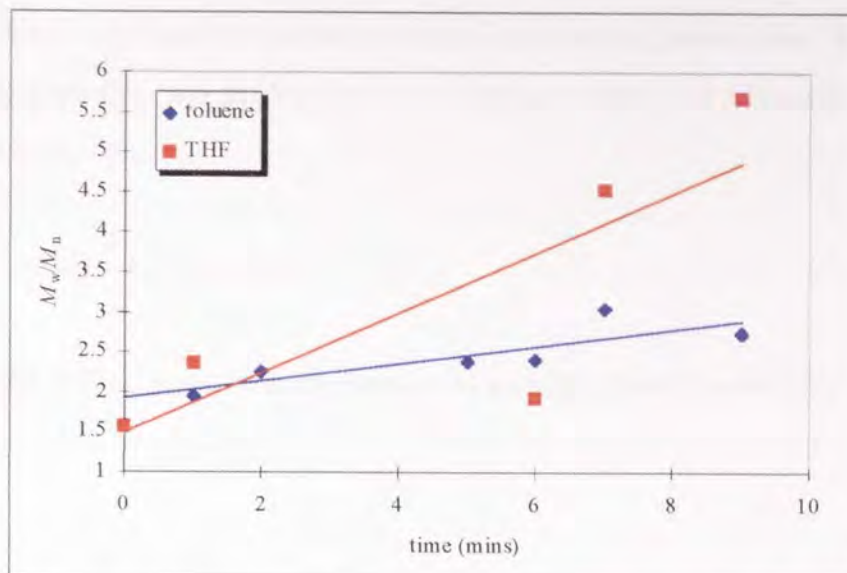


Figure 3.26. Plot of M_w/M_n versus time for the polymerisation of ϵ -caprolactone.

The plots of $\ln([M]_0/[M]_t)$ and $\ln(DP_{n,\infty}-DP_n)$ (figures 3.2 - 3.4 and 3.9 - 3.11, respectively) against time are linear, indicating that the polymerisation of caprolactone using *diisobutyl aluminium isopropoxide* as an initiator is a living system free of any termination reactions. It was also shown that the molecular weight distributions of the poly(ϵ -caprolactone) samples narrow as the reaction proceeds as would be expected of a system free of termination reactions. The most likely reason for the decrease in molecular weight and broadening of the polydispersity in the later stages of a polymerisation is a decreasing monomer concentration. Whilst propagation occurs, it could be assumed that the most reactive species present towards the aluminium alkoxide centres present is the monomer ϵ -caprolactone. Once 100% conversion is approached, or achieved, the monomer concentration at that time $[M]_t$, will be much less than the concentration of ester groups present in the polymer chain. Therefore reaction occurs with the polyester groups in the polymer chain, it is statistically more likely that reaction occurs here rather than at the monomer ester groups.

The back biting reaction and propagation reaction are essentially two different reactions, having rate constants k_b and k_p respectively. It can be expected therefore that the formation of degraded products be dependent in some way on the

ratio of k_p/k_b . It would be expected that if k_p is much greater than k_b , then the propagation reaction will predominate over the back biting and a linear polymer will result assuming that

$$k_p[M] > k_b([M]_0 - [M]) \quad 3.18.$$

where $([M]_0 - [M])$ is equal to concentration of ester groups in the polymer

and

$$k_p \propto [M] \quad 3.19.$$

then as the concentration of monomer decreases as quantitative conversion is approached so the ratio k_p/k_b favours k_b as k_p decreases.

The transesterification reactions appear to be unaffected by the nature of the reaction medium. It might be expected that the degree of transesterification would be lessened when using a co-ordinating solvent because of the need for the ester group to displace the solvent molecules from the aluminium's co-ordination sphere. This does not appear to be the case, however as the percentage of molecular weight lost appears to be similar for both solvents used.

Teysse ⁽¹²²⁾ in his paper on the polymerisation of lactides noted that the molecular weight distribution of the polymers increased with time and that percentage conversion decreased with increasing molecular weight. This they claimed was an indication of the presence of side reactions. Furthermore they reported that intramolecular transesterification reactions cause a decrease in the weight average molecular weight, thus broadening the molecular weight distribution.

Intramolecular transesterification reactions are most likely to be the cause of the decrease in molecular weight of the samples of poly(ϵ -caprolactone) removed from the polymerisation reactions after all of the monomer has been consumed.

3.5.2. Effect of temperature on transesterification reactions.

The effect of temperature on the simultaneous increase in the molecular weight distribution and decrease in molecular weight is reported in this section. An oil bath was used to heat the solvent and monomer in a dried vessel under argon at atmospheric pressure. When the solvent/monomer solution had reached the desired temperature the initiator solution was added and samples removed at recorded intervals. The samples removed were analysed by GPC and the results are in table 3.11

| Temp °C | Time (mins) | M_n | M_w | M_w/M_n |
|---------|-------------|-------|-------|-----------|
| 40°C | 5 | 6870 | 9820 | 1.43 |
| | 30 | 19460 | 25960 | 1.32 |
| | 40 | 28340 | 42230 | 1.49 |
| | 50 | 23760 | 43480 | 1.83 |
| 60°C | 5 | 19720 | 29580 | 1.5 |
| | 10 | 17900 | 23270 | 1.3 |
| | 14 | 22640 | 41430 | 1.83 |
| | 45 | 19220 | 40360 | 2.1 |
| | 105 | 17690 | 35380 | 2 |
| | 230 | 20730 | 45610 | 2.2 |
| | 1225 | 15000 | 31500 | 2.1 |
| 80°C | 0 | 2920 | 3210 | 1.1 |
| | 1 | 35240 | 42290 | 1.2 |
| | 4 | 22100 | 43760 | 1.98 |
| | 30 | 20010 | 36220 | 1.81 |
| | 60 | 14380 | 31630 | 2.2 |
| | 200 | 13220 | 22350 | 1.69 |
| | 1080 | 11420 | 23300 | 2.04 |
| | 1260 | 10520 | 24840 | 2.36 |
| 100°C | 1 | 700 | 1940 | 2.75 |
| | 5 | 18080 | 32360 | 1.79 |
| | 20 | 21830 | 40610 | 1.86 |
| | 75 | 11620 | 24530 | 2.11 |
| | 180 | 10110 | 23860 | 2.36 |
| | 345 | 11910 | 24880 | 2.09 |
| | 1380 | 8520 | 21400 | 2.51 |

Table 3.11. Molecular weights obtained from the polymerisation of ϵ -caprolactone at a range of temperatures from 40°C to 100°C using diisobutyl aluminium isopropoxide initiator in toluene. ($[M]_0 = 2.1 \text{ ml}^{-1}$, $[I]_0 = 1.8 \times 10^{-2} \text{ ml}^{-1}$)

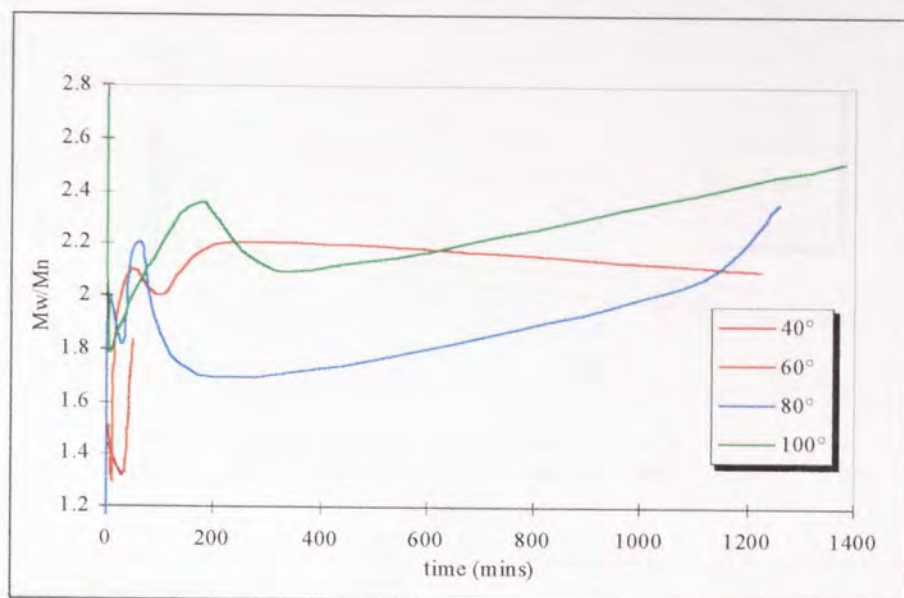


Figure 3.27. Effect of reaction temperature on a plot of polydispersity against time for the polymerisation of ϵ -caprolactone at various temperatures.

The values obtained for the polydispersity of the samples vary from around 1.1-1.5 at the start of the reaction and increase to around 2.1-2.5 after around 22-23 hours. This broadening of the distribution, (figure 3.27.) can be seen to be greater in the reaction carried out at 100°C where the M_w/M_n value increases to 2.51 from around 1.79, assuming the point taken at $t=0$ is somewhat erroneous. The broadening of the molecular weight distribution as time proceeds helps to indicate the change in size of the polymer chains present as the back biting takes place

The number average molecular weight, M_n of the poly(ϵ -caprolactone) samples removed from the reaction decrease with time as the reaction proceeds (figure 3.28.). According to Teyssie ⁽¹²²⁾, a decrease in the number average molecular weight coupled with an increase in the polydispersity signifies the presence of **intramolecular** transesterification reactions.

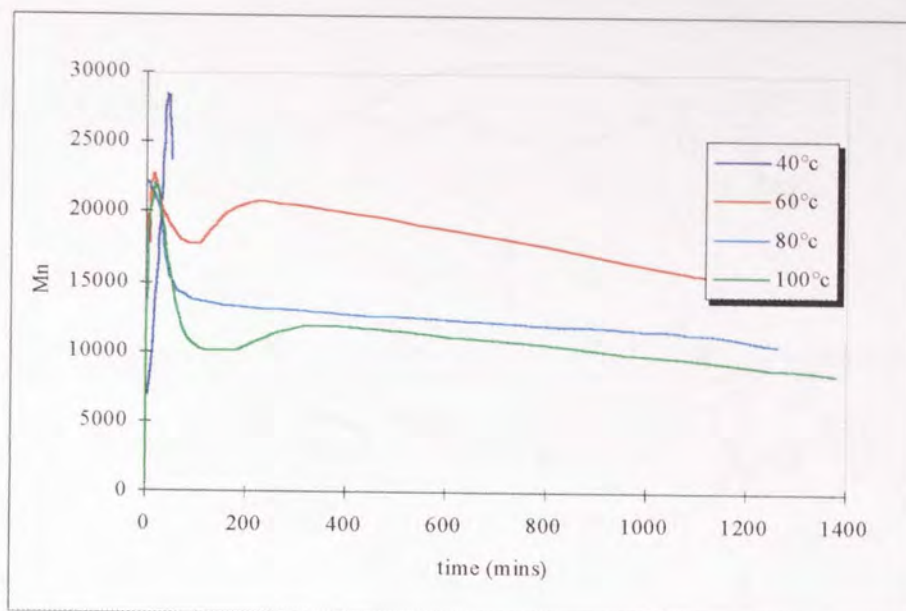
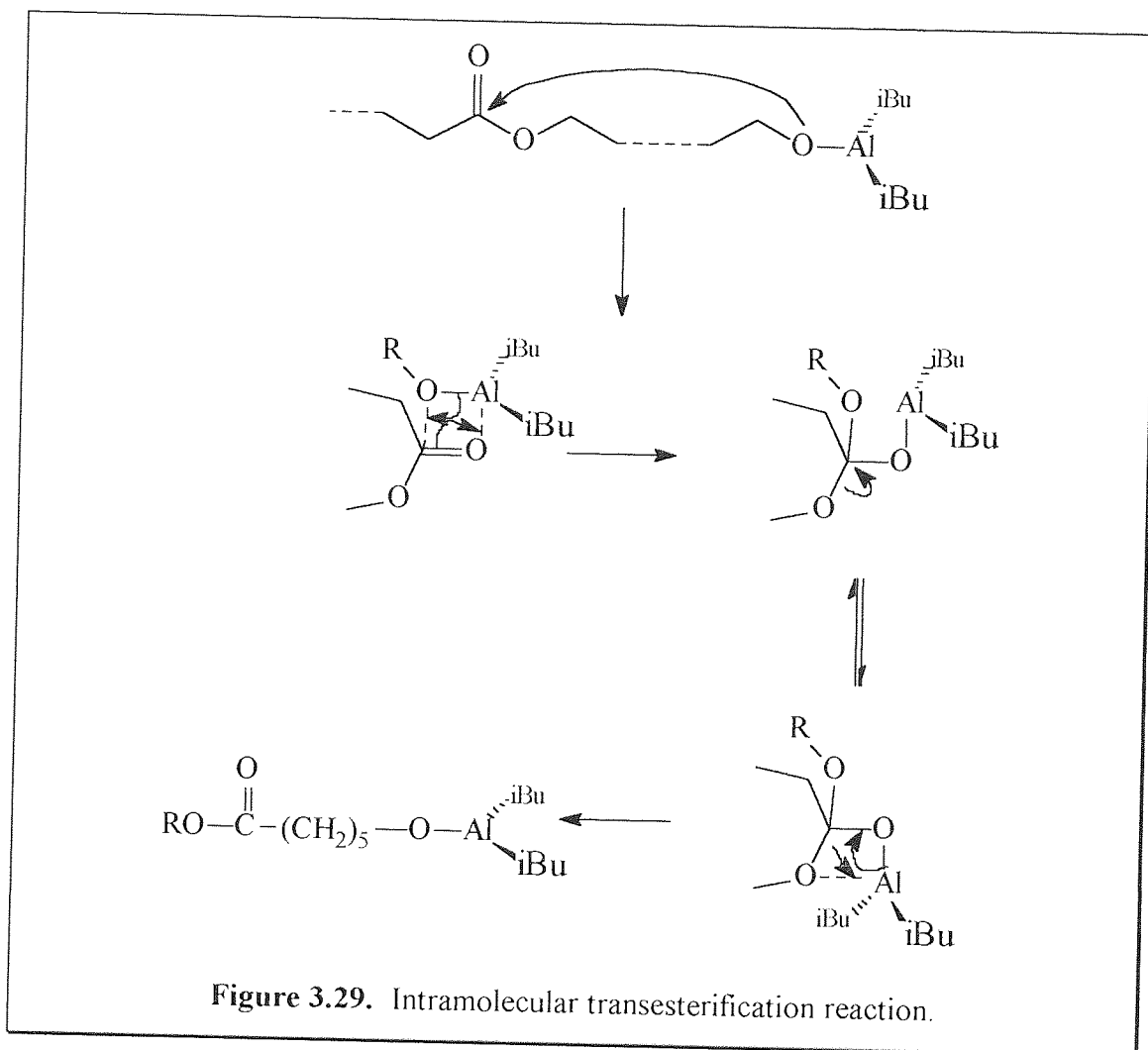


Figure 3.28. Plot of molecular weight against time the polymerisation of caprolactone at various temperatures.

Transesterification reactions would appear to be taking place at all temperatures and in both co-ordinating and non co-ordinating solvents. Increasing the reaction temperature exaggerates the effects of the transesterification. At higher temperatures the decrease in molecular weight from the maximum values reached of 22-23000 are greater than at lower temperatures. Presumably increased molecular motion at higher temperatures leads to an increased likelihood of transesterification side reactions occurring.



Intramolecular transesterification appears to be the predominant side reaction over intermolecular transesterification since in all cases both the number and weight average molecular weights decrease. This is not to say however that intermolecular transesterification is not taking place, merely that the effects of the intramolecular reaction predominate over intermolecular.

Chapter 4.

The polymerisation of ϵ -caprolactone using functional aluminium alkoxides.

4.1. Introduction.

The polymerisation of ϵ -caprolactone using aluminium alkoxide or dialkyl aluminium alkoxide initiators is known to occur via a co-ordination insertion mechanism (section 1.3.3.1.). Since the monomer complexes with the initiator, it is likely that the immediate environment around the aluminium centre will affect the complexing of the monomer and initiator. It was believed therefore that the structure of both the alkoxide and alkyl groups might affect this complexation reaction. To gain an understanding of these effects an investigation into the effects that the structure of both the alkyl and alkoxide group have on the reaction kinetics has therefore been carried out.

4.1.1. Synthesis of functional aluminium alkoxides

All dialkyl aluminium alkoxides initiators used were formed by the reaction of an alcohol and the corresponding trialkyl aluminium in toluene solution. *Triisobutyl* aluminium was added to dried, distilled toluene using the Schlenk technique and the dried and distilled alcohol was then added slowly to the toluene and alkyl aluminium solution using a dry syringe. An argon bubbler kept the vessel at atmospheric pressure whilst *isobutane* was evolved. Solid alcohols such as phenol, *p*-methoxy phenol and 2,6-di-*tert*-butyl phenol were dried under vacuum at 40°C for 48 hours and then dissolved in toluene before being added to the toluene/alkyl aluminium solution.

4.1.2. Functional aluminium alkoxides synthesised.

The aluminium alkoxides shown in table 4.1. have been synthesised and used as initiators for the polymerisation of ϵ -caprolactone. The alcohol was reacted under the conditions previously described and stored under argon and used as required. Each alkoxide was used as an initiator for the ring opening polymerisation of caprolactone in toluene at 25°C.


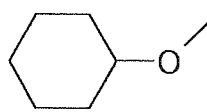
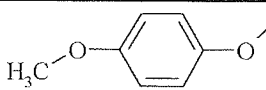
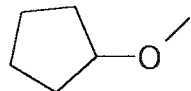
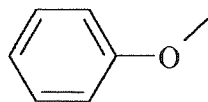
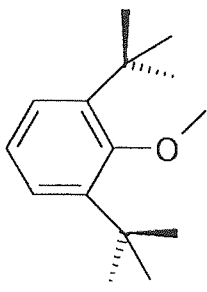
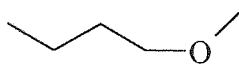
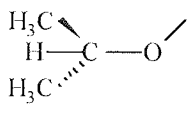
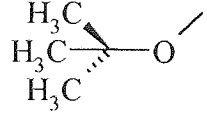
|  | | | |
|-----------------------------------------------------------------------------------|-------------------------------------------------------------------------------------|--------------------------|---------------------------------------------------------------------------------------|
| Alcohol | X= | Alcohol | X= |
| cyclo hexanol |  | <i>p</i> -methoxy phenol |  |
| cyclopentanol |  | phenol |  |
| 2,6-di- <i>tert</i> -butyl phenol |  | <i>n</i> -butanol |  |
| <i>i</i> -propanol |  | <i>t</i> -butanol |  |

Table 4.1. Alcohols used in synthesis of aluminium alkoxides

4.1.3. Unsuccessful dialkyl aluminium alkoxide synthesis.

The synthesis of the alkoxides of *p*-nitrophenol and *p*-aminophenol was attempted.

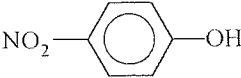
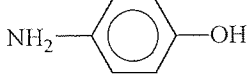
| X= | Alcohol | X= | Alcohol |
|-----------------------|-----------------------------------------------------------------------------------|-----------------------|-------------------------------------------------------------------------------------|
| <i>p</i> -nitrophenol |  | <i>p</i> -aminophenol |  |

Table 4.2. Aluminium alkoxides attempted.

The synthesis of the aluminium alkoxide of *p*-nitrophenol was unsuccessful. It was found that the dried alcohol would not dissolve in toluene at room temperature. Heating the solution to about 60°C dissolved the alcohol. Upon adding the aluminium alkyl the nitro group reacted with the aluminium alkyl.

Dried *p*-aminophenol would not dissolve in toluene at any temperature and hence it could not be used to form an aluminium alkoxide.

4.2. The polymerisation of ϵ -caprolactone using functional aluminium alkoxide initiators.

The reaction conditions were identical to those used for the polymerisation of ϵ -caprolactone using *diisobutyl* aluminium *isopropoxide* in chapter 3.

The reaction conditions were,

- Temperature 25°C
- $[\epsilon\text{-CL}] = 2.1 \text{ ml}^{-1}$
- $[I]_0 = \text{varied}$
- Inert atmosphere
- Toluene solvent

Samples were removed from the polymerisation at recorded intervals, transferred to a beaker containing a small volume of toluene and then precipitated from methanol.

It was found that direct precipitation in methanol made the polymer insoluble in both THF and chloroform and GPC analysis was found subsequently to be difficult. The solvent was removed by evaporation and the polymer was dried to a constant weight under vacuum.

4.2.1. The polymerisation of ϵ -caprolactone using aromatic alkoxide initiators.

Diisobutyl aluminium *di-tert*-butyl phenoxide and *diisobutyl* aluminium *p*-methoxy phenoxide were used as initiators for the polymerisation of ϵ -caprolactone. The polymers produced using these initiators have been compared to those produced using *diisobutyl* aluminium phenoxide as an initiator.

4.2.2. The polymerisation of ϵ -caprolactone using *diisobutyl* aluminium phenoxide initiator.

Diisobutyl aluminium *p*-methoxyphenoxide was used as an initiator for the polymerisation of ϵ -caprolactone in toluene. The results are in table 4.3.

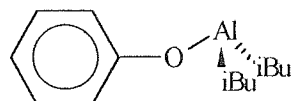


Figure 4.1. Dialkyl aluminium phenoxide.

| $[I]_0 \text{ ml}^{-1}$ | Time (mins) | % Conv | M_n | M_w | M_w/M_n |
|---------------------------------|-------------|--------|-------|--------|-----------|
| 3.6×10^{-2} (GKS51) | 5 | 2.8 | - | - | - |
| | 10 | 3.4 | - | - | - |
| | 17 | 3.7 | - | - | - |
| | 24 | 4.1 | - | - | - |
| | 30 | 4.3 | 400 | 1450 | 3.6 |
| | 45 | 2.7 | 12160 | 23610 | 1.9 |
| | 650 | 7.9 | - | - | - |
| | 100 | 13.2 | - | - | - |
| | 130 | 28.1 | - | - | - |
| | 185 | 64.9 | - | - | - |
| 1.8×10^{-2} (GKS50) | 5 | 1.8 | - | - | - |
| | 15 | 3.1 | - | - | - |
| | 43 | 10.6 | 4800 | 6800 | 1.4 |
| | 65 | 27.2 | 12500 | 18000 | 1.5 |
| | 90 | 55.1 | 30400 | 40600 | 1.1 |
| | 150 | 85.3 | 52300 | 103000 | 2.0 |
| | 240 | 91.1 | 28200 | 70800 | 2.5 |
| | 300 | 94.0 | 70400 | 114000 | 1.6 |
| 1.0×10^{-2} (GKS52) | Time (mins) | % Conv | M_n | M_w | M_w/M_n |
| | 10 | 0.2 | - | - | - |
| | 40 | 2.0 | - | - | - |
| | 70 | 3.5 | - | - | - |
| | 90 | 5.7 | - | - | - |
| | 135 | 43.3 | - | - | - |
| | 180 | 34.5 | - | - | - |
| | 220 | 69.0 | - | - | - |
| | 330 | 89.3 | - | - | - |

Table 4.3. Molecular weight and conversion data from the polymerisation of ϵ -caprolactone using diisobutyl aluminium phenoxide as an initiator.

The samples of poly(ϵ -caprolactone) removed from the polymerisation using diisobutyl aluminium phenoxide initiator were difficult to dissolve in either THF or chloroform. Molecular weight calculations using GPC were therefore difficult to obtain. Only the GPC analysis of the reaction carried out at $[I]_0 = 1.8 \times 10^{-2} \text{ ml}^{-1}$ produced enough molecular weight data to be meaningful.

A plot of M_n against conversion (figure 4.2) for GKS50 shows the actual molecular weight (solid line) is greater than the theoretical molecular weight (dashed line). It is possible that the alkoxide initiator did not form properly or that initiation was incomplete.

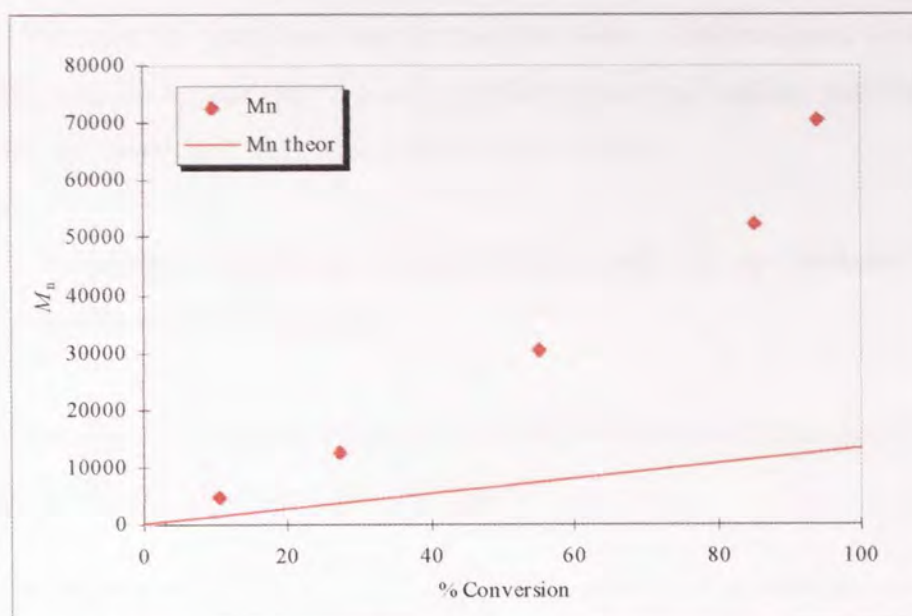


Figure 4.2. Dependence of M_n on conversion for the polymerisation of ϵ -caprolactone using diisobutyl aluminium phenoxide as an initiator.

A plot of $\ln([M]_0/[M]_t)$ against time shows that the plot does not pass through the origin. An acceleration period is noticeable at the start of the reaction, the gradient of the plot increases with time. This build up period is believed to be related to the ability of the monomer to co-ordinate with the initiator and consequently the slow initiation process observed in these systems.

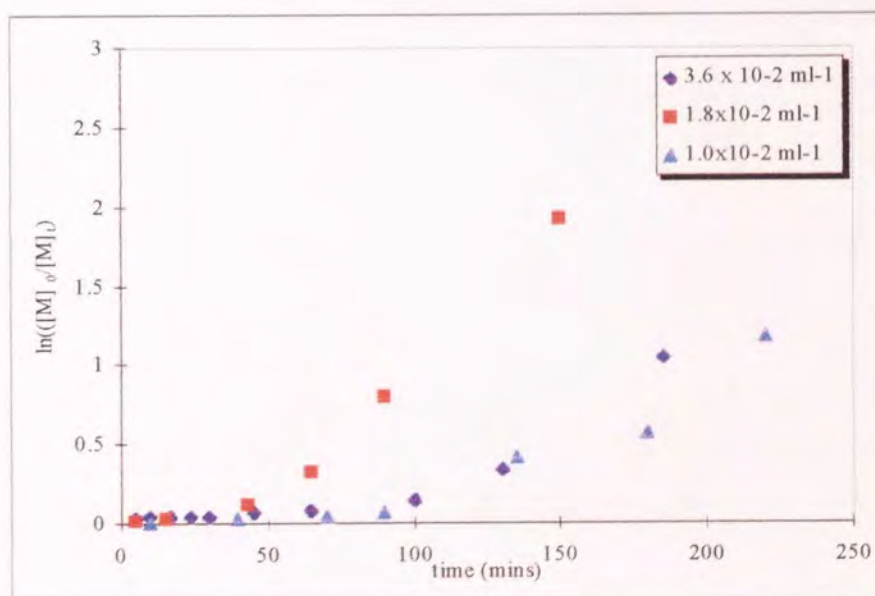


Figure 4.3. First order for the polymerisation of ϵ -caprolactone using diisobutyl aluminium phenoxide as an initiator.

However the plot does tend to become linear. This indicates that that the initiation reaction is slow but it is not possible to say that transfer and termination reactions are absent and that the polymerisation is living.

4.2.3. Diisobutyl aluminium *p*-methoxyphenoxide as an initiator for the polymerisation of ϵ -caprolactone.

Diisobutyl aluminium *p*-methoxyphenoxide (figure 4.4.) has also used as an initiator for the polymerisation of ϵ -caprolactone in toluene.

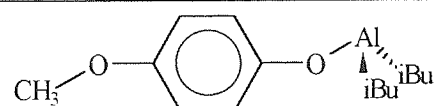


Figure 4.4. Diisobutyl aluminium *p*-methoxyphenoxide.

| $[I]_0 \text{ ml}^{-1}$ | Time (mins) | % Conv | M_n | M_w | M_w/M_n |
|---------------------------------|-------------|--------|-------|-------|-----------|
| 3.6×10^{-2} (GKS65) | 5 | 6.6 | 500 | 800 | 1.6 |
| | 10 | 9.8 | 900 | 1600 | 1.8 |
| | 20 | 24.0 | 2500 | 4100 | 1.7 |
| | 30 | 51.3 | 6000 | 8900 | 1.5 |
| | 40 | 79.3 | 10400 | 14200 | 1.4 |
| | 50 | 99.0 | 13600 | 17300 | 1.3 |
| 1.8×10^{-2} (GKS67) | 5 | 2.5 | - | - | - |
| | 15 | 4.1 | 900 | 1400 | 1.6 |
| | 30 | 15.3 | 3400 | 4600 | 1.4 |
| | 45 | 71.5 | 18100 | 28900 | 1.6 |
| | 50 | 84.5 | 17800 | 27500 | 1.5 |
| | 55 | 94.5 | 30000 | 38000 | 1.3 |
| | 60 | 97.6 | 30800 | 39000 | 1.3 |
| 1.0×10^{-2} (GKS64) | 18 | 2.2 | 200 | 210 | 1.1 |
| | 30 | 4.3 | 3300 | 4300 | 1.3 |
| | 45 | 11.4 | 7700 | 10800 | 1.4 |
| | 60 | 26.0 | 15800 | 22700 | 1.4 |
| | 80 | 64.6 | 38900 | 49700 | 1.3 |
| | 90 | 95.2 | 40800 | 49700 | 1.2 |
| | 105 | 80.5 | 42300 | 54500 | 1.3 |
| | 130 | 85.2 | 54000 | 64000 | 1.2 |
| 6.7×10^{-3} (GKS66) | 50 | 21.1 | 16500 | 29700 | 1.8 |
| | 57 | 40.0 | 21200 | 28200 | 1.3 |
| | 65 | 69.6 | 43200 | 54300 | 1.3 |

Table 4.5. Molecular weight and conversion data obtained from the polymerisation of ϵ -caprolactone using *diisobutyl* aluminium *p*-methoxyphenoxide.

Again the polymerisation of ϵ -caprolactone using *diisobutyl* aluminium *p*-methoxyphenoxide produces polymers with higher molecular weights than expected from initial monomer/initiator ratios (see Figure 4.5).

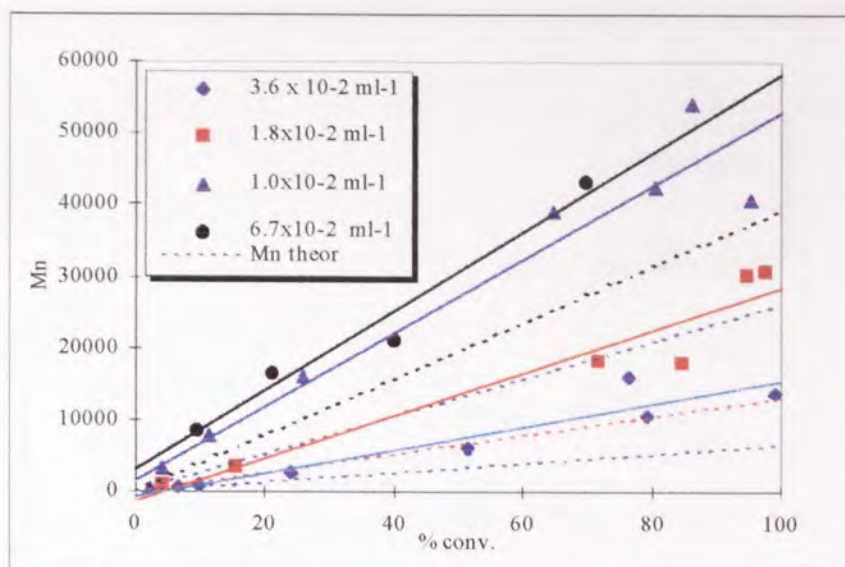


Figure 4.5. Dependence of M_n on conversion for the polymerisation of ϵ -caprolactone using *diisobutyl* aluminium *p*-methoxy phenoxide in toluene at 25°C.

The plot of M_n against conversion for the polymerisation of ϵ -caprolactone using *diisobutyl* aluminium *p*-methoxy phenoxide (Figure 4.5) shows that the observed molecular weights of the polymers (solid lines) are greater than the theoretical molecular weights calculated from the initial monomer/initiator ratio. It may be that the methoxy group on the phenol ring is co-ordinating with aluminium centres on other initiator molecules (figure 4.6). This will prevent the aluminium centres from complexing with the monomer and propagating.

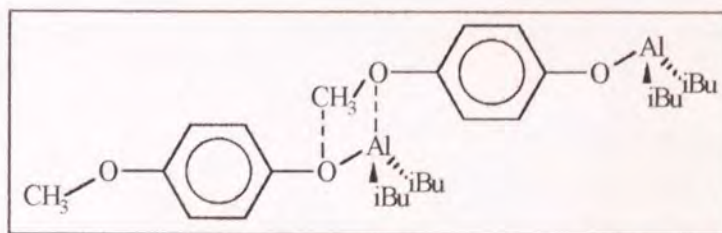


Figure 4.6. Interactions between aluminium centre and *p*-methoxy group

The molecular weight distributions are quite narrow however so such intermolecular interactions are not causing the growing polymers to be terminated prematurely. It is possible therefore that the interactions between initiator molecules are causing some initiator to be destroyed or rendered ineffective.

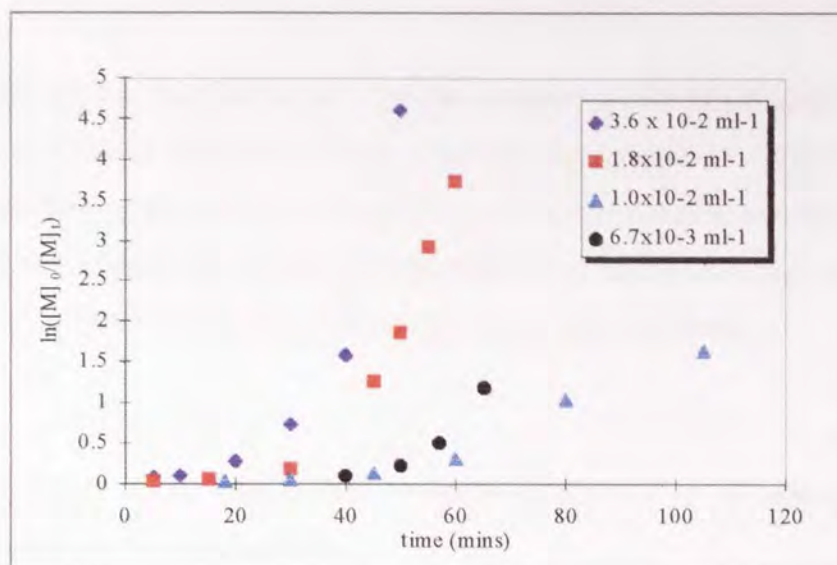


Figure 4.7. First order plot for the polymerisation of ϵ -caprolactone using diisobutyl aluminium *p*-methoxy phenoxide initiator.

The rate of polymerisation of ϵ -caprolactone using diisobutyl aluminium *p*-methoxy phenoxide initiator is dependent on concentration of initiator. The gradient of the linear section of the plot of $\ln([M]_0/[M]_t)$ against time after the build up period increases with initiator concentration (figure 4.7). The plots at $[I]_0 = 1.0 \times 10^{-2} \text{ ml}^{-1}$ and $6.7 \times 10^{-3} \text{ ml}^{-1}$ appear to be incorrect. This is either because of experimental error, or because of impurities such as air or moisture leaking into the reaction. An induction period shows that propagation does not occur instantly. In common with all the other initiators used there is a period where the concentration of living species increases and then remains constant throughout propagation.

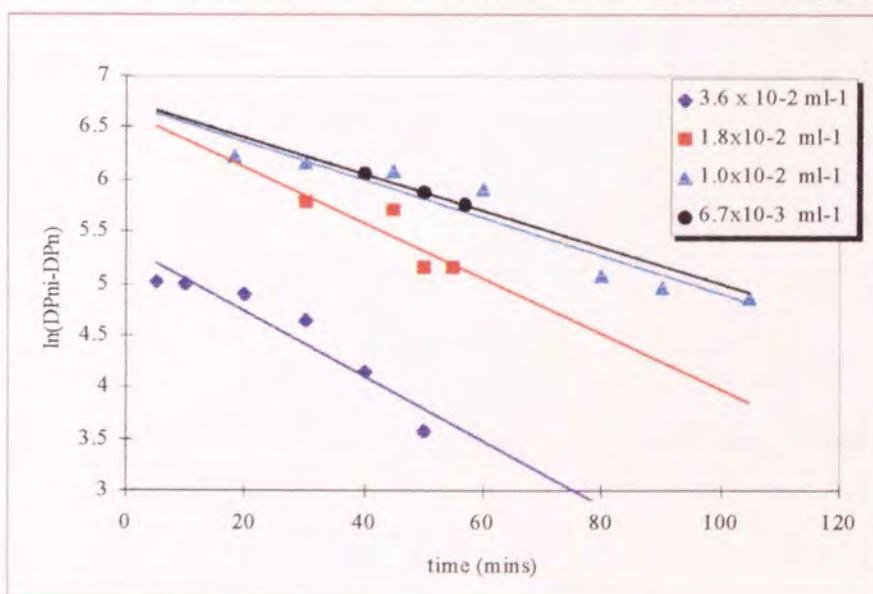


Figure 4.8. Plot of $\ln(DP_{n\infty}-DP_{nt})$ against time for the polymerisation of ϵ -caprolactone.

It is known that the negative of the gradient of the $\ln(DP_{n_{\infty}} - DP_n)$ against time plot is equal to the apparent rate constant of propagation. Figure 4.8 shows that the gradient of the plot is proportional to the initial initiator concentration used as would be expected of a living polymerisation. It also shows that as the slope increases, then the concentration of growing species also increases.

4.2.4. Diisobutyl aluminium 2,6-di *tert*-butyl phenoxide as an initiator for the polymerisation of ϵ -caprolactone.

Diisobutyl aluminium 2,6-di-*tert*-butyl phenoxide (figure 4.9) was chosen as an aromatic initiator that would be able to provide steric hindrance around the active site. Table 4.4 summaries the data obtained for polymerisations of caprolactone using diisobutyl aluminium 2,6-di-*tert*-butyl phenoxide initiator.

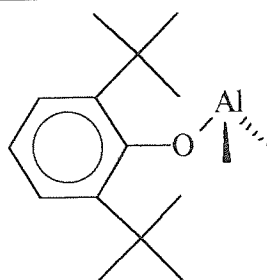


Figure 4.9. Diisobutyl aluminium di-*tert*-butyl phenoxide

| $[I]_0 \text{ ml}^{-1}$ | Time (mins) | % Conv | M_n | M_w | M_w/M_n |
|---------------------------------|-------------|--------|-------|--------|-----------|
| 3.6×10^{-2} (GKS69) | 30 | 6.6 | - | - | - |
| | 70 | 20.7 | 37500 | 60700 | 1.6 |
| | 120 | 32.7 | 52500 | 92300 | 1.8 |
| | 155 | 40.9 | 76300 | 149800 | 2.0 |
| | 240 | 60.6 | 86500 | 214000 | 2.5 |
| 1.8×10^{-2} (GKS68) | 13 | 3.4 | 5400 | 6000 | 1.1 |
| | 20 | 2.9 | 10000 | 19900 | 2.0 |
| | 30 | 2.9 | 12500 | 22900 | 1.8 |
| | 45 | 7.5 | 15000 | 27700 | 1.9 |
| | 75 | 8.2 | 23400 | 42200 | 1.8 |
| | 105 | 9.8 | 33500 | 50400 | 1.5 |
| | 160 | 14.8 | 38400 | 54800 | 1.4 |
| | 215 | 18.7 | 40300 | 59500 | 1.4 |
| | 245 | 13.5 | 45500 | 59500 | 1.3 |
| | 285 | 20.0 | 46300 | 63100 | 1.3 |
| | 375 | 34.7 | - | - | - |
| 6.7×10^{-3} (GKS70) | 30 | 2.2 | - | - | - |
| | 75 | 6.5 | - | - | - |
| | 135 | 13.9 | 31600 | 42900 | 1.4 |
| | 160 | 19.3 | 22300 | 28600 | 1.3 |
| | 240 | 40.7 | 50100 | 80200 | 1.6 |
| | 280 | 48.9 | 64600 | 116000 | 1.8 |

Table 4.5. Molecular weight and conversion data obtained from the polymerisation of ϵ -caprolactone using diisobutyl aluminium 2,6-di-*tert*-butyl phenoxide in toluene at 25°C.

The molecular weights of the samples of polymer withdrawn from the reaction are greater than would be expected from the initial monomer/initiator ratios. The dashed lines in Figure 4.10. show the expected molecular weights whilst the solid lines show the actual molecular weight obtained by GPC. It is probable that the all of the alkoxide moieties did not take part in initiation.

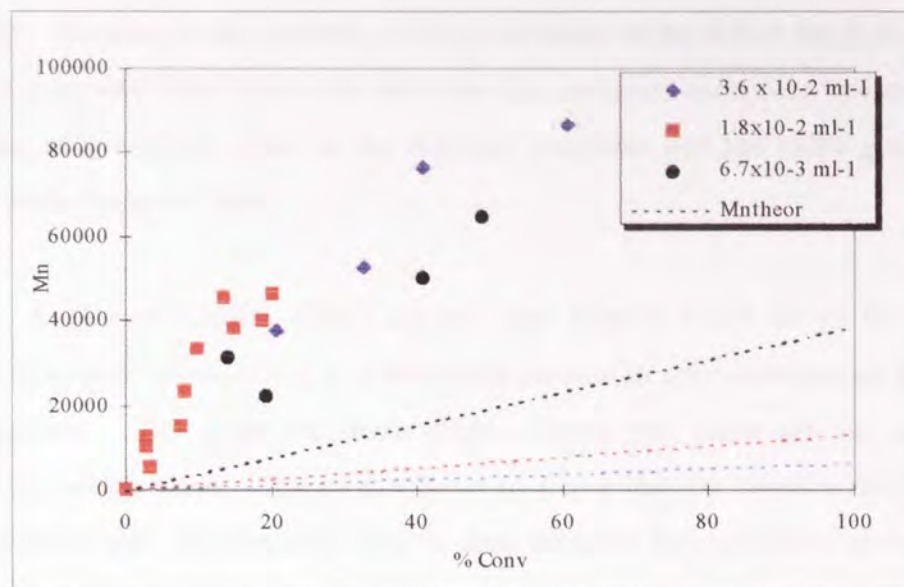


Figure 4.10. Dependence of M_n on conversion for the polymerisation of ϵ -caprolactone using *diisobutyl* aluminium *di-tert*-butyl phenoxide initiator in toluene at 25°C.

The inefficient initiation of the polymerisation can be assigned to the bulky structure of the initiator. The *tert*-butyl groups β - to the alkoxide oxygen atom hinder the complexation of the monomer with the active alkoxide sites. *Diisobutyl* aluminium *di-tert*-butyl phenoxide is shown from the side (a), and from above (b) in Figure 4.11. Whilst approach of the monomer to the alkoxide from viewpoint Figure 4.11 (a) will almost certainly be blocked or hindered, approach from the viewpoint of Figure 4.11 (b) will be less hindered, although probably not entirely unhindered.

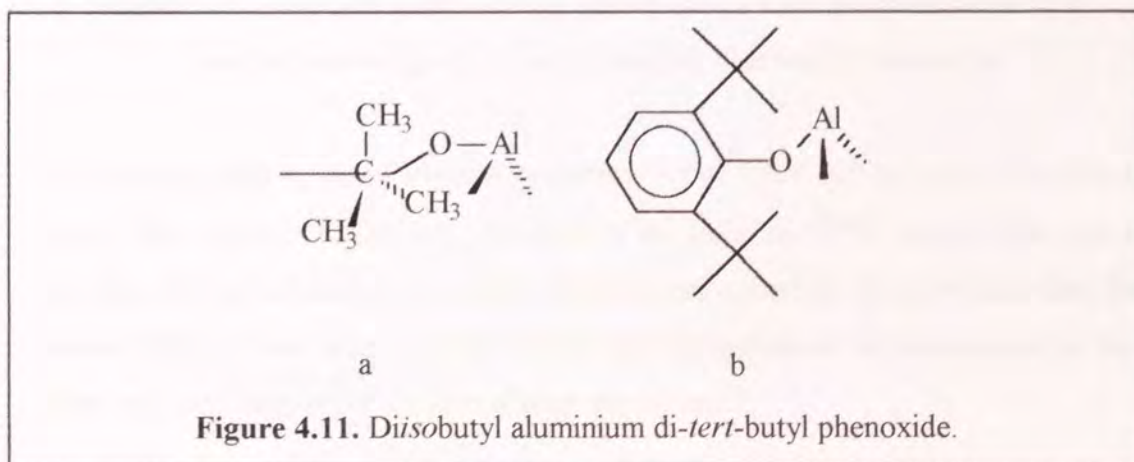


Figure 4.11. *Diisobutyl* aluminium *di-tert*-butyl phenoxide.

The molecular weight distributions of the polymers formed are broader than would be expected for a living polymerisation. The broad distribution of molecular

weights is probably due to slow initiation rather than termination of the propagating species. Because of the sterically hindered location of the active site it is likely that initiation is very slow, and once initiation has occurred monomer insertion should become progressively easier as the polymer lengthens and the bulky group moves away from the active site.

A plot of $\ln(DP_{n\infty}-DP_n)$ against time (Figure 4.12) shows the effect of initial diisobutyl aluminium 2,6-di-*tert*-butyl phenoxide concentration on the rate of propagation. The plots are linear which shows that there are no termination reactions taking place. This in part helps to prove that the broader than expected molecular weight distribution is due to slow initiation as opposed to termination or transfer reactions.

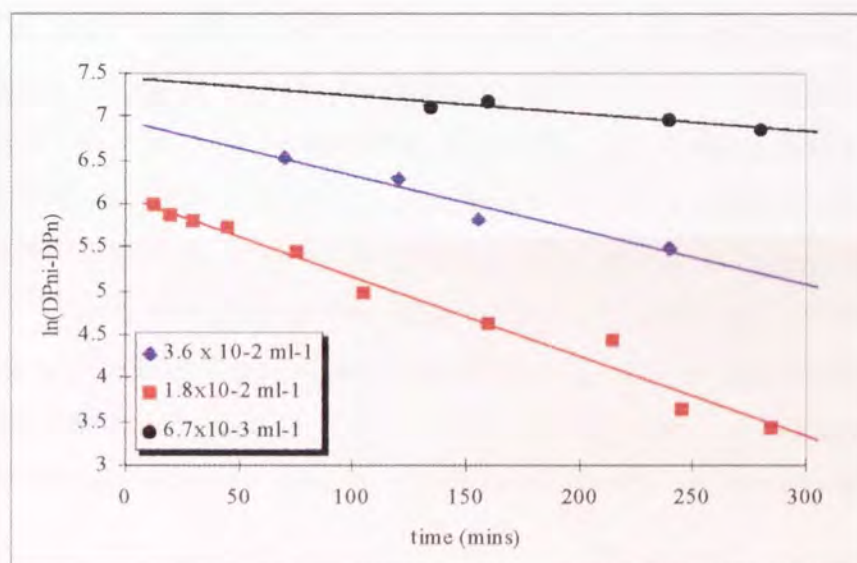


Figure 4.12. Plot of $\ln(DP_{n\infty}-DP_n)$ against time for the polymerisation of ϵ -caprolactone using diisobutyl aluminium ditert-butyl phenoxide

The reaction with an initial initiator concentration of $3.6 \times 10^{-2} \text{ ml}^{-1}$ has a rate that is slower than would be expected, the slope of the $\ln(DP_{n\infty}-DP_n)$ against time plot is less than that of a reaction at a higher initiator concentration. It is probable that the cause of this slower than expected rate is that the initiation was incomplete or that there was an experimental error in adding the initiator.

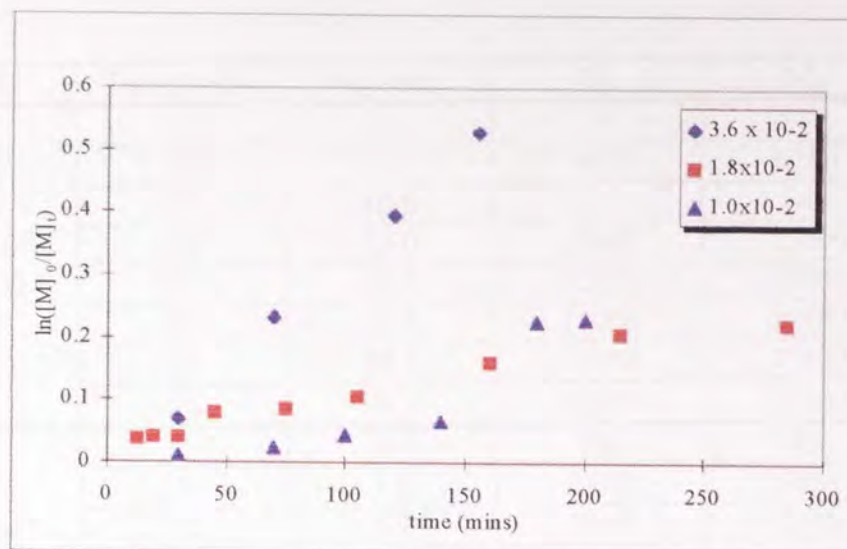


Figure 4.13. First order plot for the polymerisation of ϵ -caprolactone using diisobutyl aluminium 2,6-di-*tert*-butyl phenoxide initiator.

The plot of $\ln([M]_0/[M]_t)$ against time for the polymerisation of ϵ -caprolactone using diisobutyl aluminium 2,6-di-*tert*-butyl phenoxide initiator (Figure 4.13) shows no noticeable build up period. The build up period is usually observed at around 7-10% conversion and the polymerisations here have all reached at least 95% conversion so the build up period might not be occurring. Jerome and Teyssie⁽¹¹³⁾ stated that the build up period was an indication of the ability of the initiator to accommodate the monomer molecules. It could be that the bulky nature of the alkoxide group prevents the formation of aggregates and therefore is no rearrangement or formation of such aggregates required and slowing the rate of reaction.

4.2.5. Diisobutyl aluminium cyclohexanoxide as an initiator for the polymerisation of ϵ -caprolactone.

Diisobutyl aluminium cyclohexanoxide was chosen as a cyclic and non aromatic alkoxide group. The structure of diisobutyl aluminium cyclohexanoxide (figure 4.14) is similar to that of diisobutyl aluminium isopropoxide up to the carbon atom β to the alkoxide oxygen atom.

| $[I]_0 \text{ ml}^{-1}$ | Time (mins) | % Conv | M_n | M_w | M_w/M_n |
|---------------------------------|-------------|--------|-------|-------|-----------|
| 3.6×10^{-2} (GKS59) | 4 | 3.3 | - | - | - |
| | 10 | 6.6 | 4800 | 6300 | 1.3 |
| | 15 | 18.0 | - | - | - |
| | 20 | 23.0 | 10900 | 15000 | 1.4 |
| | 25 | 38.3 | 12200 | 17000 | 1.4 |
| | 30 | 53.8 | 13000 | 20300 | 1.6 |
| | 40 | 98.1 | 21000 | 33300 | 1.6 |
| | 50 | 96.2 | 18800 | 30400 | 1.6 |
| 1.8×10^{-2} (GKS60) | 3 | 3.4 | 580 | 900 | 1.5 |
| | 7 | 4.0 | 2300 | 5800 | 1.9 |
| | 15 | 7.7 | 3600 | 8300 | 2.3 |
| | 28 | 30.1 | 5800 | 10000 | 1.7 |
| | 33 | 43.4 | 10800 | 14000 | 1.3 |
| | 40 | 67.0 | - | - | - |
| | 50 | 87.5 | 12900 | 21300 | 1.7 |
| | 60 | 94.2 | - | - | - |
| 1.0×10^{-2} (GKS62) | 15 | 10.3 | 7900 | 10800 | 1.4 |
| | 30 | 27.5 | 17200 | 23600 | 1.4 |
| | 45 | 47.6 | 24300 | 34700 | 1.4 |
| | 60 | 72.9 | 35600 | 50600 | 1.4 |
| | 75 | 86.2 | 46850 | 59000 | 1.3 |
| | 105 | 97.7 | 72400 | 84000 | 1.2 |
| | 135 | 96.5 | 59300 | 78600 | 1.3 |
| | 180 | 98.1 | - | - | - |
| 6.7×10^{-3} (GKS61) | 10 | 2.4 | 4700 | 13900 | 2.9 |
| | 22 | 15.0 | 4600 | 6500 | 1.4 |
| | 32 | 10.7 | 7000 | 9800 | 1.4 |
| | 45 | 18.8 | 11800 | 16500 | 1.4 |
| | 60 | 34.5 | 18400 | 25000 | 1.4 |
| | 75 | 60.4 | - | - | - |
| | 90 | 79.7 | - | - | - |
| | 120 | 97.4 | - | - | - |
| | 150 | 97.7 | - | - | - |

Table 4.6. Molecular weight and conversion data obtained from the polymerisation of ϵ -caprolactone using diisobutyl aluminium cyclo-hexanoxide in toluene at 25°C.

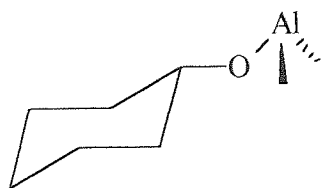


Figure 4.14 Dialkyl aluminium cyclohexanoxide.

The plot of M_n against conversion (Figure 4.15) shows that the experimental molecular weights are greater than the theoretical molecular weights (dashed lines) calculated from initial monomer/initiator ratios but the differences are much less significant in this case than when *diisobutyl* aluminium 2,6-*di-tert*-butylphenoxide was used as the initiator.

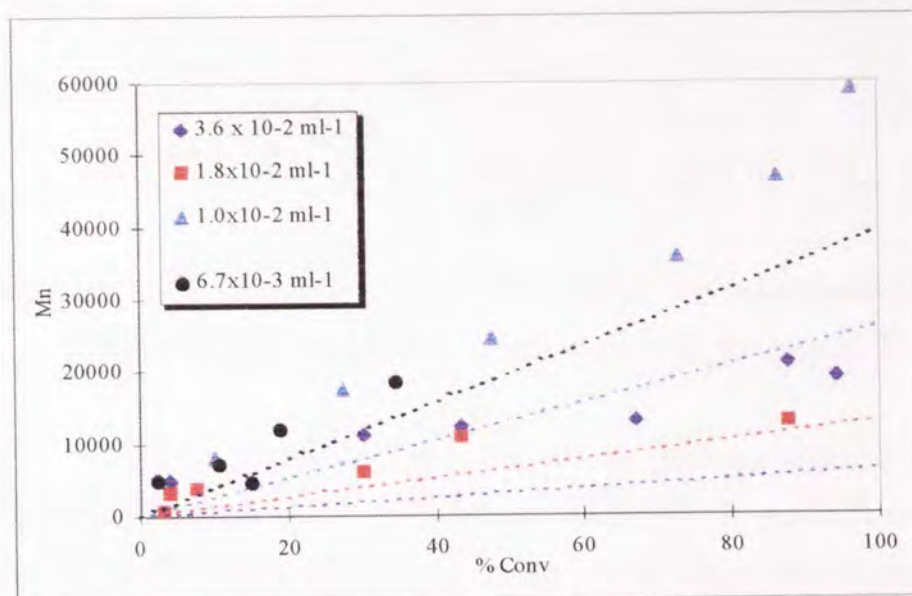


Figure 4.15. Dependence of M_n on conversion for the polymerisation of ϵ -caprolactone in toluene using *diisobutyl* aluminium cyclohexanoxide at 25°C.

It is likely either that initiation is incomplete, or that the initiator was not completely formed, thus lowering the effective initiator concentration. Transfer and termination reactions are unlikely to have been present because of the linear nature of the M_n against conversion plots. The presence of termination reactions would have caused the plots to be not linear. The slope of the plot at $[I]_0 = 1.0 \times 10^{-2} \text{ ml}^{-1}$ increases slightly after approximately 80% conversion. It is possible that some of the initiator had been destroyed and this is most probably because impurities accidentally leaked into the system.

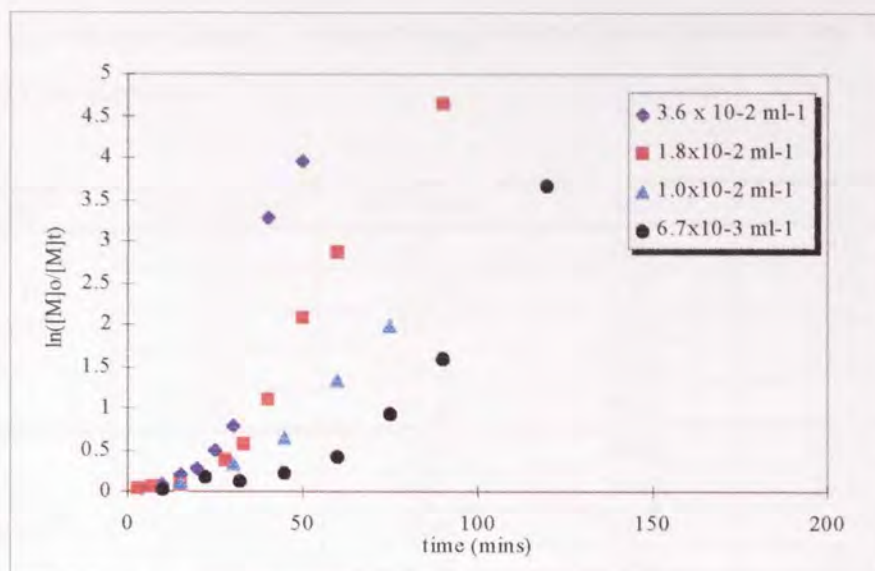


Figure 4.16. First order plot for the polymerisation of ϵ -caprolactone using diisobutyl aluminium cyclohexanoxide initiator in toluene at 25°C .

The first order plot shows again that a build up period is present at the beginning of each reaction. The structure of the alkoxide group of the initiator (Figure 4.16) is sufficiently bulky as to possibly prevent immediate complexation of the monomer with the initiator. The molecular weight distribution of the polymer produced in each reaction is broader than would be expected if initiation were instantaneous. The length of the build up period appears to be related to the initial initiator concentration. After the build up period, the rate of propagation increases significantly but remains linear until the reaction nears 100% conversion. This indicates that the polymerisation of ϵ -caprolactone using diisobutyl aluminium cyclohexanoxide initiator is first order in monomer. The gradient of the plot decreases as monomer concentration decreases when the reaction is almost complete. The gradient of the plot after the inflexion point is proportional to the initial concentration $[I]_0$.

4.2.6. The polymerisation of ϵ -caprolactone using diisobutyl aluminium cyclopentoxide as an initiator.

Cyclopentanol was chosen to use in the formation of an alkyl aluminium alkoxide because it is cyclic and planar. The results obtained from the polymerisations using isopropoxide and cyclohexanoxide groups in the initiator suggested that the structure and the volume occupied in space of the alkoxide group does have an

effect on the reaction kinetics. It was thought that a planar alkoxide may an effect on the reaction kinetics.

| $[I]_0 \text{ ml}^{-1}$ | Time (mins) | % Conv | M_n | M_w | M_w/M_n |
|---------------------------------|-------------|--------|-------|-------|-----------|
| 3.6×10^{-2} (GKS87) | 20 | 5.2 | 200 | 200 | 1.0 |
| | 35 | 15.6 | 330 | 540 | 1.7 |
| | 47 | 79.2 | 2900 | 3700 | 1.3 |
| | 55 | 90.9 | 7900 | 10000 | 1.3 |
| | 60 | 97.0 | 8800 | 11100 | 1.3 |
| 18×10^{-2} (GKS88) | 20 | 2.6 | 1800 | 2800 | 1.6 |
| | 30 | 4.3 | 2400 | 2600 | 1.1 |
| | 50 | 28.8 | 12800 | 15700 | 1.2 |
| | 55 | 36.4 | 15500 | 18800 | 1.2 |
| | 60 | 56.3 | 22000 | 25600 | 1.2 |
| | 70 | 84.2 | 14000 | 17500 | 1.2 |
| | 105 | 98.6 | - | - | - |
| 1.0×10^{-2} (GKS89) | 15 | 1.4 | 540 | 910 | 1.7 |
| | 30 | 9.3 | 5100 | 6300 | 1.2 |
| | 38 | 25.8 | 12200 | 13800 | 1.1 |
| | 42 | 40.9 | 15600 | 18900 | 1.2 |
| | 45 | 52.4 | 20000 | 23200 | 1.2 |
| | 50 | 69.0 | 23500 | 28400 | 1.2 |
| 6.7×10^{-3} (GKS90) | 15 | 1.2 | - | - | - |
| | 30 | 1.9 | 710 | 900 | 1.2 |
| | 40 | 1.6 | 1200 | 1700 | 1.4 |
| | 55 | 5.4 | 4100 | 4800 | 1.2 |
| | 70 | 15.1 | 9400 | 10800 | 1.1 |
| | 85 | 35.1 | 17700 | 26900 | 1.5 |
| | 95 | 59.3 | 21000 | 24300 | 1.2 |
| | 120 | 87.3 | 37100 | 50600 | 1.4 |

Figure 4.7 Molecular weight and conversion data obtained from the polymerisation of ϵ -caprolactone using diisobutyl aluminium cyclopentoxide in toluene at 25°C.

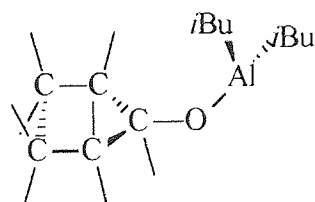


Figure 4.17. Dialkyl aluminium cyclopentoxide

The plot of M_n against conversion (Figure 4.18) shows again that the molecular weights of the polymers produced in these reactions are higher than expected from initial monomer/initiator ratios (dashed lines). The actual molecular

weights do seem to be closer to the theoretical weights than when diisobutyl aluminium cyclo-hexanoxide was used as initiator and much closer than when diisobutyl aluminium 2,6-di-*tert*-butylphenoxide was used as the initiator. It may be that the smaller cyclopentyl ring does not hinder the formation of the monomer and initiator complex. Initiation is therefore likely to be more efficient. The molecular weight distributions seem to be narrower than the corresponding diisobutyl aluminium hexanoxide reaction. Assuming an absence of termination reactions, initiation appears to be faster than the corresponding hexanoxide reactions. The living nature of the polymerisation is indicated by the general linearity of the plots.

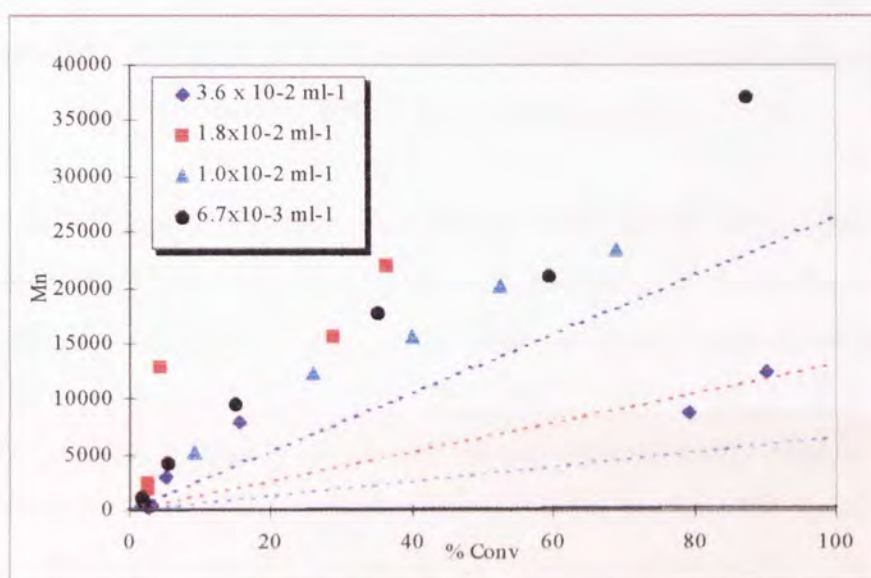


Figure 4.18. Dependence of M_n on conversion for the polymerisation of ϵ -caprolactone using diisobutyl aluminium cyclopentoxide in toluene at 25°C.

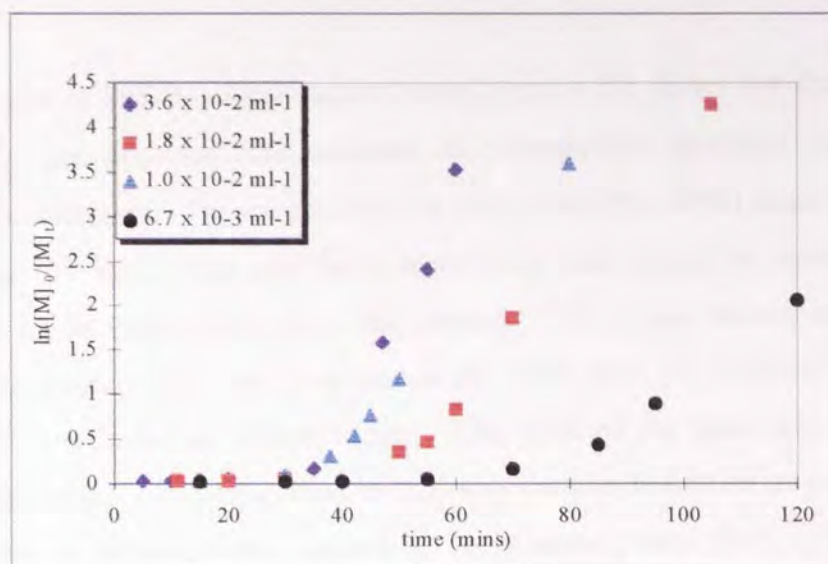


Figure 4.19. First order plot for the polymerisation of ϵ -caprolactone using *diisobutyl* aluminium cyclopentoxide in toluene at 25°C .

The plot of $\ln([M]_0/[M]_t)$ against time (Figure 4.19) clearly shows the build up period which appears to be present in all polymerisations of ϵ -caprolactone using dialkyl aluminium alkoxide initiators. The build up period seems to be related to the initial initiator concentration used. The reaction carried out at $1.8 \times 10^{-2} \text{ ml}^{-1}$ appears to be slightly slower than would be expected, probably because of poor initiator efficiency. The gradient of the first order plot after the build up period does appear to be directly related to the initial initiator concentration, the rate of propagation is directly proportional to the initial initiator concentration $[I]_0$.

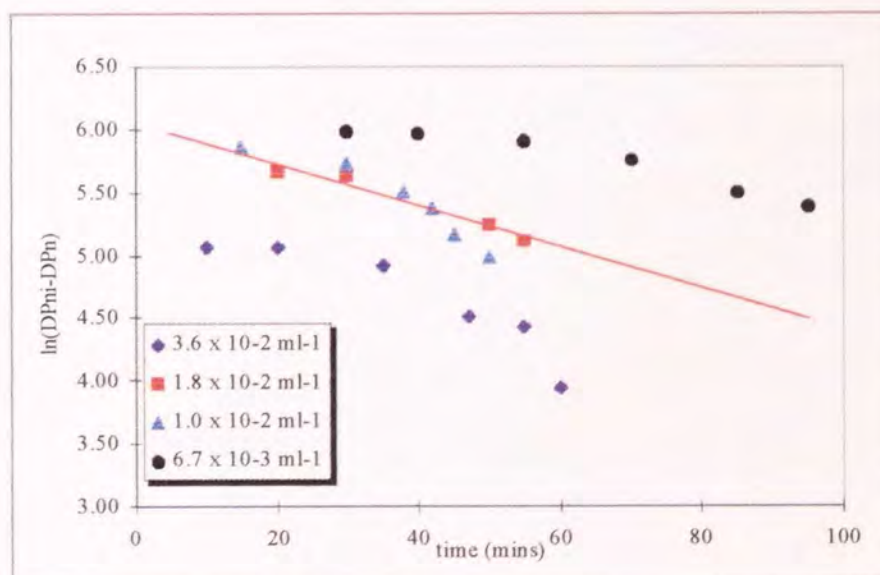


Figure 4.20. Plot of $\ln(\text{DP}_{n\infty}-\text{DP}_{ni})$ against time for the polymerisation of ϵ -caprolactone using *diisobutyl* aluminium cyclopentoxide initiator in toluene at 25°C .

The plot of $\ln(DP_{n_{\infty}} - DP_{n_t})$ against time (figure 4.20) shows that the negative gradient (i.e. the apparent rate constant of propagation) increases as initiator concentration increases. The exception is the plot of $\ln(DP_{n_{\infty}} - DP_{n_t})$ against time for $[I]_0 = 1.0 \times 10^{-2} \text{ ml}^{-1}$. This plot has a higher rate than would be expected from comparison to the other plots using this initiator. The actual amount of initiator added to the reaction may have been inaccurate. The plots are not linear as would be expected from a living polymerisation. The slope of the plots and hence the apparent rate constant of propagation increases as the polymerisation proceeds. The concentration of active centres appears to be increasing with time. This is also apparent from the plots of $\ln([M]_0/[M]_t)$ against time where there is a build up period at the beginning of the reaction.

4.2.7. Diisobutyl aluminium *n*-butoxide as an initiator for the polymerisation of ϵ -caprolactone.

Previous studies had shown that the initiation of the polymerisation of ϵ -caprolactone was dictated by steric factors. A linear alkoxide which should hinder the complexing of the monomer with the initiator to a lesser degree was then chosen. This was expected to allow a greater understanding of the mechanism of polymerisation using aluminium alkoxide initiators

| $[I]_0$ ml ⁻¹ | Time (mins) | % Conv | M_n | M_w | M_w/M_n |
|---------------------------------|-------------|--------|-------|-------|-----------|
| 3.6×10^{-2} (GKS54) | 3 | 26.4 | 400 | 2200 | 5.1 |
| | 6 | 46.6 | 1800 | 3800 | 2.2 |
| | 9 | 76.9 | 2800 | 5800 | 2.1 |
| | 12 | 93.8 | 5900 | 8100 | 1.4 |
| | 15 | 97.0 | 6300 | 9300 | 1.5 |
| | 20 | 95.6 | 6800 | 10200 | 1.5 |
| | 25 | 99.9 | 7000 | 11000 | 1.6 |
| | 30 | 98.7 | 7700 | 10600 | 1.4 |
| | 45 | 98.9 | 7900 | 12700 | 1.6 |
| 1.8×10^{-2} (GKS53) | 5 | 21.3 | 2100 | 3700 | 1.7 |
| | 13 | 47.8 | - | - | - |
| | 17 | 71.5 | 12400 | 14600 | 1.2 |
| | 20 | 90.1 | - | - | - |
| | 25 | 98.0 | 17200 | 22000 | 1.3 |
| | 30 | 95.3 | 20500 | 26300 | 1.3 |
| | 35 | 95.6 | 21600 | 27600 | 1.3 |
| | 45 | 94. | - | - | - |
| | 80 | 98.7 | 21700 | 32800 | 1.5 |
| 1.0×10^{-2} (GKS55) | 2 | 2.4 | - | - | - |
| | 6 | 5.0 | 260 | 700 | 2.7 |
| | 10 | 7.8 | - | - | - |
| | 15 | 14.0 | 4300 | 5600 | 1.3 |
| | 25 | 37.8 | 8400 | 13000 | 1.6 |
| | 35 | 65.5 | - | - | - |
| | 45 | 72.3 | 14800 | 22800 | 1.5 |
| | 60 | 89.2 | 29800 | 43200 | 1.5 |
| | 90 | 95.6 | 34800 | 55000 | 1.6 |
| 6.7×10^{-3} (GKS56) | 6 | 0.2 | - | - | - |
| | 14 | 4.0 | - | - | - |
| | 25 | 10.1 | 4700 | 7300 | 1.6 |
| | 35 | 20.6 | 6200 | 9000 | 1.4 |
| | 45 | 29.3 | 10100 | 15500 | 1.5 |
| | 55 | 50.3 | 19100 | 27000 | 1.4 |
| | 70 | 71.9 | 25600 | 39400 | 1.5 |
| | 105 | 82.0 | 30300 | 53600 | 1.8 |
| | 150 | 97.8 | 32200 | 54100 | 1.7 |

Table 4.8. Molecular weight and conversion data from the polymerisation of ϵ -caprolactone using diisobutyl aluminium *n*-butoxide in toluene at 25°C.

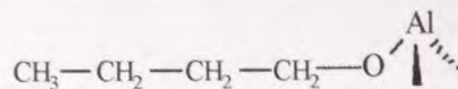


Figure 4.21. Dialkyl aluminium *n*-butoxide.

The polymerisation of ϵ -caprolactone using *diisobutyl* aluminium *n*-butoxide appears to have produced polymers with a molecular weight close to those expected from initial monomer/initiator ratios (figure 4.22). All of the actual molecular weights are greater than the theoretical molecular weights except those from the reaction carried out at $[\text{I}]_0 = 6.7 \times 10^{-3} \text{ ml}^{-1}$ which gave a lower molecular weight than expected. It is unlikely that more than one alkoxide moiety is active on each aluminium centre. It is more likely that the initial monomer concentration was lower than calculated, that the initiator concentration was greater, or that trace amounts of impurities, such as water or a nitrogen-containing compound were activating an otherwise inactive alkyl group.

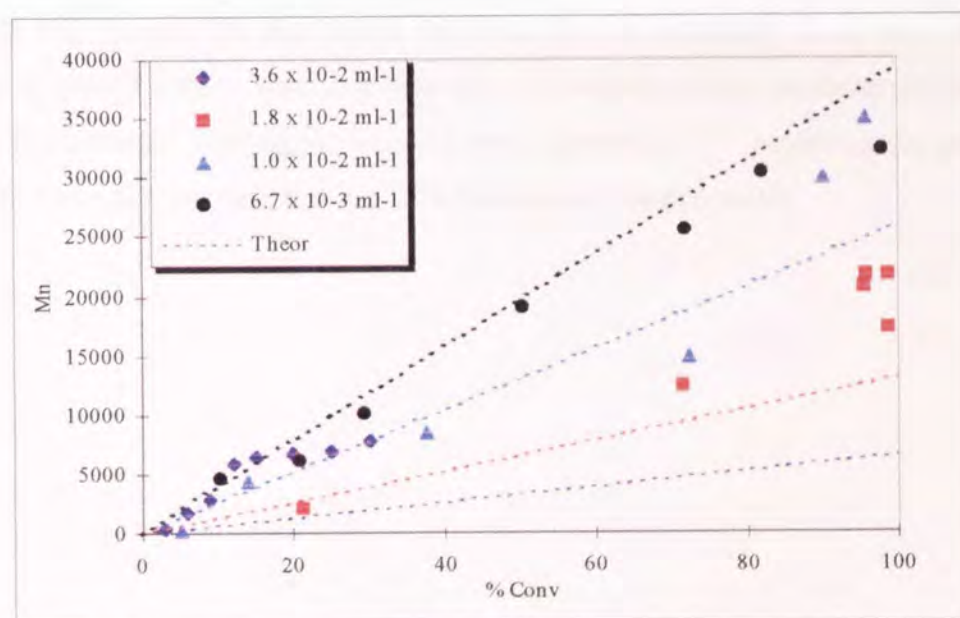


Figure 4.22. Dependence of M_n on conversion for the polymerisation of ϵ -caprolactone using *diisobutyl* aluminium *n*-butoxide in toluene at 25°C.

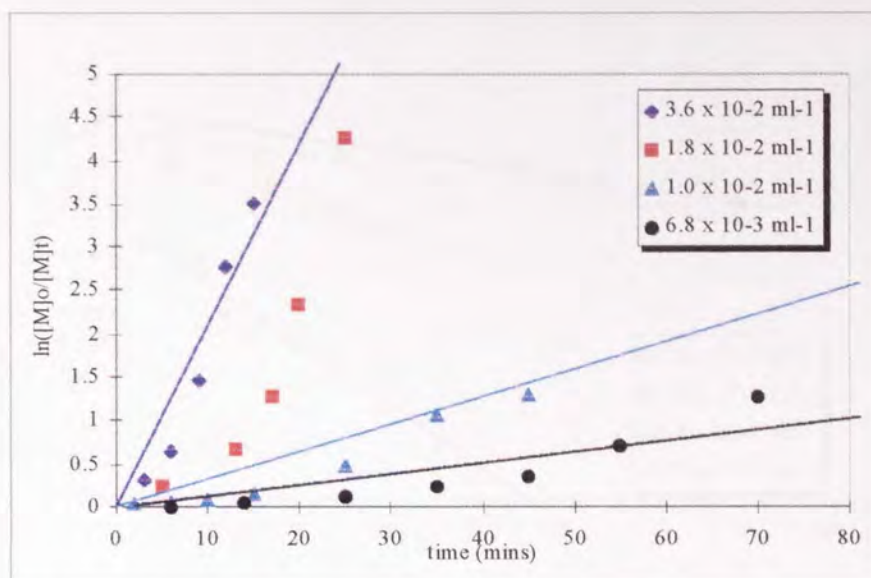


Figure 4.23. First order plot for the polymerisation of ϵ -caprolactone in toluene using diisobutyl aluminium *n*-butoxide in toluene at 25°C.

The plot of $\ln([M]_0/[M]_t)$ against time (figure 4.23) shows that the build up period noted when other functional alkoxide initiators have been used is absent when the alkoxide group is *n*-butoxide. Since *n*-butoxide is the alkoxide group which will provide the least steric hindrance to the monomer, it is clear that the build up period may be seen as a measure of the ability of the monomer to complex with the initiator. This agrees with Jerome's hypothesis⁽¹¹³⁾ regarding the build up period when polymerising lactides with aluminium triisopropoxide.

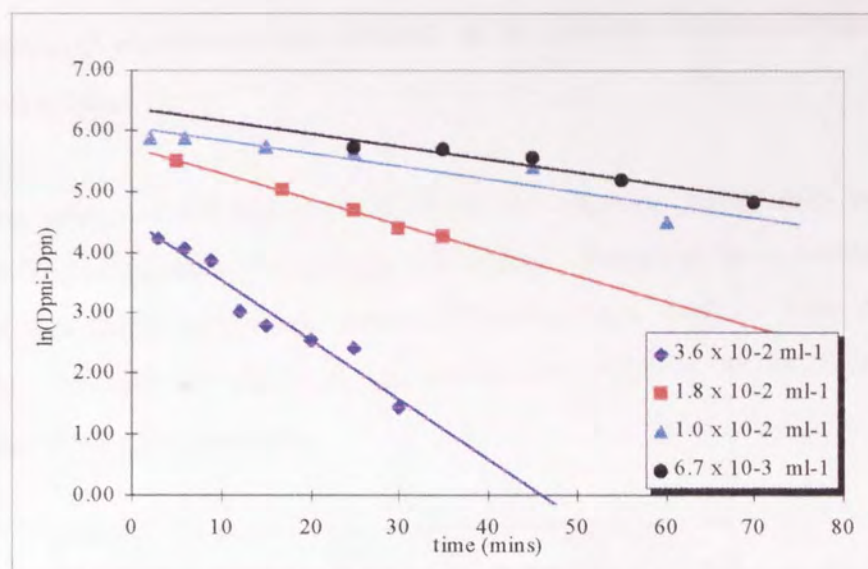


Figure 4.24. Plot of $\ln(DP_{n\infty} - DP_n)$ against time for the polymerisation of ϵ -caprolactone in toluene using diisobutyl aluminium *n*-butoxide in toluene at 25°C.

The plot of $\ln(DP_{n\infty} - DP_n)$ against time shows that the apparent rate constant of propagation, or the negative gradient of the plot increases with initiator concentration.

4.2.8. Diisobutyl aluminium *tert*-butoxide as an initiator for the polymerisation of ϵ -caprolactone.

The effect of the structure alone of the alkoxide group may be clearly illustrated if two isomers are used as alkoxides. Therefore as a comparison to diisobutyl aluminium *n*-butoxide, *tert*-butyl alcohol was used to form diisobutyl aluminium *tert*-butoxide (figure 4.25), which was used as an initiator for the polymerisation of ϵ -caprolactone.

| $[I]_0 \text{ ml}^{-1}$ | Time (mins) | % Conv |
|---------------------------------|-------------|--------|
| 3.6×10^{-2} (GKS57) | 3 | 3.9 |
| | 9 | 3.0 |
| | 14 | 3.2 |
| | 20 | 3.5 |
| | 30 | 3.6 |
| | 45 | 3.2 |
| | 60 | 4.3 |
| | 110 | 5.1 |
| | 140 | 4.9 |
| | 210 | 6.4 |
| 275 | 8.3 | |
| 1.8×10^{-2} (GKS58) | 55 | 1.2 |
| | 125 | 2.6 |
| | 170 | 4.3 |
| | 1110 | 9.5 |
| | 1170 | 9.2 |
| | 1230 | 10.2 |
| | 1290 | 10.0 |
| | 1350 | 10.9 |
| | 1410 | 9.3 |

Table 4.9. Molecular weight data from the polymerisations of ϵ -caprolactone using diisobutyl aluminium *tert*-butoxide in toluene at 25°C.

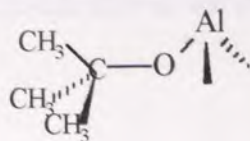


Figure 4.25. Dialkyl aluminium *tert*-butoxide.

The polymerisation of ϵ -caprolactone using diisobutyl aluminium *tert*-butoxide is so slow that the conversion of monomer to polymer reached 10% after 24 hours at $[I]_0 = 1.8 \times 10^{-2} \text{ ml}^{-1}$. Such low conversions prevented the use of GPC to calculate the molecular weight of the polymer produced in each sample withdrawal. The polymerisation of ϵ -caprolactone using the corresponding linear alkoxide, *n*-butoxide is rapid and without a build up period. The opposite is true of diisobutyl aluminium *tert*-butoxide. The greater inductive effect of the *tert*-butyl group would give a higher electron density around the alkoxide oxygen than *n*-butoxide. This should give a faster rate of polymerisation when using diisobutyl aluminium *tert*-butoxide than diisobutyl aluminium *n*-butoxide. Since this has not happened then the structure of the alkoxide group is responsible for the decreased rate.

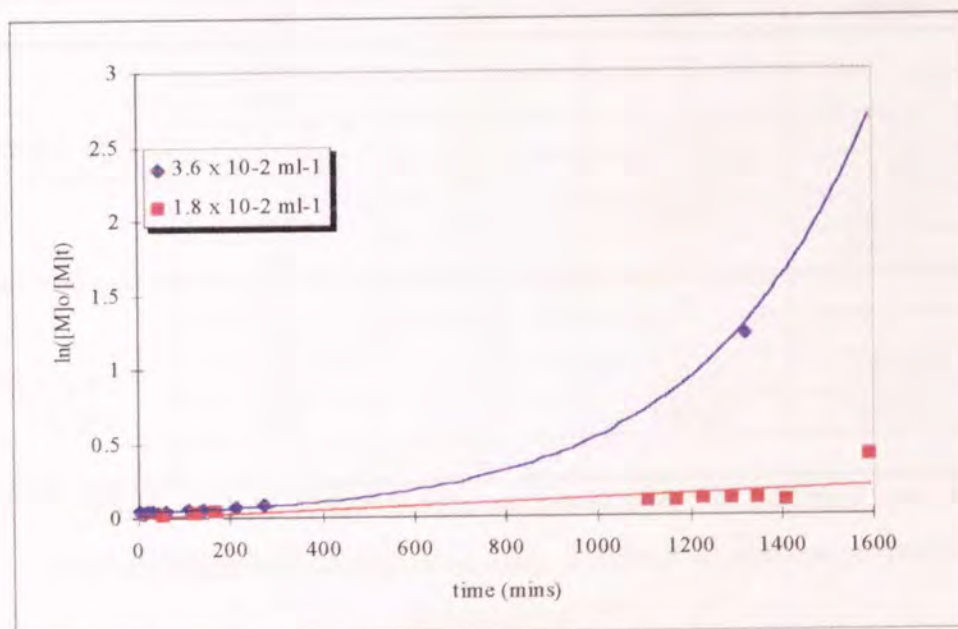


Figure 4.26. First order plot for the polymerisation of ϵ -caprolactone in toluene

4.2.9. Diisobutyl aluminium *iso*-propoxide as an initiator for the polymerisation of ϵ -caprolactone.

Since previous studies have shown that the initiation of the polymerisation of ϵ -caprolactone was dictated by steric factors then a secondary alkoxide, diisobutyl aluminium *iso*-propoxide (figure 4.27), was used as comparison to the linear and tertiary alkoxides, *n*-butoxide and *tert*-butoxide. The secondary alkoxide should hinder the complexing of the monomer with the initiator to a greater degree than the linear alkoxide *n*-butoxide.

| $[I]_0 \text{ ml}^{-1}$ | Time (mins) | % Conv | M_n | M_w | M_w/M_n |
|---------------------------------|-------------|--------|-------|-------|-----------|
| 3.6×10^{-2} (GKS02) | 4 | 4.3 | 5000 | 10400 | 2.1 |
| | 8 | 6.4 | 6500 | 10200 | 1.6 |
| | 15 | 17.1 | 11200 | 16000 | 1.4 |
| | 21 | 42.3 | 16800 | 21900 | 1.3 |
| | 42 | - | 18700 | 24900 | 1.3 |
| | 60 | 98.1 | 17400 | 26400 | 1.6 |
| 1.8×10^{-2} (GKS05) | 8 | 4.0 | 1900 | 3270 | 1.7 |
| | 18 | 16.3 | 4600 | 7500 | 1.6 |
| | 28 | 48.8 | 8400 | 11500 | 1.4 |
| | 34 | 87.6 | 15200 | 18900 | 1.3 |
| 1.0×10^{-2} (GKS27) | 20 | 1.0 | - | - | - |
| | 35 | 2.0 | - | - | - |
| | 60 | 3.6 | 2400 | 12700 | 2.4 |
| | 105 | 14.4 | 11900 | 18700 | 1.6 |
| | 125 | 69.4 | 14800 | 24100 | 1.6 |
| | 185 | 94.6 | 17500 | 25700 | 1.5 |
| 6.7×10^{-3} (GKS28) | 45 | 2.4 | - | - | - |
| | 65 | 2.0 | - | - | - |
| | 100 | 11.6 | 10000 | 13500 | 1.3 |
| | 150 | - | 14300 | 28100 | 2.0 |
| | 275 | 74.0 | - | - | - |

Table 4.10. Molecular weight and conversion data obtained from the polymerisation of ϵ -caprolactone using diisobutyl aluminium *iso*-propoxide in toluene at 25°C.

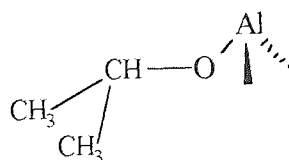


Figure 4.27. Dialkyl aluminium *iso*propoxide.

The expected value for the molecular weight using this initiator with an initial initiator concentration of $[I]_0 = 3.6 \times 10^{-2} \text{ ml}^{-1}$ would be approximately 6730 at 100% conversion. Since a value for $M_n = 17390$ was obtained at 98% conversion it is likely that less than one chain is being initiated per alkoxide moiety. The polydispersity of the sample narrows to 1.3 at the peak molecular weight at 42 minutes and then increases to 1.5 as molecular weight decreases. It is likely that some form of degradation of the polymer, such as transesterification, is taking place once maximum conversion has been achieved. Indeed the presence of transesterification reactions has been reported under such circumstances^(53,68,116)

In the reaction carried out at $[I]_0 = 1.0 \times 10^{-2} \text{ ml}^{-1}$ the very small amount of polymer produced at the start of the reaction in the first two samples prevented any analysis by GPC being carried out. It is unlikely that such a low conversion is entirely due to the presence of initiator residue. The initiator concentration was $[I]_0 = 1.0 \times 10^{-2} \text{ ml}^{-1}$, so there would approximately 0.002 grams of initiator per 2ml aliquot removed from the reaction. This equates to 0.4% so any value for the percentage conversion over 0.4% undoubtedly contains polymer.

It is noticeable that the polydispersity of the samples decreases as the reaction proceeds. This is indicative of a living polymerisation system in which the rate of initiation k_i is greater than that of propagation k_p . As the molecular weights of the polymer chains increase, the small differences between the chain lengths become statistically less significant, leading to a decrease in the distribution of chain lengths.

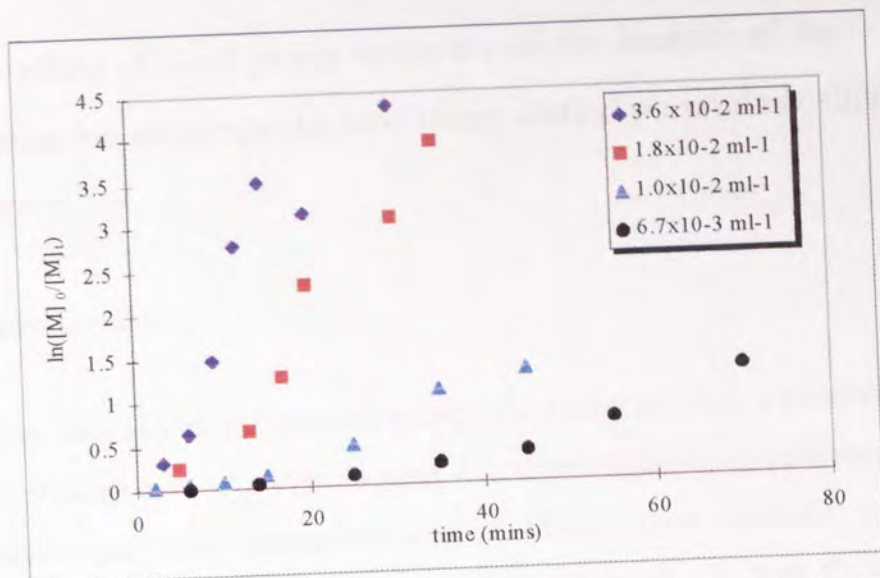


Figure 4.28. First order plot for the polymerisation of ϵ -caprolactone using diisobutyl aluminium *iso*-propoxide initiator.

Linear alkoxides such as *n*-butoxide also show no or a very small build up period when a $\ln([M]_0/[M]_t)$ versus time plot is constructed (Figure 4.28). Since the build up period is said to be related to the ability of the monomer to co-ordinate with the initiator ⁽¹¹³⁾ then a linear and therefore less bulky alkoxide may allow the monomer to co-ordinate with initiator more easily.

4.3. The effect of alkyl group structure on the kinetics of the polymerisation of ϵ -caprolactone using dialkyl aluminium alkoxide initiators.

4.3.1. Introduction.

The structure of the alkoxide group of a dialkyl aluminium alkoxide initiator for the polymerisation of ϵ -caprolactone was found to have a significant effect on the initiation, and hence propagation rate of polymerisation, molecular weight and molecular weight distribution of the polymer produced. It was thought likely therefore that the structure of the alkyl group would also have an effect on the system. The effect of the structure of the alkyl group on the reaction kinetics when using dialkyl aluminium *n*-butoxide initiator has been investigated by varying the nature of the alkyl group whilst keeping the other reaction parameters constant. The reaction conditions were,

- Temperature 25°C
- $[\epsilon\text{-CL}] = 2.1 \text{ ml}^{-1}$
- $[I]_0 = \text{varied}$
- Inert atmosphere
- Toluene solvent

The results of these studies are summarised in table 4.8 and table 4.11 for the polymerisation of ϵ -caprolactone using *diisobutyl* aluminium *n*-butoxide and diethyl aluminium *n*-butoxide respectively.

| $[I]_0 \text{ ml}^{-1}$ | Time (mins) | % Conv | M_n | M_w | M_w/M_n |
|---------------------------------|-------------|--------|-------|-------|-----------|
| 3.6×10^{-2} (GKS86) | 4 | 36.5 | 3800 | 5100 | 1.4 |
| | 8 | 75.6 | 7800 | 10200 | 1.3 |
| | 10 | 97.7 | 12200 | 14100 | 1.2 |
| | 12 | 95.9 | 13300 | 16600 | 1.3 |
| | 15 | 97.3 | 14200 | 18000 | 1.3 |
| | 20 | 98.7 | 13500 | 17900 | 1.3 |
| 1.8×10^{-2} (GKS83) | 2 | 3.7 | 950 | 1200 | 1.3 |
| | 5 | 12.1 | 3700 | 5200 | 1.4 |
| | 10 | 40.1 | 4500 | 7400 | 1.6 |
| | 16 | 71.8 | 18900 | 23500 | 1.2 |
| | 20 | 81.1 | 18100 | 26000 | 1.4 |
| 6.7×10^{-3} (GKS85) | 8 | 7.4 | 4600 | 5700 | 1.2 |
| | 20 | 23.3 | 15200 | 19800 | 1.3 |
| | 28 | 36.3 | 23700 | 27500 | 1.2 |
| | 33 | 46.5 | 26000 | 31700 | 1.2 |
| | 38 | 55.4 | 31000 | 39100 | 1.2 |
| | 45 | 60.9 | 37600 | 48600 | 1.3 |

Table 4.11. Molecular weight and conversion data obtained from the polymerisation of ϵ -caprolactone using diethyl aluminium *n*-butoxide in toluene at 25°C.

4.3.2. The effects of alkyl group structure on the dependence of $\ln(DP_{n_{\infty}}-DP_{n_t})$ versus time.

Plots of $\ln(DP_{n_{\infty}}-DP_{n_t})$ against time have been constructed using the molecular weight data shown in table 4.8 and Table 4.11. From equation 3.12 the gradient of a plot of $\ln(DP_{n_{\infty}}-DP_{n_t})$ against time maybe used to obtain the apparent rate of polymerisation, k_p . The plots of $\ln(DP_{n_{\infty}}-DP_{n_t})$ against time (figures 4.29 and 4.30) show that the apparent rate of propagation increases as the initiator concentration increases irrespective of the initiator, diethyl or *diisobutyl* aluminium alkoxide.

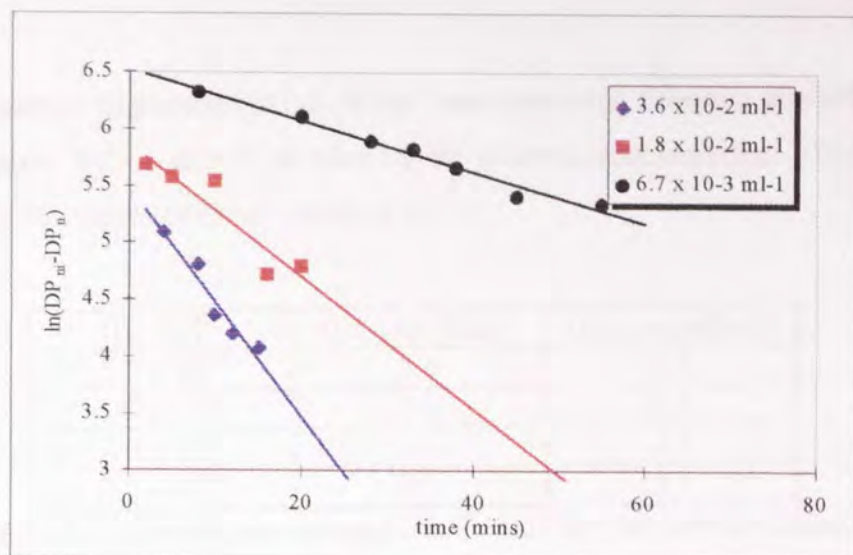


Figure 4.29. Plot of $\ln(DP_{n_{\infty}} - DP_{n_t})$ against time for the polymerisation of ϵ -caprolactone using diethyl aluminium *n*-butoxide initiator and toluene as a solvent at 25°C.

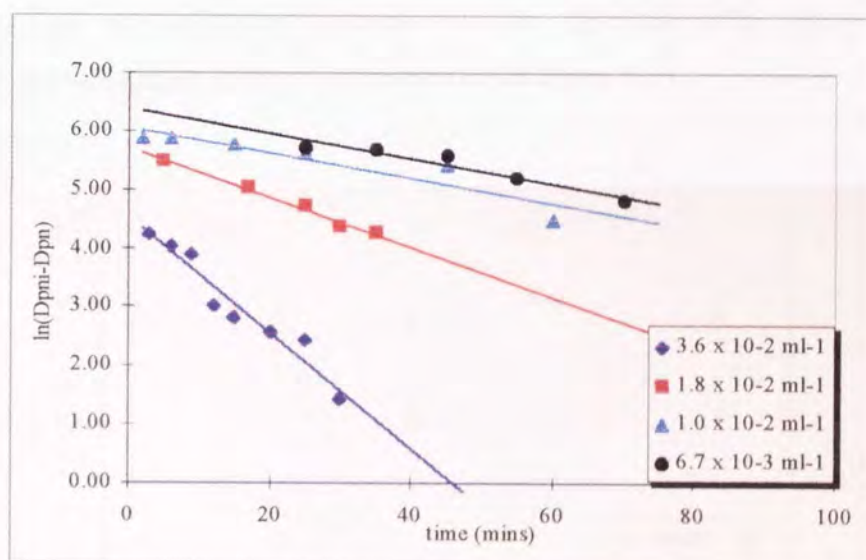


Figure 4.30. Plot of $\ln(DP_{n_{\infty}} - DP_{n_t})$ against time for the polymerisation of ϵ -caprolactone using diisobutyl aluminium *n*-butoxide initiator and toluene as a solvent at 25°C.

The plot of $\ln(DP_{n_{\infty}} - DP_{n_t})$ against time for the polymerisation of ϵ -caprolactone using diisobutyl aluminium *n*-butoxide in toluene (figure 4.30) also shows that the rate of polymerisation increases with initiator concentration. The plots at $[I]_0 = 1.0 \times 10^{-2} \text{ ml}^{-1}$ and $6.7 \times 10^{-3} \text{ ml}^{-1}$ have similar gradients, probably because of a slower rate of polymerisation in the reaction at $1.0 \times 10^{-3} \text{ ml}^{-1}$. This slower rate was most likely due to termination reactions brought about by impurities such as water or oxygen.

The rate constant of polymerisation, k_p has been calculated from the gradient of the plots in figures 4.29 and 4.30 divided by the initiator concentration. The values obtained for this value are listed in table 4.12.

| $[I]_0 \text{ mol l}^{-1}$ | $(\text{Et})_2\text{Al}(n\text{BuO})$ | $(i\text{Bu})_2\text{Al}(n\text{BuO})$ |
|----------------------------|---------------------------------------|----------------------------------------|
| 3.6×10^{-2} | 3.0 | 2.5 |
| 1.8×10^{-2} | 3.0 | 2.5 |
| 1.0×10^{-2} | - | 2.1 |
| 6.7×10^{-3} | 3.1 | 2.4 |

Table 4.12. Apparent rate constant $\text{l mol}^{-1} \text{sec}^{-1}$ for the polymerisation of ϵ -caprolactone using diisobutyl aluminium n -butoxide and diethyl aluminium n -butoxide initiator and toluene as a solvent at 25°C .

The rate of propagation is clearly slower when the bulkier alkyl group *isobutyl* is used as the initiator compared to the less bulky ethyl group. These results are plotted against initiator concentration in figure 4.31.

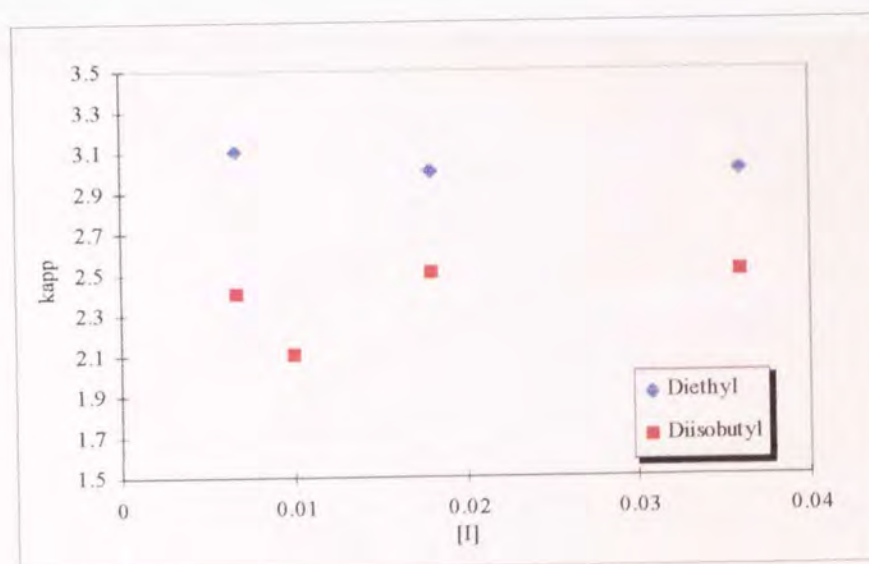


Figure 4.31. Plot of apparent rate constant against initial initiator concentration to show the effect of alkyl group structure.

From figure 4.31 it is clear that the apparent rate constant of polymerisation is greater when using diethyl aluminium n -butoxide rather than diisobutyl aluminium n -butoxide initiator for the polymerisation of ϵ -caprolactone in toluene. The structure of alkyl group appears therefore to have an effect of the polymerisation kinetics.

First order kinetic plots of $\ln([M]_0/[M]_t)$ against time (figures 4.32 and 4.33) confirm that the apparent rate increases with initiator concentration and that the rate constant is greater for diethyl aluminium *n*-butoxide.

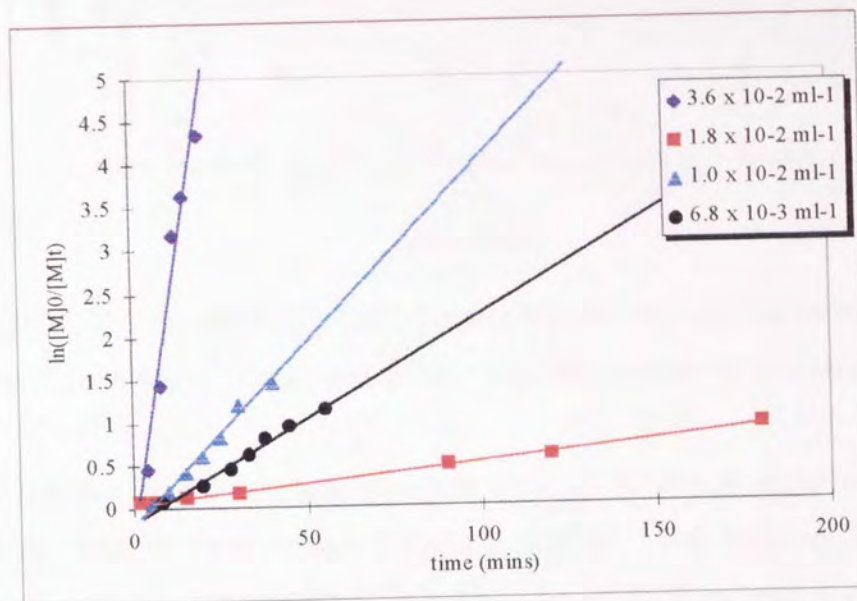


Figure 4.32. Plot of $\ln([M]_0/[M]_t)$ against time for the polymerisation of ϵ -caprolactone using diethyl aluminium *n*-butoxide initiator in toluene at 25°C.

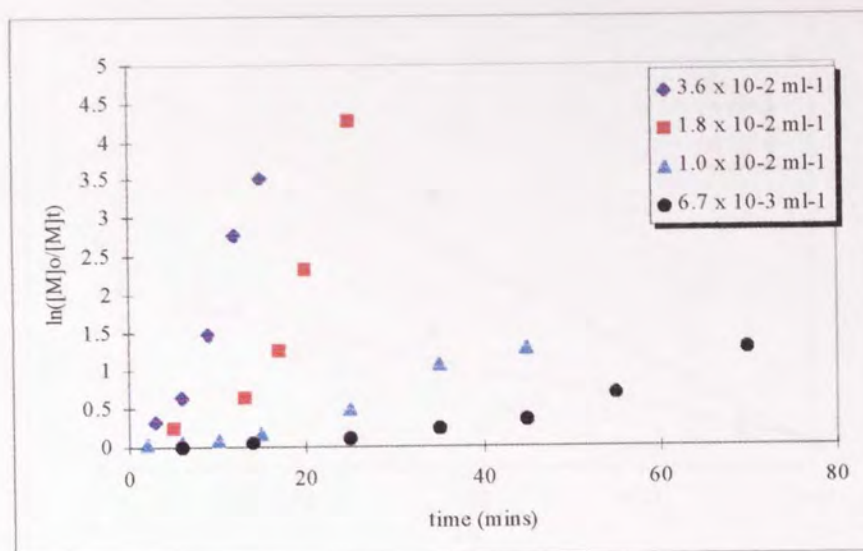


Figure 4.33. Plot of $\ln([M]_0/[M]_t)$ against time for the polymerisation of ϵ -caprolactone using diisobutyl aluminium *n*-butoxide initiator in toluene at 25°C.

Expanded plots of the type shown in figures 4.32 to 4.33 show an induction or build up time between around 2 and 12 minutes. This build up period was observed to a greater degree when bulkier alkoxide groups were used in the initiator. The diethyl aluminium *n*-butoxide initiator has a shorter build up period for the corresponding reaction carried out using diisobutyl aluminium alkoxide (figure 4.34).

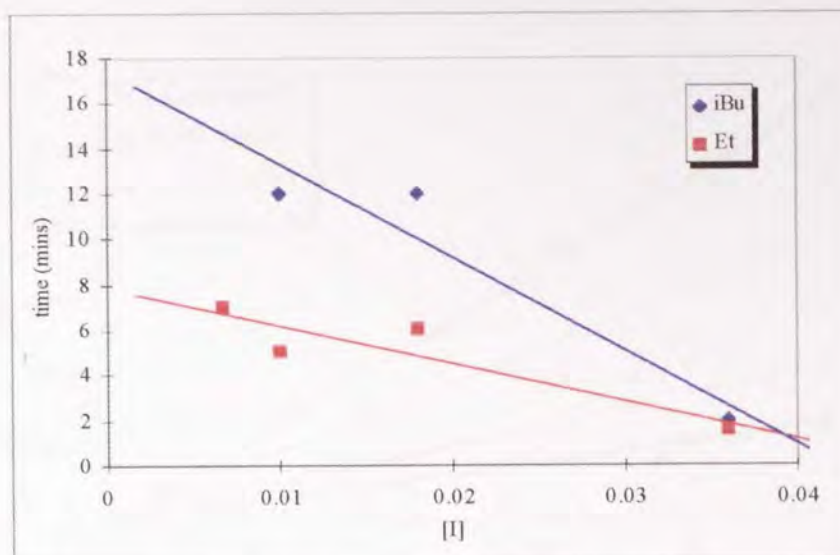


Figure 4.34. Build up period against initial initiator concentration for the polymerisation of ϵ -caprolactone using dialkyl aluminium *n*-butoxide in toluene at 25°C.

Jerome ⁽¹¹³⁾ proposed that the build up period is related to the ability of the monomer to co-ordinate with the initiator. Accordingly the bulkier the alkyl groups the longer this build up period would be expected. However the length of the build up period is probably related more to the structure of the alkoxide group than to the structure of the alkyl moiety. This is not to say however that the build up period is unrelated to the structure of the alkyl group, merely that the alkoxide probably has the greater effect. The build up period by nature occurs at the start of the reaction when the functional alkoxide is closer to the active aluminium alkoxide centre. The alkyl group stays adjacent to the reaction site throughout the reaction, therefore any effect it may have on monomer complexing with initiator should be present throughout propagation. Therefore the increased build up period when *diisobutyl* rather than diethyl aluminium *n*-butoxide is used as an initiator is probably because the reaction is slower anyway, rather than because the alkyl group promotes a longer build up period.

The dependence of M_n against conversion has been plotted for each of the initiators used (figure 4.35 and 4.36). Both show that the actual molecular weight (solid lines) is greater than the theoretical molecular weight calculated from initial monomer/initiator ratios (dashed lines).

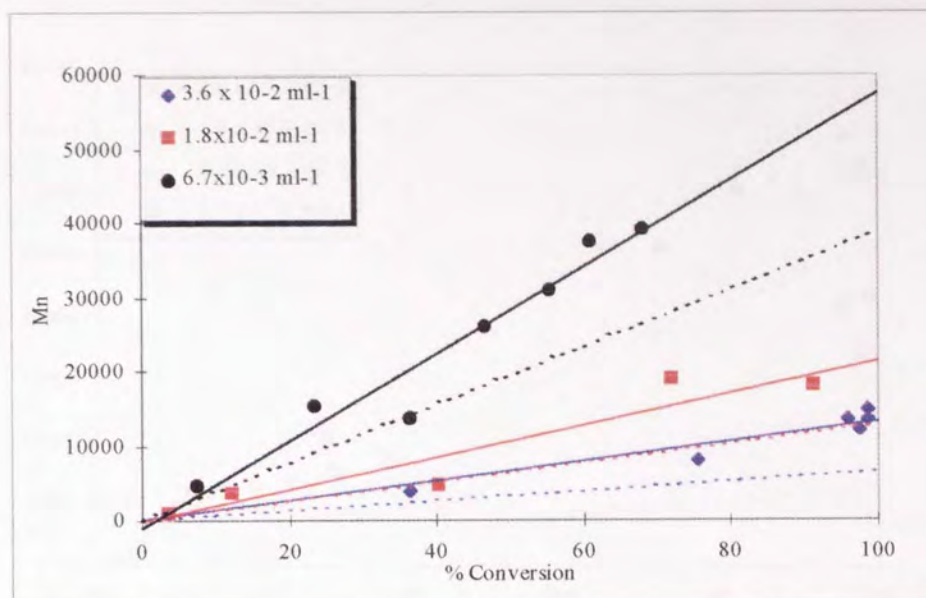


Figure 4.35. Plot of M_n against conversion for the polymerisation of ϵ -caprolactone using diethyl aluminium *n*-butoxide initiator in toluene at 25°C

Using diethyl aluminium *n*-butoxide as the initiator appeared to result in a polymer which had a molecular weight closer to the theoretical molecular weight than the corresponding reactions using diisobutyl aluminium *n*-butoxide initiator.

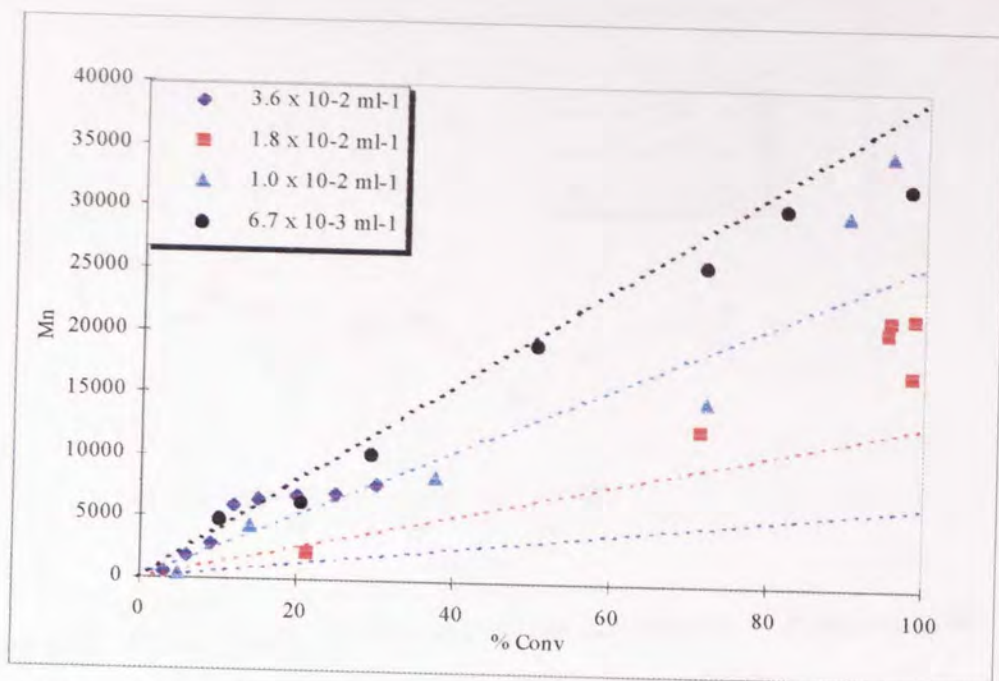


Figure 4.36. Plot of M_n against conversion for the polymerisation of ϵ -caprolactone using diisobutyl aluminium *n*-butoxide in toluene at 25°C.

The initiation of ϵ -caprolactone using diethyl aluminium using *n*-butoxide may be more efficient than the corresponding reaction using diisobutyl aluminium *n*-butoxide. A greater amount of steric hindrance around the active site is likely to be the cause of incomplete initiation.

The nature of the alkyl group also appears to have an effect on the molecular weight distribution of the polymer samples produced. Plots of M_w/M_n against time have been constructed, (figures 4.37 and 4.38)

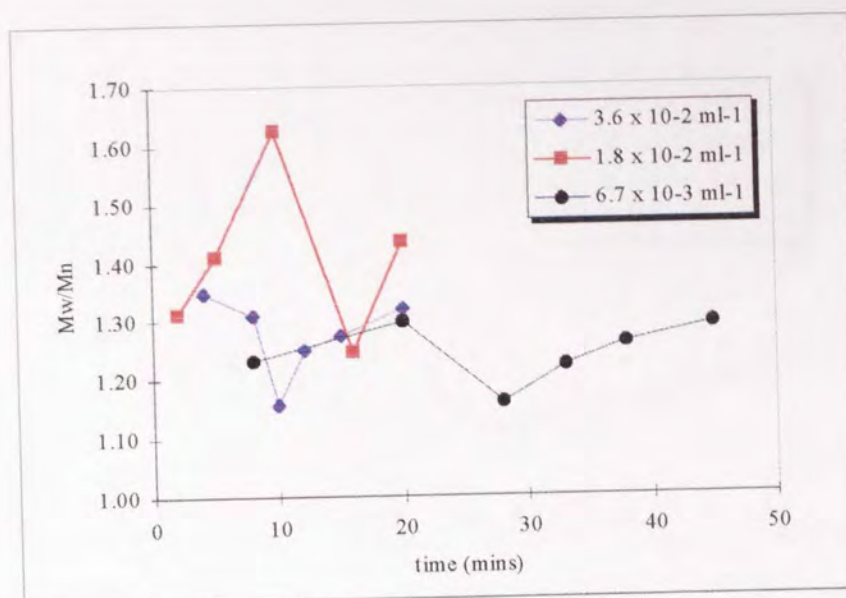


Figure 4.37. Plot of M_w/M_n against time for the polymerisation of caprolactone using diethyl aluminium *n*-butoxide as an initiator.

The molecular weight distributions of the samples of polymer removed from the reaction decrease as the reaction proceeds. This would be expected since according to equation 5.1., the molecular weight distribution is inversely proportional to DP_n ;

$$M_w/M_n = 1 + DP_n/(1 + DP_n)^2 \quad 5.1.$$

Therefore for living systems for which k_i is fast, as the chain length increases, the molecular weight distribution, M_w/M_n decreases.

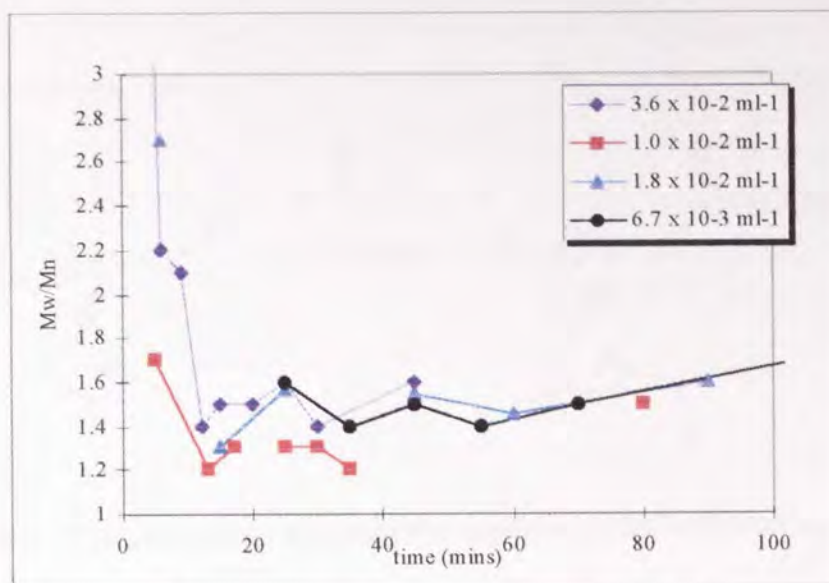
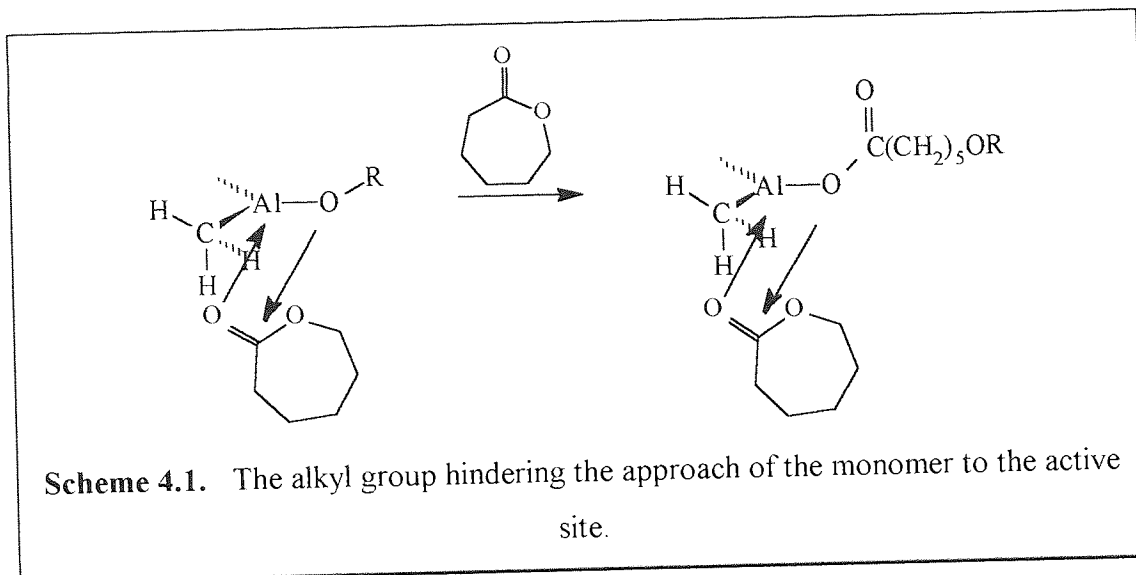


Figure 4.38. Plot of M_w/M_n against time for the polymerisation of caprolactone using diisobutyl aluminium *n*-butoxide as an initiator.

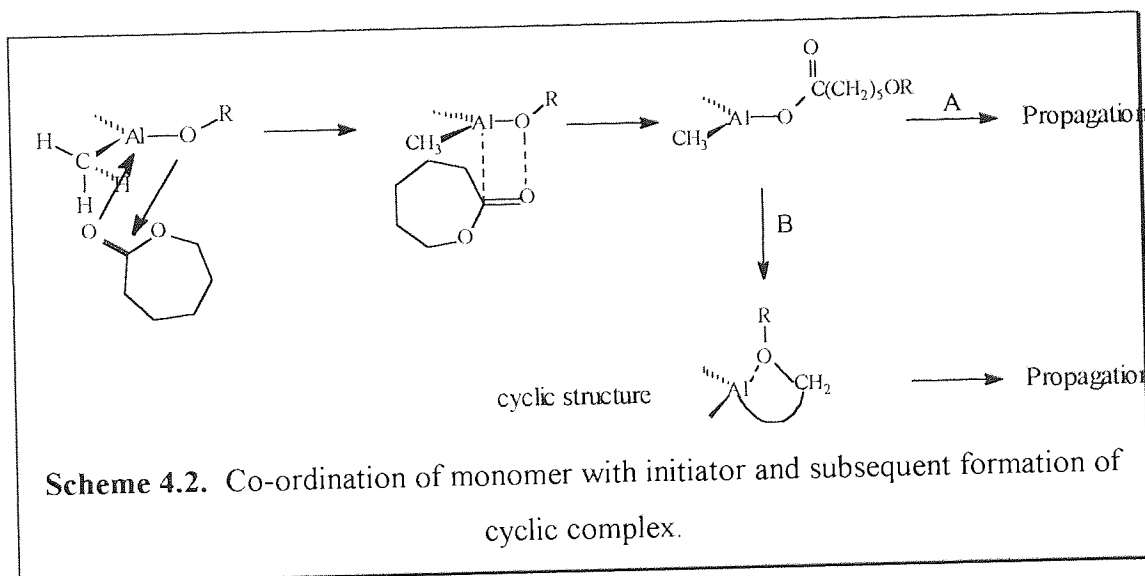
The molecular weight distributions of polymer samples produced using diethyl aluminium *n*-butoxide are narrower than those produced with diisobutyl aluminium *n*-butoxide. The less bulky structure of the ethyl group compared to an *isobutyl* group may decrease steric hindrance and thus initiation may be faster. The molecular weight distribution is consequently likely therefore to be narrower and closer to a Poisson type.

In order to summarise this section it is clear that the structure of the alkyl group when using dialkyl aluminium alkoxide initiators does have an effect on the reaction kinetics and the nature of the polymers produced, which helps an understanding of the mechanism of polymerisation.

Both of the mechanisms postulated by Teysie and Shelton (section 1.3.3.1.) may cause the structure of the alkyl group to have an effect on the rate of polymerisation. Under anhydrous conditions the monomer does not insert between the alkyl group and the aluminium centre. Therefore the effect a bulkier alkyl substituent will have on monomer insertion is likely to be present throughout propagation. Scheme 4.1. shows how the alkyl group may hinder the approach of the monomer to the aluminium alkoxide. Whilst the alkoxide group R moves away from the aluminium centre as propagation continues whereas the alkyl groups may continue to have an effect on propagation throughout.



Shelton proposed that a cyclic compound is formed after the first monomer insertion into the active alkoxide bond whereby the active alkoxide bond forms a weak bond with the original alkoxide moiety (scheme 4.2. route B). This is statistically unlikely as there are many other sites other than the in the same polymer chain with which the aluminium can complex with.



The strain that would exist within such a cyclic structure would also be prohibitive to this ring enlargement mechanism being followed. If formation of a cyclic complex does not occur and route A (Scheme 4.2.) is followed, then the alkyl groups will still effect the complexing of monomer with initiator.

The effect the alkyl group has on the monomer complexing with the initiator is probably related to the volume it occupies in space. Rotation about Al-C bonds will cause the alkyl moiety over time to occupy a greater effective volume in space. Such movement of the alkyl moiety in space however may be beneficial to the monomer insertion. As the alkyl group rotates in space it will periodically leave a slightly easier route for the monomer to the alkoxide site before rotating around to occupy a space that hinders the monomer complexing with the initiator.

In general larger, bulkier alkyl groups slow the rate of propagation by slowing the rate at which the monomer complexes with the active aluminium alkoxide centre. It is possible that sufficiently bulky alkyl groups may hinder propagation totally and in combination with a bulky alkoxide group may prevent propagation entirely. It was proved in section 4.2.8 that *t*-butyl alkoxide was able to suppress propagation to a large degree.

4.4. Summary of the effect of alkoxide group structure on the kinetics of the polymerisation of ϵ -caprolactone using dialkyl aluminium alkoxide initiators.

The data obtained from the experiments in section 4.1 has been compared and contrasted in this section.

The plots of $\ln(DP_{n\infty}-DP_n)$ against time have been analysed and the values of rate constants are summarised in table 4.13.

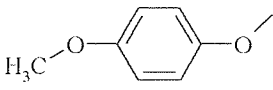
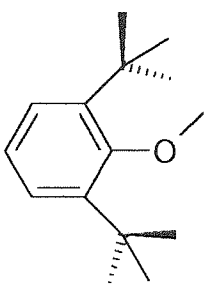
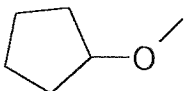
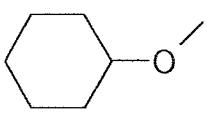
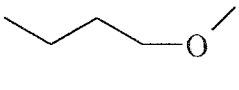
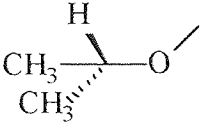
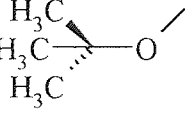
| $[I]_0 \times 10^{-2} \text{ ml}^{-1} \rightarrow$ | 3.6 | 1.8 | 1.0 | 0.67 |
|-------------------------------------------------------------------------------------|-------|-------|-------|-------|
| Alkoxide \downarrow | | | | |
|  | 0.031 | 0.027 | 0.018 | 0.017 |
|  | 0.006 | 0.009 | - | 0.002 |
|  | 0.021 | 0.016 | 0.024 | 0.009 |
|  | 0.010 | 0.024 | 0.022 | 0.017 |
|  | 0.100 | 0.058 | - | 0.022 |
|  | 0.069 | 0.031 | 0.007 | - |
|  | - | | - | - |

Table 4.13. Apparent rate constants of polymerisation for the polymerisation of ϵ -caprolactone using *diisobutyl* aluminium alkoxide initiators in toluene at 25°C.

The values obtained in this table have been plotted against initial initiator concentration and this graph is below (figure 4.39).

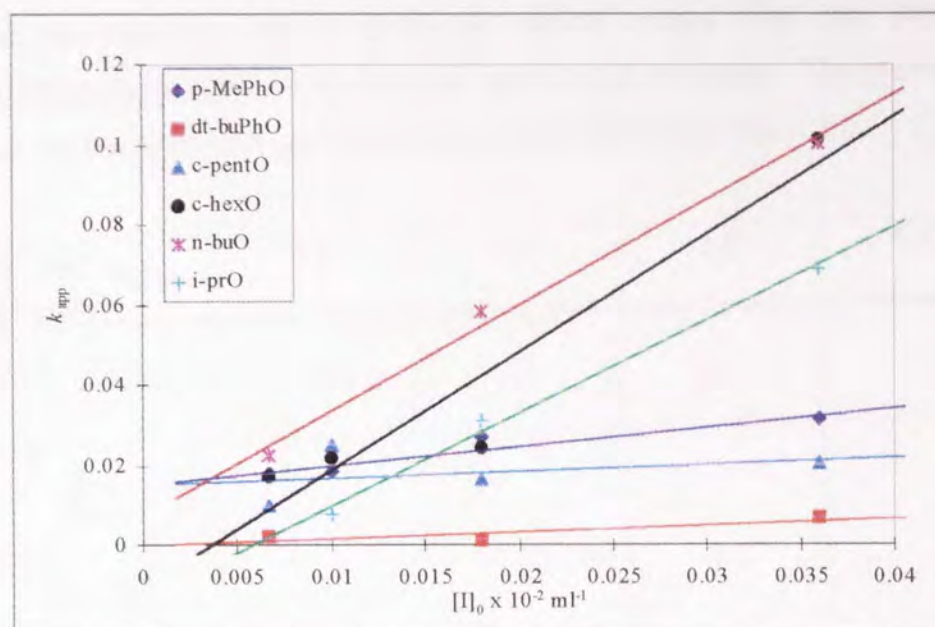


Figure 4.39. The effect of the alkoxide group structure on the apparent rate constant k_{app} .

The alkoxides can be ranked according to rate of polymerisation calculated from the $\ln(DP_{n\infty}-DP_n)$ against time plot. This data is summarised in figure 4.39 and according to this graph, the fastest rate of polymerisation is obtained when the linear alkoxide *n*-butoxide is used. A list of alkoxides, with the alkoxide that produces the fastest rate of polymerisation first, is shown below;

- *n*-butoxide
- cyclo-hexanoxide
- iso-propoxide
- para-methoxyphenoxide
- cyclo-pentanoxide
- *tert*-butyl phenoxide.

↓
decreased
rate of
polymerisation

The gradient of a plot, $\{1/[I]_0\} \ln([M]_0/[M]_t)$ against time is taken to be equal to the rate of propagation, assuming that initiation is instantaneous. In these reactions the presence of a build up period means that the plot of $\{1/[I]_0\} \ln([M]_0/[M]_t)$ against time does not pass through the origin. The gradient of the linear section of the plot has been calculated and is listed in table 4.14.

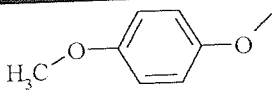
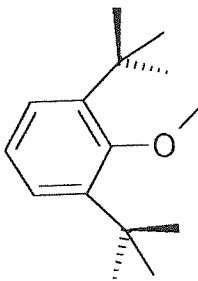
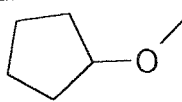
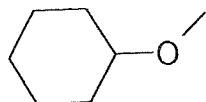
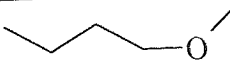
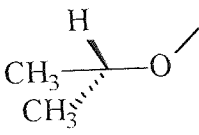
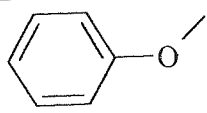
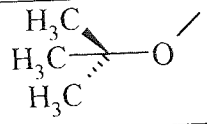
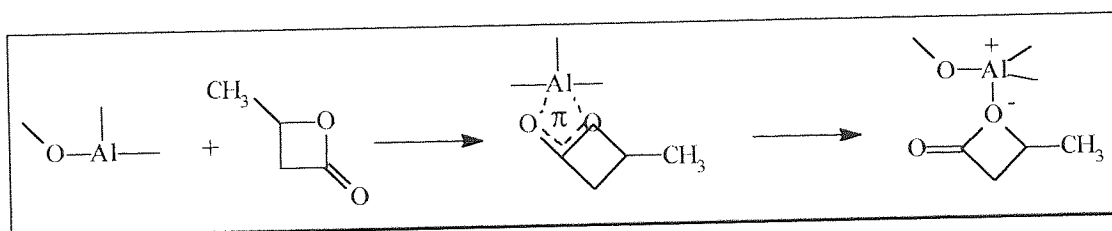
| $[I]_0 \times 10^{-2} \text{ ml}^{-1} \rightarrow$ | 3.6 | 1.8 | 1.0 | 0.67 |
|-------------------------------------------------------------------------------------|------|------|-----|------|
| Alkoxide \downarrow | | | | |
|  | 3.8 | 6.5 | 2.7 | 9.6 |
|  | 1.1 | 0.4 | 0.2 | - |
|  | 3.6 | 3.3 | 8 | 0.04 |
|  | 3.9 | 3.9 | 8.8 | 7.8 |
|  | 7.9 | 10.8 | 4 | 4.5 |
|  | 2.4 | 3.4 | 2.4 | 10.4 |
|  | 0.47 | 0.6 | 0.9 | - |
|  | - | - | - | - |

Table 4.14. Slope of linear section of $\{1/[I]_0\} \ln([M]_0/[M]_t)$ against time plot.

The gradient of the linear section of the $\{1/[I]_0\} \ln([M]_0/[M]_t)$ against time plot, i.e. after the build up period appears from the table 4.14 to be independent of the structure of the alkoxide group. Whilst there are variations from one alkoxide to another, all of the rate constants are of the same order of magnitude as corresponding reactions using other alkoxides. There are of course exceptions,

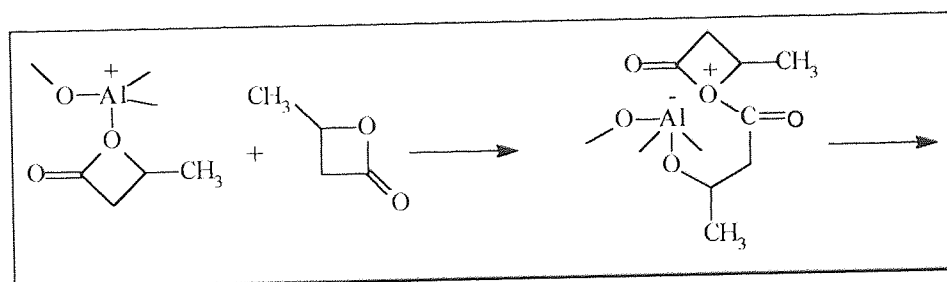
diisobutyl aluminium di-*tert*-butylphenoxide has a very slow rate of polymerisation and a long build up period. The bulky nature of the alkoxide group may be preventing initiation from occurring rapidly.

The rate of propagation after the build up period appears to be largely independent of initiator structure. Therefore the propagation mechanism that involves the formation of cyclic structures, which was proposed by Shelton ⁽⁷⁴⁾ (schemes 4.3 and 4.4.), is most likely to be inaccurate.



Scheme 4.3. π -complexation of the monomer with the aluminium centres.

If the cyclic structures proposed in schemes 4.3 and 4.4 were indeed correct, then the alkoxide structure would continue to have an effect throughout the reaction. This clearly does not happen, therefore the alkoxide group does not remain directly associated with the aluminium centre throughout propagation.



Scheme 4.4. Complexation of monomer with initiator.

That is not to say that the aluminium centre does not associate with any terminal group or indeed any other polar group, merely that the structure of the alkoxide group does not appear to affect the rate of propagation and that therefore the alkoxide moiety is not associated with the aluminium centre for the duration of propagation.

The polymerisation of ϵ -caprolactone using dialkyl aluminium alkoxide initiators appears to have a build up period present at the start of each reaction. Jerome ⁽¹¹³⁾ proposed that the build up period was related to the ability of the monomer to complex with the initiator. It is possible therefore that the length of this build up period may be related to the structure of the alkoxide group used as the initiator. The length in minutes of the build up period, which is apparent when a first order kinetic plot of $\ln([M]_0/[M]_t)$ against time has been studied and is tabled in table 4.15.

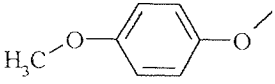
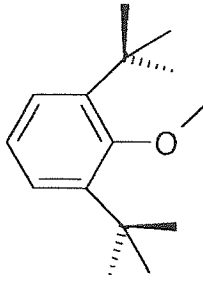
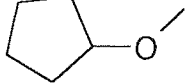
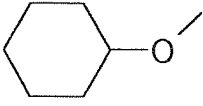
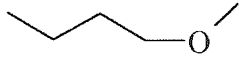
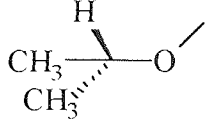
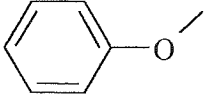
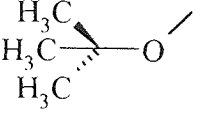
| $[I]_0 \times 10^{-2} \text{ ml}^{-1} \rightarrow$ | 3.6 | 1.8 | 1.0 | 0.67 |
|-------------------------------------------------------------------------------------|-----|-----|-----|------|
| Alkoxide ↓ | | | | |
|  | 22 | 31 | 43 | 47 |
|  | 9 | 25 | 102 | - |
|  | 24 | 40 | 25 | 70 |
|  | 20 | 23 | 27 | 57 |
|  | 3 | 8 | 12 | 30 |
|  | 14 | 9 | 73 | 81 |
|  | 92 | 41 | 104 | - |
|  | - | - | - | - |

Table 4.15. Build up period, t_i in minutes for the polymerisation of ϵ -caprolactone using diisobutyl aluminium alkoxide initiators in toluene at 25°C.

The length of the build up period has been plotted against initial initiator concentration for each alkoxide structure used and is shown in figure 4.30.

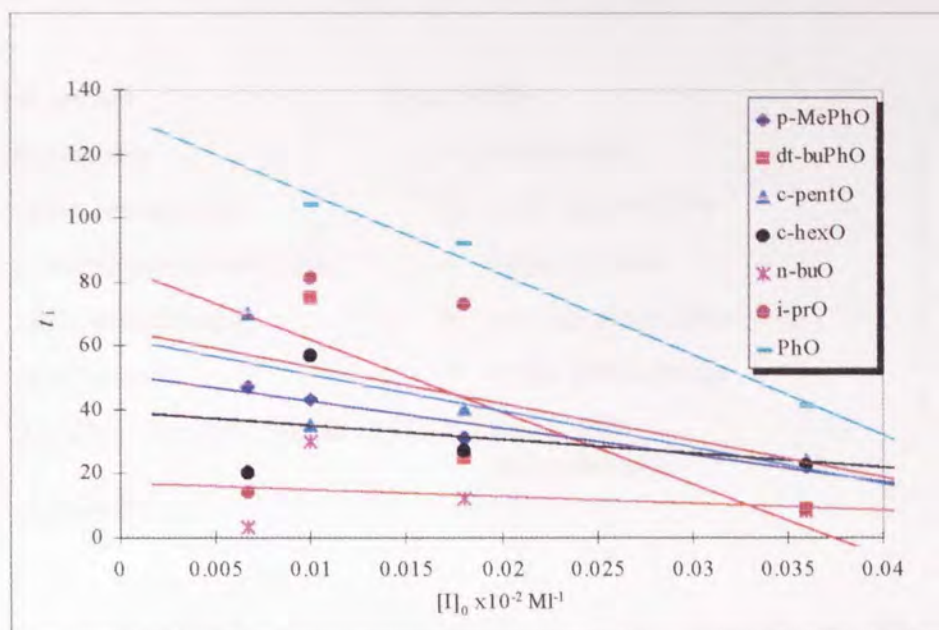


Figure 4.40. The effect of the alkoxide group structure on the length of the build up period.

The structure of the alkoxide group has a significant effect on the length of the build up period (figure 4.40 and table 4.14). Clearly the structure of alkoxide group has an effect at the start of the reaction. Since the structure does not appear to have an effect throughout the reaction this points to the mechanism being one in which the alkoxide group moves away from the aluminium centre as the reaction proceeds, or at least does not influence propagation. The mechanisms of initiation and propagation are likely to be the one that was proposed by Jerome and Penczek.

The length of the build up period is greater when phenolic initiators are used (figure 4.40). Using *diisobutyl* aluminium *n*-butoxide as an initiator gives the shortest build up period. The full order of build up period length is listed in table 4.14, with the order calculated from the plot of k_{app} against $[I]_0$. The shortest build up period is at the top of the list and the longest at the bottom.

Build up period

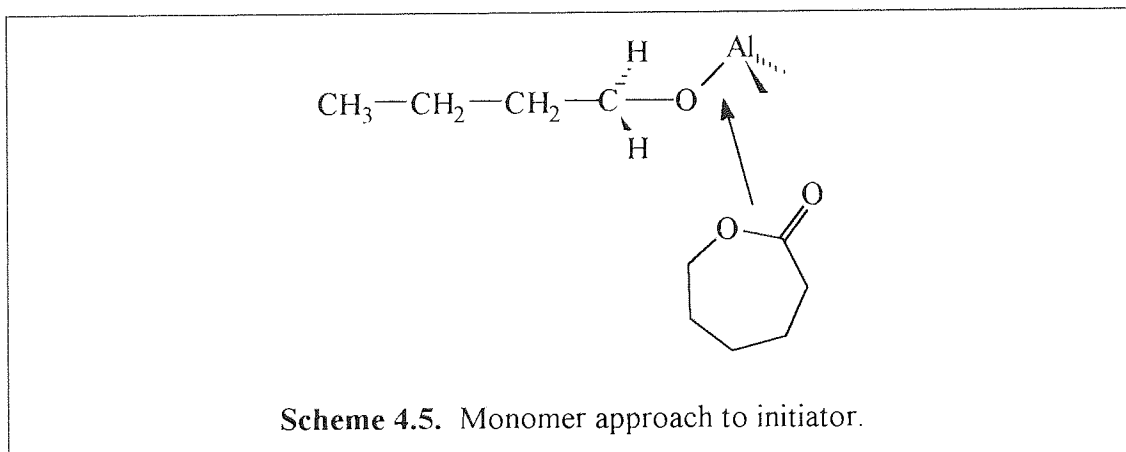
- *n*-butoxide
- cyclo-hexanoxide
- *para*-methoxyphenoxide
- cyclo-pentanoxide
- *isopropoxide*
- 2,6-di-*tert*-butylphenoxide
- phenoxide

k_{app} vs $[I]_0$

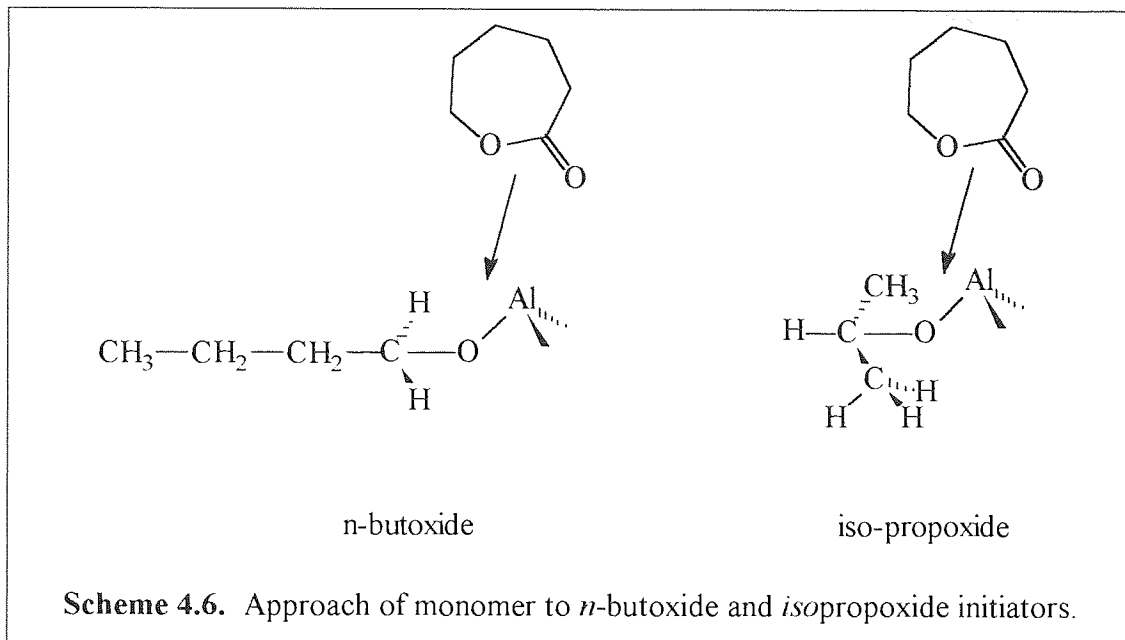
- *n*-butoxide
- cyclo-hexanoxide
- *isopropoxide*
- *para*-methoxyphenoxide
- cyclo-pentanoxide
- 2,6-di-*tert*-butylphenoxide

Increased
build up
period

A direct link between the structure of the alkoxide and the rate of polymerisation can now be drawn. *Diisobutyl aluminium n*-butoxide has the fastest rate regardless of the method of calculation. This is because it has a linear structure and does not hinder the complexation of the monomer with the active aluminium centre. Movement about the C-O bond and Al-O will result in the monomer being given more space to approach the aluminium centre (scheme 4.5).

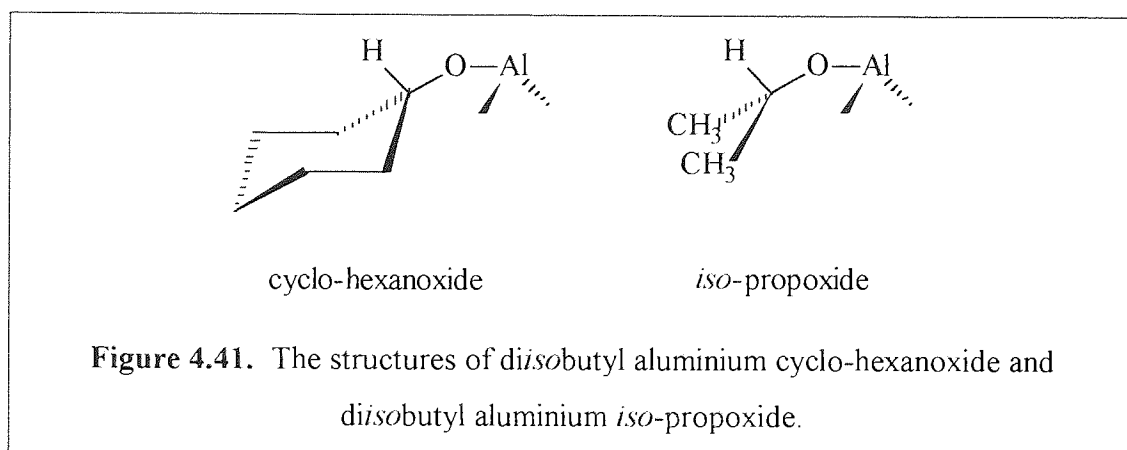


The branched alkoxide, *isopropoxide*, has a slower rate than the corresponding reactions using *diisobutyl aluminium n*-butoxide. The inductive effect of an *isopropoxide* group is likely to be little different from that of an *n*-butoxide group, although the inductive effect of a secondary alkyl group is greater than that of a primary alkyl group. This will probably affect the reaction far less than the increased steric hindrance around the active alkoxide bond. Scheme 4.6. shows the increased hindrance around the alkoxide bond.

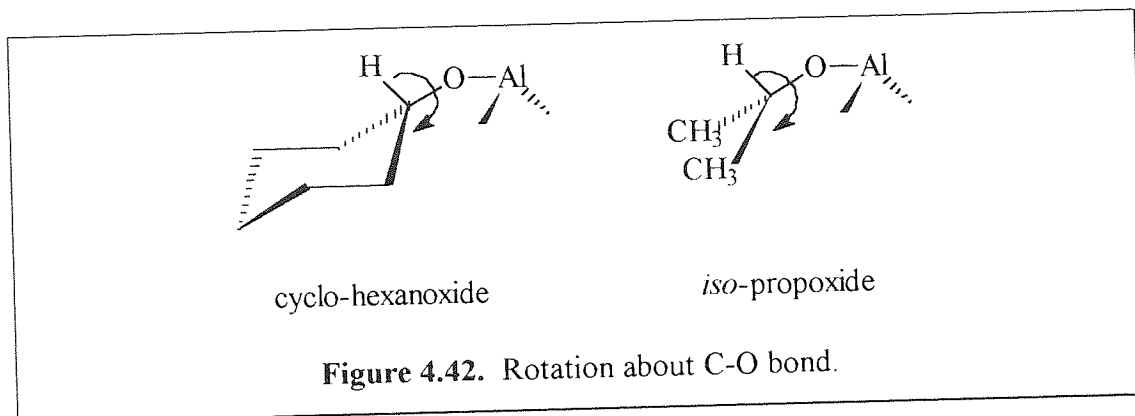


This diagram does not necessarily mean that the configuration shown is the one that is adopted when monomer approaches the initiator, merely that steric hindrance has increased. Of course the actual system is three-dimensional and the approach of the monomer can take place from any direction. However the alkoxide can also move in space and so on average the hindrance will be greater than when the initiator was *diisobutyl* aluminium *n*-butoxide.

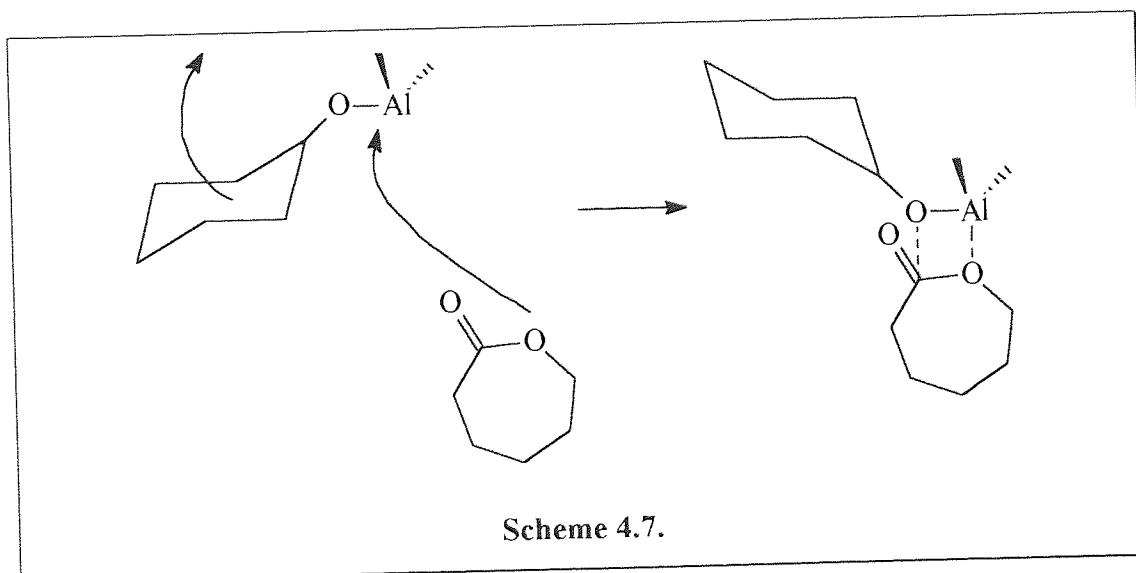
When the cyclic alcohol, cyclo-hexanol was used to form an initiator for the polymerisation of ϵ -caprolactone the rate of polymerisation appears to be faster than that when *iso*-propoxide was the alkoxide group.



The structures of both alkoxides up to the β -carbon are essentially the same. Therefore electronic effects cannot be causing the differences in rate since these are generally considered to be only effective over about 1 carbon atom. The structure of the alkoxide is the same (figure 4.41) and structural effects are probably not directly responsible for the differences in reaction rate. Rotation about the C-O bond certainly occurs (figure 4.42) and this may be behind the disparities in the rate of reaction.



Cyclo-hexanol occupies a larger volume in space than *iso*-propanol, and thus rotation about the C-O bond may be slower for cyclo-hexanol than for *iso*-propanol. Rotation may be slower because there is more resistance to rotation from the reaction medium. This slower rotational frequency may allow more time for the monomer to approach the active alkoxide site without being hindered by the alkoxide group. It may even be possible that the resistance to rotation is such that the cyclo-hexanol group is forced to adopt one fixed position orientated away from the monomer.



Using the planar, cyclic, alkoxide cyclo-pentoxide to initiate the polymerisation of ϵ -caprolactone produces a reaction that has a slower rate of polymerisation than the corresponding reactions using *diisobutyl* aluminium cyclohexanoxide initiator. Van der Waal's and other intermolecular forces probably cause the cyclohexanol ring to be orientated away from the monomer. A planar molecule such as cyclo-pentanol may not allow as much space for the monomer to complex. The planar molecule probably rotates quicker around the C-O bond and does not allow time for the monomer to complex with the initiator.

Although insufficient data was collected for the molecular weight studies to be meaningful the polymerisation using *diisobutyl* aluminium *tert*-butoxide initiated polymerisations clearly have a slower rate than corresponding reaction using the linear butoxide. The structure of the bulkier *diisobutyl* aluminium *tert*-butoxide initiator is hindering the approach of the monomer to the active alkoxide site and slowing the rate of initiation.

The use of phenolic groups shows some interesting results, the bulkier *diisobutyl* aluminium 2,6-*di**tert*butylphenoxide appears to have a faster rate than corresponding reaction using *diisobutyl* aluminium phenoxide. Using *diisobutyl* aluminium *para*-methoxyphenoxide initiator gives a rate of polymerisation faster than the corresponding reaction using either of the other phenolic initiators. A methoxy substituent on a phenol ring is an ortho- and para- directing activator. The electron density at the alkoxide oxygen is therefore likely to be higher than when an unsubstituted phenol is the alkoxide group. The low electron density of the carbonyl carbon on the monomer is therefore likely to be more attracted to the alkoxide oxygen. This will increase the rate of initiation compared to phenoxide and 2,6-*di**tert*butylphenoxide. Using *diisobutyl* aluminium 2,6-*di**tert*butylphenoxide as an initiator gives a polymerisation that is faster than corresponding *diisobutyl* aluminium phenoxide initiated reactions. Potassium 2,6-*di**tert*butyl phenoxide is known to be a strong base. Therefore the increased electron density around the alkoxide oxygen in 2,6-*di**tert*butylphenoxide is likely to increase the rate of initiation in the same way as the *p*-methoxy group increases the rate of polymerisation.

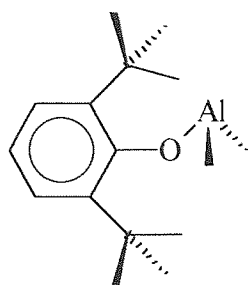


Figure 4.43. Diisobutyl aluminium 2,6-di-*tert*butylphenoxide.

In addition, the *tert*-butyl groups may interact with the aluminium and oxygen atoms, possibly holding the alkoxide group in place and preventing free rotation around the C-O bond. This would assist the monomer to complex with the initiator by providing a clear route to the active alkoxide site.

Both the structure of the alkoxide moiety, and the electronic effects caused by the different alkoxide structures appear to have a direct effect on the reaction kinetics. It is possible therefore to choose an initiator that would produce the desired combination of molecular weight and molecular weight distribution with a terminal functional group.

4.5. NMR analysis of functional terminated poly(ϵ -caprolactone).

4.5.1. ^{13}C NMR analysis of poly(ϵ -caprolactone).

Samples of poly(ϵ -caprolactone) have been analysed using ^{13}C NMR. The NMR spectrum of poly(ϵ -caprolactone) is shown below (figure 4.44.).

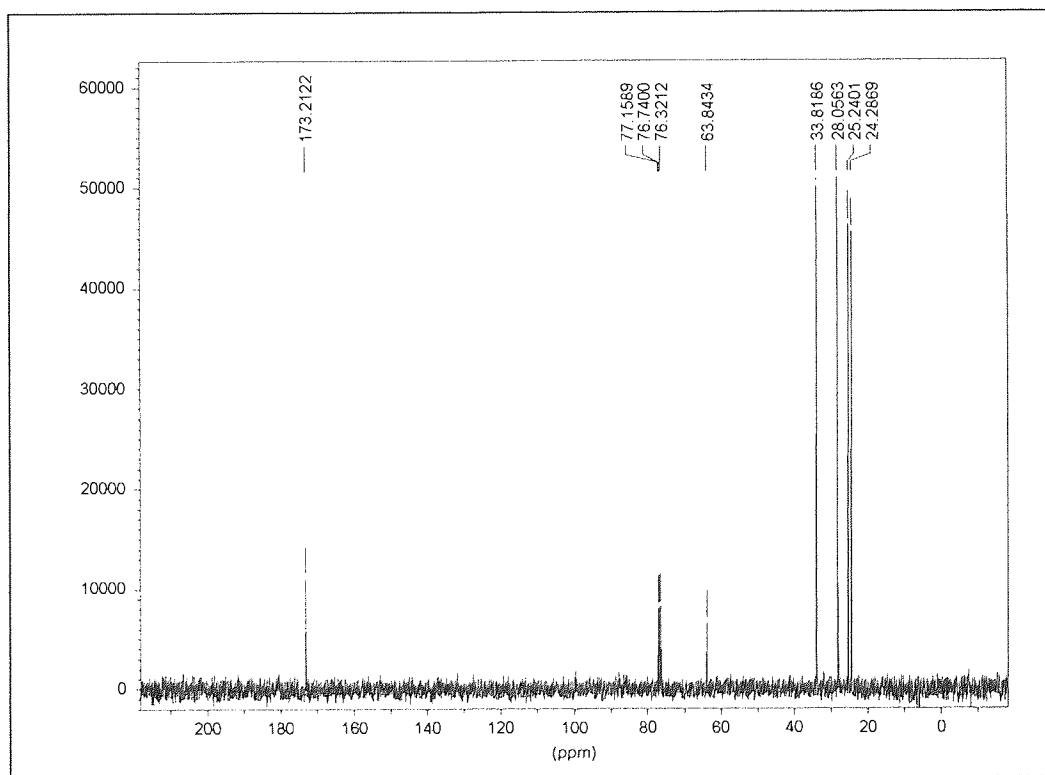
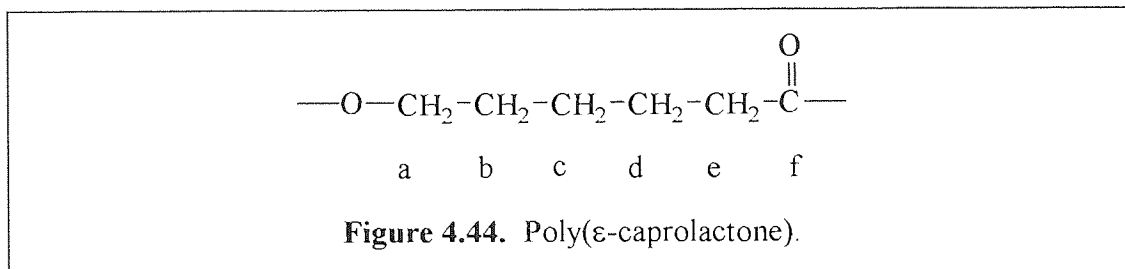


Figure 4.45. ^{13}C NMR of poly(ϵ -caprolactone).

Poly(ϵ -caprolactone) shows a resonance at approximately 175 ppm due to the carbonyl carbon ('f' figure 4.44.) which is strongly deshielded by the electron rich π -bond and the oxygen atom. The reference used is CDCl_3 in CHCl_3 . The reference shows three resonances because the carbon is decoupled from the C-H but it is not decoupled from the C-D. The middle line is known to have a chemical shift

of 77.0ppm. At 63ppm the carbon labelled 'a' (figure 4.44.) deshielded by the adjacent acyl oxygen resonates. The central four-methylene carbon atoms 'b-d' (figure 4.44.) resonate at between 24 and 33 ppm. The methylene carbon adjacent to the carbonyl carbon resonates furthest downfield at 34ppm.

The structure of the terminal functional group does not appear to affect the ^{13}C NMR spectrum of poly(ϵ -caprolactone). It is more than likely that the NMR spectrometer is not of sufficient power to provide the resolution required to observe this particular resonance.

4.5.2. ^1H NMR analysis of poly(ϵ -caprolactone).

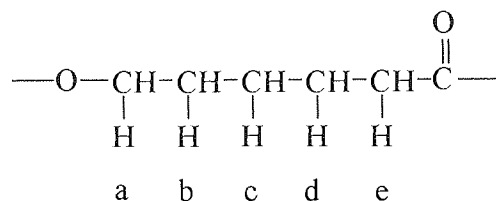


Figure 4.46. Poly(ϵ -caprolactone).

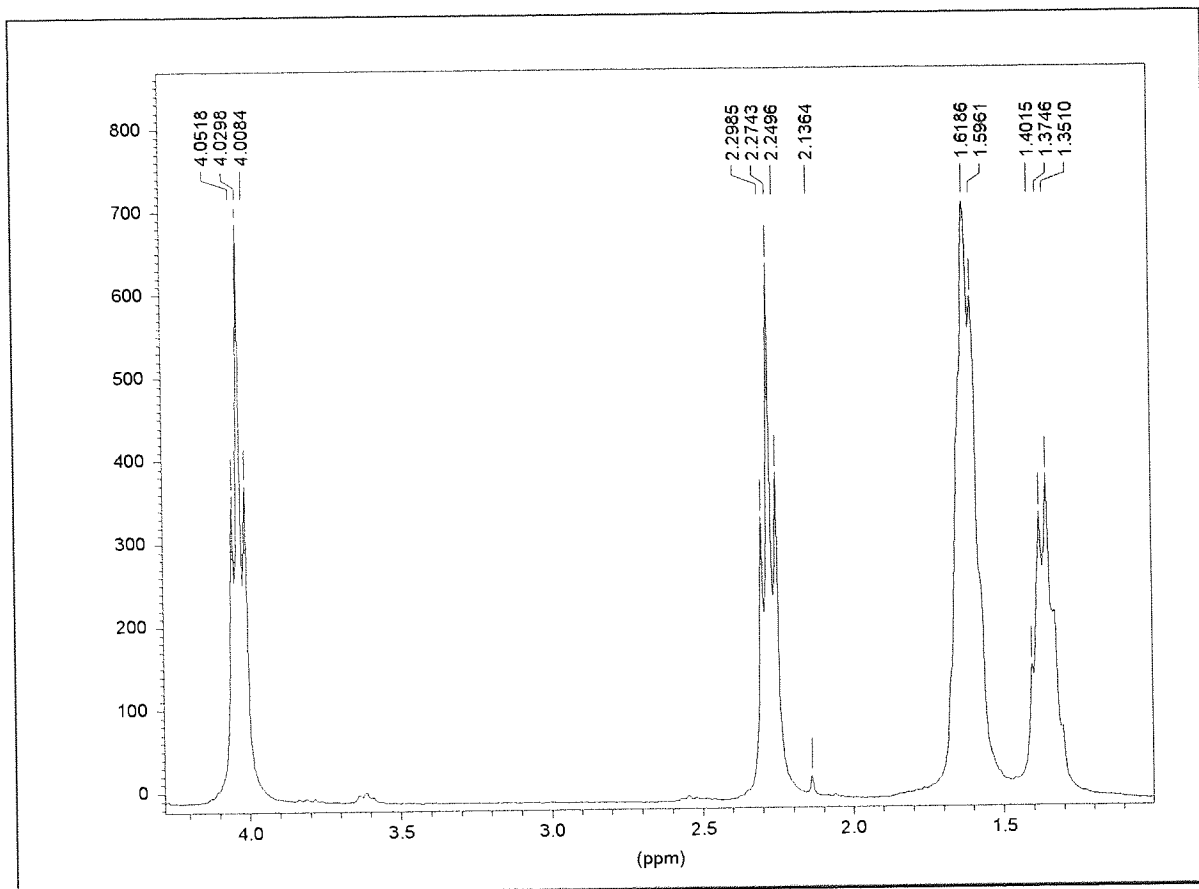


Figure 4.47. ¹H NMR of poly(ε-caprolactone).

Figure 4.47 shows the ¹H NMR of *diisobutyl aluminium n*-butoxide initiated poly(ε-caprolactone). This was chosen as the standard spectrum because the structure of the terminal group is little different from that of the repeat unit so it is unlikely to affect the spectrum.

The proton NMR of poly(ε-caprolactone) shows a resonance due the protons on the carbon adjacent to the acyl oxygen atom ('a' figure 4.46.) at approximately 4.0ppm. Slightly upfield at 2.3 ppm a triplet shows due to the resonance of the protons on the carbon atom next to the carbonyl carbon atom. The protons located more centrally in the monomer repeat unit appear further upfield still between 1.3 and 1.6 ppm. The protons labelled 'c' and 'd' resonate at 1.6 ppm as a triplet of double the intensity of the other protons, indicating that there are two identical protons resonating.

4.5.3. NMR analysis of *diisobutyl aluminium 2,6-di-tert butyl phenoxide* initiated poly(ϵ -caprolactone).

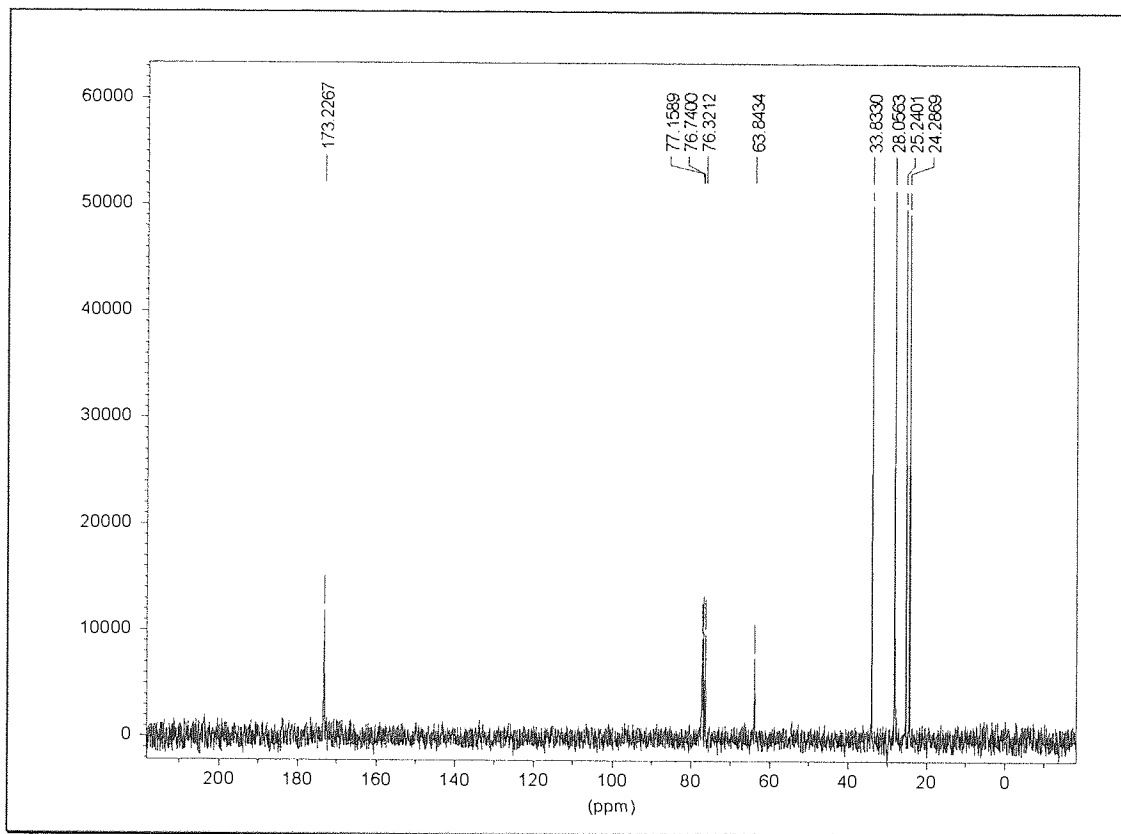


Figure 4.48. ^{13}C NMR of *diisobutyl aluminium di-tert-butyl phenoxide* initiated poly(ϵ -caprolactone).

The ^{13}C NMR spectrum of *diisobutyl aluminium di-tert-butyl phenoxide* initiated poly(ϵ -caprolactone) (figure 4.48.) shows very little difference to the spectrum of poly(ϵ -caprolactone) initiated using *diisobutyl aluminium n-butoxide*. According to the mechanism of lactone polymerisation using alkoxide initiators the alkoxide moiety should be the terminal group at one end of the polymer. It would be expected therefore that an aromatic group would appear in the ^{13}C NMR spectrum of this polymer in the region of 120-160 ppm. No obvious peaks are apparent in this range although there may be a small peak at about 132 ppm. This could be merely noise and therefore be irrelevant.

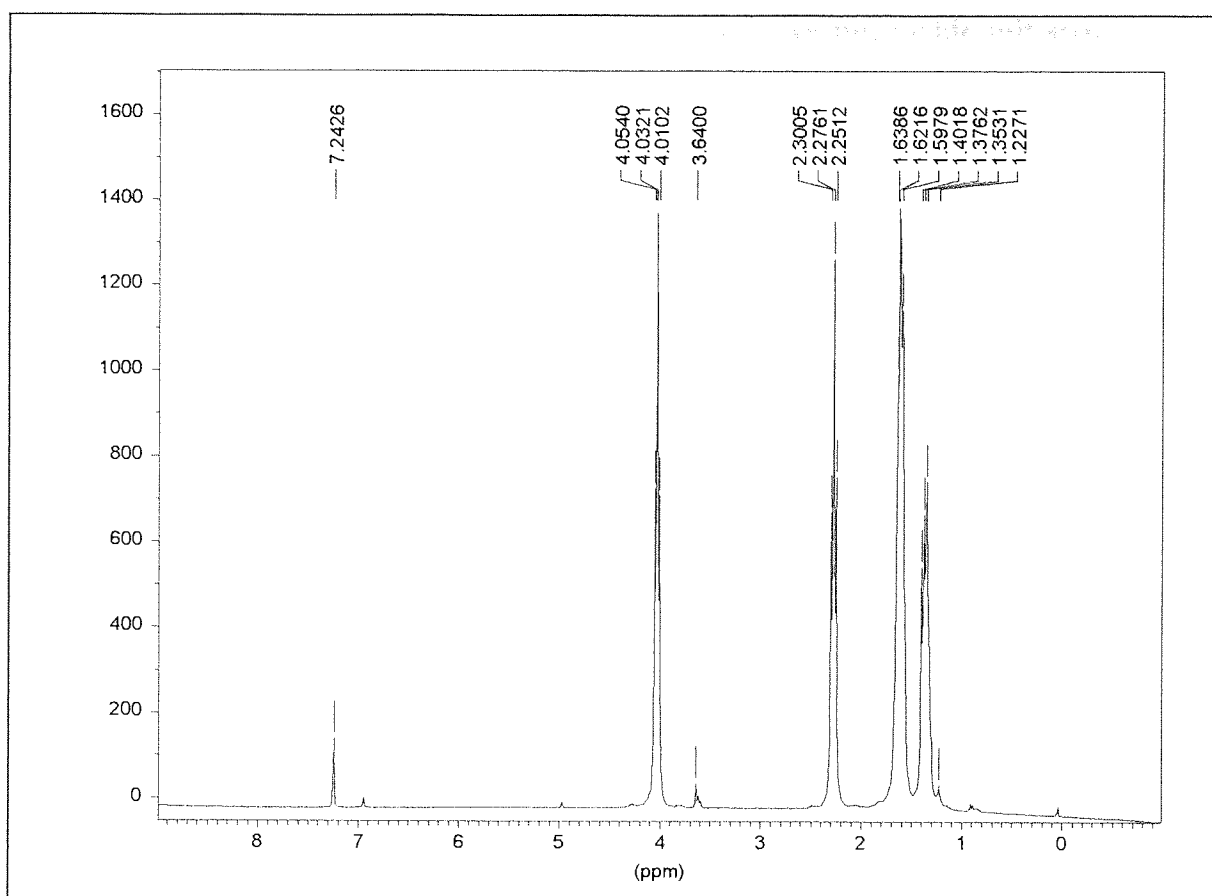


Figure 4.49 ^1H NMR spectrum of di-*tert*-butyl phenoxide initiated poly(ϵ -caprolactone).

Two peaks appear at 7.0 - 7.3 ppm (figure 4.49.) and these are probably due to the resonance of aromatic protons. The larger of the two peaks could be residual solvent, toluene, or it could be due to the protons on the terminal. A much smaller peak is visible at 6.9 ppm although this is most likely to be residual toluene which was the solvent used in the polymerisation. A small peak to the right of the methylene proton peak is visible at approximately 1.2 ppm. This is most probably the resonance caused by the methyl protons of the *tert*-butyl groups in the terminal di-*tert*-butyl phenoxides moieties.

4.5.4. NMR analysis of diisobutyl aluminium *p*-methoxy phenoxide initiated poly(ϵ -caprolactone).

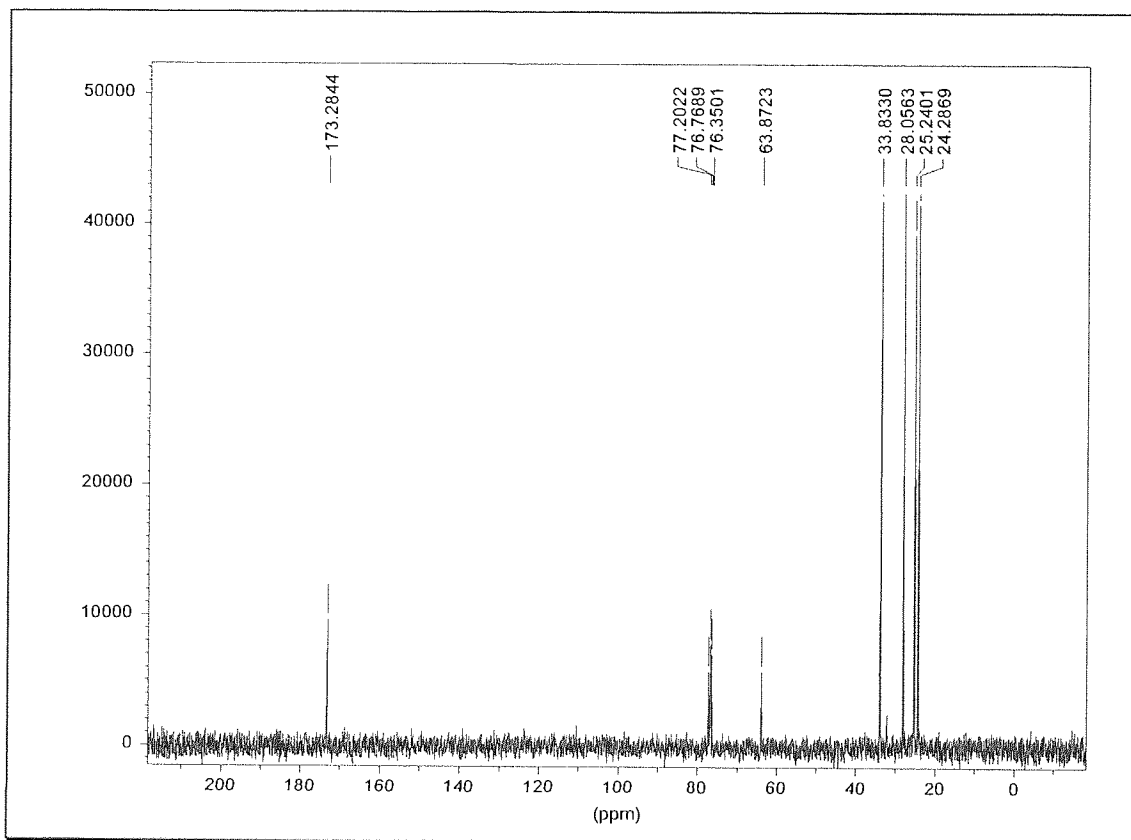


Figure 4.50. ^{13}C NMR of diisobutyl aluminium *para*-methoxy phenoxide initiated poly(ϵ -caprolactone).

The ^{13}C NMR of diisobutyl aluminium *para*-methoxy phenoxide initiated poly(ϵ -caprolactone) (figure 4.50) shows little difference from the ^{13}C NMR of diisobutyl aluminium di-*tert*-butyl phenoxide initiated poly(ϵ -caprolactone). There is however a small resonance at about 32 ppm which is due to the resonance of the *para*-methoxy carbon atom.

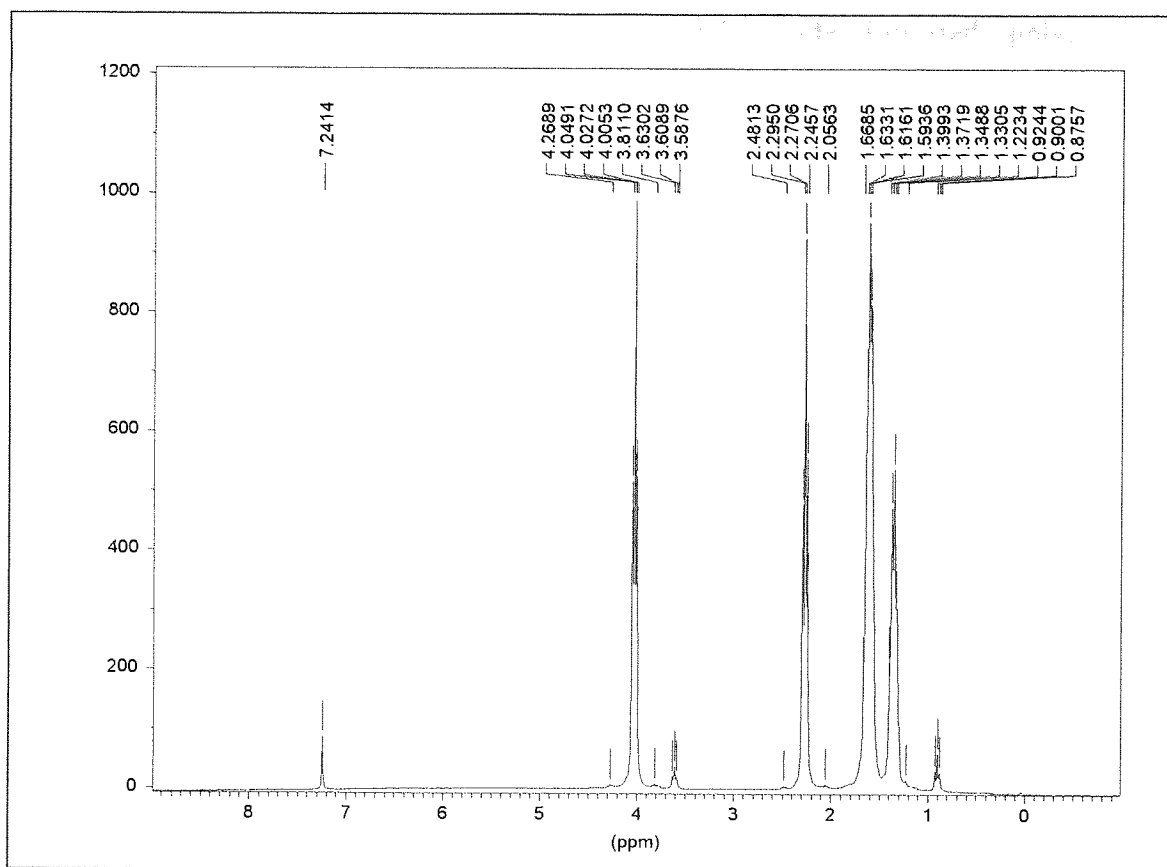


Figure 4.51. ^1H NMR of diisobutyl aluminium *p*-methoxy phenoxide initiated poly(ϵ -caprolactone).

The ^1H NMR spectrum of diisobutyl aluminium *p*-methoxy phenoxide initiated poly(ϵ -caprolactone) (figure 4.51) shows very few differences from that of poly(ϵ -caprolactone) without a terminal aromatic group (figure 4.47). There is a resonance at 7.2 ppm, which may be due to the protons on the terminal phenols or because of some solvent trapped amongst the polymer. A very small peak shows at about 3.5 ppm and this is most probably because of the resonance of the *para*-methoxy protons.

4.5.5. NMR analysis diisobutyl aluminium *n*-butoxide initiated poly(ϵ -caprolactone).

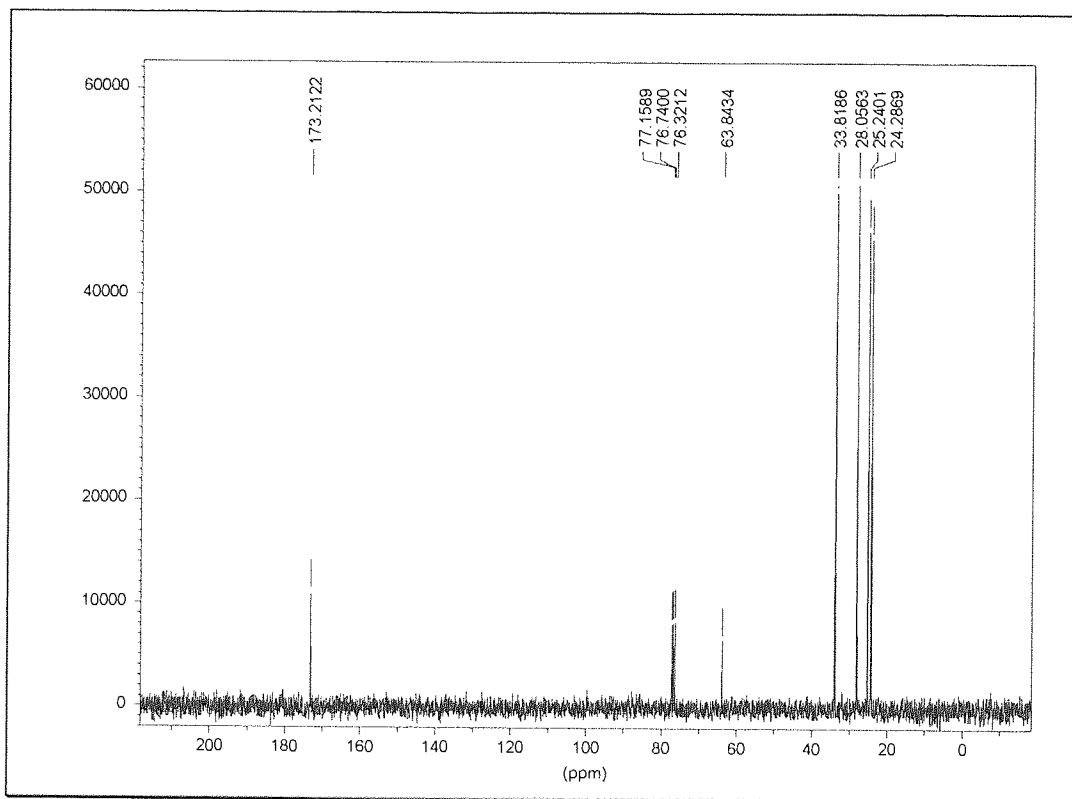


Figure 4.52. ^{13}C NMR of *n*-butoxide initiated poly(ϵ -caprolactone).

The ^{13}C NMR spectrum of diisobutyl aluminium *n*-butoxide initiated poly(ϵ -caprolactone) (figure 4.52) shows no real evidence of the inclusion of butanol as a terminal functional group. However the terminal group contains only $-\text{CH}_2-$ and $-\text{CH}_3$ groups that are also present in the polymer. It is likely that the *n*-butoxide resonances are obscured by the resonances due to the protons in the polymer.

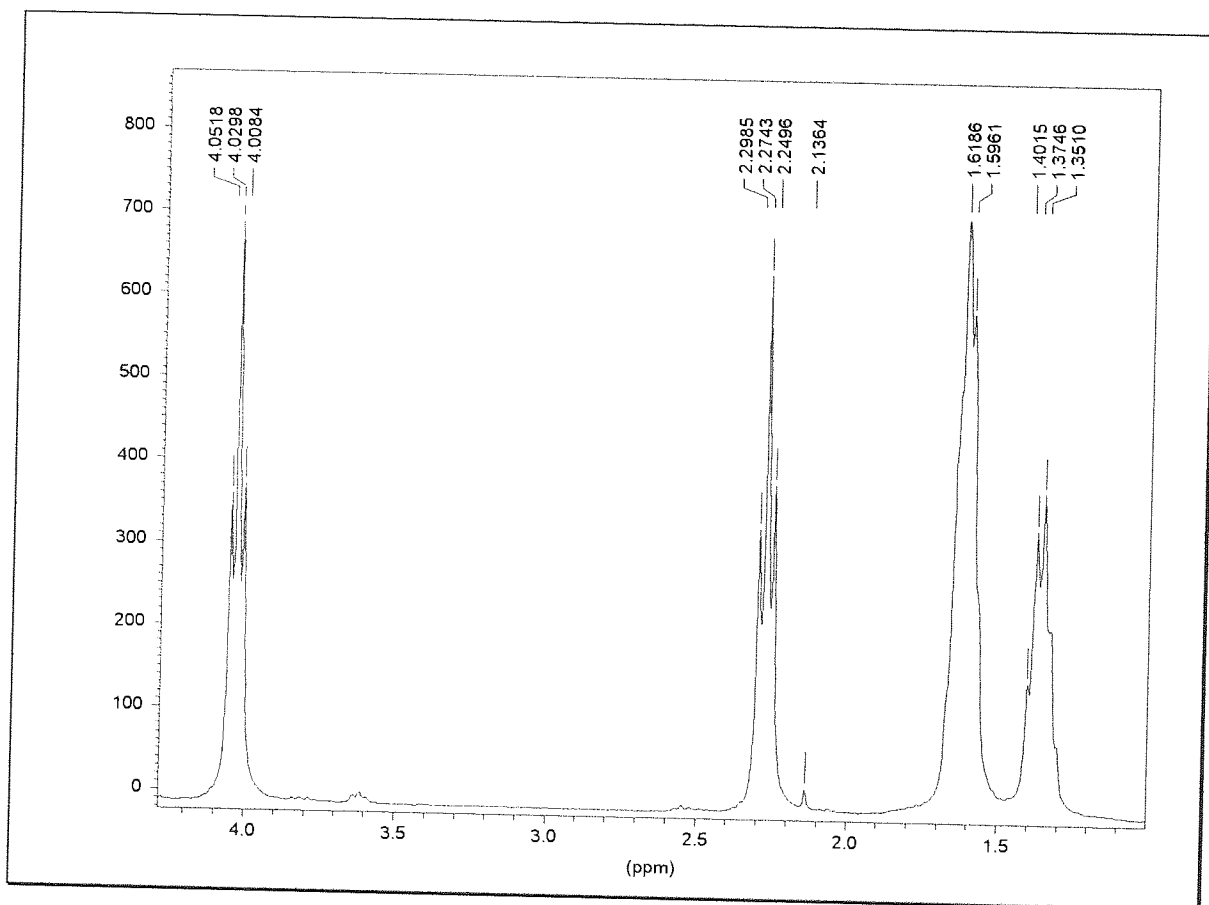


Figure 4.53 ¹H NMR of of diisobutyl aluminium *n*-butoxide initiated poly(ϵ -caprolactone).

The proton NMR of diisobutyl aluminium *n*-butoxide initiated poly(ϵ -caprolactone) (figure 4.53) shows no peaks that could solely be attributed to the telechelic group. *n*-Butanol only has groups which are present in the monomer repeat units so the resonance due to the terminal groups are likely to be swamped by the polymer resonances.

Chapter 5.

Homo-polymerisations of δ -valerolactone.

Introduction.

In order to understand further the mechanism of the polymerisation of lactones using aluminium alkoxide initiators it was necessary to vary the ring size of the lactone monomer.

5.1. Polymerisation of δ -valerolactone.

δ -Valerolactone was polymerised using *diisobutyl* aluminium *isopropoxide* as an initiator in dried and distilled solvents of different polarity. The reaction was maintained under a slight positive pressure of argon throughout and aliquots of a known volume removed at recorded intervals. These aliquots were analysed for molecular weight and molecular weight distribution using GPC, and percentage conversion.

The reaction conditions were identical to those used for the polymerisation of ϵ -caprolactone using *diisobutyl* aluminium *isopropoxide* in chapter 3.

The reaction conditions were,

- Temperature 25°C
- $[\epsilon\text{-CL}] = 2.1\text{m l}^{-1}$

- $[\text{I}] = \text{varied}$
- Inert atmosphere
- Toluene solvent

Samples were removed at recorded intervals and transferred to a beaker containing a small volume of toluene and then precipitated from methanol. It was found that direct precipitation in methanol made the polymer insoluble in both THF and chloroform and subsequently GPC analysis was found to be difficult. The solvent was removed by evaporation and the polymer was dried to a constant weight under vacuum.

5.1.1. The polymerisation of δ -valerolactone in THF using diisobutyl aluminium isopropoxide initiator.

| $[I]_0 \text{ ml}^{-1}$ | Time (mins) | % Conv | M_n | M_w | M_w/M_n |
|---------------------------------|-------------|--------|-------|-------|-----------|
| 3.6×10^{-2} (GKS39) | 10 | 12 | 960 | 2000 | 2.1 |
| | 25 | 32 | 1400 | 3300 | 2.3 |
| | 60 | 40 | 3000 | 5600 | 1.9 |
| | 120 | 79 | 4500 | 7200 | 1.6 |
| | 240 | 98 | 6700 | 9600 | 1.5 |
| 1.8×10^{-2} (GKS40) | 30 | 9 | 1100 | 3200 | 2.9 |
| | 60 | 45 | 3000 | 5000 | 1.7 |
| | 140 | 91 | 3400 | 6800 | 2.0 |
| | 215 | 95 | 3600 | 7300 | 2.0 |
| | 275 | 95 | 3900 | 7300 | 1.9 |
| | 340 | 98 | 5800 | 9600 | 1.7 |
| | 390 | 96 | 6200 | 9500 | 1.5 |
| 1.0×10^{-2} (GKS41) | 30 | 7 | 370 | 800 | 2.0 |
| | 60 | 26 | 3600 | 4100 | 1.1 |
| | 90 | 45 | 3200 | 4900 | 1.5 |
| | 140 | 88 | 4000 | 5900 | 1.5 |
| | 210 | 95 | - | - | - |
| | 280 | 98 | 4400 | 6700 | 1.5 |
| | 370 | 98 | 4400 | 6700 | 1.5 |
| | 470 | 99 | 5200 | 7100 | 1.4 |
| 6.7×10^{-3} (GKS42) | 25 | 3 | 4490 | 6300 | 1.4 |
| | 55 | 8 | 860 | 2300 | 2.6 |
| | 145 | 75 | 5200 | 7400 | 1.4 |
| | 190 | 72 | 6600 | 9700 | 1.4 |
| | 250 | 98 | 6600 | 7600 | 1.2 |

Table 5.1. Molecular weight and conversion data obtained from polymerisations of δ -valerolactone using diisobutyl aluminium isopropoxide initiator in THF.

The molecular weights of polymers produced from these polymerisations of δ -valerolactone are closer to the predicted theoretical values than the corresponding polymerisation of ϵ -caprolactone. The theoretical value of the molecular weight of the polymer obtained from the reaction with $[I]_0 = 3.6 \times 10^{-2} \text{ ml}^{-1}$ at 100% conversion would be 6740, compared to the recorded value at quantitative conversion of 6670. It may be that better control of the reaction is obtained because the rate of propagation is slower than the rate of propagation of ϵ -caprolactone.

This is borne out by the molecular weight distribution of the samples removed from this reaction, which narrow as the polymerisation proceeds, a phenomenon, which would be expected for a polymerisation that proceeds with the absence of termination or transfer reactions if the rate of initiation is fast.

The theoretical molecular weight distribution M_w/M_n is given by equation 5.1. assuming a Poisson distribution and that initiation is fast compared to propagation,⁽⁴¹⁾

$$M_w/M_n = 1 + \nu/(\nu+1)^2 \quad 5.1.$$

where ν is the kinetic chain length.

Therefore as the chain lengthens, the molecular weight distribution would be expected to narrow.

The molecular weights of the polymers produced in the reactions carried out with $[I]_0 = 1.8 \times 10^{-2} \text{ ml}^{-1}$, $1.0 \times 10^{-2} \text{ ml}^{-1}$ and $6.7 \times 10^{-3} \text{ ml}^{-1}$ (table 5.1.) are much lower than would be expected. With an initial initiator concentration of $[I]_0 = 1.8 \times 10^{-2} \text{ ml}^{-1}$, at 100% conversion and assuming 100% initiator efficiency then a molecular weight of around 11700 would be expected. A number average molecular weight of around 6200 was achieved at quantitative conversion. Similarly in the polymerisations of δ -valerolactone with $[I]_0 = 1.0 \times 10^{-2} \text{ ml}^{-1}$ and $[I]_0 = 6.7 \times 10^{-3} \text{ ml}^{-1}$, the molecular weight values obtained are significantly lower than those which would be expected, around 20000 and 31000 respectively. It may be that the molecular weight as calculated by GPC is not an exact value but rather relative to poly(styrene) samples and therefore inaccurate. In both cases quantitative conversion is achieved, and it may be that more than one polymer chain is being initiated per initiator molecule, resulting lower than expected molecular weight values. It is also possible that the batch of initiator used was incorrectly made, or that the solvent is being polymerised by the initiator.

5.1.1.1. NMR analysis of poly(δ -valerolactone).

Samples of poly(δ -valerolactone) polymerised in toluene and THF have been analysed using ^1H NMR. The molecular weights of the polymers produced when THF was used as a solvent are lower than would be expected compared to those obtained from predicted theoretical molecular weights. It may be that the solvent THF is being ring opened by the dialkyl aluminium alkoxide initiator. An inspection of the ^1H and ^{13}C NMR spectra of the polymers produced should show if this is the case.

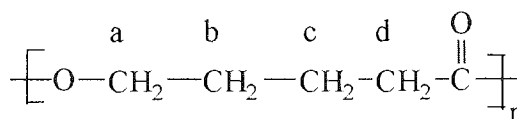


Figure 5.1. Structure of poly(δ -valerolactone).

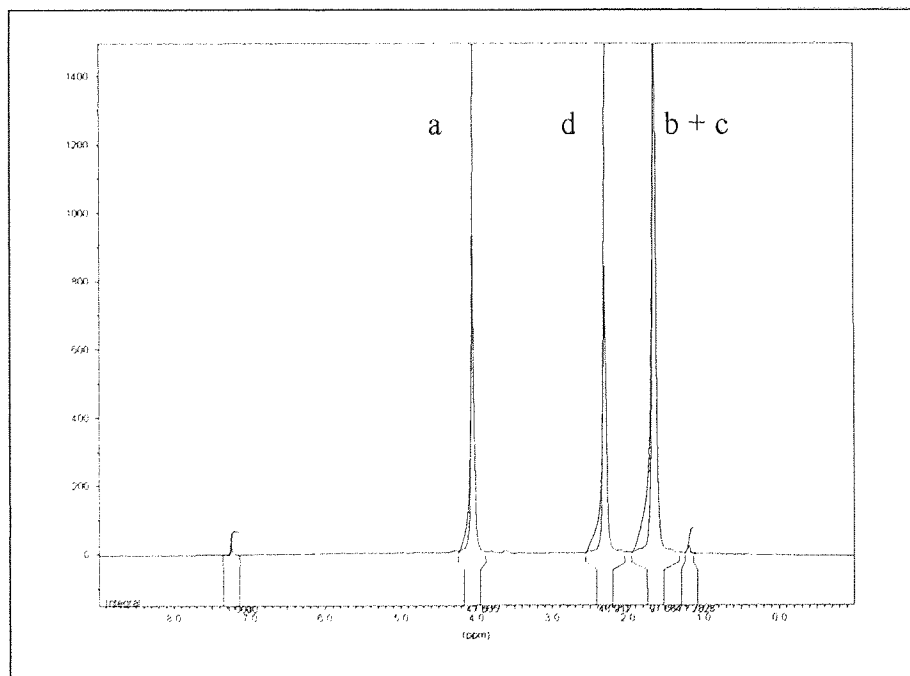


Figure 5.2. ^1H NMR spectra of poly(δ -valerolactone).

There are four main proton resonances in the ^1H NMR of poly(δ -valerolactone). The protons on the carbon atom adjacent to the acyl oxygen ('a' figure 5.1.) shows at 4.0 ppm. Further upfield, the less shielded protons adjacent to the carbonyl carbon resonate at approximately 2.3 ppm ('a' figure 5.1.). The resonance due to the central methylene groups in each monomer unit (figure 5.1. 'b' and 'c') are at 1.6 ppm. The relative intensity of this resonance (97.6) is approximately twice those of the resonances at 2.3 and 4.0 ppm (48.9 and 47.0 respectively) showing that the resonance is in fact due to the two identical methylene groups. The resonance at approximately 7.2 ppm is probably due to residual solvent (toluene) from the polymerisation. The small peak at 1.2 ppm is probably due to resonance of the protons in the end groups.

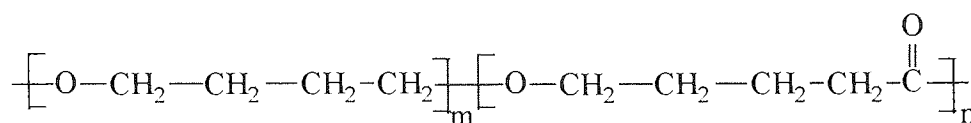


Figure 5.3. Structure of poly(δ -valerolactone)-poly(THF) co-polymer.

If the solvent, THF, is being incorporated into the polymer, then comparison of the peaks at 4.0 ppm and 2.3 ppm should show the presence of THF in the polymer if transfer to monomer is occurring. In poly(tetrahydrofuran) there are no carbonyl groups, only methylene groups and ether oxygens (figure 5.3.). Therefore in a co-polymer of δ -valerolactone and THF, the ratio of protons adjacent to carbonyl groups and those adjacent to oxygen atoms should change if THF is being incorporated in to the growing polymer chain. This ratio is demonstrated in figure 5.4.

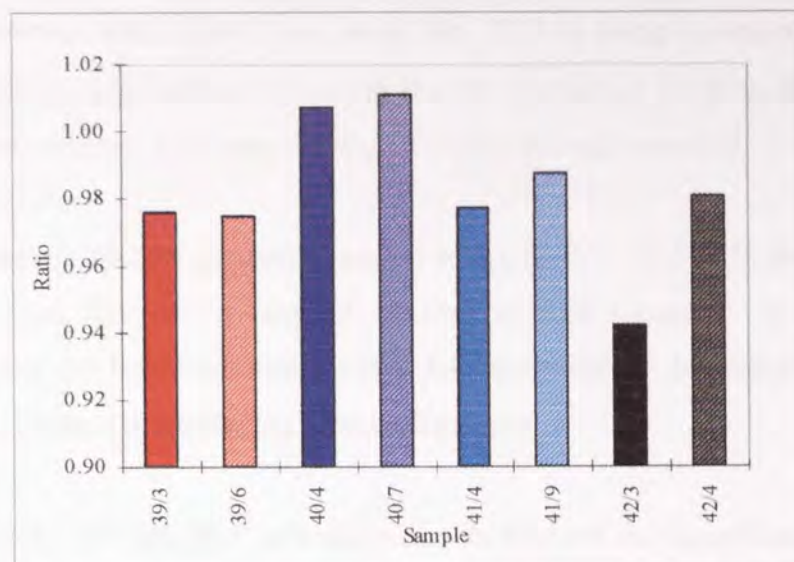


Figure 5.4. Ratio of intensities of protons adjacent to carbonyl carbon and acyl oxygen as reaction proceeds.

It is conceivable that this plot is detecting experimental error. However there is a definite trend to the change in intensities of the proton resonances being compared. It is unlikely that this is because of experimental error alone and it is more likely that the following explanation holds.

If no THF had been incorporated into the polymer, then the ratio of protons adjacent to carbonyl groups and those adjacent to acyl oxygen atoms would remain constant at all times during the polymerisation. The shaded peaks in figure 5.4. represent the measurements which were taken at a later point in the reaction. In all cases except reaction GKS39, ($[I]_0 = 3.6 \times 10^{-2} \text{ ml}^{-1}$) the ratio of protons adjacent to carbonyl groups and those adjacent to acyl oxygen atoms is greater at earlier points in the reaction. This is more pronounced in the reactions with a lower initial initiator concentration and thus a slower rate of propagation. There appears to be a greater proportion THF being incorporated into the polymer in the early stages of the reaction than at a later point. It is possible that the initiator can polymerise the solvent, which complexes with the initiator, whilst initiation of the monomer is slow at the beginning of the reaction. As the rate of propagation increases, then the more reactive species, δ -valerolactone is polymerised rather than the monomer.

However whilst this is not proof that THF is being incorporated into the growing poly(δ -valerolactone) it is clear that the number of ' α ' protons is changing as would be expected if the ring opening of THF is indeed occurring.

Reaction GKS39 samples /3 and /4 where $[I] = 3.7 \times 10^{-2} \text{ M dm}^{-3}$ appear to have the same ratio of ' α ' and ' α' ' protons in both samples. At the initiator concentration and hence the reaction rate decrease, then the difference between the ratio of the protons present in the samples increases.

It is known that THF can compete with lactones for co-ordination with the aluminium centre when aluminium alkoxides are used for the ring opening polymerisation of lactones. Therefore it may not be entirely unexpected if the solvent may also ring open during the course of the reaction, especially if the rate of reaction is slow.

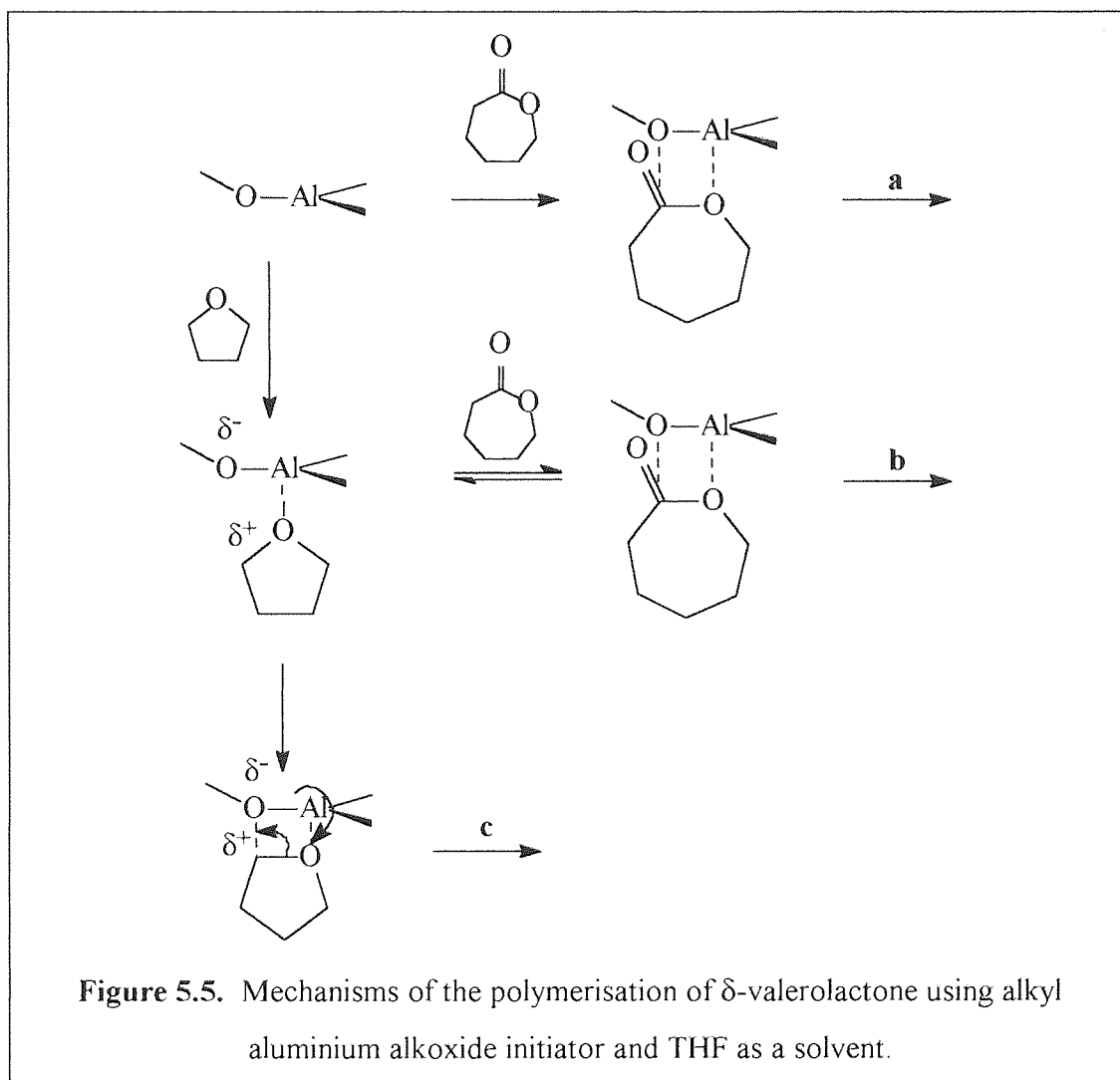


Figure 5.5. Mechanisms of the polymerisation of δ -valerolactone using alkyl aluminium alkoxide initiator and THF as a solvent.

Three routes to propagation (a, b and c figure 5.5.) might be possible using using alkyl aluminium alkoxide initiator and THF as a solvent. The first two, a and b, involve the polymerisation of δ -valerolactone, either by direct monomer coordination with the initiator, or by replacing a co-ordinated solvent molecule with monomer. The slower rate of reaction of δ -valerolactone may lead to route c being possible. The carbon atoms adjacent to the oxygen atom in THF are slightly positively charged because of the electron withdrawing effect of the oxygen. The carbon can then co-ordinate with the alkoxide oxygen atom and subsequent rearrangement of the electrons may occur leading to the ring opening of the solvent molecule.

Diisobutyl aluminium isopropoxide was also synthesised in the usual manner but using THF rather than toluene as the solvent. After standing under argon overnight a white precipitate appeared that did not occur when the preparation was carried out in toluene.

5.1.2. The polymerisation of δ -valerolactone in toluene.

Toluene was used as a solvent in the polymerisation of δ -valerolactone using *diisobutyl aluminium isopropoxide* as an initiator. Samples of a recorded volume were removed from the polymerisation at recorded intervals and dried under vacuum to a constant weight.

| [I] ml ⁻¹ | Time (mins) | % Conv | M_n | M_w | M_w/M_n |
|----------------------|-------------|--------|-------|-------|-----------|
| 18 (GKS34) | 24 | 13 | 8170 | 11730 | 1.44 |
| | 35 | 25 | 8710 | 13300 | 1.53 |
| | 50 | 54 | 15130 | 22590 | 1.49 |
| | 65 | 40 | 17020 | 26370 | 1.55 |
| | 85 | 65 | 12430 | 21600 | 1.74 |
| 10 (GKS33) | 45 | 17 | 15430 | 26770 | 1.7 |
| | 70 | 37 | 16020 | 26010 | 1.6 |
| | 100 | 66 | 22110 | 31270 | 1.4 |
| | 140 | 71 | 18290 | 28880 | 1.6 |
| | 170 | 64 | 22080 | 34560 | 1.6 |
| | 240 | 70 | 21990 | 36030 | 1.6 |
| 6.7 | 30 | 24 | 19880 | 26250 | 1.3 |
| | 50 | 65 | 30050 | 41950 | 1.4 |
| | 100 | 100 | 30860 | 44800 | 1.5 |

Table 5.2. Molecular weight and conversion data obtained from polymerisations of δ -valerolactone using *diisobutyl aluminium isopropoxide* initiator in toluene.

In the first two reactions (GKS34 and GKS33) there appears to be a decrease in the molecular weight of the samples taken at 40% and 65% conversion respectively. It is possible that back biting reactions are taking place. This is supported by an increase in the molecular weight distribution of the samples removed from the polymerisation.

The polymerisation of δ -valerolactone described in table 5.2. using diisobutyl aluminium isopropoxide in toluene at ($[I]_0 = 1.8 \times 10^{-2} \text{ ml}^{-1}$) corresponds to a theoretical molecular weight of 13100 at 100% conversion. This had almost been reached after 85 minutes and 65% conversion, which equates to approximately 65% initiator efficiency. This feature was found in the other polymerisations of δ -valerolactone in toluene. At $[I]_0 = 1.0 \times 10^{-2} \text{ ml}^{-1}$, the molecular weights of the polymers produced are greater than the theoretical maximum value even at 21000, and this has been exceeded by after about 100 minutes. At $[I]_0 = 6.6 \times 10^{-3} \text{ ml}^{-1}$, a M_n of 32000 would be expected at maximum conversion and a figure of 31000 was reached, showing that 0.94 chains are being initiated per alkoxide moiety. Such a small discrepancy could well be due to experimental error.

The molecular weight distribution either broadens ($[I]_0 = 1.8 \times 10^{-2} \text{ ml}^{-1}$ and $[I]_0 = 6.6 \times 10^{-3} \text{ ml}^{-1}$) or does not narrow greatly ($[I]_0 = 1.0 \times 10^{-2} \text{ ml}^{-1}$) as the polymerisation proceeds. The higher than expected molecular weights are probably a result of incomplete initiation due to either destruction of the dialkyl aluminium alkoxide initiator or because of termination at an early stage of the polymerisation. The most likely cause of both of these is the inclusion of trace impurities into the reaction vessel.

5.1.3. The polymerisation of δ -valerolactone in dichloromethane.

| [I] ml ⁻¹ | Time (mins) | % Conv | M_n | M_w | M_w/M_n |
|----------------------|-------------|--------|-------|-------|-----------|
| 36 (GKS35) | 15 | 24 | - | - | - |
| | 35 | 46 | 8400 | 12020 | 1.4 |
| | 85 | 89 | 8710 | 12900 | 1.5 |
| | 105 | 94 | 5090 | 9780 | 1.9 |
| | 180 | 98 | 9180 | 16920 | 1.8 |
| | 215 | 97 | 10660 | 16960 | 1.6 |
| 18 (GKS36) | 10 | 4.9 | - | - | - |
| | 40 | 6.8 | - | - | - |
| | 95 | 17.6 | 6830 | 9960 | 1.46 |
| | 150 | 29.3 | 9000 | 12942 | 1.44 |
| | 210 | 50.7 | 10620 | 14848 | 1.40 |
| | 240 | 56.7 | 10700 | 14930 | 1.40 |
| 10 (GKS41) | 30 | 4.5 | 590 | 860 | 1.45 |
| | 50 | 11.2 | - | - | - |
| | 105 | 17.3 | 7450 | 8042 | 1.10 |
| | 170 | 52.4 | 8920 | 11080 | 1.24 |
| | 250 | 59.1 | 15090 | 23080 | 1.53 |
| | 300 | 68.1 | 15240 | 20830 | 1.37 |
| | 420 | 66.4 | 24470 | 33710 | 1.38 |

Table 5.3. Molecular weight and conversion data obtained from polymerisations of δ -valerolactone using di*i*sobutyl aluminium *i*sopropoxide initiator in DCM.

When dichloromethane was used as a solvent, the molecular weights of the polymers obtained were closer to the theoretical values than the corresponding polymers produced using THF as a solvent. Initiator efficiency is not however 100% and in all cases less than one chain per aluminium centre appears to have been initiated.

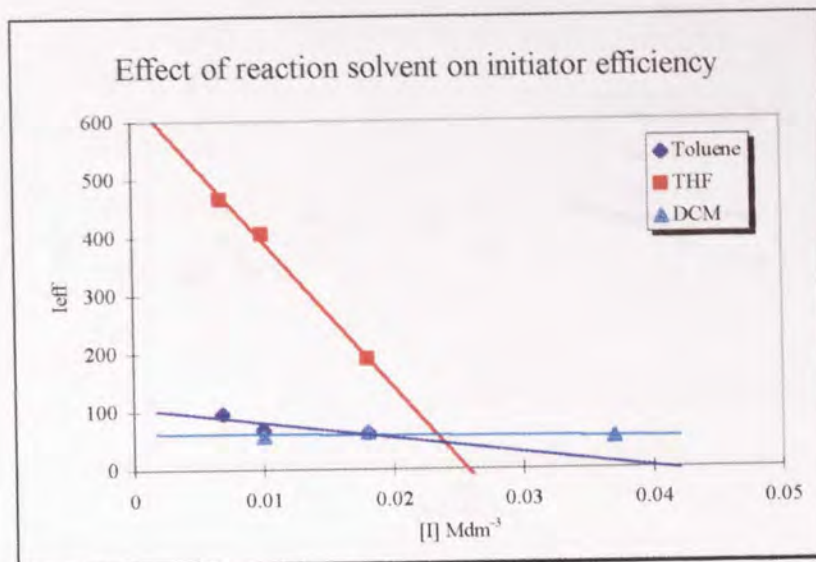


Figure 5.6. Dependence of initiator efficiency on initiator concentration in all solvent used for the polymerisation of δ -valerolactone.

Polymers formed in THF appear to have more than one chain initiated per alkoxy moiety and the initiator efficiency is therefore greater than 100%. This is further support to the theory that the solvent may be being polymerised by the initiator. The polymerisations carried out in THF and toluene have similar initiator efficiencies, from around 50% in DCM at higher initiator concentrations to 65% and in between 60% and 95% in toluene.

The values obtained via GPC for the molecular weight distribution of the polymers produced are quite narrow with values as low as $M_w/M_n = 1.2$ being achieved. Values for M_w/M_n in excess of 2.5 have been obtained at the beginning of a reaction before decreasing to 1.2-1.4 as the reaction proceeds. Such narrowing is an indication of the living nature of this system which is borne out by linear plots of $\ln(DP_{n\infty} - DP_n)$ versus time and $\ln[(M)_0/(M)_t]$ versus time. Jerome and Teyssie⁽¹¹³⁾ and co-workers have quoted values for the polydispersity as low as $M_w/M_n = 1.10$ for the polymerisation of caprolactone using alkyl aluminium alkoxides.

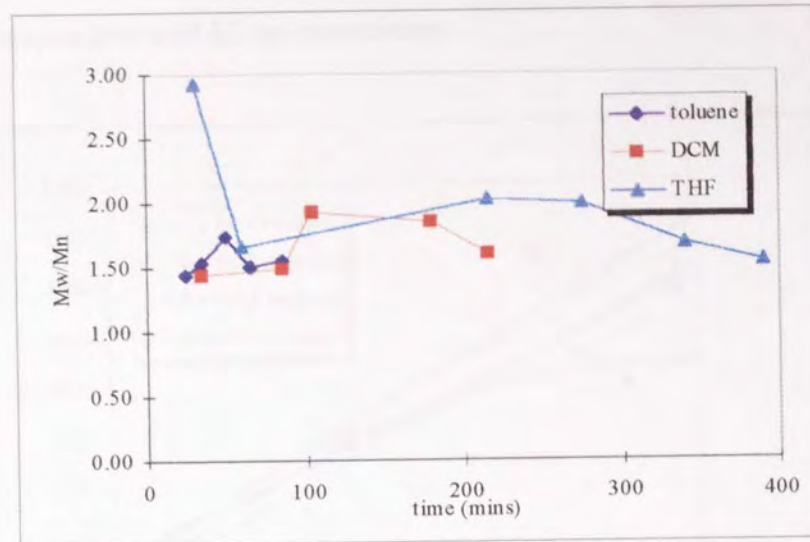


Figure 5.7. Dependence of polydispersity on time for the polymerisation of δ -valerolactone.

Throughout the studies of this system the polydispersities of the polymers produced have been broader than would be perhaps expected for a living system. It is most likely that the Omnifit sampling equipment used does allow the contamination of the reaction by very small amounts of moisture or oxygen, thus terminating some chains and broadening the molecular weight distribution.

5.1.4. The dependence of M_n on conversion.

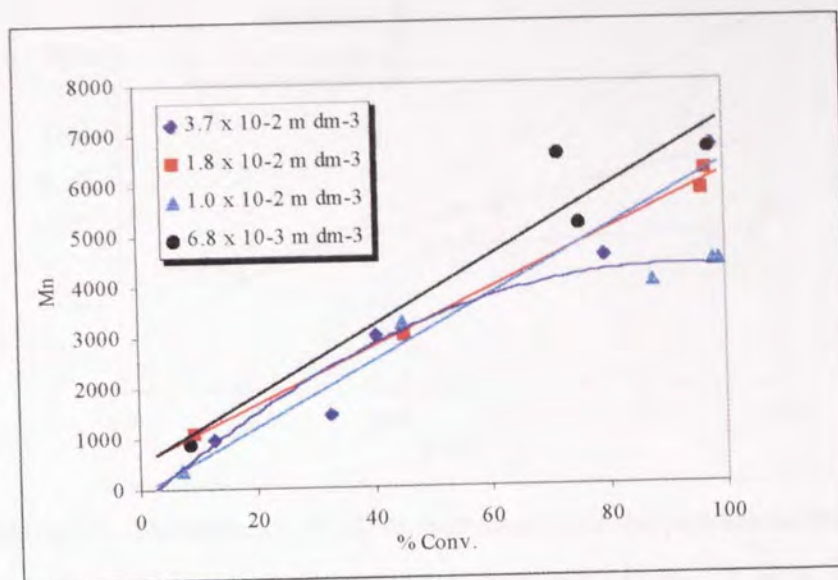


Figure 5.8. Dependence of M_n on conversion for the polymerisation of δ -valerolactone using diisobutyl aluminium isopropoxide and THF as a solvent.

The dependence of M_n on conversion should be linear if the polymerisation is living, i.e. the polymer chains are growing equally as monomer is consumed. The plot of M_n versus conversion for the polymerisation in THF is linear at all initiator concentrations except $1.0 \times 10^{-2} \text{ m dm}^{-3}$. The gradient of this plot decreases after about 50% conversion indicating the presence of termination reactions. Transfer to solvent could also be the reason for this decrease in gradient but the other plots do not have this decrease so it is unlikely. It is also possible that the results are incorrect, possibly because of an error in the GPC analysis for one or more points on the plot.

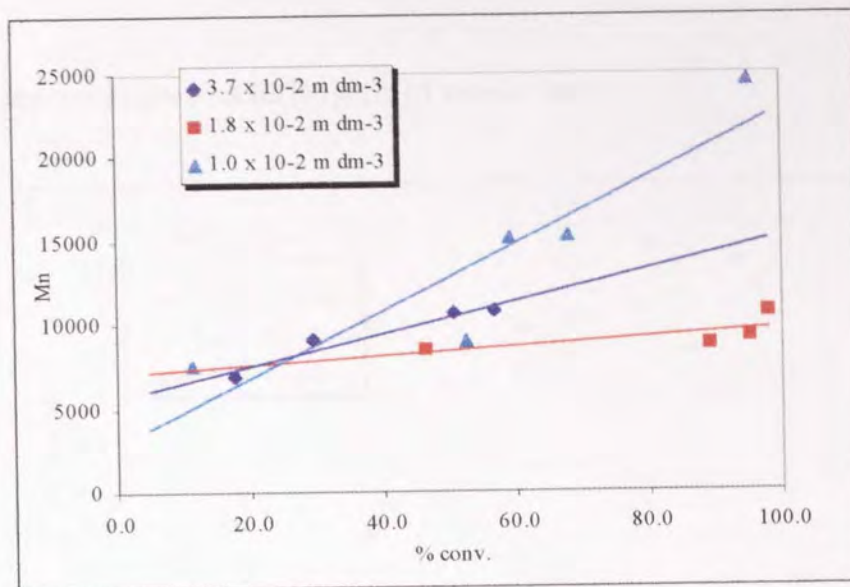


Figure 5.9. Dependence of M_n on conversion for the polymerisation of δ -valerolactone using diisobutyl aluminium isopropoxide and DCM as a solvent.

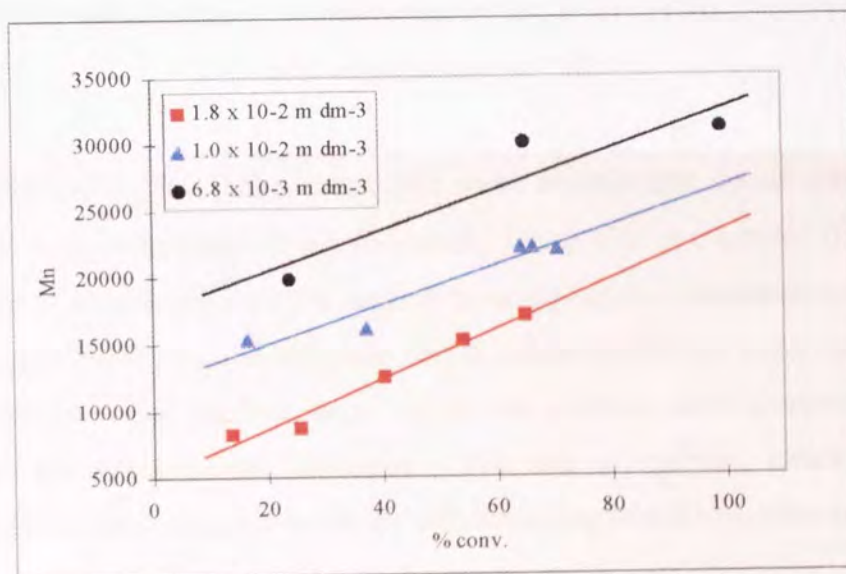


Figure 5.10. Dependence of M_n on conversion for the polymerisation of δ -valerolactone using diisobutyl aluminium isopropoxide and toluene as a solvent.

Like the polymerisations carried out in THF, both the polymerisations on DCM and toluene have a positive intercept on the y -axis. This a further confirmation of the induction period was seen on the $\ln([M]_0/[M]_t)$ versus time plots in section 5.1.5. The polymer seems to be growing slowly at the beginning of the reaction before the rate suddenly accelerates.

5.1.5. First order plots of $\ln([M]_0/[M]_t)$ versus time.

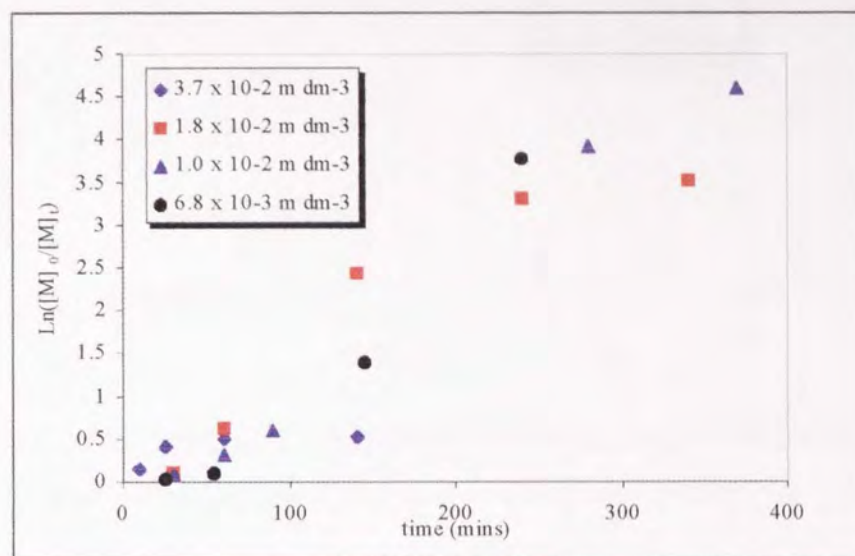


Figure 5.11. Effect initiator concentration on first order plot for the polymerisation of δ -valerolactone in THF.

Plots of $\ln([M]_0/[M]_t)$ versus time show an induction period similar to the reactions using ϵ -caprolactone as a monomer. Using THF as a solvent, (figure 5.11) the induction period appears to be dependent on the initiator concentration. The plot is reasonably linear after the induction period indicating the first order nature of the polymerisation. The gradient decreases as the reaction nears completion as the monomer concentration has decreased. The rate of reaction, indicated by the gradient of the linear segment increases with increasing initiator concentration.

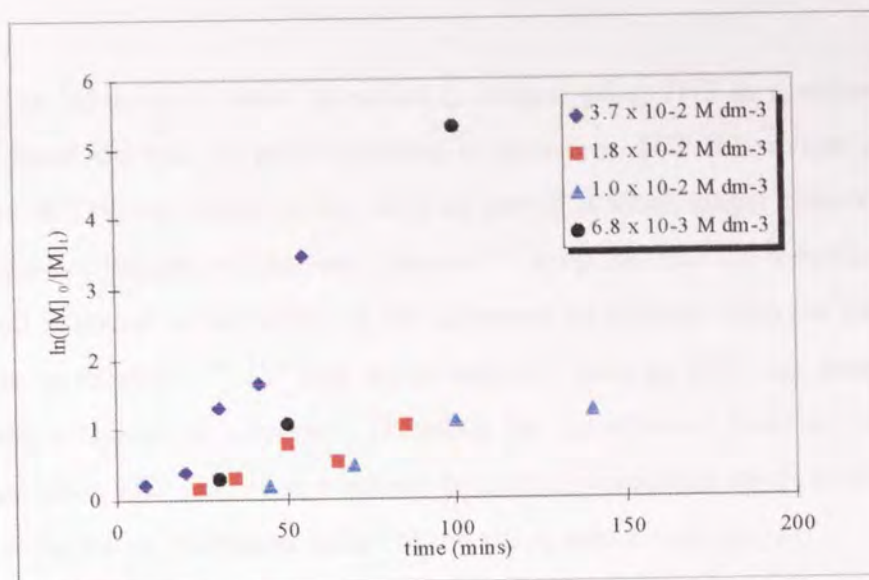


Figure 5.12. Effect of initiator concentration on first plot of $\ln([M]_0/[M]_t)$ versus time for the polymerisation of δ -valerolactone in toluene.

The plots of $\ln([M]_0/[M]_t)$ versus time for the reactions carried out in toluene (figure 5.12) also show an induction period at the beginning of the reaction. The rate of reaction shown by the gradient of the linear section of the plot slows as initiator concentration decreases. An exception is the reaction at $6.7 \times 10^{-3} \text{ ml}^{-1}$ of initiator although this may be a result of experimental error. This appears to be faster than expected, perhaps because of a high initiator efficiency initiating more chains than higher concentrations of initiator with a lower initiator efficiency.

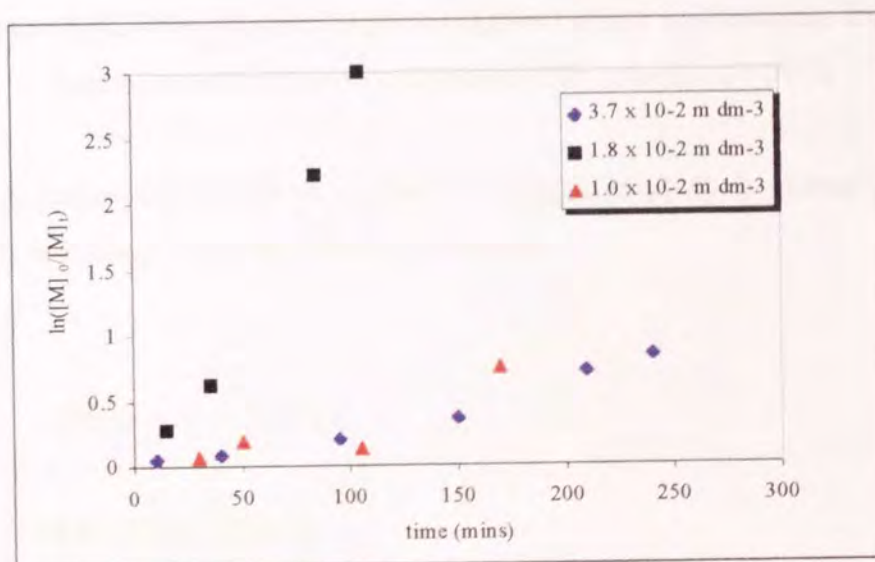


Figure 5.13. First order plot for the polymerisation of δ -valerolactone in DCM.

The induction or build up period is longest using THF as a solvent, (figure 5.14). Since the rate of polymerisation is slower in THF this is not surprising. However in THF the length of the build up period is much longer than when using either DCM or toluene as a solvent. Jerome⁽¹¹³⁾ proposed that the induction or build up period is linked to the ability of the monomer to complex with the initiator. It has been established^(106, 113) that donor solvents such as THF can complex with aluminium alkoxides in solution. Therefore the induction or build up period t_i is increased when THF is used as a solvent because the monomer needs to displace the solvent from the co-ordination sphere of the active centre to propagate.

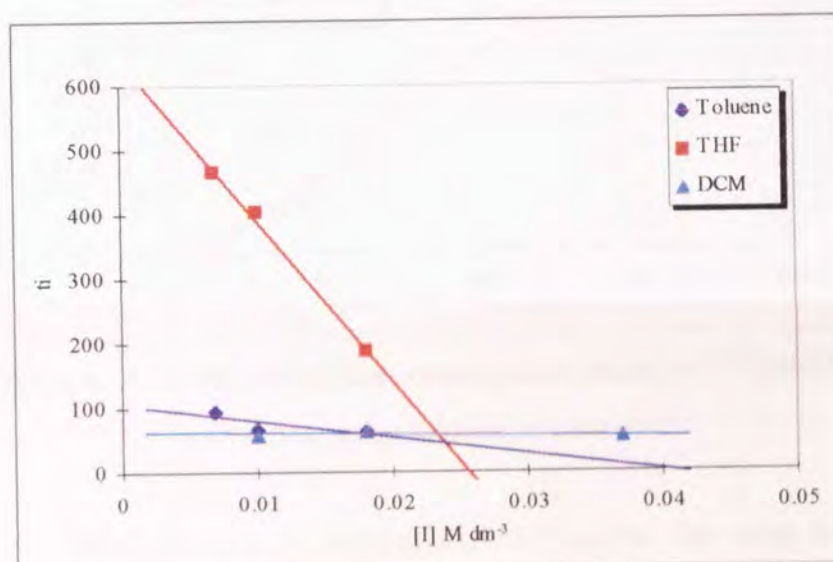


Figure 5.14. Plot of induction period against initiator concentration for the polymerisation of δ -valerolactone in THF, toluene and DCM.

A linear plot should be obtained if $1/[I]_0 \cdot \ln[M]_0/[M]_t$ is plotted against t . This plot is obtained from the following derivation,

If

$$-d[M]/dt = k_p [M][A^*] \quad 5.2.$$

Then

$$\ln[M]_0/[M]_t = k_p [A^*]t \quad 5.3.$$

So

$$1/[A^*] \ln([M]_0/[M]_t) = k_p t$$

5.4.

All points should then lie on a straight line for a living polymerisation. The gradient of this plot is k_p , the rate of polymerisation. The plot is like the first order plot, that is linear after an initial build up period. This build up period presumably occurs because of a gradual increase in the concentration of growing centres.

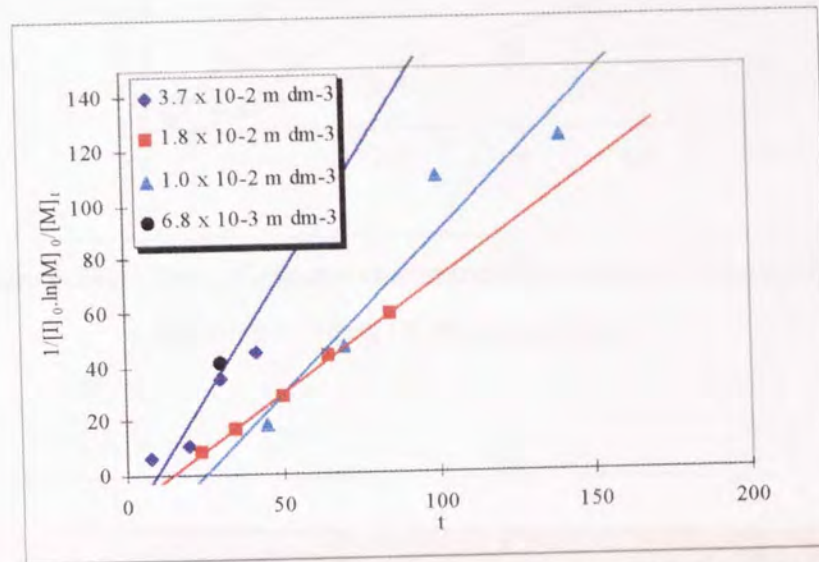


Figure 5.15. Effect of initiator concentration on plot of $1/[I]_0 \ln([M]_0/[M]_t)$ against time using toluene as a solvent.

Both the plots of $1/[I]_0 \ln([M]_0/[M]_t)$ against time using toluene as a solvent (figure 5.15) and DCM (figure 5.16) are slightly curved. It is likely that the concentration of active species builds to a constant level and then remains constant throughout propagation until the concentration of monomer decreases causing the rate of propagation to decrease.

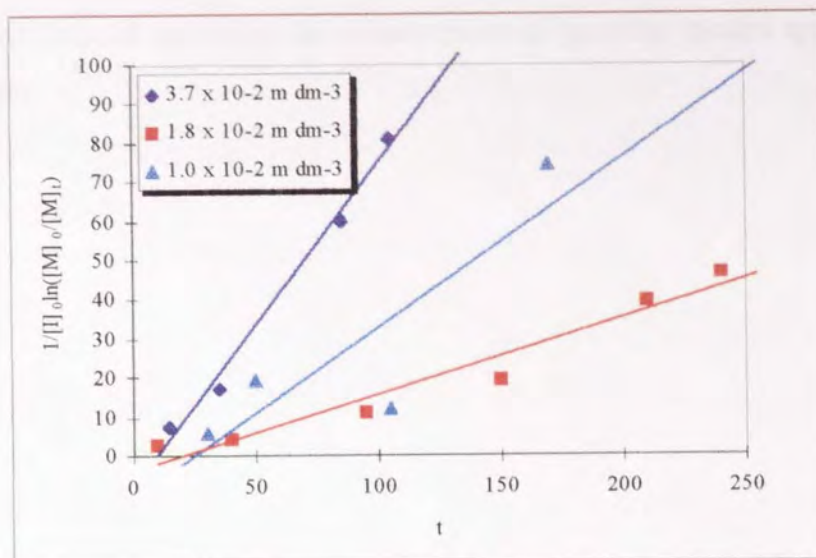


Figure 5.16. Effect of initiator concentration on plot of $1/[I]_0 \ln([M]_0/[M]_t)$ against time using DCM as a solvent.

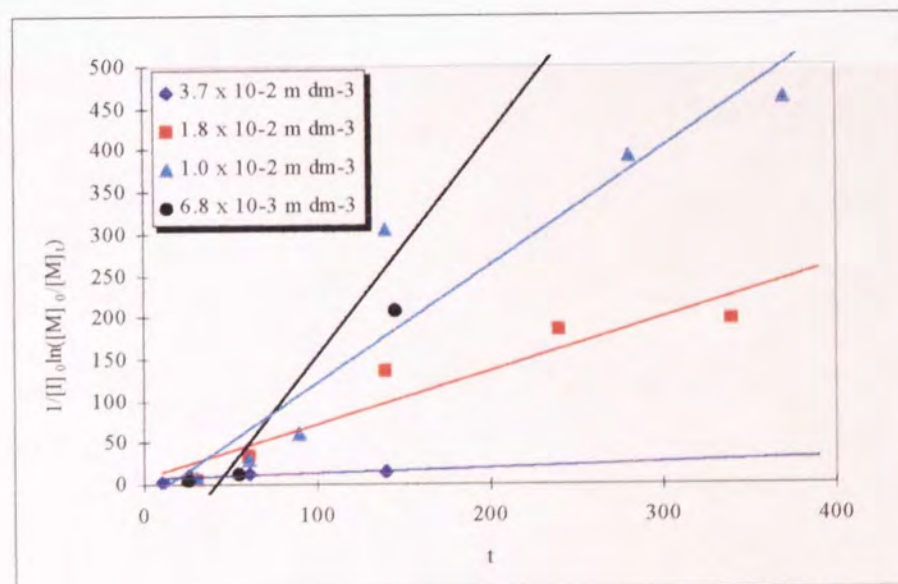


Figure 5.17. Effect of initiator concentration on plot of $1/[I]_0 \ln([M]_0/[M]_t)$ against time using THF as a solvent.

The plot of $1/[I]_0 \ln([M]_0/[M]_t)$ against time when THF was used as the reaction solvent (figure 5.17.) appears to have a build up period at the start of the reaction. It can probably be said that the concentration of growing species does not

remain constant throughout the reaction but in fact increases until after the build up period. After this build up period the concentration of growing species appears to remain constant.

5.1.6. The effect of reaction solvent on plots of $\ln(DP_{n\infty} - DP_n)$ versus time.

Plots of $\ln(DP_{n\infty} - DP_n)$ vs time have been constructed for the polymerisation of δ -valerolactone using tetrahydrofuran as a solvent. (Figure 5.18. below).

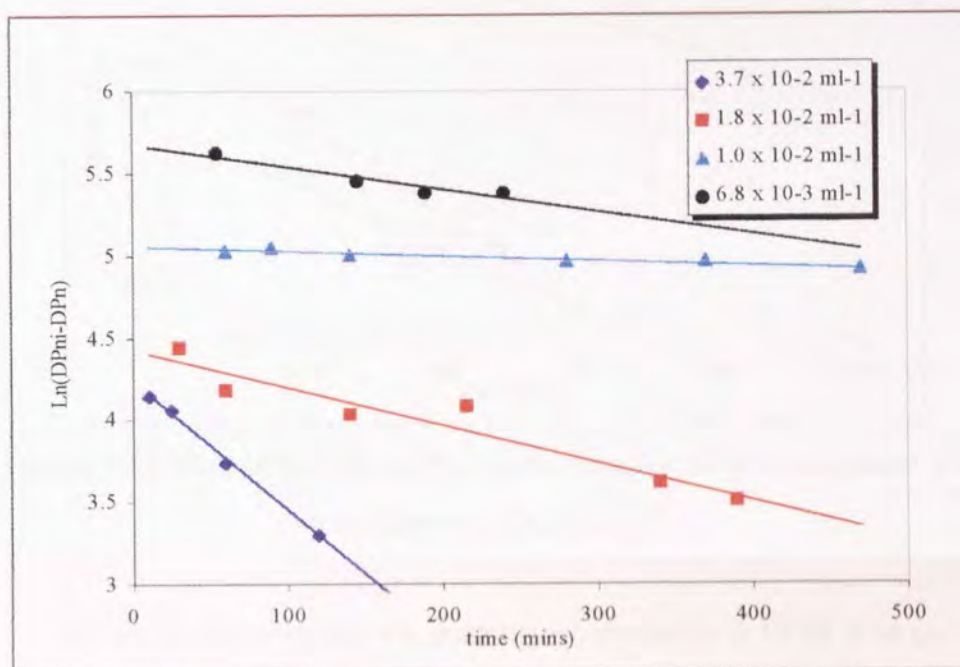


Figure 5.18. The effect of initiator concentration on plot of $\ln(DP_{n\infty} - DP_n)$ vs time for the polymerisation of δ -valerolactone in THF at 25°C .

It can be seen that as the concentration of initiator used decreases that the apparent rate of polymerisation also decreases. The linearity of the plots indicates a living system, there are no termination present in the polymerisation mechanism. However the reaction carried out at $[I] = 1.0 \times 10^{-2} \text{ ml}^{-1}$ has a gradient which is less than might be expected. Assuming that the gradient of the graph is equal to the apparent rate constant k_p , then it may be assumed that this reaction is slower than would perhaps be expected, not fitting the general trend shown in figure 5.18. It is most probable therefore that termination, either by impurities introduced by inadequate drying of materials or the glassware or by a leak of air and moisture into the reaction system has destroyed some of the initiator. Indeed it is known that trace amounts of water can act as a catalyst for the polymerisation of caprolactone with

alkyl aluminium initiators. This is a likely explanation for both a decreased rate of polymerisation and a lower than expected molecular weight of the final polymer.

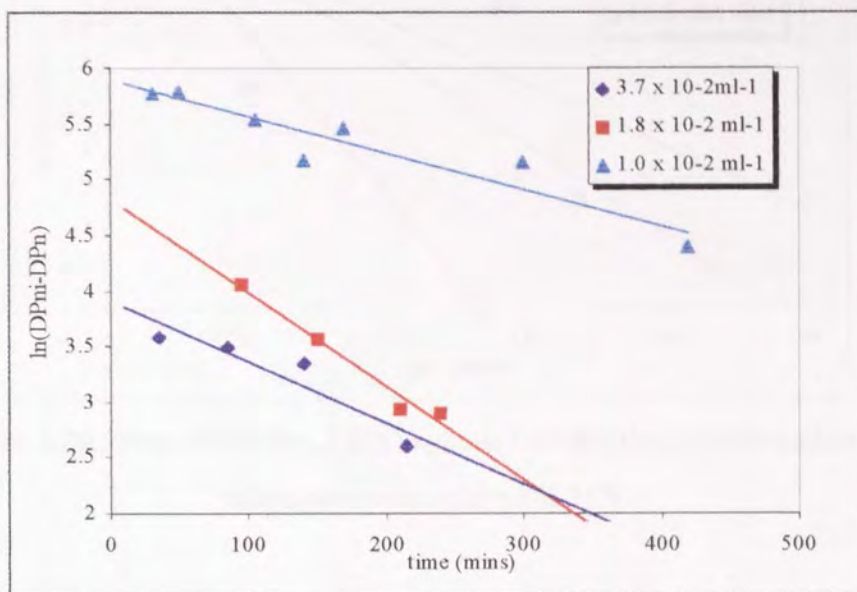


Figure 5.19. Plot of $\ln(DP_{n\infty} - DP_n)$ against time for the polymerisation of δ -valerolactone in DCM at 25°C .

The effect of decreasing the initiator concentration in DCM is in general to decrease the rate of polymerisation. The values of $(DP_{n\infty})$ at the y -intercept are not the same as the $[M]_0/[I]_0$ values. The value of $(DP_{n\infty})$ used is the one which gives the closest agreement with the y -intercept value. The linear plots indicate a living polymerisation free of termination reactions.

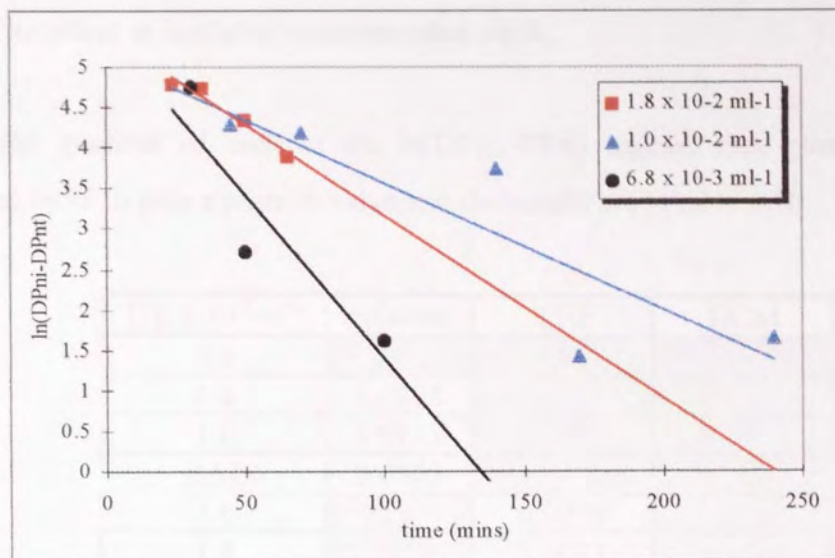


Figure 5.20. Plot of $\ln(DP_{n\infty} - DP_{nt})$ against time for the polymerisation of δ -valerolactone in toluene at 25°C .

In toluene the plots of $\ln(DP_{n\infty} - DP_{nt})$ versus time are linear again indicating a lack of termination reactions. The rate increases as initiator concentration increases.

5.1.7. The effect of initiator concentration on k_p .

The gradient of each of the $\ln(DP_{n\infty}-DP_n)$ against time plots has been multiplied by -1 to give a positive value and the results are in table 5.10.

| $[I]_0 \times 10^{-2} \text{ml}^{-1}$ | toluene | THF | DCM |
|---------------------------------------|---------|--------|--------|
| 3.6 | | | |
| 1.8 | 0.0225 | | |
| 1.0 | 0.0157 | | |
| 0.67 | 0.0405 | | |
| 3.6 | | 0.0078 | |
| 1.8 | | 0.0023 | |
| 1.0 | | 0.0003 | |
| 0.67 | | 0.0013 | |
| 3.6 | | | 0.0084 |
| 1.8 | | | 0.0055 |
| 1.0 | | | 0.0032 |
| 0.67 | | | |

Table 5.4. Apparent rate constant of polymerisation of δ -valerolactone in solvents of differing polarity.

The values of k_p in table 5.4. are equal to the apparent rate constant of propagation and these have been plotted in figure 5.21.

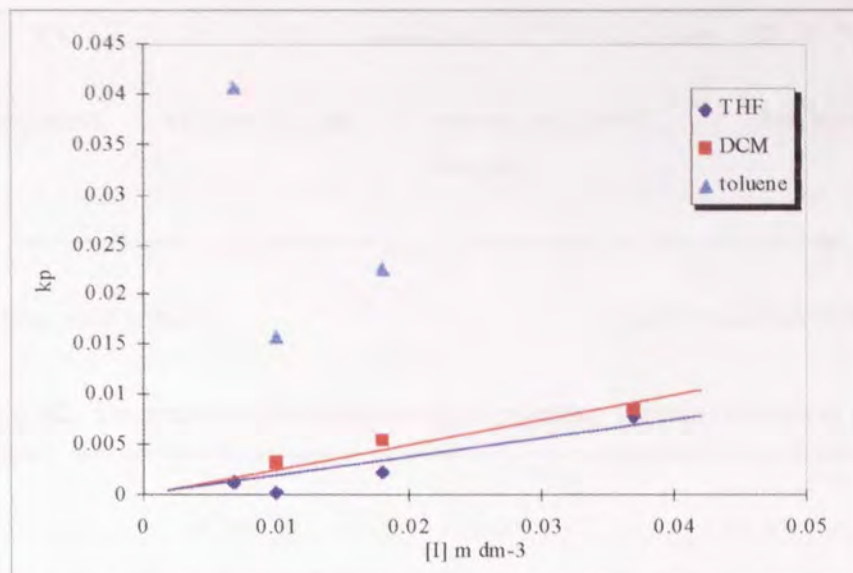
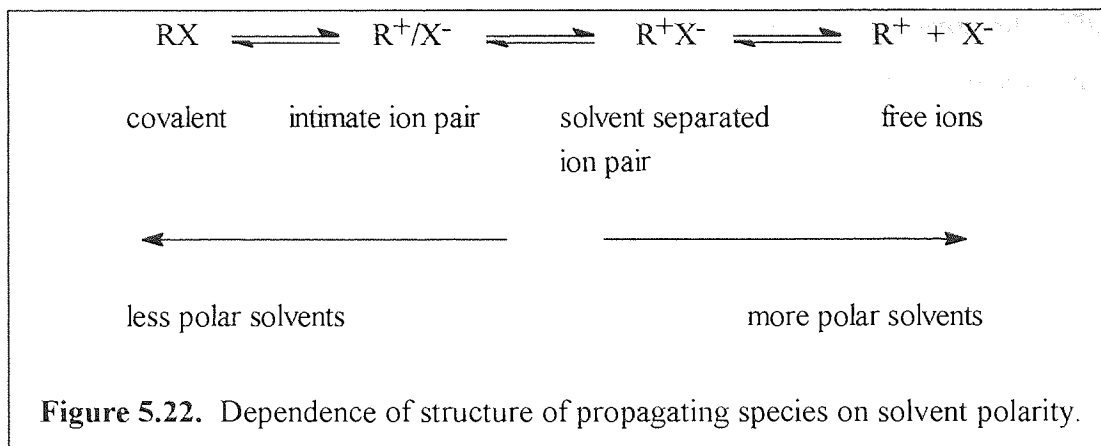


Figure 5.21. Graph of apparent rate of propagation versus initiator concentration for the polymerisation of δ -valerolactone in DCM, THF and toluene.

The rate of polymerisation appears to be fastest in toluene of the three solvents used. Whilst the first point in toluene at $[I]_0 = 3.7 \times 10^{-2} \text{ mol dm}^{-3}$ appears to be faster than would perhaps be expected, in general the polymerisation proceeds at a greater rate in toluene than in DCM or THF. Solvent polarity is usually expressed in terms of dielectric constant ϵ which measure the ability of a solvent to act as an insulator of electric charges. In general solvents of low dielectric constant such as toluene are non-polar, and vice versa. Toluene has a dielectric constant $\epsilon = 2.4$ at 25°C compared to THF ($\epsilon = 7.6$) and DCM ($\epsilon = 8.9$).

It has been suggested that when considering purely ionic polymerisation reactions the position of the gegen ion can be altered by varying the dielectric constant of the solvent used.

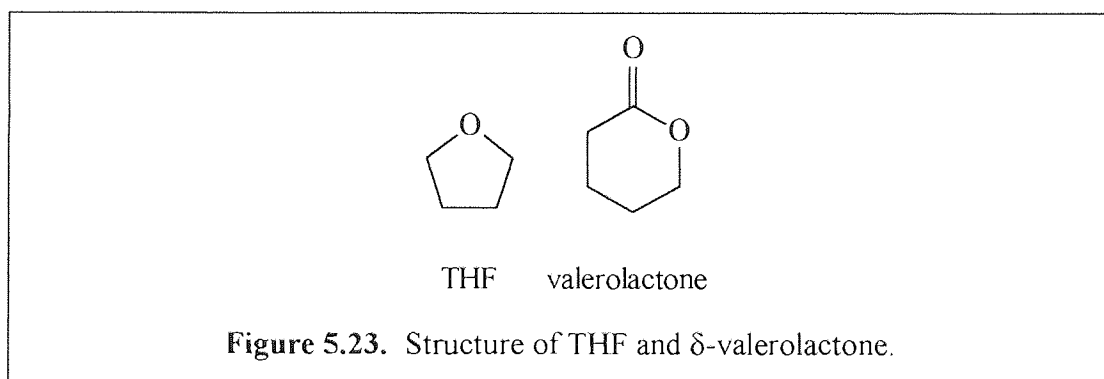


The increasing polarity of the solvent changes the distance between the ions from ion pairs to free ions. Since free ions propagate faster than ion pairs an increase in k_p is associated with the increased free ion concentration as solvent polarity increases. Both the active aluminium centre and the lactone monomer have a dipolar structure and the solvent dielectric constant (ϵ) should have an effect on the rate constant k_p . The dependence of the rate of propagation on the solvent used in co-ordination polymerisations is known to be reverse to those involving ionic species. Co-ordination polymerisations proceed faster in less polar solvents such as toluene than in more polar solvents. This behaviour may be related to the specific solvation of the growing species by dipolar solvents such as THF and indeed ethers do form stable complexes with organoaluminium compounds⁽¹⁰⁶⁾. The co-ordination sphere of the complex then needs to be re-arranged in order to accommodate the monomer. Thus extra energy has to be found to weaken the complex which has been formed between the solvent and the initiator in order to allow the monomer to complex with the alkoxide species.

The polymerisation of δ -valerolactone using *diisobutyl* aluminium *isopropoxide* has been found to be faster in toluene than in THF and DCM, which are both more polar than toluene. This is consistent with the co-ordination - insertion mechanism which has been proposed for the ring opening polymerisation of ϵ -caprolactone using aluminium alkoxides. A less polar solvent which favours the formation of species to the left of figure 5.22. increases the rate of co-ordination

- insertion polymerisations because closely associated species are favoured. The monomer is thus held closer to the active alkoxide bond, effectively increasing the monomer concentration around this active bond. As solvent polarity increases, favouring the more separated species to the right of figure 5.22., the monomer is co-ordinated to the aluminium alkoxide but is held further away from the active site than in less polar solvents. Therefore the effective monomer concentration around the aluminium alkoxide bond is lower, slowing the rate of propagation.

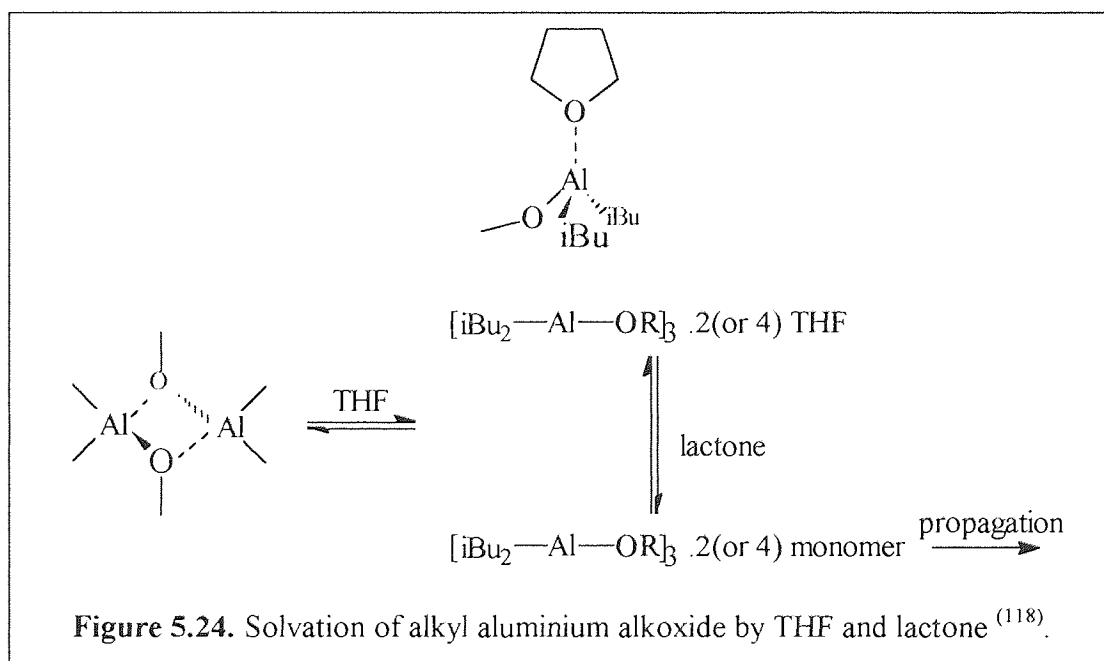
The rate of polymerisation in dichloromethane has been found to be faster than when the less polar solvent tetrahydrofuran is used. Should the mechanism be an ionic one, then the polymerisation would be expected to proceed faster in more polar solvents. However this is not the case and the phenomenon can be explained when the structure of THF is compared to that of δ -valerolactone.



The oxygen atom present in the solvent THF molecules has a lone pair of electrons, as has the monomer, δ -valerolactone. Both of these are able to compete to occupy the vacant sp^3 orbital of the aluminium atom. An equilibrium exists between the solvent co-ordinated and monomer co-ordinated species. Teyssie and colleagues ⁽¹¹³⁾ observed that the rate of polymerisation of ϵ -caprolactone was slower in THF than in toluene using aluminium *triisopropoxide* as an initiator. The incorporation of THF into a co-polymer may slow the reaction further.

In pure toluene the ^{27}Al NMR of diethyl aluminium bromoethoxide shows only one absorption corresponding to a tetrahedrally co-ordinated aluminium atom.⁽¹¹⁸⁾ This is consistent with the structure of the initiator aggregate being the trimer reported for ethyl substituents on aluminium alkoxides. Dimeric species may also be present but ^{27}Al NMR is unable to differentiate between the two species. When a lactone is added, a new peak is observed corresponding to an octahedral aluminium which is attributed to the solvation of the aluminium by two lactone molecules or the dissociation of the trimer into single alkoxide species. Since the alkoxide is known to be kept aggregated during the polymerisation so the first hypothesis is true.

The same experiment carried out in THF observed a two new additional ^{27}Al NMR peaks which can be attributed to alkyl aluminium alkoxide trimers solvated by one THF per aluminium, or two THF molecules per alkyl aluminium alkoxide trimer. Again when a lactone is added, another peak is observed due to solvation of the initiator by the lactone. These peaks indicate competition between the solvent and monomer for the solvation of the aluminium atoms.



So it is likely that the polymerisation of δ -valerolactone in THF is slower than in the more polar solvent DCM because of co-ordination of the solvent with the monomer

According to theory then the initiator is aggregated as a dimer before it dissociates into a monomer to propagate. Plots of $\ln k_p$ versus $\ln[I]_0$ have been plotted for each solvent used (figure 5.25.)

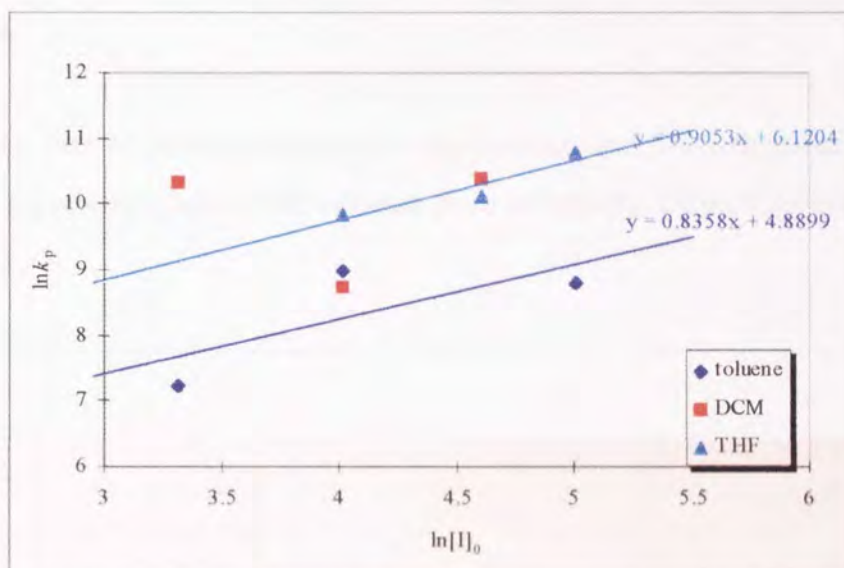


Figure 5.25. Effect of solvent on plot of $-\ln k_p$ versus $-\ln[I]_0$ for the polymerisation of δ -valerolactone using diisobutyl aluminium isopropoxide in toluene, THF and DCM at 25°C.

| Solvent | Gradient | MDA |
|---------|----------|-----|
| THF | 0.91 | 1.1 |
| Toluene | 0.84 | 1.2 |

Table 5.5. Mean degree of association in THF and DCM.

The reciprocal of the gradient of the plots is equal to the degree of aggregation of the initiator molecules (section 1.3.4.). The mean degree of association of the diisobutyl aluminium isopropoxide molecules in both solvents is approximately 1.1-1.2. It is most likely therefore that in the presence of δ -valerolactone in DCM or THF, that diisobutyl aluminium isopropoxide exists as a

monomeric unit. This does not differ greatly from the mean degree of association of the diisobutyl aluminium isopropoxide initiator when the monomer used was ϵ -caprolactone. Thus the initiator does not appear to aggregated in a different manner, regardless of the monomer used, whether it is ϵ -caprolactone or δ -valerolactone.

5.1.8. Comparison of rate of polymerisation of ϵ -caprolactone and δ -valerolactone using diisobutyl aluminium isopropoxide in solvents of different polarities.

The rate of polymerisation of ϵ -caprolactone and δ -valerolactone obtained from the negative gradient of the relevant plots of $\ln(DP_{n\infty}-DP_n)$ have been plotted in figure 5.26.

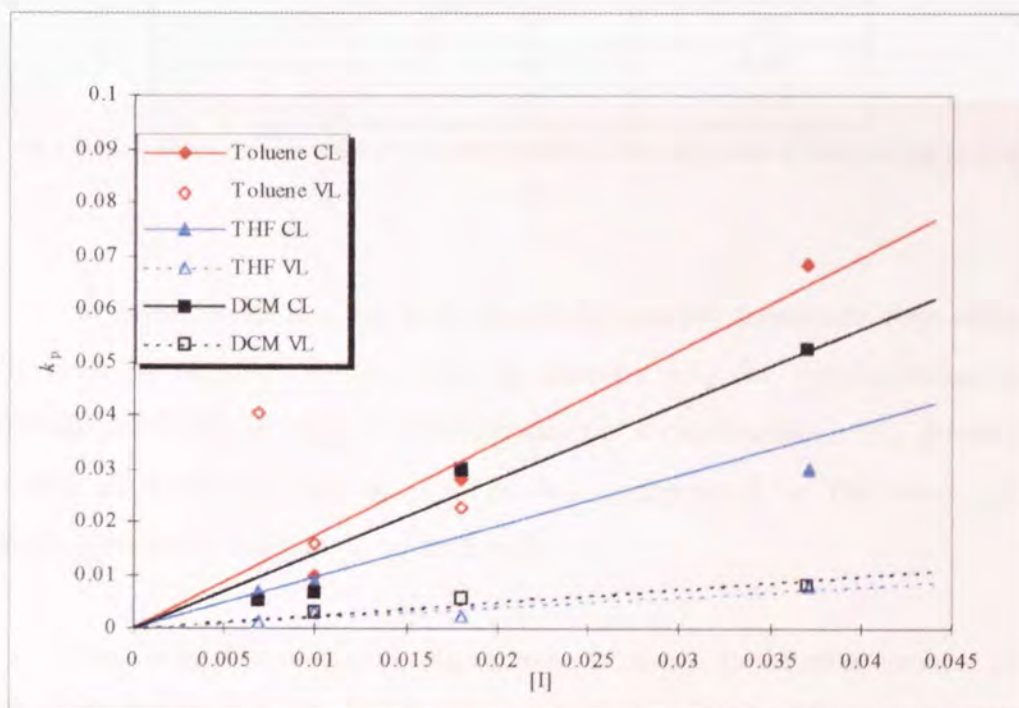


Figure 5.26. Graph of apparent rate constant of propagation for the polymerisation of ϵ -caprolactone and δ -valerolactone in toluene, DCM and THF.

It is apparent from figure 5.26. that the rate of propagation of ϵ -caprolactone using diisobutyl aluminium isopropoxide is faster than the rate of propagation of δ -

valerolactone using the same catalyst and solvent. ϵ -Caprolactone is a seven membered heterocyclic ring whilst δ -valerolactone is a six membered ring.

As discussed in section 1.2.2.2. the thermodynamic polymerisability of cyclic monomers may be estimated by the change in free energy during the ring opening process. In order for a ring opening reaction to proceed, the reaction must be thermodynamically favourable, $\Delta G_p < 0$. Assuming that the polymer has the same functional group as the monomer, i.e. that the reaction is a ring opening polymerisation, then the free energy of polymerisation ΔG_p is affected by the size and nature of the ring being polymerised independent of polymerisation mechanism. Values of ΔG_p for the ring opening polymerisation of lactones have been published⁽⁴⁶⁾ and are displayed in table 5.6.

| | Ring Size | ΔG_p (kJ mol ⁻¹) |
|--------------------------|-----------|--------------------------------------|
| γ -butyrolactone | 5 | + 12.6 |
| δ - valerolactone | 6 | - 8.0 |
| ϵ -caprolactone | 7 | - 12.8 |

Table 5.6. Values of free energy of ring opening for lactones of increasing ring size.

(46)

In order for the reaction to be thermodynamically favourable, then values of ΔG_p must be negative, it then becomes apparent why the polymerisation of δ -valerolactone is slower than the polymerisation of ϵ -caprolactone. ΔG_p for the ring opening of δ -valerolactone is -8.0 kJ mol^{-1} , compared to the value for ϵ -caprolactone which is equal to $-12.8 \text{ kJ mol}^{-1}$.

The Gibbs free energy of ring opening is related to the strain present in the ring, may be linked to the deviation from equilibrium bond angles that exist within the ring. The deviations from equilibrium bond angles are detailed in table 5.7.

| | Ring Size | Bond angle (°) | | |
|--------------------------|-----------|----------------|--------------|--------------|
| | | C-O-(C=O) | O-(C=)-C | C-C-C |
| δ -valerolactone | 6 | 121.0 | 114.9 | 113.9 |
| ϵ -caprolactone | 7 | 125.5 | 117.6 | 114.4 |
| Equilibrium value | | 109.5 | 110.0 | 110.5 |

Table 5.7. Comparison of bond angles of lactones.⁽⁴⁶⁾

The deviations from equilibrium bond angles present in δ -valerolactone are less than those present in ϵ -caprolactone. It may be assumed therefore that the ring strain present in δ -valerolactone is less than that in ϵ -caprolactone. Thus the Gibbs free energy of ring opening of δ -valerolactone is less than that of ϵ -caprolactone.

The ring opening polymerisation of δ -valerolactone is therefore thermodynamically less favourable than the ring opening polymerisation of ϵ -caprolactone at the same temperature and using the same initiator. This is because the six membered lactone is less strained than the seven membered lactone and hence has a less negative value of ΔG_p .

Chapter 6.

The synthesis of block co-polymers using aluminium alkoxide macroinitiators.

ABA type triblock co-polymers have been synthesised using diisobutyl aluminium PHBV-alkoxide macroinitiators and ϵ -caprolactone. Molecular weights have been predictable from initiator/monomer ratios and have been confirmed by GPC and NMR analysis.

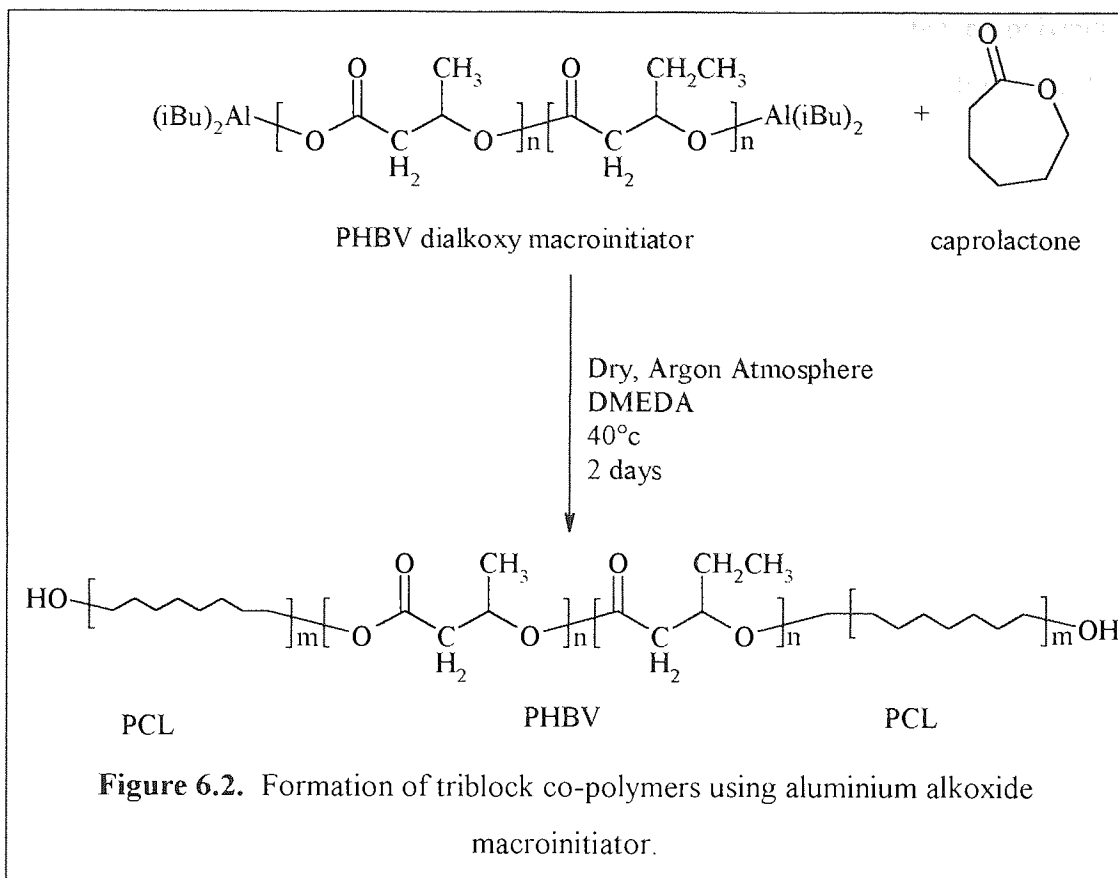
6.1. Synthesis of triblock co-polymers.

The macroinitiator was formed by the reaction of triisobutyl aluminium with α,ω -dihydroxy terminated PHBV.



Figure 6.1. Formation of macroinitiator.

This was subsequently reacted with the monomer, ϵ -caprolactone in the presence of an amine, DMEDA which prevents the formation of initiator aggregates to form a co-polymer (figure 6.2.)



The PHBV pre-polymer was dried under vacuum at 40°C for 72 hours before use. It was transferred to a dried vessel and then placed under vacuum overnight to remove any remaining moisture. The vacuum oven was released to atmospheric pressure using a dry inert gas supply and the reaction vessel sealed immediately. The PHBV was then dissolved in freshly distilled DCM.

An appropriate volume of DCM was distilled into a separate vessel and *triisobutyl* aluminium and DMEDA were added using Schlenk techniques. This was then transferred to the vessel containing the PHBV solution and stirred under an argon blanket at atmospheric pressure for three hours to form the PHBV-alkoxide macroinitiator. The monomer was added to the initiator solution using a dry syringe and an argon blanket. The vessel was sealed and placed in an oven at 40°C for 48 hours.

Once the reaction had been completed, it was found that the co-polymer solution was soluble in both methanol and hexane at room temperature. Cold methanol, which had been cooled to -30°C was found to be sufficient for the isolation of the product which was removed by vacuum filtration using a cold grade 3 sintered glass funnel.

The dried product was found to take the form of pale yellow crystals, which were insoluble in THF, DCM or chloroform. The product was stirred for 3 hours in an excess of acetyl acetone to remove any residual aluminium compounds present. This acetyl acetone solution was dissolved in dichloromethane and further precipitated in cold methanol. When filtered and dried this produced a purified polymer as a white powder, which was soluble in both dichloromethane and chloroform.

The molecular weights of the polymers were analysed using GPC and the results are in table 6.1.

The number average molecular weight of the PHBV pre-polymer was found to be 1500 by GPC. The hydroxy valerate content of the PHBV co-polymer was found to be 8%.

| Ratio OH:PHBV:CL | M_n theoretical | M_n GPC | M_w GPC | M_w/M_n |
|------------------|----------------------|--------------|--------------|-----------|
| 2:16:16 | 3300 | 3600 | 4600 | 1.3 |
| 2:16:24 | 4200 | 4700 | 6400 | 1.4 |
| 2:16:32 | 5600 | 8900 | 11000 | 1.2 |
| 2:16:48 | 7000 | 9500 | 12500 | 1.3 |
| 2:16:96 | 12500 | 14000 | 21800 | 1.5 |

Table 6.1. Results of the formation of PCL-PHBV-PCL block co-polymers using alkyl aluminium PHBV-alkoxide macroinitiator.

The molecular weights of the polymers obtained by GPC are in close agreement with the theoretical molecular weights. They are slightly higher than the

molecular weights calculated from monomer/initiator ratios (figure 6.3.) but are within the limits of experimental error. Any difference may be because of incomplete initiation of the poly(ϵ -caprolactone) segment, either due to termination or destruction of the living end by impurities such as water, carbon dioxide or oxygen, or because of incomplete alkoxide formation. It may also be because the GPC used was calibrated with poly(styrene) standards and PCL-PHBV-PCL co-polymers may not have the same hydrodynamic volume as the standards.

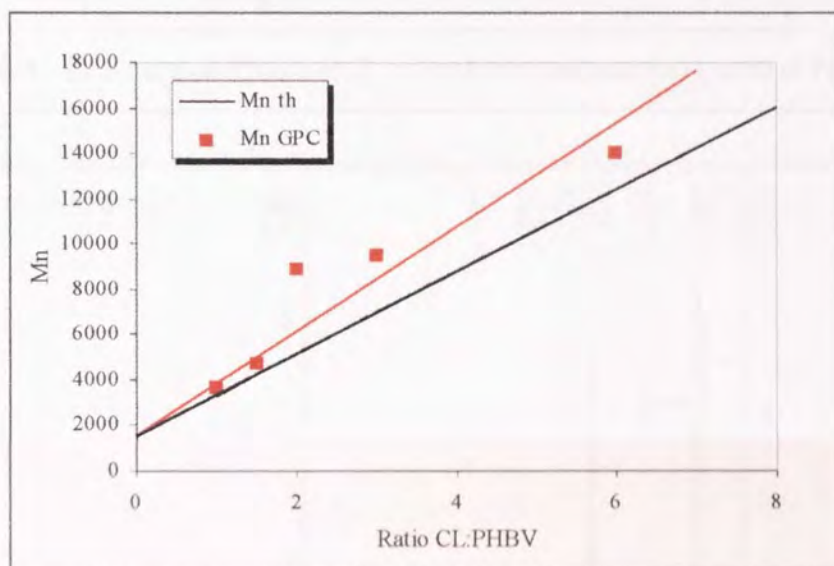


Figure 6.3. Effect of volume of ϵ -caprolactone added on molecular weight of co-polymers.

6.2. NMR analysis of co-polymers.

^{13}C and ^1H NMR has been used to study the structure and molecular weight of the co-polymers produced.

6.2.1. ^1H NMR of co-polymers.

A ^1H NMR of PCL-PHBV-PCL co-polymers is shown below (figure 6.5).

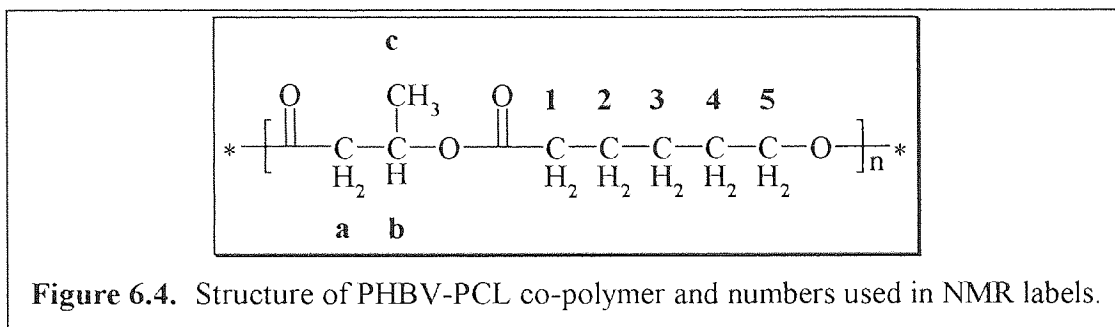


Figure 6.4. Structure of PHBV-PCL co-polymer and numbers used in NMR labels.

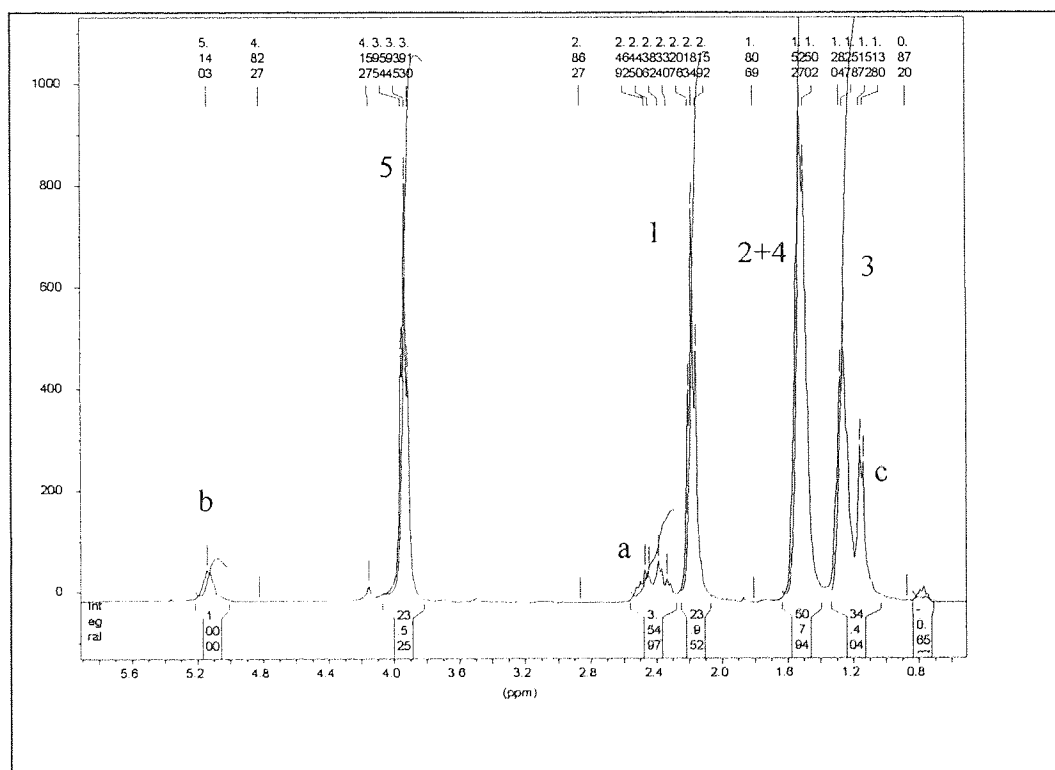


Figure 6.5. ^1H NMR spectrum of PCL-PHBV-PCL co-polymer. (GK50)

| Chemical shift (δ) ppm | Description | Proton |
|---------------------------------|-------------|--------|
| 5.1 | doublet | b |
| 3.9 | triplet | 5 |
| 2.4 | multiplet | a |
| 2.2 | triplet | 1 |
| 1.5 | triplet | 2+4 |
| 1.2 | doublet | 3 |
| 0.8 | doublet | c |

Table 6.2. Resonances in ^1H NMR spectrum of PCL-PHBV-PCL co-polymer.

The poly(ϵ -caprolactone) segment of the co-polymer shows four main proton resonances. At approximately 3.9 ppm the protons labelled '5' (figure 6.4.) resonates and a triplet results.

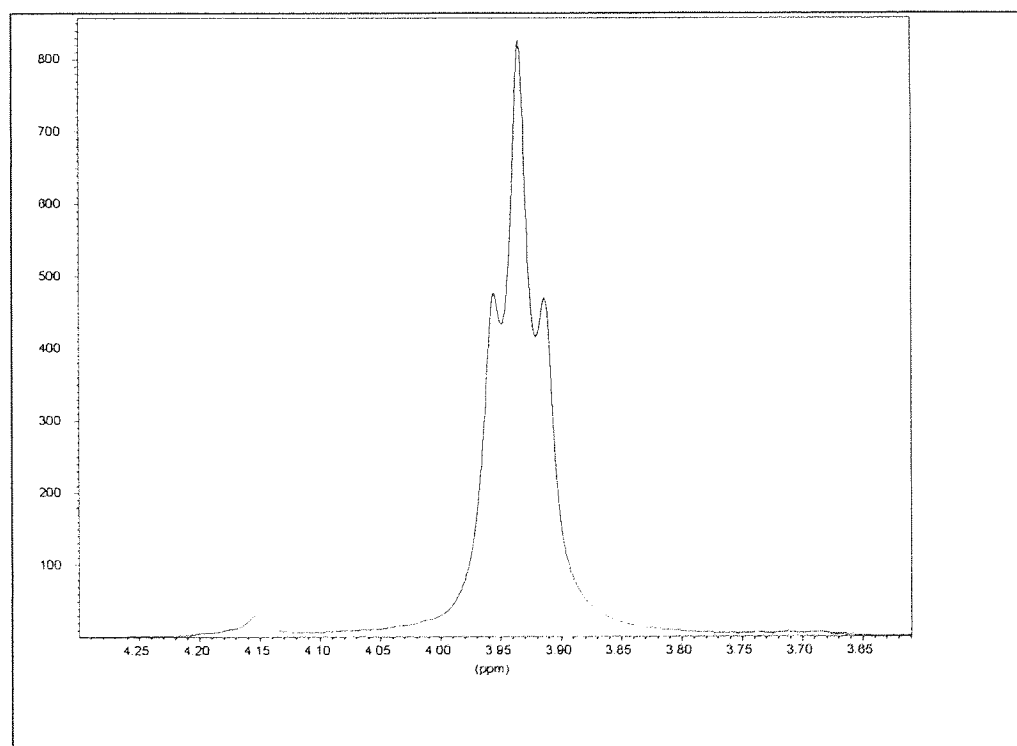


Figure 6.6. Expansion of methylene protons adjacent to acyl oxygen in poly(ϵ -caprolactone) segment.

The ^1H NMR spectrum also shows another triplet further upfield at 2.2 ppm and this is due to the resonance caused by the protons adjacent to the carbonyl carbon ('1' figure 6.4.). Slightly further upfield, three peaks show in between 1.1 and 1.6 ppm. The peaks at 1.3 and 1.5 ppm are due to the central methylene protons in poly(ϵ -caprolactone). The outer protons ('2+4' figure 6.4.) resonate at about 1.5 ppm. There is a slight shoulder to this peak (figure 6.7.) which is most probably caused by the slightly different environments of the two methylene groups. The relative intensity is twice that of the other methylene protons showing that there are definitely twice the number of resonating groups compared to the other resonances at 1.6 and 3.95 ppm. Proton '3' resonates at 1.2 ppm and is a triplet.

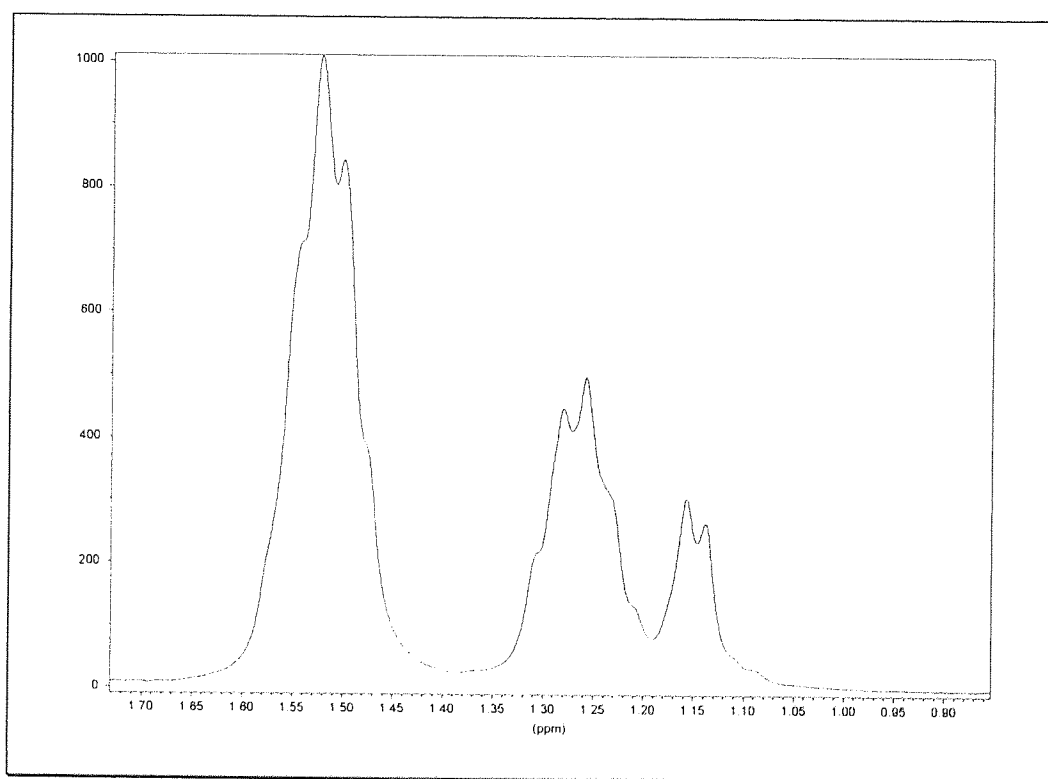


Figure 6.7. Expansion of 0.9 ppm - 1.70 ppm area of ^1H NMR of PCL-PHBV-PCL co-polymer.

The PHBV segment shows three separate resonances at 5.1 ppm, 2.4 ppm, and 1.1 ppm. The protons labelled 'b' (figure 6.4.) resonate as a doublet at 5.1 ppm. The shoulders on either side of the peak (figure 6.8.) may be due to the resonance

caused by the same protons where they join onto the PCL segments, the slightly different environment causing a change in the chemical shift at which they resonate.

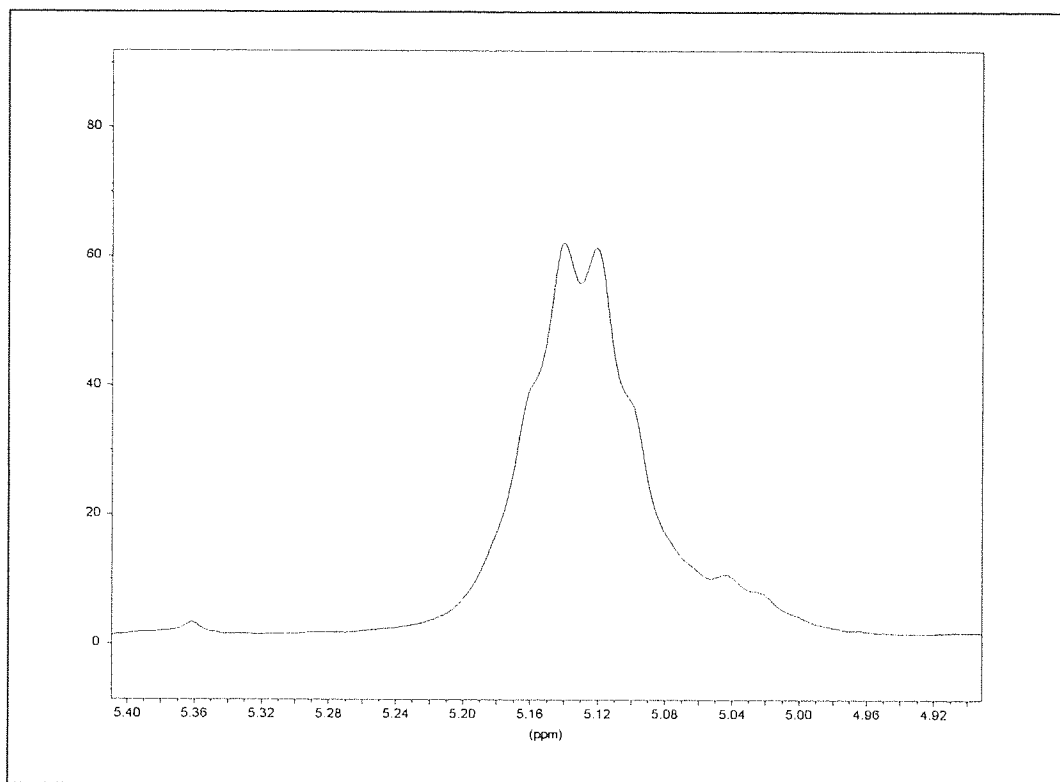


Figure 6.8. ^1H NMR of PHBV-PCL co-polymer, proton on tertiary carbon resonance ('b' figure 6.4.)

The pendant methyl groups in the PHB show as a doublet at 1.1 ppm (figure 6.7). The ethyl group which is present in PHV show as a small multiplet at about 0.8 ppm (figure 6.5.)

6.2.2. Calculation of molecular weights using ^1H NMR.

The molecular weight of the polymers has been calculated from the areas of the methylene protons in the PHBV and PCL units (labelled 'a' and '1', figure 6.4.) The spectrum of the co-polymer with a target molecular weight of 12500 is figure 6.10. and the relative intensities of the methylene resonances at 2.4 ppm and 4.16 ppm are 3.5 and 23.5 respectively.

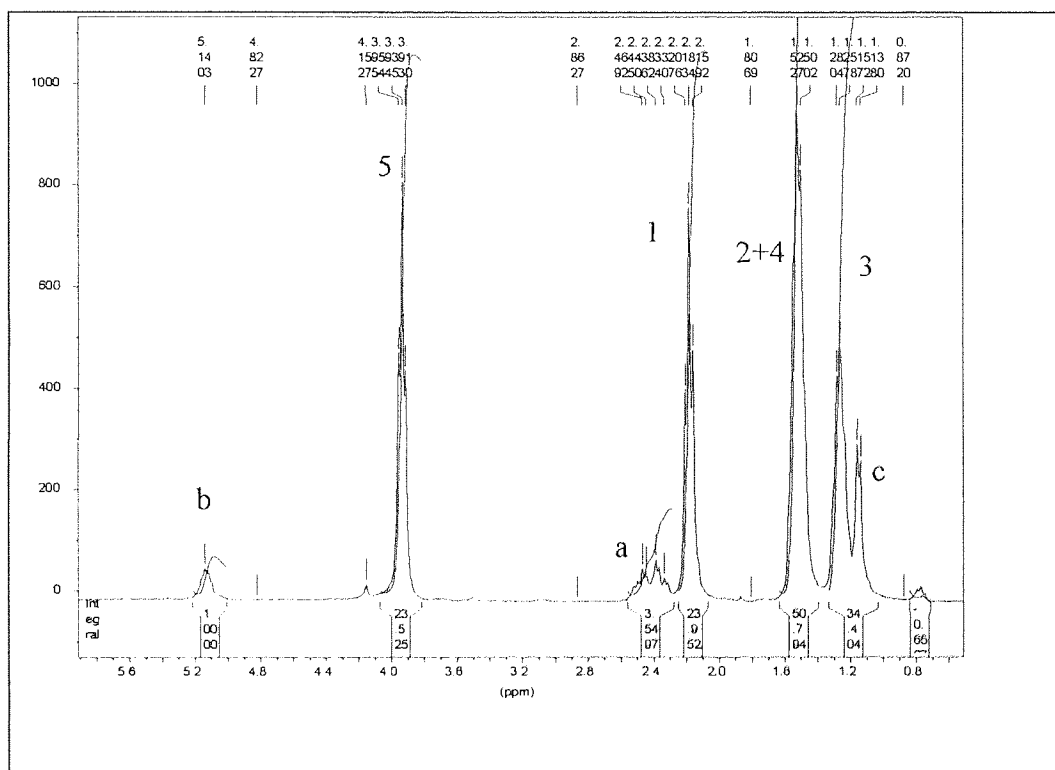


Figure 6.9. ^1H NMR spectrum of PCL-PHBV-PCL co-polymer. (GK50)

| Sample | PHBV methylene proton resonance at 2.4 ppm | PCL methylene proton resonance at 4.16 ppm | M_n theoretical | MW NMR | M_n GPC |
|--------|--------------------------------------------|--------------------------------------------|-------------------|--------|-----------|
| GK46 | | 6.8 | 3300 | 3100 | 3600 |
| GK47 | 8.8 | 14.0 | 4200 | 3900 | 4700 |
| GK48 | 8.5 | 15.9 | 5600 | 4300 | 8900 |
| GK49 | 21.0 | 59.8 | 7000 | 5800 | 9500 |
| GK50 | 3.5 | 23.5 | 12400 | 11600 | 14000 |

Table 6.3. Molecular weights by GPC and NMR of PHBV-PCL co-polymers.

Molecular weights calculated by NMR are in close agreement with both theoretical and GPC calculated values. Errors of differences appear to be only as great as about 5% when the NMR values are compared to the theoretical values obtained from the monomer/initiator ratios.

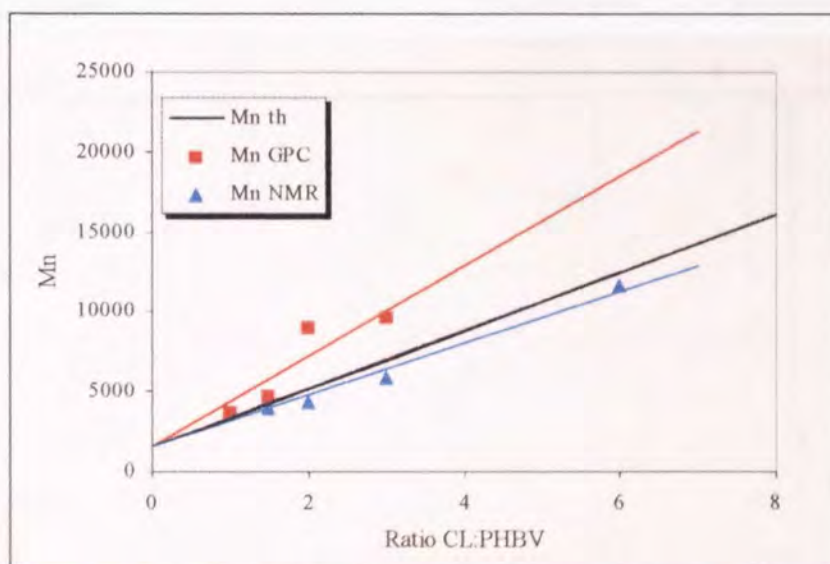


Figure 6.10. Plot of molecular weight of co-polymer against caprolactone added.

^1H NMR would seem to be a more accurate method of molecular weight analysis for co-polymers such as these. Molecular weights calculated using ^1H NMR have values almost identical to those that were expected from initial monomer/initiator ratios (figure 6.10). GPC has given M_n values in excess of what was expected. That is not to say however that GPC is an inaccurate technique for

the calculation of these co-polymer molecular weights, but that it appears to be less suitable than ^1H NMR.

6.2.3. ^{13}C NMR spectra.

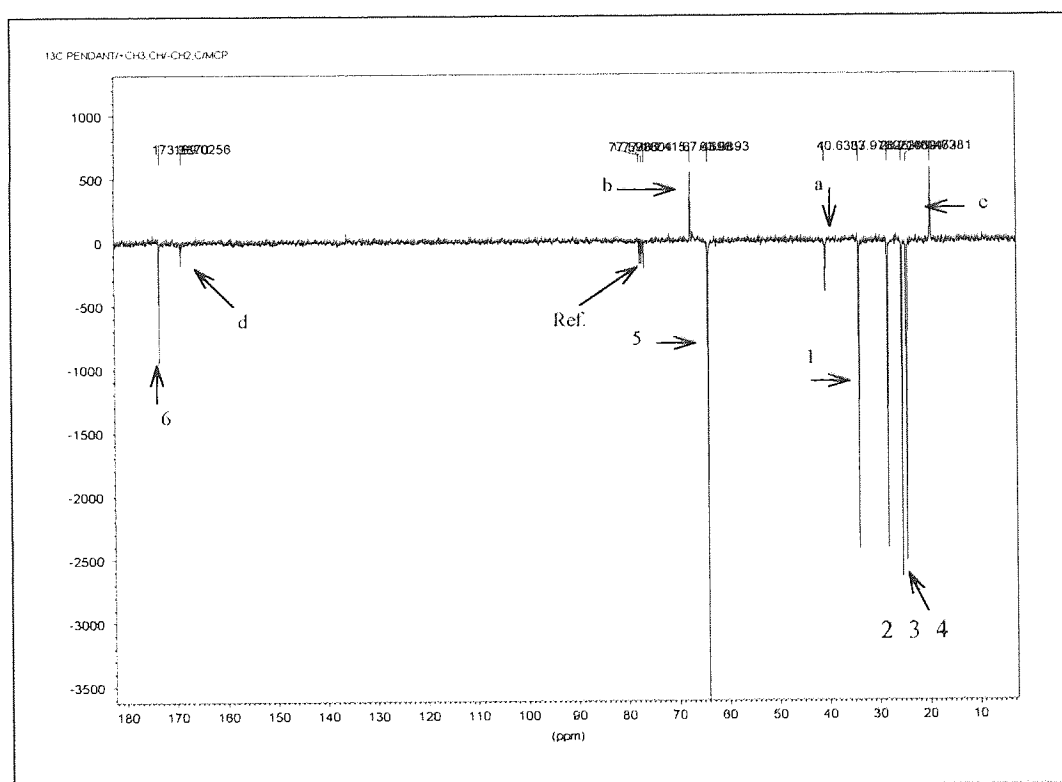
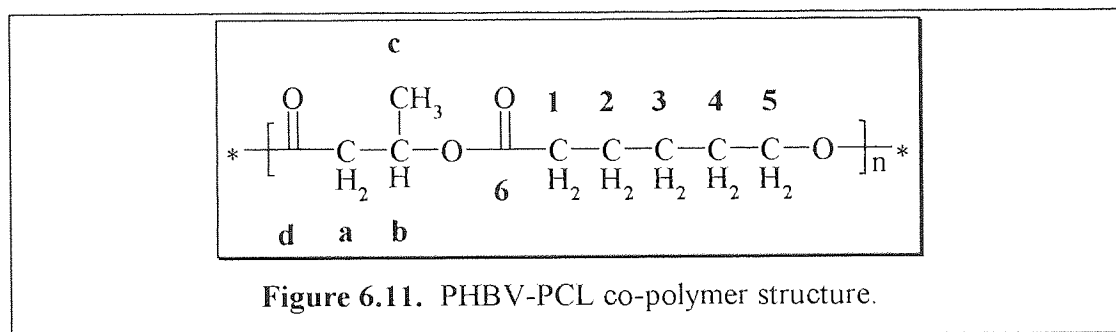


Figure 6.12. ^{13}C NMR spectra of PCL-PHBV-PCL co-polymer. (GK50)

^{13}C NMR spectra of the co-polymers produced show two different carbonyl resonances in the 168-174 ppm area. Whilst ^{13}C NMR is not a quantitative technique, it is possible to observe the change in composition of the co-polymers as

the two carbonyl peaks change intensity as the caprolactone of the co-polymer content increases. (Figure 6.13)

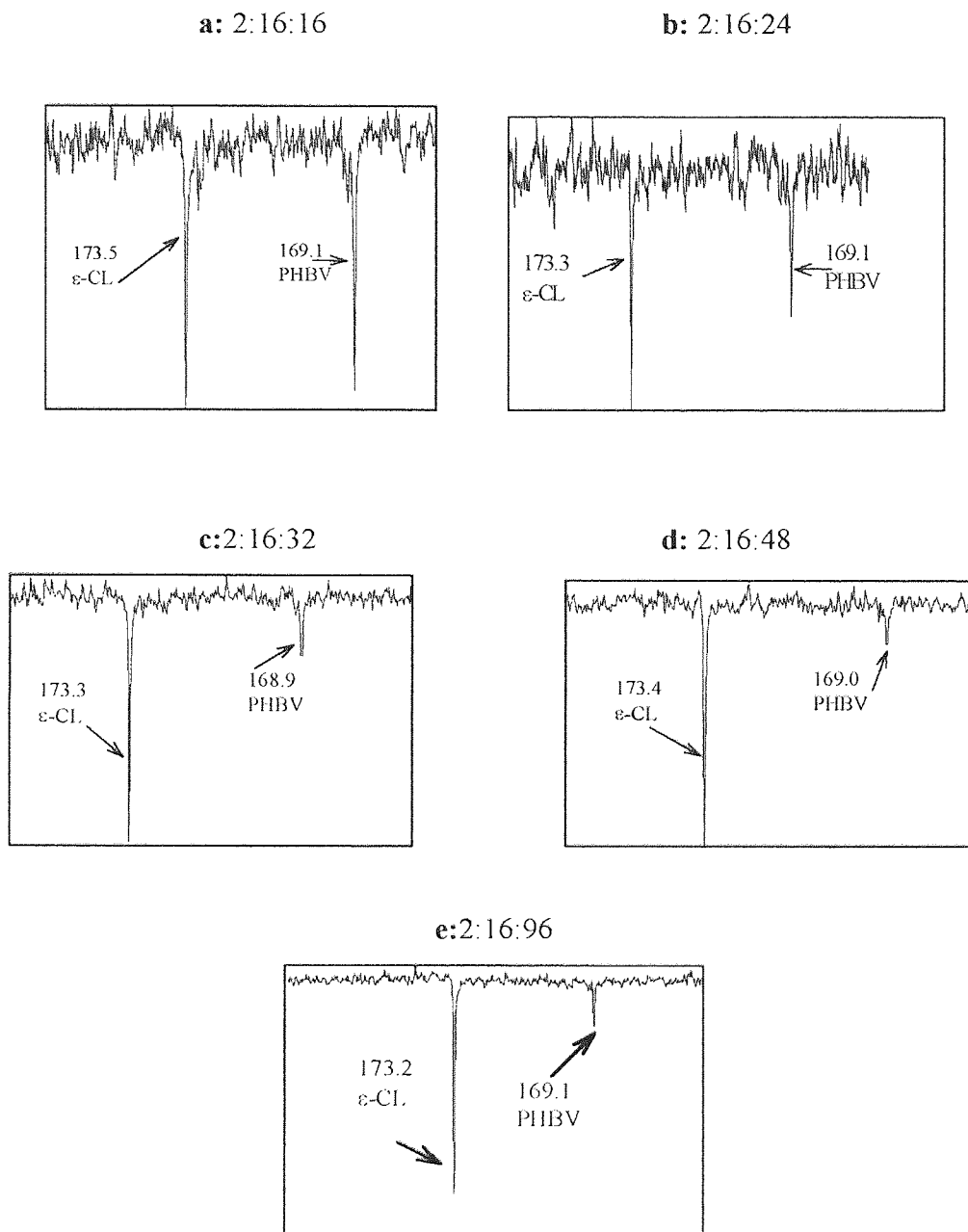


Figure 6.13 (a-e). Close up of carbonyl peaks in ^{13}C NMR spectra of PHBV-PCL block co-polymers.

6.3. Effect on molecular weight of aluminium alkyl added.

The ratio of aluminium alkyl to hydroxy groups present was varied. The reaction was carried out in exactly the same way as section 6.1. but the volume of aluminium added was altered according to the ratio in table 6.4.

| | | | |
|----|-------|--------------|----------------------|
| OH | DMEDA | caprolactone | Al(iBu) ₃ |
| 1 | 2 | 4 | x |

Table 6.4. Ratio of reactants in co-polymerisation.

The polymers formed were isolated in the same way as described in section 6.1. and molecular weight was calculated by GPC. The results of the polymerisations are in table 6.4.

| x | M_n | M_w | M_w/M_n |
|---|-------|-------|-----------|
| 1 | 2300 | 3400 | 1.4 |
| 4 | 2200 | 2900 | 1.3 |
| 8 | 1800 | 2500 | 1.4 |

Table 6.5. Molecular weight with varying aluminium alkyl concentration.

The theoretical molecular weight was 2400. The polymer produced when the ratio of aluminium alkyl to hydroxy groups was 1:1, i.e. there was no excess of aluminium produced a polymer with molecular weight in good agreement with the theoretical molecular weight. When the aluminium alkyl was in a 4 times excess, the molecular weight of the co-polymer is still in good agreement with the theoretical molecular weight. When an 8 times excess of aluminium alkyl has been used, the molecular weight of the co-polymer is approximately 600 less than that of what would be expected.

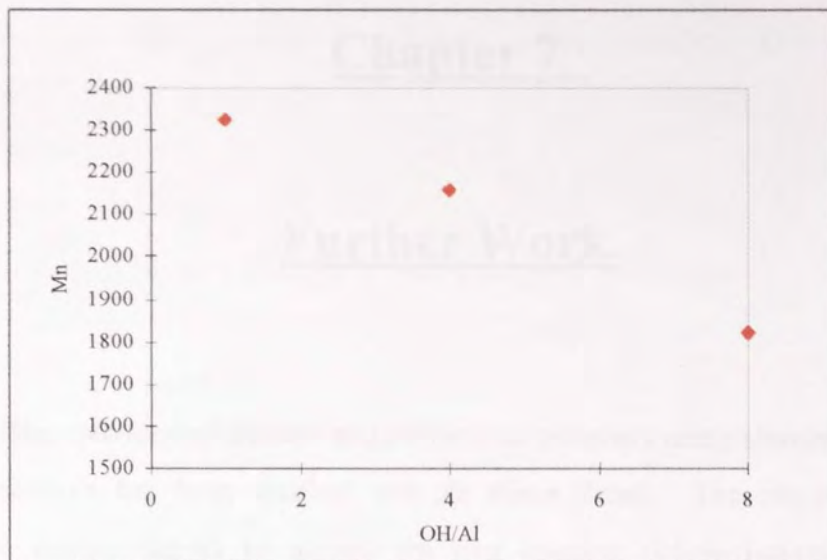


Figure 6.14. Plot of molecular weight of PHBV-PCL co-polymer against volume of aluminium alkyl.

The molecular weight of the polymers produced appears to be largely independent of the volume of *triisobutyl* aluminium added to the reaction. However, there is a small decrease in the molecular weight of the polymers. It may be that the excess aluminium alkyl is co-ordinating with the excess DMEDA and monomer present in the reaction solution and polymerising the monomer to form poly(ϵ -caprolactone) oligomers.

Chapter 7.

Further Work.

The synthesis of diblock and triblock co-polymers using aluminium alkoxide macroinitiators has been touched only in minor detail. The use of aluminium alkoxide macroinitiators to initiate the ring opening polymerisation of both ϵ -caprolactone and δ -valerolactone has been studied. Co-polymers of PHBV and P ϵ -CL and P δ -VL with predictable properties have been formed. The use of aluminium alkoxides to initiate the ring opening polymerisation of lactides has also been reported by Jerome and Teyssie^(68, 92, 106, 110-124, 135-137). It is probable therefore that the technique of using PHBV/aluminium alkoxide macroinitiators could be extended to the ring opening polymerisation of lactides. There should be no reason why other parent polymers with an ω -hydroxy function such as poly(ϵ -caprolactone) could not be reacted with trialkyl aluminium. Using a poly(ϵ -caprolactone) aluminium alkoxide to initiate the ring opening polymerisation of lactides would form poly(lactic acid)-*b*- poly(ϵ -caprolactone) block co-polymers could be useful as compatibilisers in poly(ϵ -caprolactone)/ poly(lactic acid) blends.

Tranesterification reactions appear to occur after the reaction has reached quantitative conversion. It is known⁽¹³⁷⁾ that amines prevent initiator aggregates from forming by occupying co-ordination sites on the initiator aluminium centres and increasing the rate of polymerisation. It has also been found in this thesis that using THF or DMF as solvents slows the rate of propagation by competing with the monomer for the vacant co-ordination site on the aluminium centre. Beila and Duda⁽¹⁰⁶⁾ reported the same result when using acetonitrile as a solvent. Tranesterification primarily occurs after all or most of the monomer has been consumed because the polymer ester groups are less reactive than the lactone ester

groups. It is possible therefore that adding a compound containing a co-ordinating centre such as a nitrogen may prevent transesterification from occurring.

Adding a second polyester to a polymerisation vessel after polymerisation of ϵ -caprolactone has been completed may have interesting results. Intermolecular transesterification occurs between the active aluminium alkoxide chain end and ester groups in other polymers. If a second polyester is subsequently added and, providing that the reaction conditions are maintained, then attack by the active chain end on the secondary polymer should occur. A new route to the formation of co-polymers would then be possible.

THF has been found to be incorporated into δ -valerolactone polymers. A further investigation into the ring opening of THF solvent using ^{18}O labelled solvent would prove conclusively whether this is actually the case. DSC analysis of poly(δ -valerolactone) produced in THF and toluene solvents should show a difference between the homo polymer poly(δ -valerolactone) and poly(δ -valerolactone)-co-poly(tetrahydrofuran).

Functional aluminium alkoxides have been thoroughly investigated both here and by Jerome, Teyssie and Penzcek ^(111-116, 132-134). Bromine terminated polymers have been used to form block co-polymers with styrene and methacrylates. Using bromine functional aluminium alkoxides as initiators for the polymerisation of ϵ -caprolactone and then the subsequent polymerisation of olefinic monomers in the same vessel would provide an interesting route to co-polymers.

It has been proved in this thesis that the rate of polymerisation of lactones is affected by the nature of the alkoxide substituent. Assuming that bulkier alkoxide groups hinder propagation, then it may be possible that some alkoxide groups such as *t*-butyl alkoxide will hinder propagation to such an extent that polymer formation is negligible in the timescale of a polymerisation carried out with say, aluminium *n*-butoxide. Another monomer may not be hindered by this alkoxide and will

propagate. Selective polymerisation of two monomers at the same time may be possible. Certainly the formation of two polymers, a homo polymer A, and a random co-polymer AB, should be possible with careful selection of the alkoxide groups using a difunctional alkoxide aluminium alkyl initiator.

Chapter 8.

Conclusions.

The polymerisation of lactones using alkyl aluminium alkoxide initiators is affected by the polarity and donor power of the solvent used in the polymerisation (chapter 3). It was found that using more polar solvents such as DCM and THF resulted in a slower rate of polymerisation compared to toluene. Solvents of higher polarity are known to decrease the rate of polymerisation when the mechanism is a coordination-insertion type. It was found however that the rate of polymerisation when THF was used as a solvent was slower than in DCM, which has a higher dielectric constant. The oxygen atom in the THF ring has a lone pair and this occupies the vacant sp^3 orbital on the aluminium atom. The monomer therefore has to displace the solvent from the co-ordination sphere of the aluminium alkoxide before propagation can occur. The same effect was observed when DMF was used as the solvent. The polymerisation was very slow with low conversions being achieved even after a reaction time of 72 hours.

Transesterification reactions were also found to occur when polymerising ϵ -caprolactone after approximately >95% conversion had been reached. The monomeric ester groups are presumably more reactive than the polymeric ester groups. The backbiting reaction predominates over propagation once the monomer concentration has decreased to such an extent that the backbiting reaction is kinetically favoured. The effect of transesterification is exaggerated with temperature.

Jerome and Teyssie reported that alkyl aluminium alkoxides form aggregates in solution⁽¹¹³⁾. It was found in this study that *diisobutyl* aluminium *isopropoxide* does not form aggregates in THF, DCM or toluene. It was also found that a di alkoxide as an initiator produces polymers with a molecular weight approximately half that of the corresponding reaction with a mono alkoxide initiator.

The structure of both the alkyl group and the alkoxide moiety were found to have an effect on the kinetics of the polymerisation of ϵ -caprolactone (chapter 4). An induction or a build up period was present at the beginning of each polymerisation. The length of this build up period was related to the structure of the alkoxide moiety. When bulkier alkoxide groups such as cyclohexoxide and phenoxide were used as initiators then the build up period was longer than when smaller alkoxide groups such as *n*-butoxide were used. The rate of propagation, the slope of the plot of $[\{1/t\}\ln([M]_0/[M]_t)]$ against time after the induction period was independent of the alkoxide structure. This proves that the mechanism of propagation is one where the alkoxide group is at the dead end of the polymer moving away from the active centre as propagation continues. The bulkier alkoxide groups cause steric hindrance around the active site, which hinders the complexation of the monomer with the initiator. As well as steric effects the electronic effects in the alkoxide moiety also had an effect on the reaction kinetics. The electron donating *para*-methoxy substituent increased the rate of polymerisation of ϵ -caprolactone compared to the unsubstituted phenoxide was part of initiator. The electron donating effect of the *para*-methoxy group increases the electron density around the active alkoxide bond. This makes the complexation of the monomer and initiator easier and increases the rate of initiation.

When the alkyl group *isobutyl* was part of the initiator the build up period was also longer than when the less bulky ethyl group was used. This is again because steric hindrance around the active site prevents complexation of the monomer and initiator. However the rate of propagation was slower when *diisobutyl* aluminium *n*-butoxide was used as the initiator compared to diethyl aluminium *n*-

butoxide. The alkyl group therefore appears to have an effect on the reaction rate throughout the polymerisation. It is likely that the alkyl groups remain close to the active site unlike the alkoxide moieties throughout the reaction and the steric hindrance provided by bulkier alkyl groups may also affect propagation as well as initiation.

The size of the lactone ring was also found to be important in the reaction kinetics (chapter 5). The kinetics of the six membered ring δ -valerolactone were compared with the seven membered ring ϵ -caprolactone. It was found that δ -valerolactone, which has less ring strain and a less negative Gibbs free energy of ring opening has a slower rate of polymerisation than ϵ -caprolactone.

A method of synthesising co-polymers with accurately predictable properties was developed (chapter 6). Di hydroxy terminated poly(hydroxybutyrate-co-hydroxyvalerate) was reacted in DCM with triisobutyl aluminium in the presence of a bulky diamine to form a polymer with an aluminium alkoxide group at each end. This was then used as an initiator for the polymerisation of ϵ -caprolactone. The co-polymers formed were precipitated in cold methanol and dried under vacuum. The molecular weights of the triblock polymers were found by both GPC and ^1H NMR to be close to the theoretical molecular weights calculated from initial monomer/initiator ratios. The formation of a co-polymer was confirmed by ^{13}C NMR, which showed resonances from carbonyl carbons in both the PHBV and the PCL segments.

- 1 Kawai F.
Mechanisms of Bacterial degradation of Polyethers and Their Copolymers
Biodegradable Polymers and Plastics. Ed. Vert M., Feijen J., Albertsson A.,
Scott G. and Chiellini E. Royal Society of Chemistry 1992
- 2 Intveld P.J.A., Shen Z.R., Takens G.A.J., Feijen F.
Glycolic acid based Copolymers
Journal of Polymer Science: Part A: Polymer Chemistry 1994 **32** 1063
- 3 Uhrich K.E., Gupta A., Thomas T.T., Laurencin C.T., Langer R
Synthesis and Characterisation of Degradable Poly(anhydride-co-imides).
Macromolecules 1995 **28** 2184-2193
- 4 Okada M., Okada Y., Ao K.
*Synthesis and Degradabilities of Polyesters from 1,4/3,6 Dianhydrohexitols
and Aliphatic Dicarboxylic acids.*
Journal of Polymer Science: Part A: Polymer Chemistry 1995 **33** 2813-2820
- 5 Yasin M., Amass A.J., Tighe B.J.
*'Environmentally Friendly' Fate of Plastic Waste' Polymers and Other
Advanced Materials: Emerging Technologies and Business Opportunities.* Ed.
P.N. Prasad *et al.*
Plenum Press, New York 1995
- 6 Hrabak O.
PHB-Part of a New Waste Management System Biodegradable Polymers and
Plastics. Ed. Vert M., Feijen J., Albertsson A., Scott G. and Chiellini E.
Royal Society of Chemistry 1992
- 7 Chandra R., Rustgi R.
Biodegradable Polymers.
Prog. Polym. Sci. **23** 1273-1335 1998
- 8 McNeill I.C.
Fundamental Aspects of Polymer Degradation Polymers in Conservation Ed.
Allen N.S., Edge M., Hori C.U.
Royal Society of Chemistry 1992
- 9 Nakamura T., Hitomi S., Shimamoto T., Hyon S., Watanbe S., Shimizu Y.
Biomaterials and Clinical Applications Elsevier Science, Amsterdam 1987
- 10 Bostman O.M.
Absorbable implants for the fixation of fractures
J. Bone Joint Surgery **73A** 1 148-153 1991
- 11 Encyclopaedia of pharmaceutical technology, Ed James Swarbrick James C.
Boylan Vol.2, Biodegradable polyester polymers as drug carriers to clinical
pharmacokinetics and pharmacodynamics New York, Dekker, 1990

- 12 Schindler A., Jeffcoat R., Kimmel G.L., Pitt C.G., Wall M.E., Zweidinger R.,
Biodegradable Polymers for Sustained Drug Delivery.
Contemporary Topics in Polymer Science. Vol. 2. Plenum Press 1977
- 13 Encyclopaedia of pharmaceutical technology, Ed James Swarbrick James C.
Boylan Vol.2, Biodegradable polyester polymers as drug carriers to clinical
pharmacokinetics and pharmacodynamics New York, Dekker
- 14 Holland S.J.
Paper given at Biocompatibility seminar, 09/11/93. Notes given as part of final
year lectures at Aston University 1995/6.
- 15 Lt Yan C.X., and Chen X.
Biomaterials **45** 303-310 1993
- 16 McMurray J.
Organic Chemistry 3rd Ed.
Brooks/Cole Publishing California 1992
- 17 Lewis D.H.
Controlled release of bioactive agents from Lactide/Glycolide polymers
Biomaterials **9** 1987
- 18 Birmingham Polymers Inc.
Biodegradation Web page.
[Http://www.bpi-sbs.com](http://www.bpi-sbs.com)
- 19 Cha Y., Pitt C.G.
*The Acceleration of Degradation Controlled Drug Delivery From Polyester
Microspheres.*
Journal of Controlled Release. **8**, (3) 259-265 1989
- 20 Kreiser-Saunders I., Kricheldorf H.R.
Polylactones 39a. *Zn lactate catalysed co-polymerisation of L-lactide with
glycolide or ε-caprolactone.*
Macromolecular Chemistry and Physics. **199** 1081-1087 1998
- 21 Schindler A., Jeffcoat R. Kimmel G.L., Pitt C.G., Wall M.E., Zweidinger R.
Biodegradable Polymers for Sustained Drug Delivery.
Contemporary Topics in Polymer Science, Vol 2. Plenum Press 1977
- 22 McGrath J.E. *Synthetic Importance and Industrial Applications of Ring
Opening Polymerisation*
Makromol. Chem. Macromol. Symp. **42/43** 69-91 1991
- 23 John J., Tang J., Bhattacharya M.
*Processing of biodegradable blends of wheat gluten and modified
polycaprolactone.*
Polymer **39** 2883-2895 1998

- 24 Pouton C.W. Akhtar S.,
Biosynthetic Polyhydroxyalkanoates and their potential in drug delivery.
Adv. Drug Del. Rev. **18** 133-162 1996
- 25 Pouton C.W. Akhtar S.
Biodegradable Polymers in Drug Delivery
Drug News Perspect. 2. 89-93 1989
- 26 Gatenholm P., Kubat I, Mathiasson A.,
Biodegradable Natural Composites 1. Processing and Properties.
J App. Polym. Sci. **45**. 1667-1677 1992
- 27 Holland S.J., Jolly A.M, Yasin M., Tighe B.J.
Polymers for Biodegradable medical devices (II). Hydroxybutyrate - hydroxyvalerate copolymers: Hydrolytic studies
Biomaterials **8** 289-295 1987
- 28 Howells E.R.
Single Cell Protein and Related Technology
Chem. Ind 508-511 1982
- 29 Barham P.J., Organ S.J.,
Mechanical Properties of Polyhydroxybutyrate-hydroxybutyrate-hydroxyvalerate copolymer blends
J. Mat. Sci. **29**. 1676-1679 1994.
- 30 Jaimes. C., Collet A., Giani-Beaune O., Schue F., Amass W., Amass A.
Ring Opening Polymerisation of Lactones Part 1. Homo- and Copolymerisations of Racemic β -butyrolactone and δ -valerolactone by Tetraisobutylaluminumoxane (TIBAO) Catalyst.
Polymer International **45** 5-13 1998
- 31 Cox M.K.
The Effect of Material Parameters on the Properties and Biodegradation of 'BIOPOL' Biodegradable Polymers and Plastics Copolymers Biodegradable Polymers and Plastics. Ed. Vert M., Feijen J., Albertsson A., Scott G. and Chiellini E.
Royal Society of Chemistry 1992
- 32 Yasin M., Amass A.J., Tighe B.J.
Biodegradable Polymer Blends. Polymers and other advanced materials: emerging technologies and business opportunities. Ed. Prasad P.N. et al. Plenum Press N.Y. 1995

- 33 Yasin M Tighe B.J.
Polymers for biodegradable medical devices. VIII. Hydroxybutyrate-hydroxyvalerate copolymers: physical and degradative properties of blends with polycaprolactone.
Biomaterials. **13**. 9-16 1992
- 34 Yasin M., Tighe B.J.
Strategies for the design of biodegradable polymer systems. Manipulation of polyhydroxybutyrate based materials.
Plastics, Rubber and Composites Processing and Applications. **19** 15-27 1993
- 35 Fukada K., *An overview of the activities of the Biodegradable Plastics Society.*
Ed M. Vert et al. Royal Society Chemistry 1992
- 36 Ali S.A.M., Zhong S.P., Doherty P.J., Williams D.F.
Mechanisms of Polymer Biodegradation in Implantable Devices. 1. Poly(caprolactone)
Biomaterials **9** 548-655 1993
- 37 McNeill I.C.
Fundamental Aspects of Polymer Degradation Polymers in Conservation
Ed. Allen N.S., Edge M., and Hori C.U.
Royal Society of Chemistry 1992
- 38 Cox M.K.,
The Effect of Material Parameters on the Properties and Biodegradation of 'BIOPOL' Biodegradable Polymers and Plastics Copolymers Biodegradable Polymers and Plastics. Ed. Vert M., Feijen J., Albertsson A., Scott G. and Chiellini E.
Royal Society of Chemistry 1992
- 39 Scott J
Biodegradable Polymers
[Http://www.denison.edu/chem/DCS/journal/scottv1n1.html](http://www.denison.edu/chem/DCS/journal/scottv1n1.html)
- 40 Carothers W.H.
Studies on polymerisation and ring formation.
I. An introduction to the general theory of condensatio polymerisation.
J. Am. Chem. Soc. **51** 2548-2560 1929
- 41 Cowie J.M.G.
Polymers: Chemistry and physics of modern materials. 2nd Edition.
Blackie academic and professional. London 1993
- 42 Hocker H., Keul H.
Ring opening polymerisation and ring closing depolymerisation.
Advanced Materials. **6** 21-36 1994

- 43 Chujo Y., Saegusa T.
Ring opening polymerisation.
Encyclopedia of Polymer Science and Technology. Vol 14 2nd Ed. Wiley New York 1988
- 44 Wolinski L.E., Mington
The effect of C-substitution of caprolactam on the ring opening polymerisation reaction.
J. Polym. Sci. **49** 217-223 1961
- 45 McMurray J.
Organic Chemistry
Brooks/Cole Publishing California 1992
- 46 Saiyasombat W., Molloy R., Nicholson T.M., Johnson A.F., Ward I.M., Posyachinda S.
Ring strain and polymerisability of cyclic esters
Polymer. **39** 5581-5585 1998
- 47 Lundberg R.D., Cox E.F.
Lactone Polymerisation in Ring Opening Polymerisation Ed. Frisch K.C., Reegan S.L.
Marcel Dekker London 1969
- 48 Van Natta F.J., Hill J.W. Carothers W.H.
Studies of Polymerisation and Ring Formation.
XIII. ϵ -caprolactone and its Polymers.
J. Am. Chem. Soc. **56** 455-457 1934
- 49 Szwarc M., Levy M., Milkovich R.
Polymerisation initiated by electron transfer to monomer. A new method of formation of block co-polymers/
J. Am. Chem. Soc. **78** 2656-2657 1956
- 50 Morton M., Wu M.
Organolithium polymerisation of ϵ -caprolactone
ACS symposium series. **286** 175 1985
- 51 Ito K., Yamashita Y.,
Propagation and depropagation rates in the anionic polymerisation of ϵ -caprolactone cyclic oligomers
Macromolecules **11** 68-72 1978
- 52 Ito K., Hashizuka Y., Yamashita Y.
Equilibrium cyclic oligomer formation in the anionic polymerisation of ϵ -caprolactone.
Macromolecules. **10** 821-824 1977

- 53 Hofman A., Slomkowski S., Penczek S.,
Polymerisation of ϵ -caprolactone with kinetic suppression of macrocycles
Macromol. Chem. Rapid Commun. **8** 387-391 1987
- 54 Matyjaszewski K., Zielinski M., Kubisa P., Slomkowski S., Chojnowski J.,
Penczek S.,
*Kinetically controlled formation of macrocyclic oligomers in the ring opening
polymerisation.*
Mackromol. Chem. **181** 1469-1482 1980
- 55 Slomkowski S.
*Ring opening polymerisation with kinetically controlled enhancement of
macrocyclic oligomers or linear molecules.*
Mackromol. Chem. **186** 2581-2594 1985
- 56 Bailey W.J., Wu S.R., Ni Z.
*Synthesis of Poly- ϵ -caprolactone via a Free Radical Mechanism. Free
Radical Ring Opening Polymerisation of 2-methylene-1,3-dioxepane*
J. Polym. Sci. Polym. Chem. Ed. **20** 3021-3030 1982
- 57 Jin S., Gonsalves K.E.
*Synthesis and Characterisation of Functionalised Poly(ϵ -caprolactone)
Copolymers by Free Radical Polymerisation.*
Macromolecules **31** 1010-1015 1998
- 58 Lundberg R.D., Cox E.F.
Lactone Polymerisation in Ring Opening Polymerisation Ed. Frisch K.C.,
Reegan S.L.
Marcel Dekker London 1969
- 59 Cherdrón H., Ohse H., Korte F.
*The polymerisation of lactones. Part One, Homo-polymerisation of 4, 6, 7
membered lactones with cationic initiators.*
Makromol. Chem. **56** 179-186 1962
- 60 Kricheldorf H.R., Jonte J.M., Dunsing R.
*Polylactones 7a. The mechanism of cationic polymerisation of β -
propiolactone and ϵ -caprolactone.*
Makromol. Chem. **187** 771-785 1986
- 61 Rangel I., Ricard M., Ricard A.,
*Polymerisation of L-lactide and ϵ -caprolactone in the presence of methyl
trifluoromethanesulfonate.*
Macromol. Chem. Phys. **195** 3095-3101 1994
- 62 Gresham T.L., Jansen J.E., Shaver F.W.
J. Am. Chem. Soc. **70** 998-999 1948

- 63 Hofman A., Szymanski R., Slomkowski S., Penczek S.
Structure of active species in the cationic polymerisation of β -propiolactone and ϵ -caprolactone
Makromol. Chem. **185** 655-667 1984
- 64 Pierre G., Limosin D., Djelali NE.
Electroinitiated cationic polymerisation of ϵ -caprolactone using sacrificial anodes.
Makromol. Chem. **192** 2767-2775 1991
- 65 Tsubokawa N. Yoshihara T.,
Grafting of polyesters onto carbon whisker surface.
Polymer Bulletin **30** 421-428 1993
- 66 Kricheldorf H.R., Sumbel M.V., Krieser Saunders I.
Polylactones 20. Polymerisation of ϵ -caprolactone with tributyl tin derivatives: A mechanistic study.
Macromolecules **24** 1944-1949 1991
- 67 Kricheldorf H.R., Soo-Ran Lee, Schanagl N.
Polylactones 28. Syndiotactic poly(β -D,L-hydroxybutyrate) by ring opening polymerisation of β -D,L-butyrolactone with butyltin metoxides
Macromolecules **27** 3139-3146 1994
- 68 Kricheldorf H.R., Berl M., Schanagl N.,
Poly(lactones) 9. Polymerisation mechanism of metal alkoxide initiated polymerisations of lactide and various lactones
Macromolecules **21** 286-293 1988
- 69 Kowalski A., Duda A., Penczek S.
Kinetics and mechanism of cyclic esters polymerisation initiated with tin(II) octoate, 1. Polymerisation of ϵ -caprolactone
Makromol Rapid Commun. **19** 567-572 1998
- 70 Ething B., Gogolewski S., Pennings A.J.,
Biodegradable materials of poly(L-lactic acid) 1. Melt spun and solution spun fibers
Polymer **23** 1587-1593 1982
- 71 Vasantharamari R., Pennings A.J.
Crystallisation kinetics of poly(L-lactic acid)
Polymer **24** 175-178 1983
- 72 Dubois Ph., Degee Ph., Jerome R., Teyssie Ph.,
Macromolecular engineering of polylactones and polylactides 8. Ring opening polymerisation of ϵ -caprolactone initiated by primary amines and trialkylaluminium.
Macromolecules **25** 2614-2618 1992

- 73 Barakat I., Dubois Ph., Jerome R., Teyssie Ph.
Living Polymerisation and selective end functionalisation of ϵ -caprolactone using zinc alkoxides as initiators
Macromolecules **24** 6542-6545 1991
- 74 Agostini D.E., Lando J.B., Shelton J.R.
Synthesis and characterisation of poly β -hydroxybutyrate.
I. Synthesis of crystalline DL- poly β -hydroxybutyrate from DL- β -butyrolactone.
J.Polym Sci Polym Chem Ed. **9** 2775-2787 1971
- 75 Shelton J.R Agostini D.E., Lando J.B.
Synthesis and characterisation of poly β -hydroxybutyrate.
I. Synthesis of D- poly β -hydroxybutyrate and the mechanism of ring opening polymerisation of β -butyrolactone
J.Polym Sci Polym Chem Ed. **9** 2789-2799 1971
- 76 Teranishi K., Iida M. Araki T., Yamashita S., Tani H.
Stereospecific polymerisation of β -alkyl- β -propiolactone
Macromolecules **7** 421-427 1974
- 77 Iida M. Araki T., Teranishi K., Tani H.
Effect of substituents on stereospecific polymerisation of β -alkyl and β -chloroalkyl- β -propiolactones
Macromolecules **10** 275-284 1977
- 78 Bloembergen S., Holden D.A, Bluhm T.L., Hamer G.K. Marchessault R.H.
Stereoregularity in synthetic β -hydroxybutyrate and β -hydroxyvalerate
Macromolecules **22** 1656-1663 1989
- 79 Yan Zhang, Gross R.A., Lenz R.W.
Stereochemistry of the ring opening polymerisation of (S)- β -butyrolactone
Macromolecules **23** 3206-3212 1991
- 80 Evans W.J., Katsumata H.
Polymerisation of ϵ -caprolactone by divalent samarium complexes.
Macromolecules **27** 2330-2332 1994
- 81 Evans W.J., Katsumata H.
Polymerisation of ethylene carbonate and ϵ -caprolactone using samarium complexes
Macromolecules **27** 4011-4013 1994
- 82 Stevels W.M., Ankone M.J.K., Dijkstra P.J., Feijen J.
Kinetics and mechanism of ϵ -caprolactone polymerisation using yttrium alkoxides as initiators
Macromolecules **29** 8296-8303 1996

- 83 Stevels W.M., Ankone M.J.K., Dijkstra P.J., Feijen J.
A versatile and highly efficient catalyst system for the preparation of polyesters based on lanthanide tris(2,6-ditertbutylphenolate)s and various alcohols.
Macromolecules **29** 3332-3333
- 84 Stevels W.M., Ankone M.J.K., Dijkstra P.J., Feijen J.
Kinetics and mechanism of L-lactide polymerisation using two different yttrium alkoxides as initiators.
Macromolecules **29** 6132-6138 1996
- 85 Li S.M., Espartero J.L., Foch P., Vert M.
Structural characterisation and hydrolytic degradation of a Zn metal initiated copolymer of L-lactide and ϵ -caprolactone
J. Biomater Sci. Polym Ed, **4** 165-187 1996
- 86 Tanahashi N., Doi Y.
Thermal properties and stereoregularity of poly(3-hydroxybutyrate) prepared from optically active β -butyrolactone with a zinc based catalyst
Macromolecules **24** 5732-5733
- 87 Yan Zhang, Gross R.A., Lenz R.W.
Stereochemistry of the ring opening polymerisation of (S)- β -butyrolactone
Macromolecules **23** 3206-3212 1991
- 88 Gross R.A., Zhang Y., Konrad G., Lenz R.W.
Polymerisation of β -monosubstituted β -propiolactone using trialkylaluminium/water catalytic systems and polymer characterisation.
Macromolecules **21** 2657-2668 1988
- 89 Agostini D.E., Lando J.B., Shelton J.R.
Synthesis and characterisation of poly β -hydroxybutyrate.
I. Synthesis of crystalline DL- poly β -hydroxybutyrate from DL- β -butyrolactone.
J. Polym Sci Polym Chem Ed. **9** 2775-2787 1971
- 90 Teranishi K., Iida M., Araki T., Yamashita S., Tani H.
Stereospecific polymerisation of β -alkyl- β -propiolactone
Macromolecules **7** 421-427 1974
- 91 Iida M., Araki T., Teranishi K., Tani H.
Effect of substituents on stereospecific polymerisation of β -alkyl and β -chloroalkyl- β -propiolactones
Macromolecules **10** 275-284 1977

- 92 Dubois Ph., Degee Ph., Jerome R., Teyssie Ph.
Macromolecular engineering of polylactones and polylactides 8. Ring opening polymerisation of ϵ -caprolactone initiated by primary amines and trialkylaluminium.
Macromolecules **25** 2614-2618 1992
- 93 Kowalski A., Duda A., Penczek S.
Kinetics and mechanism of cyclic esters polymerisation initiated with tin(II) octoate, 1. Polymerisation of ϵ -caprolactone
Macromol Rapid Commun. **19** 567-572 1998
- 94 Knani D., Gutman A.L., Kohn D.H.
Enzymatic polyesterification in organic synthesis of linear polyesters. I. Condensation polymerisation of linear hydroxyesters. II. Ring opening polymerisation of ϵ -caprolactone.
J. Appl Polym. Sci. Part A, Polym. Chem. Ed. **31** 1221-1232 1993
- 95 Uyama D., Kobayashi S.
Enzymatic polymerisation of lactones
Chem Lett. 1149-1158 1987
- 96 MacDonald R.T., Pulapura S.K., Svirikin Y.Y., Gross R.A., Kaplan D.I., Akkara J., Swift G. Wolk S
Enzyme catalysed ϵ -caprolactone ring opening polymerisation.
Macromolecules. **28** 73-78 1995
- 97 Nobes G.A.R., Kazlauskas R.J., Marchessault R.H.
Lipase catalysed ring opening polymerisation of lactones: A novel route to poly(hydroxyalkanoates).
Macromolecules **29** 4829-4833 1996
- 98 Cordova A. Iverson T., Hult K., Martinelle M.
Lipase-catalysed formation of macrocycles by ring opening polymerisation of ϵ -caprolactone.
Polymer **39** 6519-6524 1998
- 99 Kullmer K. Kilkuchi H., Uyama H, Kobayashi S.
Lipase-catalysed ring opening polymerisation of α -methyl- δ -valerolactone and α -methyl- ϵ -caprolactone.
Macromol. Rapid Commun. **19** 127-130 1998
- 100 Kobayashi S., Takeya K. Uyama H.
Lipase-catalysed ring opening polymerisation of medium size lactones to polyesters.
Macromol. Chem. Phys. **199** 1729-1736 1998

- 101 Bisht K.S., Henderson L.A., Gross R.A., Kaplan D.L., Swift G.
Enzyme catalysed ring opening polymerisation of ω -pentadecalactone.
Macromolecules **30** 2705-2711 1997
- 102 Henderson L.A., Svirkin Y.Y., Gross R.A., Kaplan D.L., Swift G
Enzyme catalysed polymerisation of ϵ -caprolactone: Effects of initiator on product structure, propagation kinetics, and mechanism.
Macromolecules **29** 7759-7766 1996
- 103 Szwarc M., Levy M., Milkovich R.
Polymerisation initiated by electron transfer to monomer. A new method of formation of block co-polymers/
J. Am. Chem. Soc. **78** 2656-2657 1956
- 104 Szwarc M.
Living polymers. Their discovery, characterisation and properties.
J. Appl. Polym. Sci. Part A., Polymer. Chem. **36** ix-xv 1998
- 105 Odian G.
Principles of Polymerisation 2nd Edition
J.Wiley & Sons 1981
- 106 Beila T., Duda A.
Solvent effect in the polymerisation of ϵ -caprolactone initiated with diethyl aluminium ethoxide.
J. Polym. Sci. Part A. Polym Chem Ed. **34** 1807-1813 1996
- 107 Hamitou A., Ouhadi T., Jerome R., Teyssie Ph.
Soluble binetallic μ -oxo alkoxides. VII. Characteristics and mechanisms of ring opening polymerisation of lactones.
J. Polym Sci **15** 865-873 1977
- 108 Heuchen J., Jerome R., Teyssie Ph.
Soluble bimetallic μ -oxo alkoxides VIII. Kinetic behavior of the catalytic species in unsubstituted lactone ring opening polymerisation
Macromolecules **14** 242-246 1981
- 109 Hamitou A., Ouhadi T., Jerome R., Teyssie Ph.
Polycaprolactone based co-polymers I. Synthesis by anionic co-ordination type catalysts
9 927-930 1976
- 110 Jacobs C., Dubois Ph., Jerome R. Teyssie Ph.
Macromolecular Engineering of Polylactones and Lactides. 5. Synthesis and Characterisation of diblock Copolymers Based on Poly- ϵ -caprolactone and Poly(L,L or D,L)lactide by Aluminium Alkoxides.
Macromolecules. **24** 11 3027-3034 1991

- 111 Dong Tian, Dubois Ph., Jerome R. Teyssie Ph.
Macromolecular Engineering of Polylactones and Lactides 18. Synthesis of Star Branched Aliphatic Polyesters Bearing Various Functional End Groups.
Macromolecules **27** 4134-4144 1994
- 112 Jedlinski Z., Kurcok P., Kowalczyk M., Matuszowicz A., Dubois Ph., Jerome R., Kricheldorf H.R.
Anionic Polymerisation of Pivalactone Initiated by Alkali Metal Alkoxides
Macromolecules **28** 7276-7280 1995
- 113 Ropson N., Dubois Ph., Jerome R. Teyssie Ph.
Macromolecular Engineering of Polylactones and Lactides 20. Effect of Monomer, Solvent, and Initiator on the Ring Opening Polymerisation As Initiated with Aluminium Alkoxides
Macromolecules **28** 7589-7598 1995
- 114 Tortosa K., Miola C., Hamaida T.
Synthesis of low molecular weight hydroxy poly(ϵ -caprolactone) macromonomers by co-ordinated anionic polymerisation in protic conditions
J. Appl Polym Sci. **65** 2357-2372 1997.
- 115 Yoshida E., Osagawa Y.,
Synthesis of Poly(ϵ -caprolactone) with a stable Nitroxyl Radical as a Functional Group and its Application to a Counter Radical
Macromolecules **31** 1446-1453 1998.
- 116 Duda A, Floranczyk Z., Hofman A., Słomkowski S., Penczek S.
Living Pseudoanionic Polymerisation of ϵ -caprolactone Free of Cyclics with Controlled End Groups.
Macromolecules **23** 1640-1646
- 117 Endo M., Aida T., Inoue S.
Immortal Polymerisation of ϵ -caprolactone Initiated by Aluminium Porphyrin in the Presence of Alcohol
Macromolecules **20** 2982-2988 1987
- 118 Duda A., Penczek S.
On the Difference of Reactivities of various Aggregated Forms of Aluminium Triisopropoxide in Initiating Ring Opening Polymerisations
Macromol. Rapid Commun. **16** 67-76 1995
- 119 Isoda M. Sugimoto H., Aida T., Inoue S
Lewis Acid Driven Accelerated Living Polymerisation of Lactones Initiated with Aluminium Porphyrins. Chemoselective Activation of Ester Groups by Lewis Acid
Macromolecules **30** 57-62 1997

- 120 Dubois Ph. Jerome R., Teyssie Ph.
Macromolecular Engineering of Polylactones and Lactides 3. Synthesis, Characterisation, and Applications of Poly(ϵ -caprolactone) Macromonomers
Macromolecules **24** 977-981 1991
- 121 Miola C., Hamiade T., Spitz R.
End Functionalised Poly(ϵ -caprolactone) Oligomers Trough Heterogeneous Catalysis in Protic Conditions: A Mechanistic Approach.
Polymer **38** 5667-5676 1997
- 122 Dubois Ph., Jacobs C., Jerome R., Teyssie Ph.
Macromolecular Engineering of Polylactones and Lactides 4. Mechanism and Kinetics of Lactide Homopolymerisation by Aluminium Isopropoxide.
Macromolecules **24** 2266-2270 1991
- 123 Vion J.M, Jerome R., Teyssie Ph., Aubin M., Prud'homme R.E.
Synthesis, Characterisation and Miscibility of ϵ -Caprolactone Random Copolymers
Macromolecules **19** 1828-1838 1986
- 124 Dubois Ph., Barakat I., Jerome R., Teyssie Ph.
Macromolecular Engineering of Polylactones and Lactides. 12 Study of the Depolymerisation Reactions of Poly(ϵ -caprolactone) with Functional Aluminium Alkoxide Groups
Macromolecules **26** 4407-4412 1993
- 125 Bero M., Adamus G., Kaspercyck J., Janeczek H.,
*Synthesis of Block Copolymers of ϵ -caprolactone and lactide in the Presence of Li *t*-BuO*
Polym. Bull. **31** 9-14 1993
- 126 Osgan M. Teyssie Ph.
Bimetallic μ -oxo alkoxides as catalysts for the insertion polymerisation of epoxides.
J. Polym. Sci Part B **5** 789-7792 1967
- 127 Osgan M., Price C.C.
Polyethers V.
New catalysts for the preparation of isotactic polypropylene oxide
J. Polym Sci **34** 153-156 1959
- 128 Ropson N., Jerome R., Dubois Ph., Teyssie Ph.
Living (co)-polymerisation of adipic anhydride and selective end functionalisation of the parent polymers
Macromolecules **25** 3820-3821 1992

- 129 Ropson N., Jerome R., Dubois Ph., Teyssie Ph.
Macromolecular engineering of polylactones and polylactides 14. A 13C and 27Al study of the effect of γ -butyrolactone on the structure of aluminium isopropoxide in toluene
Macromolecules **26** 6378-6385 1993
- 130 Ropson N., Jerome R., Dubois Ph., Teyssie Ph.
Living (co)-polymerisation of adipic anhydride and selective end functionalisation of the parent polymers
Macromolecules **25** 3820-3821 1992
- 131 Hamitou A., Ouhadi T., Jerome R., Teyssie Ph.
Soluble bimetallic μ -oxo alkoxides. 8. Kinetic behaviour of the catalytic species in unsubstituted lactone ring opening polymerisation
Macromolecules **9** 927-930 1976
- 132 Hawker C.J., Hedrick J.L., Malmstrom E.E., Trollsas Mecerreyes D., Moineau G., Dubois Ph., Jerome R.
Dual living free radical and ring opening polymerisations from a dual headed initiator
Macromolecules **31** 213-219 1998
- 133 Carter K.R., Richter R., Kricheldorf H.R., Hedrick J.L.
Synthesis of amine terminated aliphatic poly(carbonates) via $Al(Et)_2(OR)$ initiated polymerisations.
Macromolecules **30** 6074-6076 1997
- 134 Reeve M.S., McCarthy S.P., Gross R.A.
Preparation and characterisation of (R)-poly(β -hydroxybutyrate)-poly(ϵ -caprolactone) and (R)-poly(β -hydroxybutyrate)-poly(lactide) degradable diblock co-polymers
Macromolecules **26** 888-894
- 135 Yau W.W., Kirkland J.J., Bly D.D.
Modern size exclusion liquid chromatography. Practice of gel permeation and gel filtration chromatography.
J. Wiley New York 1979.
- 136 Mole T., Jefferey E.A.
Organoaluminium compounds
Elsevier Science Amstersam 1972
- 137 Duda A., Penzcek S.
Kinetics of ϵ -caprolactone polymerisation on alkyl aluminium alkoxides.
Macromol. Chem. Macromol. Symp. **47** 127-140 1991